

Risk Assessment of Mildly Flammable Refrigerants

2014 Progress Report

June 2015

The Japan Society of Refrigerating and
Air Conditioning Engineers

Copyright © 2014 by the authors and JSRAE

All rights reserved. This report or any portion thereof may not be reproduced or used in any manner whatsoever without the express written permission of JSRAE except for the use of brief quotations in a book review.

Although the authors and JSRAE have made every effort to ensure that the information in this report was correct at press time, the authors and JSRAE do not assume and hereby disclaim any liability to any party for any loss, damage, or disruption caused by errors or omissions, whether such errors or omissions result from negligence, accident, or any other cause.

The Japan Society of Refrigerating and Air Conditioning Engineers, JSRAE

Nihonbashi-Otomi Bldg. 5F

13-7 Nihon-bashi Odenma-cho

Chuo-ku, Tokyo, 103-0011 Japan

TEL + 81-3-5623-3223, FAX +81-3-5623-3229

Foreword

While great successes have been achieved in climate change mitigation, global emissions of greenhouse gases continue to rise. Greenhouse gas emissions from fossil fuels are the main issue, but emissions of fluorocarbon refrigerants from refrigeration and air conditioning appliances should not be ignored because of the large global warming potential (GWP) of fluorocarbons.

The progressively more severe impact of fluorocarbon refrigerants makes the need for urgent action abundantly clear. The basic measure to reduce the impact of refrigerants is the replacement of conventional hydrofluorocarbons (HFCs) with low-GWP refrigerants. Low-GWP refrigerants are not very stable in atmosphere and thus are sometimes flammable. According to Japan's High Pressure Gas Safety Act, the use of flammable refrigerants in refrigeration and air conditioning equipment is restricted in practice. For the safe use of flammable refrigerants and relaxation of the regulation, a risk assessment needs to be performed; only a scientific risk assessment can provide a sound basis for judgment and change in regulation.

The Ministry of Economy, Trade and Industry (METI) and the New Energy and Industrial Technology Development Organization (NEDO) have been subsidizing research to obtain basic information on mildly flammable refrigerants since 2011. In addition, a research committee was set up by the Japan Society of Refrigerating and Air Conditioning Engineers to assess the risks associated with mildly flammable refrigerants. The Japan Refrigerating and Air Conditioning Industry Association and the Japan Automobile Manufacturers Association are presently conducting very definitive risk assessments, and the results are being discussed by the research committee.

This 2014 progress report provides state-of-the-art information concerning the risk of mildly flammable refrigerants. I am sure that its information will be of much interest for the risk assessment. I thank all the members and observers of the committee who helped produce this progress report. I hope that you will find it a useful and stimulating summary of the ever-sustainable story at the heart of human progress.

Chairperson of the Committee

Professor at the University of Tokyo

Eiji HIHARA

June 2015

Table of Contents

ABSTRACT	1
1. Introduction	15
1.1 Trends in Refrigerant Regulation	15
1.2 Research trends on the Safety of Mildly Flammable Refrigerants	18
2. Fundamental Flammability	20
2.1 Introduction	20
2.2 Effect of Humidity on Flammability Limits of Refrigerants	23
2.2.1 Effect of laboratory level humidity on flammability limits of some flammable compounds	
2.2.2 Effect of high humidity on flammability properties of non-flammable refrigerants	
2.2.3 Effect of high humidity on flammability limits of mildly flammable refrigerants	
2.2.4 Adiabatic flame temperatures	
2.3 Burning Velocity	27
2.4 Minimum ignition energy and quenching distance	30
2.4.1 Quenching distance measurement	
2.4.2 Estimation of minimum ignition energy	
2.4.3 Comparison with ignition energy under practical conditions	
2.5 Extinction Diameter	34
2.6 Thermal Decomposition of Lower-GWP Refrigerants	37
2.6.1 Introduction	
2.6.2 Experimental methods and results	
2.6.3 Conclusion	
3. Physical Hazard Evaluation of A2L Refrigerants Based on Several Conceivable Handling Situations	43
3.1 Introduction	43
3.2 Hazard Evaluation of Handling Situation #1: -Use with Fossil-Fuel Heating System-	44
3.2.1 Outline	
3.2.2 Experiment	
3.2.3 Results and discussions	
3.3 Hazard Evaluation of Handling Situation #2-(a): -Ignition and Flame Propagation Possibility by a Lighter -	46
3.3.1 Outline	

3.3.2	Details of experimental evaluation of the possibility of ignition and flame propagation using piezo-type gas lighter and fuel-premixed turbo lighter	
3.3.3	Details of experimental evaluation of the possibility of ignition and flame propagation using kerosene cigarette lighter	
3.4	Hazard Evaluation of Situation #2-(b): -Physical Hazard of Rapid Leakage from a Pinhole-	51
3.4.1	Outline	
3.4.2	Experiment	
3.4.3	Results and discussions	
3.5	Hazard Evaluation of Situation #2-(c): - Physical Hazard of Leakage into the Collection Device	56
3.5.1	Outline	
3.5.2	Experiment	
3.5.3	Results and discussions	
3.6	Hazard Evaluation of Situation #2-(d) - Diesel Combustion of Oil and Refrigerant Mixture during Pump-Down of Air Conditioners-	59
3.6.1	Outline	
3.6.2	Materials and methods	
3.6.3	Results	
3.7	Conclusions	65
3.7.1	Simultaneously used with a fossil-fuel heating system	
3.7.2	Ignition and flame propagation possibility by a lighter	
3.7.3	Physical hazard of rapid leakage from a pinhole	
3.7.4	Physical hazard evaluation of leakage into the collection device	
3.7.5	Diesel combustion of oil and refrigerant mixture during pump-down of air conditioners	
4.	Physical Hazard Assessment	68
4.1	Introduction	68
4.2	Combustion Test	68
4.2.1	Introduction	
4.2.2	Experiment	
4.2.3	Flame velocity and burning velocity	
4.3	Hazard Evaluation According to Deflagration Index	72
4.3.1	<i>KG</i> value	
4.3.2	Potential risk of combustion of A2L refrigerants compared to other flammable gases	
4.3.3	Evaluation of reduced pressure based on <i>KG</i>	
4.4	Conclusion	75

5 Procedure for Risk Assessment of Mildly Flammable Refrigerant	77
5.1 Introduction	77
5.2 Procedure of Risk Assessment	77
5.3 Air-Conditioner Equipment and Risk Assessment Situation	79
5.4 Risk Assessment Procedure for Household Air-Conditioner	80
5.4.1 Tolerance level of risk assessment	
5.4.2 Setting of leakage	
5.4.3 Setting of flammable spaces	
5.4.4 Simulation of flammable time volume	
5.4.5 Setting of ignition sources	
5.4.6 Human error probability	
5.4.7 Consistency with tolerance value	
5.4.8 Summary of household air-conditioner	
5.5 Differences of Building Multi-Air-Conditioner and Commercial Air-Conditioner	87
5.6 Difference of Chiller	89
5.7 FMEA and Other Hazards	89
5.8 Summary of Risk Assessment	90
6 Risk Assessment of Mini-Split Air Conditioners	91
6.1 Introduction	91
6.2 Refrigerant Leak Simulation	91
6.3 Ignition Source Evaluation	91
6.4 Summary of FTA	92
6.5 Diesel Explosion and Combustion Products	93
6.6 Housing Air Conditioner Risk Assessment and Results	93
6.6.1 Housing air conditioner installation modes and problems	
6.6.2 One-to-one connection floor-standing housing air conditioners (Single floor-standing air conditioners) Ignition sources and installation conditions	
6.6.3 Probability of accident occurrence and aims of single floor-standing air conditioner risk assessment	
6.6.4 Single floor-standing air conditioner risk assessment analysis	
6.6.5 Single floor-standing air conditioner risk assessment analysis considering installation in 4.5-jo space [Measure S2]	
6.7 Multi-connection Housing Air Conditioner Risk Assessment and Results	96
6.7.1 Setting conditions of analysis based on realistic housing	

6.7.2 Regarding Door Clearances Based on Housing Environment: Hinged Doors and Sliding Doors	
6.7.3 Initial refrigerant density of an indoor leakage of multi-connection floor-standing air conditioners	
6.7.4 Combustible space-time product	
6.7.5 Multi-connection floor-standing housing air conditioner risk assessment analysis	
6.7.6 Results of diffusion by the indoor unit fan	
6.7.7 Multi-connection floor-standing housing air conditioner (multi floor-standing air conditioner) risk assessment results	
6.8 Multi-connection Wall Mounted Air Conditioners (Multi-Wall Mounted Air Conditioner) Risk Assessment	101
6.9 Summary of Housing Air Conditioners Risk Assessment	102
6.10 Summary	102
7. Risk Assessment for Split Air Conditioners (Commercial Package Air Conditioners)	104
7.1 Introduction	104
7.1.1 Progress of risk assessment for split air conditioners	
7.1.2 Features of C-PAC	
7.1.3 Risk assessment methodology	
7.1.4 Assumption of the allowable risk level	
7.1.5 Factors of ignition accidents for C-PAC with A2L refrigerants	
7.2 Refrigerant Leakage Simulation	107
7.2.1 Simulation for indoor installation models	
7.2.2 Simulation for outdoor installation models	
7.3 Ignition Source	111
7.3.1 Setting of the ignition source	
7.3.2 The probability of the presence of ignition sources	
7.4 FTA	113
7.4.1 FTA of the service stage for outdoor installation	
7.4.2 FTA of the service life stage for indoor installation	
7.5 Result of the Risk Assessment for Each Model	114
7.5.1 1st step models (typical normal C-PAC models)	
7.5.2 2nd step models (severe C-PAC models less than 14 kW excluding floor-standing indoor units)	
7.6 The Risk Assessment Considering Improper Refrigerant Charge	119
7.7 Summary	120

8. Progress of Risk Assessment for VRF System	121
8.1 Introduction	121
8.2 Issues for VRF Systems Using Mildly Flammable Refrigerants	121
8.3 Identification of Risks	122
8.4 Preparations for Risk Assessment	122
8.4.1 Setting allowable levels	
8.4.2 Probability of number of leaks occurring for different refrigerant leak velocities	
8.4.3 Probability of human error	
8.4.4 Ignition source assessment	
8.4.5 Calculation method for probability of fire	
8.4.6 Setting of indoor model and analysis details	
8.4.7 Setting of outdoor model	
8.5 Results of Risk Assessment and Safety Measures	130
8.5.1 During transportation stage (manufacture of product)	
8.5.2 During installation	
8.5.3 During system operation (indoors)	
8.5.4 Investigation of floor-standing safety measures	
8.5.5 During system operation (outdoors)	
8.5.6 Safety measures for outdoor unit	
8.5.7 During repair	
8.5.8 During disposal	
8.6 Summary of Risk Assessment	139
8.6.1 Probability of fire during indoor operation	
8.6.2 Probability of fire during outdoor use	
8.6.3 Probability of fire during work	
8.6.4 Probability of fire in market	
8.7 Summary of Important Safety Matters	141
8.7.1 Regulations according to High Pressure Gas Safety Law	
8.7.2 Safety countermeasures as function of indoor unit	
8.7.3 Ideal regulations for safety and commercialization	
8.8 Summary and Future Tasks	143
9. Progress in Chiller Risk Assessment	144
9.1 Introduction	144
9.2 Prerequisites for Performing Risk Assessments	144

9.2.1 Features and tasks of the chiller	
9.2.2 Risk assessment procedure	
9.2.3 Basic model of chiller for RAs	
9.2.4 Definition of life stages	
9.2.5 Basic configuration of FTA	
9.2.6 Risk assessment map and risk assessment list	
9.3 Flammable Space Analysis Model for Refrigerant Leak	148
9.3.1 Analysis model	
9.3.2 Definition of flammable region and amount of leaked refrigerant	
9.3.3 Analysis condition	
9.3.4 Analysis results	
9.4 Ignition Probability	155
9.4.1 Ignition sources in a machine room	
9.4.2 Ignition sources	
9.4.3 Ignition by smoking	
9.4.4 Ignition by electrical components	
9.5 Probability of the Occurrence of Refrigerant Leakage	149
9.6 Risk Assessment	158
9.6.1 List of risk assessment conditions	
9.6.2 Probability of accidental fire	
9.6.3 Technical requirements for safety	
9.7 Simulation of Leakage from Chillers	161
9.7.1 Calculation method	
9.7.2 Results and discussion	
9.8 Conclusions	166
10. Thermophysical Properties and Cycle Performance of Newly Developed Low-GWP Refrigerants	168
10.1 Introduction	168
10.2 Measurements of Thermodynamic Properties and Proposal for Equation of State for Low-GWP Refrigerants	168
10.2.1 Measurements of the thermodynamic properties of R1243zf	
10.2.2 Equation of state for R1243zf	
10.2.3 Measurements of surface tension for low-GWP refrigerants	
10.3 Measurement and Estimation of Thermophysical Properties	178
10.3.1 Thermal conductivity measurement of R1234ze(Z)	

10.3.2 Viscosity measurement of R1234ze(Z)	
10.4 Assessment of Cycle Performance Using Low-GWP Refrigerant Mixtures	184
10.4.1 Experimental apparatus and method	
10.4.2 Experimental results	
10.5 Conclusions	188
Appendix 1: List of Committee Members	190
Appendix 2: List of Authors	192

ABSTRACT

1. Introduction

1.1 Trends in Refrigerant Regulation

The regulation regarding the use of stationary air conditioners is known as F-Gas Regulation (EC) No. 842/2006. The present regulation focuses on reducing refrigerant leakage from air conditioners and requires proper management; instructional courses for operators; the labeling of equipment containing F-gas; and reports by producers, importers, and exporters of F-gas. In January 2015, the European Union (EU) enhanced the existing regulations. The new amendment aims to reduce the leakage of F-gas to two-thirds of the present level and prohibits the release of equipment using F-gas in fields where an environmentally friendly refrigerant has been developed. To achieve this, a phase-down schedule has been determined that stipulates that the annual amount of hydrofluorocarbons (HFCs) sold in the EU be reduced to one-fifth of the present amount by 2030.

At the Conference of Parties, which was held with the aim of abolishing practices that damage the ozone layer, three North American countries (the United States, Canada, and Mexico) submitted a proposal to revise the Montreal Protocol and restrict the production and sale of HFCs. However, HFCs do not damage the ozone layer. The problem of global warming was caused by the replacement of prohibited chlorofluorocarbons (CFCs) and hydrochlorofluorocarbons (HCFCs), which damage the ozone layer, with HFCs, which have a high global warming potential (GWP). The proposal suggests restricting the distribution of HFCs in a manner based on the framework of the Montreal Protocol.

In Japan, the “Law on the regulation of management and rational use of fluorocarbons” was established by the National Parliament on June 5, 2013, and took effect in April 2015. The name of the law was changed from the “Law for ensuring the implementation of the recovery and destruction of fluorocarbons in specific products.” The new law requires the replacement of high-GWP HFCs, refrigerant management, and refrigerant recovery to reduce HFC leakage.

1.2 Research Trends of the Safety of Mildly Flammable Refrigerants

The low-GWP refrigerants R1234yf and R32 are promising candidates to replace conventional HFC refrigerants. However, these refrigerants are not very stable in air and are flammable. Therefore, it is essential to collect basic data on the flammability of low-GWP refrigerants and research their safety for practical use. With the objective of gathering essential data for the risk assessment of mildly flammable refrigerants, safety studies are currently being conducted by project teams from the Tokyo University of Science at Suwa, Kyushu University, the University of Tokyo, and the National Institute of Advanced Industrial Science and Technology. Since 2011, these institutions have been sponsored by the project “Development of Highly Efficient and Non-Freon Air Conditioning Systems” of the New Energy and Industrial Technology Development Organization (NEDO). In addition, a research committee was organized by the Japan Society of Refrigerating and Air Conditioning Engineers to assess the risks associated with mildly flammable refrigerants. The Japan Refrigerating and Air Conditioning Industry Association and the Japan Automobile Manufacturers Association are presently conducting risk assessments, and the results are being discussed by a research committee. The 2014 activities of the committee to assess the risks associated with mildly flammable refrigerants are compiled in this report. The committee members would be pleased if this report proved helpful to persons working in associated fields.

2. Fundamental Flammability

Because high-GWP compounds are stable in the atmosphere, less-stable compounds are now being considered as lower-GWP alternatives. The properties that cause these new compounds to have a higher reactivity in the atmosphere also make them more flammable. Considering this tradeoff in risks, low-GWP compounds with mild flammability appear to be alternatives that provide the optimum balance of acceptable safety properties and environmental

performance. Thus, risk assessments of mildly flammable (2L) compounds must be conducted before they are used in practical applications.

In the risk assessment of flammable refrigerants, we should consider the combination of the probability of a fire occurring because of the leakage of the refrigerants and the severity of that fire hazard. Accordingly, it is important to collect a set of such indices that appropriately express these two factors. We present an interim report on the fundamental flammability of refrigerants, including flammability limits, burning velocity, minimum ignition energy, minimum quenching distance, extinction diameter, and thermal decomposition.

Many alternative refrigerants are multi-fluorinated compounds, and some are flammable. In particular, their flammability properties are sometimes strongly affected by the humidity conditions. In this study, the effects of humidity on various flammable and non-flammable refrigerants were investigated. The flammability limits of R1234yf and R1234ze(E) were found to be very sensitive to the humidity conditions. The higher the humidity, the wider the flammable ranges of these compounds. In particular, although R1234ze(E) is non-flammable in dry air, it becomes flammable when the humidity exceeds 10% corrected for 23 °C. It was found that R410A, R410B, and R134a become flammable when the relative humidity exceeds 19%, 25%, and 38%, respectively, at 60 °C.

Burning velocity measurements of HFO-1234ze(Z) were conducted in a microgravity environment to remove the effect of buoyancy. The maximum burning velocity was determined to be 1.9 cm s⁻¹, which is slightly higher than that of R1234yf. To confirm these results, the increases in the pressure of HFO-1234ze(Z) mixed with R32 and the burning velocities of HFO-1234ze(Z) in a variety of concentrations of O₂-enriched air were compared with those of HFO-1234ze(Z) isomers. It was found that the burning velocity of HFO-1234ze(Z) was lower than that of R1234yf and very similar to that of R1234ze(E).

To judge whether a refrigerant is flammable under practical conditions, information on the ignition energy of the refrigerant and the ignition source in the surrounding environment is necessary. In this study, quenching distance measurements, including its concentration dependence and the estimation of the minimum ignition energy, are updated. The values were compared with the energy of a static electricity spark from the human body.

In this study, an index called the extinction diameter is newly introduced to evaluate the flammability characteristics of 2L refrigerants. This index is expected to be used to judge whether an enclosure of electrical parts with openings, such as a magnetic contactor and socket, can become an ignition source for the refrigerants. We add new data on the extinction diameter of R1234yf as a function of the distance between the ignition source and the opening of the enclosure and provide a discussion on the extinction diameter.

Regarding the thermal decomposition of refrigerants, a comparison is made between 2L refrigerants and typical non-flammable refrigerants with and without moisture. Detailed analysis is performed on the onset of thermal decomposition, concentrations of toxic products, and the difference between the materials of the hot surface. We have not yet observed significant differences between 2L and conventional non-flammable refrigerants.

3. Physical Hazard Evaluation of A2L Refrigerants Based on Several Conceivable Accident Scenarios

3.1 Introduction

We conducted a series of experimental evaluations of the physical hazards associated with A2L refrigerants, assuming occasional accident scenarios in situations in which A2L refrigerants are likely to be handled, based on discussions with developers and associations dealing with air conditioning systems in Japan, such as the Japan Refrigeration and Air Conditioning Industry Association (JRAIA).

3.2 Physical Hazard Evaluation Details for Each Scenario

3.2.1 Scenario #1: Simultaneous use with a fossil fuel heating system

Even when all the refrigerant contained within a commercial room air conditioning system with an area of approximately 11 m² leaked into the general living space (7.8 m², approximately corresponding to the area of 4.5 tatami mats) where a fossil fuel heating system was in operation, ignition and flame propagation did not occur. The amount of

HF generated as a result of the thermal decomposition of the A2L refrigerant was equivalent to the amount of refrigerant present. When flows were present inside the space, the HF concentration increased.

3.2.2 Scenario #2: Service and maintenance situation

- (1) Accident scenario (a): We evaluated the physical hazards of a commercial portable gas lighter used in a space where an A2L refrigerant leaked and accumulated. When a piezo gas lighter was used, no flame propagation was observed. Although ignition and small flame propagation was confirmed near the outlet of a turbo lighter, the flame quickly went out. Significant pressure rises from the blast wave or temperature increases were not observed. However, the ignition and flame propagation of accumulated R32 was confirmed for a kerosene cigarette lighter with a surrogate source of ignition replacing the usual generation by rubbing the flint wheel.
- (2) Accident scenario (b): We assumed that the A2L refrigerant leaked from a fracture or pinhole formed in the pipes or hoses during service and maintenance. When the refrigerant leaked from a pinhole with a diameter of 4 mm to simulate a breaking pipe, a flammable zone only formed near the refrigerant outlet. Even when energy in excess of a conceivable ignition source in a realistic situation was provided to the refrigerant jet, ignition and flame propagation to the entire refrigerant jet were not observed.
- (3) Accident scenario (c): We assumed that the A2L refrigerant leaked inside a device used for service and maintenance, such as a collection device. When there was no slit to diffuse the accumulated leaked refrigerant in the model collection device to the outside, the refrigerant ignited from an ignition source with very high energy, and the flame propagated to the entire refrigerant. However, the probability of generating an ignition spark above this high energy is extremely low in actual situations. If there is a slit of a suitable width in the model collection device, the accumulation of the refrigerant can be controlled in a very short period of time, and thus ignition can be averted.
- (4) Accident scenario (d): We reproduced the diesel combustion that may occur during the pump-down of air conditioners by adiabatic compression of the air, refrigerant, and lubricating oil with the compressor. We determined that the combustion accidents that may occur during pump-down are caused by the diesel combustion of the oil resulting from the air entering the refrigerant tube. At this time, the refrigerant itself burns, which causes the intense pressure rise and the production of HF. It was revealed that the tendency of conventional A1 refrigerants to combust is similar to that of A2L refrigerants in the flammable range.

4. Physical Hazard Assessments

To utilize mildly flammable refrigerants, such as R32, R1234yf, and R1234ze(E), it is important to evaluate the combustion safety of these refrigerants in the event of leakage into the atmosphere from accidents during installation and operation. In this study, the fundamental flammability characteristics of refrigerants were experimentally evaluated using a large spherical combustion vessel, and their safety was assessed. Flammability was investigated in terms of various parameters, such as the flame speed, burning velocity, and deflagration index K_G , under the influence of elevated temperature and moisture and the uplift behavior due to buoyancy arising from the slow burning velocity. The obtained flammable characteristics were compared with those of other flammable gases. Reduced pressure effects due to an opening were considered based on a vent design.

Mildly flammable refrigerants have such a low burning velocity (≤ 10 cm/s) that a lifting of the flame front due to buoyancy significantly affects their combustion behavior, and they are categorized into the A2L class according to ASHRAE. In this study, a large-volume spherical vessel was prepared to observe and evaluate the effect of buoyancy on the flammable properties of R32 and R1234yf; the flame propagation behaviors of these two refrigerants were observed using a high-speed video camera, and the internal pressure in the vessel was measured using a pressure sensor. In addition to R32 and R1234yf, R1234ze(E) was included in the assessment medium, and the flammability of these A2L refrigerants in the presence of elevated temperatures and moisture was experimentally investigated considering the conditions of a hot and humid summer.

The deflagration index K_G is commonly used to estimate and design the area of the explosion vent of an enclosure to release the internal pressure and protect structures where internal explosions may occur. The deflagration indices K_G for

each refrigerant were evaluated along with other properties, such as peak pressure P_{max} , flame speed S_f , and burning velocity S_u . As an implicit but useful reference, explosion characteristics, such as the minimum ignition energy (MIE), detonation limit, and K_G , of other flammable gases were listed with reference to K_G and were compared with those of A2L refrigerants obtained under elevated temperature and wet conditions. It is scheduled to make a comparison with A2L refrigerants and ammonia, which exhibits flammability similar to that of A2L refrigerants, under the same experimental condition.

A study on the severity evaluation method of combustion and explosion of A2L refrigerants under realistic situations has been promoted with the help of K_G value. An evaluation procedure to estimate the reduction effect of the severity of deflagrations caused by combustible A2L refrigerants in a full-scale environment has been developed by defining the relationship between reduced pressure and venting space in a room with the help of the venting design. According to the venting design for explosion protection, the reduced pressure effect due to the presence of an opening in the room was studied, and the effective venting area was experimentally evaluated. Venting area A is assumed to be circular or square-shaped. If the area is rectangular, the desirable ratio of the long side (L) to the short side (D) should be within 2. In an actual situation in the room, L/D may exceed 2, and the effective venting area A_v in this case was experimentally evaluated. A cubic vessel with sides measuring 50 cm was prepared for the test. A refrigerant was leaked into the vessel at a rate of 10 g/min and was premixed to a stoichiometric air–fuel ratio. The gas concentration was measured at a point 15 cm from the bottom. The flammable behavior and reduced pressure were observed under the presence of various vent shapes—circles, squares, and rectangles—with different ratios of long and short sides. The reduced pressure effect was summarized according to the vent area and aspect ratio of the rectangles. The effect of decreasing explosion severity due to the presence of the venting will be assessed by determining the relationship between the reduced pressure, the vent area, and the vent shape (L/D). The effect of the vertical concentration gradient of the A2L refrigerants on the explosion severity will be also examined in the next fiscal year (FY).

5. Risk Assessment Procedure for Mildly Flammable Refrigerants

5.1 Introduction

The risk assessment of mildly flammable refrigerants, such as R32, R1234yf, and R1234ze(E), was promoted by the sub-working groups (SWGs) of the JRAIA. In this chapter, the activity of these SWGs is described. Figure 5.1 shows the procedure for the risk assessment of mildly flammable refrigerants, with steps added from IEC Guide 51.

In general, risk assessment was performed using such methods as fault tree analysis (FTA), event tree analysis (ETA), and failure mode effects analysis (FMEA). The risk assessment of flammable refrigerants considers two individual phenomena: the presence of an ignition source

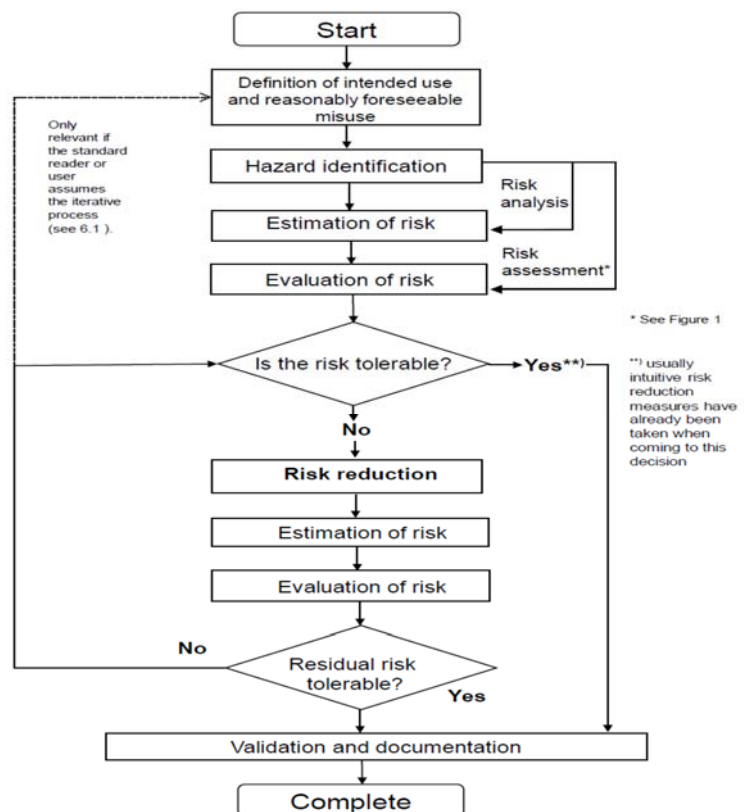


Fig. 5.1 Iterative process of risk assessment and reduction. (*Steps are described later)

and the generation of a flammable volume. Thus, we choose FTA to determine the individual phenomenon because it allows for easy calculation. We also referred to Risk-Map (R-Map). For the target setting of the equipment in the risk assessment, the product committee in JRAIA considered a household air conditioner, a building with multiple air conditioners, and a chiller.

5.2 Risk Assessment Method for Mildly Flammable Refrigerants

To implement the specific risk assessment methods, it is necessary to clarify the following terms. According to the National Institute of Technology and Evaluation (NITE), the tolerance for a home electronics unit owned by an ordinary consumer is 10^{-8} accidents/year (based on 1 million sets sold). In other words, a product is regarded as safe if a fatal accident occurs once in 100 years for 1 million sets in circulation for air conditioners and once in 10 years for a chiller. Taking household air conditioning as an example, the leakage term was set to the total amount of leaks in 4 min based on the IEC standard. The time integral of flammable volume was calculated in a 7 m² room with computational fluid dynamics (CFD) by the University of Tokyo. In addition, an open flame was used as the ignition source, and human error was set to 10^{-3} . With all of these terms set, FTA was conducted.

This FTA was expanded in detail for each stage, and the values for transport, storage, installation, usage, service, and disposal were calculated. If the obtained value was less than the tolerance value, the risk assessment ended, and the products proceeded to commercialization and release to market.

If the calculated risk exceeded the tolerance value, the review took one of two paths. One was to reduce the risk by reviewing the measures. The other was to determine an event in the critical path that raises the risk value in the FTA. If the risk of hypothesized events was roughly assumed, more accurate risk was obtained through the analysis of the information or more detailed experiments. The calculated values from the review loop of this FTA were repeated until the tolerance value was achieved. Several measures can be considered to lower the risk to below the tolerance value.

5.3 Summary of Risk Assessment

The risk assessment procedure was conducted by the mini-split risk assessment SWG (I) based on the risk assessment advanced at JRAIA through a collaboration between the University of Tokyo, Tokyo University of Science at Suwa, and the AIST Chemical Division.

A risk assessment is a preliminary evaluation of a product for future commercialization. It is only a tool to determine what hazards are present in the product. Each hazard must be addressed if it is harmful. Product engineers master this tool well; it is mandatory to provide safe equipment with a reasonable social cost. Active disclosure of residual and unexpected risks must be continued.

In general, because the risk of an air conditioner increases with the refrigerant amount and the equipment size increases with the voltage source capacity, the risk tends to be high in FTA analysis. Some countermeasures include reducing the amount of refrigerant leakage by providing a shutoff valve, diluting the concentration by adding a high-speed fan, a dispersal fan and an exhaust, eliminating the ignition source by a power-interrupting device located outside the installation compartment, and installing an alarm device. There are many options to avoid risks. These include confirming a seal during installation, reporting safety checks, and regular equipment inspections. Risk can also be avoided by enforcing regulations and standards. The characteristics, installation conditions, usage conditions, convenience, and cost of each device should be chosen to align with the best approach.

The steps are as follows:

- a) Select risk assessment method
- b) Select evaluation region for the product
- c) Select stages of the air conditioner's life cycle
- d) Investigate the air conditioner's installation circumstances
- e) Determine severity of hazard
- f) Set tolerance levels
- g) Investigate refrigerant leak rate, speed, and amount

- h) Use CFD and calculate time integral of flammable volume
- i) Consider ignition sources.
- j) Develop FTA and calculate probability, followed by inspection
- k) Compare risk (consistency with tolerance)
- l) Evaluate risk (consistency with tolerance)

If the evaluated risk is lower than tolerance, go to step p).

- m) Reduce risk (measures include the implementation of equipment, a manual, and regulations)
- n) Redevelop FTA and recalculate probability
- o) Compare risk (consistency with tolerance)
- p) Commercialize (confirm important topics) and release to market.

6. Risk Assessment of Mini-Split Air Conditioners

6.1 Introduction

The risk assessment of mini-split air conditioners, which started in 2011, has been completed for all applicable products. Consequently, this is scheduled to be the final progress report. For the assessment of the flammability risks of residential air conditioners (RACs), we reduced the risk probability by performing a refrigerant leak simulation and ignition source evaluation.

The following is a brief summary of the FTA results for wall-mounted air conditioners, one-to-one connection floor standing housing air conditioners, and multi-connection floor standing housing air conditioners, for which data were obtained during the risk assessment undertaken in this project.

6.2 Risk Assessment Procedure

According to the literature released by the NITE, products that are distributed at a rate of 1 million units a year are considered safe if a fatal accident occurs once per 100 years. The total number of RACs (including mini-split air conditioners) in Japan is approximately 100 million sets, so the target value in the calculation is 10^{-10} or fewer sets/year. An indoor space 2.4 m in height and with 7 m² of floor area using an air conditioner was used as the leakage space. The installation position of the indoor wall-mounted unit was set at a height of 1.8 m from the floor, and the floor standing unit was set on the floor. To generate the flammable region, which is important when performing a risk assessment of mildly flammable refrigerant, the values of R32 and R1234yf were obtained using the same technique for the data given in earlier literature, and the simulation results were performed at the University of Tokyo. Referencing the reports of Imamura in the Tokyo University of Science at Suwa, Takizawa in AIST, and DOE/CE/23810-92 from ADL, Inc., in 1998, the SWG describes the items that are assumed to be ignition sources as follows. Low-voltage electrical equipment in Japanese homes does not ignite. Ignition does not occur with burning tobacco that does not emit a flame. Static electricity caused by the human body within the living space does not ignite. The ignition sources of outdoor and indoor units of R32 or R1234y RACs were assumed to be open flame, and the risk assessment was conducted. We also investigated leakage conditions and human error probability, thus obtaining the ignition probability by FTA using the above items.

6.3 Summary of Fault Tree Analysis

The results of the risk assessment for RACs in the configurations outlined above are described in Table 6.1. In the case of the one-to-one connection normal wall-mounted air conditioner, the hazard occurrence probability (ignition rate) in the revised risk assessment was almost 10^{-10} during use and was below 10^{-9} during logistics, installation, service, and disposal. Because each value was below the tolerance value, no further risk assessment was performed.

To achieve equivalent performance and efficiency for R1234yf when applying mildly flammable refrigerants to conventional R410A RACs, the heat exchanger must be increased to approximately 1.4 times its size, and a new large-size compressor must be developed and its reliability ensured. While looking at Table 6.1, it is necessary to keep in mind that the values have been slightly revised from the previous progress report.

Table 6.1 Ignition probability of various refrigerants (normal wall-mounted air conditioner)

Risk: Ignition probability			
Life Stage	R32	R1234yf	R290
Logistic	4.1×10^{-17}	4.5×10^{-17}	1.9×10^{-8} – 5.0×10^{-6}
Installation	2.7×10^{-10}	3.1×10^{-10}	1.5×10^{-6} – 1.7×10^{-5}
Use (Indoor)	3.9×10^{-15}	4.3×10^{-15}	5.9×10^{-9} – 1.1×10^{-4}
(Outdoor)	1.5×10^{-10}	2.1×10^{-10}	9.7×10^{-13} – 1.9×10^{-8}
Service	3.2×10^{-10}	3.6×10^{-10}	9.3×10^{-6} – 1.7×10^{-5}
Disposal	3.6×10^{-11}	5.3×10^{-11}	1.8×10^{-5} – 1.3×10^{-4}

However, the values for single and multi floor standing air conditioners are larger than the tolerance values, even in the reviewed risk assessment. Therefore, research into the installation and actual service conditions and investigation of door clearances were conducted, primarily in Japanese-style houses, to achieve risk assessment values closer to those of actual usage. We also reviewed whether the same tolerance values could be applied for normal wall-mounted air conditioners. The latest risk assessment results, which are very important, are given in Table 6.2.

The tolerance value for single floor standing air conditioners was 10^{-9} during use and 10^{-8} during logistics, installation, etc., which almost satisfies the allowable values.

Table 6.2 Ignition probability of various RACs

Risk: Ignition probability			
Life Stage	Normal wall-mounted R32	Single floor standing R32	Multi floor standing R32
Logistic	4.1×10^{-17}	3.6×10^{-11}	1.1×10^{-9}
Installation	2.7×10^{-10}	4.0×10^{-11}	9.0×10^{-9}
Use (Indoor)	3.9×10^{-15}	4.1×10^{-10}	4.7×10^{-10}
(Outdoor)	1.5×10^{-10}	8.6×10^{-11}	1.1×10^{-9}
Service	3.2×10^{-10}	2.6×10^{-10}	4.3×10^{-9}
Disposal	3.6×10^{-11}	2.5×10^{-11}	4.1×10^{-10}

6.4 Summary

In the mini-split risk assessment SWG, we performed risk assessments of R32 and R1234yf in wall-mounted small-size commercial use air conditioners (which are substantially the same as RACs) and confirmed that there are no problems upon use. We also conducted a risk assessment of RACs using R32 and confirmed that they can be used without problems if certain measures are adhered to. To lessen the risks, we also revised the installation and service manuals for the SWG. More precisely, in the “Piping construction manual for RACs using R32 refrigerant” (internal industrial society material) issued by the JRAIA, we added caution reminders to service and installation manuals, among other materials, and proposed suggestions and manuals for measures that can be carried out when using R32.

Finally, from the results of the analysis carried out at the Tokyo University of Science at Suwa and the National Institute of Advanced Industrial Science and Technology, which participated in the project for the risk assessment of mildly flammable refrigerants, the revision of the FTA resulted in significant improvements

. In the future, we expect that once the level of harm becomes clear, we will be able to use R32 and R1234yf air conditioners with even greater safety and contribute to the prevention of global warming. This concludes our present risk evaluation of mini-split air conditioners.

7. Risk Assessment of Split Air Conditioners (Commercial Package Air Conditioners)

By comparing split air conditioners (commercial package air conditioners, C-PACs) with mini-split air conditioners (RACs) and variable refrigerant flow (VRF) air conditioners for buildings from the perspective of a risk assessment as with A2L, we conducted a risk assessment of C-PACs by the same methodology. First, we set the allowable risk level of a C-PAC as the target of the risk assessment. The allowable level was set as the probability of a serious accident occurring in the market once every 100 years. Because research on the degree of a hazardous ignition accident has not yet been completed, all ignitions were treated as serious. The probability of an ignition accident was multiplied by the leakage probability, the probability of generating a flammable region, and the probability of the presence of ignition sources. For each life cycle stage (logistics, installation, usage, service, and disposal), the ignition probability was calculated using FTA based on the assumed risk scenario. We assessed C-PAC systems in three categories.

First category – Typical C-PAC models: ceiling cassette indoor unit in an office, less than 14 kW outdoor unit installed at ground level without additional charge, and bulk storage at a warehouse.

Second category – Severe models for systems of less than 14 kW, excluding floor standing indoor units. The maximum piping length and charge amount were assumed. Indoors: kitchen with many ignition sources, airtight karaoke room. Outdoors: each floor, semi-underground, and narrow space installations. Logistics: small warehouse storage and minivan delivery.

Third category – Severe models for all C-PACs of less than 30 kW, including floor standing indoor units. The maximum piping length and charge amount were assumed. Indoors: floor standing where the leaked gas remains at a high concentration, ice thermal storage indoor unit (ceiling type), and the same outdoor models as the second step.

For the typical normal models of a C-PAC system, the ignition probability using R32 satisfied the allowable risk without additional safety measures. However, safety measures were needed to satisfy the allowable level for some severe cases included in the second and third categories.

For some stages of outdoor semi-underground installation and narrow space installation, the ignition probability did not satisfy the allowable level. The dominant risk factors during the service stages were the result of human error, such as improper refrigerant recovery, which generates a flammable region, and improper wiring of power supply, which may cause a spark, in addition to the probability of the presence of the open flame of a gas burner during welding. Thus, we proposed education for workers and carrying a leak detector, as necessary safety measures.

For the usage stage, we proposed a reduction in the probabilities of the presence of ignition sources and the generation of a flammable region as follows. Semi-underground: prohibit installation near a boiler and mechanical ventilation or the unit's fan operating with a leak detector. Narrow space: an opening of 0.6 m or more for one side or prohibit installation near a boiler.

In the case of an indoor floor standing unit, the probability of generating a flammable region was too high because the leaked gas tended to remain near the floor at a high concentration. The safety measure taken during the usage stage was to force the unit's fan to be on with a leakage detector near the floor. For the service stages, the measures of education for workers and carrying a leak detector were effective.

We plan to introduce the safety measures to the installation manual for C-PACs using R32. When additional studies (on the flammability of A2L refrigerants other than R32 for varying levels of humidity and the degree of a hazardous ignition accident with A2L) are conducted in the near future, we plan to include the latest information in our risk assessments to achieve a more practical assessment.

8. Risk Assessment of Variable Refrigerant Flow Systems

8.1 Introduction

The purpose of this risk assessment is to accurately evaluate the risk of VRF systems using mildly flammable low-GWP refrigerants and establish safety standards based on those results to ensure a sufficient level of safety in the market. To slow the advancement of global warming, these products must gain market acceptance. This will require progress in the development of viable safety standards that eliminate the need for excessive regulations. To propose safety regulations that are compatible with commercialization, the probability of fire accidents was estimated, including installation cases that are close to actual market situations, and safety standards were proposed to reduce the probability to allowable

values. In this risk assessment, R32 was used as a representative mildly flammable refrigerant.

8.2 Risk Assessment Results

First, installation cases that include significant risk were identified for each of the life cycle stages of transportation and storage, installation, operation, repair, and disposal. Next, an FTA was created for each identified case, and the probability of fire accidents for each stage was obtained. At that time, installation cases were assumed with no measures taken outside of replacing the current refrigerant R410A with R32, and the values for the probability of fire accidents were set with no measures taken. When those values exceeded the established allowable values, the execution of safety measures became necessary. When the incidence of a fire accident was less than 1 in 100 years, it was considered to be socially acceptable, and the allowable values for the probability of fire accidents were set to be equivalent to that frequency.

Tables 8.1 and 8.2 indicate the probability of fire accidents during indoor and outdoor operation, respectively. Each assumed installation case is listed vertically in the tables, and the installation site, unit type, constituent ratio of the market for each installation case, and allowable probability are indicated horizontally. Furthermore, the probability values of fire accidents occurring when no measures are taken are indicated for cases with no mechanical ventilation and for cases with mechanical ventilation in the amount specified by the Building Standards Act. Additionally, each probability of fire accidents for cases in which safety measures were implemented is indicated when the values without mechanical ventilation exceeded the allowable values. Cases exceeding the allowable values are indicated by white spaces. In the last column of each table, the probability of fire accidents is indicated for the market overall. This was obtained by multiplying the market constituent ratio by the fire probability of each installation case.

For installation cases excluding ceiling spaces, the probability of fire accidents occurring during indoor operation without mechanical ventilation was higher than the allowable values, and thus safety measures are necessary. Specifically, when ventilation is turned off at night in an

Table 8.1 Probability of fire accidents during indoor operation

In each installation cases				[time/(unit*year)]	Not allowable	Allowable	
Installation case				Fire accident probability A			
Site	Type	Constituent ratio P	Allowable probability	Without measures		With measures	
				No vent	Vented		
Indoor	Karaoke	Ceiling	2.1E-03	1.0E-09	1.8E-07	4.4E-11	0.0E+00
	Restaurant	Floor	2.0E-02		3.8E-07	5.4E-09 ^{*1)}	2.6E-10 ^{*2)}
	Hair salon	Ceiling	1.6E-03		1.3E-09	1.2E-10	6.8E-12
	BBQ restaurant	Ceiling	7.8E-04		2.8E-09	4.4E-10	1.5E-11
	Ceiling space	Ceiling concealed	1.0E-00		3.0E-10	-	3.0E-11

Ventilation turned off at night

Installation case				Fire accident probability A			
Site	Type	Constituent ratio P	Allowable probability	Without measures		With measures	
				No vent	Vented		
Indoor	Office	Ceiling	3.8E-01	1.0E-09	7.6E-09 ^{*3)}	3.5E-12	3.5E-12

Total in market

Total=Σ(P * A)	4.0E-01	1.0E-09	1.1E-08	1.1E-10	3.7E-11
----------------	---------	---------	---------	---------	---------

*1) Supply and exhaust on the ceiling surface cannot dilute refrigerant gas leaked from floor unit.

*2) Measures are mechanical ventilation with a vent opening near the floor, or, agitation by the indoor fan.

*3) Ventilation turned off 18:00 to 09:00. Ignition sources are smoking by overtime people and water heater driving after people left from office.

Table 8.2 Probability of fire accidents during outdoor operation

In each installation cases				[time/(unit*year)]	Not allowable	Allowable
Installation case				Fire accident probability A		
Site	Constituent ratio P	Allowable probability	Without measures		With measures	
			No vent	Vented		
Outdoor	Usual	9.4E-01	4.0E-09	1.9E-11	-	-
	Each floor	5.0E-02		3.0E-09	-	-
	Semi-underground	1.0E-04		1.1E-07	-	2.5E-13 ^{*1)}
	Machinery room	6.0E-03		6.1E-08	-	3.2E-09 ^{*2)}

Total in market

Total=Σ(P * A)	1.0E+00	4.0E-09	5.4E-10	-	1.9E-11
----------------	---------	---------	---------	---	---------

*1) Mechanical ventilation with suction duct

*2) Mechanical ventilation, 2times/h*2system

Table 8.3 Probability of fire accidents during each work stage

In each installation cases				[time/(unit*year)]	Not allowable	Allowable				
Installation case				Fire accident probability A						
Site	Type	Constituent ratio P	Allowable probability	Installation		Repairing		Disposal		
				Without meas.	With meas.	Without meas.	With meas.	Without meas.	With meas.	
Indoor	Office	Ceiling	3.8E-01	1.0E-08	1.9E-09	-	8.7E-11	8.8E-12	2.9E-14	2.9E-15
	Restaurant	Floor	2.0E-02		1.9E-09	-	1.2E-08	3.9E-11	3.4E-12	3.4E-13
	Karaoke	Ceiling	2.1E-03		-	-	-	-	-	-
Outdoor	Usual	-	9.4E-01	1.0E-08	1.9E-09	-	1.4E-09	1.4E-10	2.4E-10	3.2E-11
	Each floor	-	5.0E-02		1.9E-09	-	3.1E-09	3.1E-09	1.0E-09	1.4E-10
	Semi-underground	-	1.0E-04		1.1E-08	1.9E-09	3.6E-07	2.1E-09	3.3E-08	4.8E-10
	Machinery room	-	6.0E-03		1.1E-08	2.1E-09	8.6E-07	5.4E-09	2.2E-08	3.3E-10

Total in market

				Without meas.		With meas.	
Indoor total=Σ(P * A)	4.0E-01	1.0E-08		1.0E-09		4.1E-12	
Outdoor total=Σ(P * A)	1.0E+00	1.0E-08		9.0E-09		3.7E-10	

office where the constituent ratio is high, oil cigarette lighters can be ignition sources, and the fire probability exceeds the allowable values.

In outdoor operation, safety measures, such as a combination of mechanical ventilation and an outdoor unit fan, must be implemented because the probability of fire accidents exceeds the allowable values for semi-underground and machinery room installations.

In Table 8.3, the probability of fire accidents is indicated for each work stage, such as transportation and storage, installation, repair, and disposal. In semi-underground and machinery room installations, the probability of fire accidents when the burner acted as an ignition source during brazing operation exceeded allowable values. Leak detection devices are essential countermeasures to check leakage. Sufficient mechanical ventilation is necessary when repairing equipment at restaurants where floor standing units are installed.

8.3 Analysis of Probability of Fire Accidents

Figure 8.1 indicates the probability of a fire occurring during indoor operation when using refrigerants R32 and R290 in RACs and refrigerant R32 in VRF systems. The vertical axis expresses the probability of fire accidents and was derived by analyzing the probability of a flammable region (cloud) emerging from a refrigerant leak and the probability of the refrigerant leak encountering an ignition source. The probability that the flammable region encounters an ignition

source is higher when using R290 than when using R32, and if a rapid R290 refrigerant leak occurs, it is thought that this can easily become the cause of a fire accident. This is due to the fact that R290 generates a large flammable region even if the leakage amount is relatively small because its lower flammability limit (LFL) is low, and one of many electrical components found indoors, such as an electrical outlet, light switch, or electric lighter, can easily become an ignition source. Because VRF systems using R32 have a greater amount of refrigerant than do RAC systems, the flammable region is large and continues to exist for a long time. For this reason, the probability of it encountering an ignition source becomes substantial.

To lower the probability of fire accidents to below the allowable values in R290 RACs and R32 VRF systems, safety measures are necessary. Lowering the probability below approximately 1/1,000,000 in R290 RACs requires the implementation of safety measures, including refrigerant charge amount regulations, explosion proofing, and ventilation. Safety measures are necessary to reduce the probability of fire accidents to approximately 1/10 in R32 VRF systems; however,

options are not limited to regulatory control but also include official and industrial standards. Although ventilation, leak detection and warnings, and refrigerant shut-off devices have been considered as safety measures, the probability of fire accidents can be expected to fall below 1/10 by incorporating main unit safety functions.

8.4 Summary

Risk assessment was performed for VRF systems using the mildly flammable refrigerant R32, which has a low impact

Product	Residential	←	VRF
Refrigerant	R32	R290	R32
Charge [kg]	1.0	0.5	88.1
Installation site	Living room (7m ²)	←	Office (40.3m ²)
Ventilation	None	←	Off at night

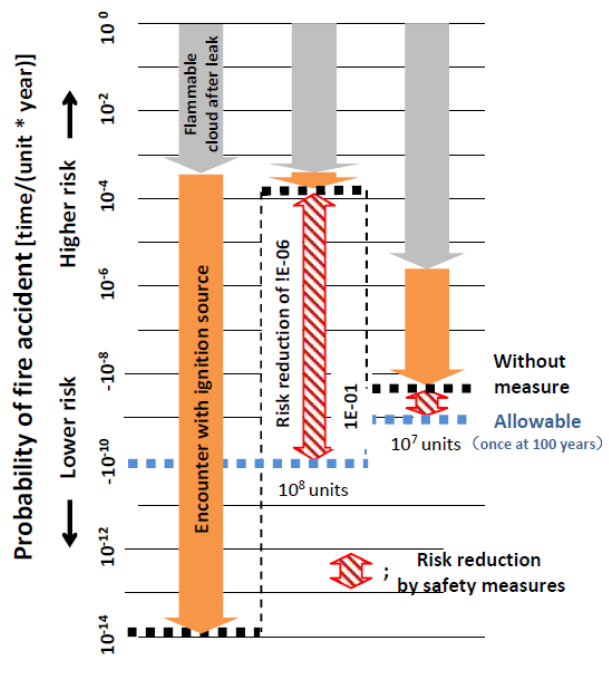


Fig. 8.1 Probability of fire accident with R290 (RAC) and R32 (RAC and VRF)

the probability of fire accidents can be expected to fall below 1/10 by incorporating main unit safety functions.

on global warming. Safety measures were proposed for stages during indoor and outdoor operations, installation, repair, and disposal to lower the probability of fire accidents for each installation case to 1 in 100 years, including even the most difficult cases. Furthermore, an estimate was performed for the probability of fire accidents occurring during use in the market overall, and it was clarified that the incidence of a fire accident can be lowered to 1 in 100 years by incorporating main unit safety measures.

From this point forward, it is desirable to gather these safety requirements as technical standards and establish industrial safety measures that are incorporated as functions of the main unit instead of regulations, such as prior application at the time of installation.

9. Risk Assessment of Chillers

9.1 Introduction

Heat source systems supplying hot or cold water to central air conditioning systems use R410A or R134a hydrofluorocarbon refrigerants. Both refrigerants have a GWP exceeding 1000 and thus could contribute to climate change. Therefore, it is necessary to ultimately replace them with low-GWP alternatives. R1234yf, R1234ze(E), R32, and mixtures thereof have been evaluated in drop-in, retrofit, and performance tests. All of these low-GWP refrigerants are mildly flammable. Risk assessments for burn injury and fires in chiller systems using these mildly flammable refrigerants have been undertaken since the 2011 FY. The scope of this study includes air-cooled heat pumps installed outdoors and water-cooled chillers installed in machine rooms and used as a central air conditioning heat source with a cooling capacity ranging from 7.5 to 175,000 kW. This year, the chiller sub-working group (chiller SWG) executed (a) a risk quantification based on the results of a refrigerant leak analysis conducted jointly by the University of Tokyo and the chiller SWG, reviewing the probability of ignition and the associated risk, (b) RAs based on the requirements for chiller design and the conditions of the facilities that incorporate the measures and the actions, (c) the drafting of JRAIA guidelines (GLs) for the generalization of technical requirements.

9.2 Risk Assessment Procedure

Risk assessments are executed according to the following procedure, which follows the basic risk assessment flow.

- (1) The basic specifications of the chiller of an RA are defined according to its application, cooling capacity, structure, and installation location.
- (2) The life cycle of the chiller is separated into six life stages (LSs), from the logistics stage to the disposal stage, and the risks associated with each stage are then analyzed.
- (3) The relationships between probable ignition sources and the cases of refrigerant leakage are clarified using the FTA method, and then the probability of the occurrence of burns and fire accidents is calculated by considering the ignition source density, leak probability, and the flammable space volume integrated with respect to the time of the leak. Because each accident or case is an independent event, the combined probability of each case indicates the annual probability of the occurrence of accidents per unit.
- (4) Safety requirements for the chiller and the facility are established to reduce high-risk hazards, and then GLs for their technical requirements are drawn up.

9.3 List of Risk Assessment Conditions

For the current calculation of the risk of burn injury and fire accidents, the time-dependent volume of the flammable space for a burst and rapid leak was calculated along with the probability of the presence of each ignition source during that time. The calculation conditions are defined as follows, and it is assumed that each of the six LSs has different ignition sources.

- (1) Four pieces of equipment that comprise the heat-source system are installed, and the startup/shutdown cycles of adjacent pieces of equipment are considered.
- (2) The ventilation of the equipment is to be $(2 \text{ air changes/h}) \times (2 \text{ lines}) = 4 \text{ air changes/h}$, and the failure rate of the duct fan is estimated to be $2.5 \times 10^{-4}/(\text{unit}\cdot\text{year})$.

- (3) The probability that the equipment is not ventilated at all is 1%, and at the LSs of the installation and disposal it is assumed to be 50%.
- (4) For each LS, logistics and disposal without the direct contact of a user are excluded from the probability of accidents while the values are specified.
- (5) The probability of the existence of a flammable space when there is no ventilation is defined as same as the probability of refrigerant leakage.
- (6) When the machine room is ventilated, the probability of a small leak existing is 0 because the existence of a flammable space is not considered.
- (7) The probability of the existence of a flammable space is given as the time-dependent volume of the flammable space [m³ min]/(target space [m³] × 8760 h × 60 min). The target space of an air-cooled heat pump is defined as the area surrounded by soundproof walls.
- (8) Ignition sources are assumed to exist throughout the flammable space, including the floor surface. For example, the existence of a lighter flame at the ground level is not excluded.
- (9) The time-dependent volume of R1234ze(E) is applied for a water-cooled chiller, and R32 is applied for an air-cooled heat pump.

9.4 Probability of Fire Accidents

The probabilities of fire accidents for each LS in the case of chillers both with and without countermeasures are listed in Table 9.1. A previously measured value describes the risk with no ventilation and shows the probability of a fire accident based on the existence of an ignition source, the occurrence of low-flammability gas leaks, and whether the concentration of the refrigerant is within the flammable range. During the LSs under the management of a user, the probability of bursts, rapid leaks, and slow leaks are summed to yield 1.32×10^{-4} accident/(unit·year), which is larger than the actual value. For example, if the machine room is narrow and without ventilation at 1% of constituent ratio, the probability is 1.32×10^{-6} accident/(unit·year), which is not acceptable. The probability of a fire accident when countermeasures have been taken is calculated from the probability of the flammable space for a standard chiller model with ventilation and a standard machine room. The probability during the LSs under the management of a user is 3.90×10^{-12} accident/(unit·year), which is evaluated as being “improbable.”

Table 9.1 Probability of fire accidents

	LS	LS ratio	Without ventilation [1/(unit·year)]		With ventilation [1/(unit·year)]	
			LS	LS under user's management	LS	LS under user's management
Suppliers	Logistics	0.0517	4.28×10^{-6}	-	1.51×10^{-13}	-
Operator	Installation [carry-in]	0.0517	4.67×10^{-6}	1.32×10^{-4}	2.40×10^{-12}	3.90×10^{-12}
	Installation [trial]	(0.0023)				
	Usage [machine room]	0.2144	6.19×10^{-5}			
	Usage [outdoor]	0.5002				
	Repair	0.1207	6.52×10^{-5}			
	Overhaul	0.0098				
Suppliers	Disposal	0.0517	1.72×10^{-5}	-	9.23×10^{-12}	-

9.5 Technical Requirements for Safety

This section describes the safety requirements and compares them with KHKS0302-3, ISO5149-3 (2014), and the Japanese domestic legal standards and requirements for the reference of this risk assessment.

- (1) Ventilation of machine room: Mechanical ventilation must be required at all times. The baseline air change rate for a machine room should be 2–4 air changes/h, depending on the size of the machine room. The ventilation system should consist of two lines. The exhaust port should be installed close to the floor where the refrigerant tends to settle, such that it can be discharged directly through a duct. Ventilation equipment should be operable from outside the machine room.
- (2) Refrigerant detector and refrigerant leakage alarm: One or more instruments that can detect refrigerants and have a sensor at an undisturbed position should be installed. The sensor should be positioned where the refrigerant will tend

to collect. The refrigerant detector and refrigerant leakage alarm should operate using an independent power supply, such as an uninterruptable power supply (UPS). The instrument is to be linked to an alarm (e.g., both audible and visible) that is noticeable from outside a machine room.

- (3) Prohibition of open flame: Any apparatus with an open flame (e.g., heating apparatus, water heater, or stove) should be prohibited in a machine room.
- (4) Smoking and other uses of fire should be strictly prohibited.
- (5) Inspection: The machine ventilation, refrigerant detector, refrigerant leak alarm, and UPS should be periodically inspected during installation, and the air change rate should be as recommended by the manufacturer; all inspection records should be stored.
- (6) Instrument protection: The normal operation of the refrigerant detector and the mechanical ventilation of the machine room should be configured to be interlocked with the startup of the chiller.

9.6 Conclusions

The risk assessments performed by the chiller SWG confirmed that the frequency of fire accidents and burns was sufficiently low for water-cooled chillers and heat pumps using low-flammability refrigerants when considering the probabilities of refrigerant leakage and the existence of ignition sources. In addition, it was confirmed that the probability of an accident occurring was smaller than once every 100 years in the machine room with appropriate machine ventilation (2–4 air changes/h with two ventilation lines). The general safety requirements determined through the risk assessments are: (1) Guarantee mechanical ventilation with the required air flow rate in a machine room, (2) Monitor the refrigerant leakage using at least one refrigerant detector, (3) Interlock the chiller with the refrigerant detector and the mechanical ventilation system, and (4) Guarantee the refrigerant detector and the refrigerant leakage alarm device run on an independent power supply, such as a UPS. Furthermore, a draft of the GLs for the chilling equipment based on these technical requirements has been drawn up. In the next FY, the SWG will work towards the development of GLs and a general overview of risk assessments.

10. Thermophysical Properties and Cycle Performance of Newly Developed Low-Global Warming Potential Refrigerants

In the present study, the measurement of the thermodynamic properties of HFO-1243zf, the proposed equation of state for HFO-1243zf, measurements of the surface tension of some low-GWP refrigerants, measurements of the transport properties of HFO-1234ze(Z), and the cycle performance test for the binary refrigerants mixture of HFO-32 and HFO-1234yf were performed. The obtained results are as follows.

- (1) The pressure–density–temperature ($P\rho T$) properties, vapor pressures, and saturated liquid and vapor densities of HFO-1243zf were measured using two types of isochoric methods. Then, the critical temperature T_c and the critical density ρ_c were determined from the present measured data. The critical pressure P_c and the saturated vapor pressure correlation were also determined for HFO-1243zf.
- (2) A fundamental equation of state explicit in the Helmholtz energy was formulated for R1243zf using the critical parameters and saturated liquid and vapor densities obtained in the present study. It was confirmed that the thermodynamic properties predicted by the formulated equation of state agree with the existing experimental data. An FLD file for REFPROP based on the equation of state was also provided.
- (3) The surface tensions of HFO-1243zf, HFO-1234ze(Z), and HCFO-1233zd(E) were measured using the capillary elevation method. Then, empirical correlations of the van der Waals type were proposed.
- (4) The thermal conductivity of HFO-1234ze(Z) was measured using a transient hot-wire technique with two fine wires of different lengths for HFO-1234ze(Z) both in the saturated liquid and superheated vapor states in the temperature range of 280–350 K. The extended corresponding model to predict the thermal conductivity of HFO-1234ze(Z) was also developed based on the present study. It was confirmed that there was good agreement between the measured and predicted values.

- (5) The viscosity thermal conductivity of HFO-1234ze(Z) was measured using the tandem capillary tubes method based on Hagen–Poiseuille theory in both the subcooled liquid and superheated vapor states. The extended corresponding model for predicting the viscosity of HFO-1234ze(Z) was also developed based on the present study. The predictions of the extended corresponding model were in good agreement with the experimental data.
- (6) In the present study, the cycle performances of several refrigerants were evaluated using a water source heat pump loop. This year, binary zeotropic mixtures of HFC-32 and HFO-1234yf (42/58 mass% and 28/72 mass%) were tested. The cycle performance of the refrigerant mixtures of HFC-32 and HFO-1234yf (42/58 mass% and 28/72 mass%) was compared to that of HFC-32 and HFO-1234ze(E) mixtures (42/58 mass% and 28/72 mass%) and R410A. It was found that the coefficients of performance (COPs) of the HFC-32/HFO-1234ze(E) and HFC-32/HFO-1234yf mixtures were almost comparable when their compositions yielded the same GWP. For the compositions that yielded a GWP of 300, the COPs of these mixtures exceeded that of R410A.

1. Introduction

The use of chlorofluorocarbons (CFCs) and hydrochlorofluorocarbons (HCFCs) is severely restricted and, in an effort to protect the ozone layer, they are being replaced with hydrofluorocarbons (HFCs). However, leakage of this refrigerant into the air from active or end-of-life air conditioners is a serious environmental issue owing to its high global warming potential (GWP). Thus, it is now universally acknowledged that replacing HFCs with lower-GWP refrigerants is essential to rectifying this problem. The main types of air-conditioning equipment produced in Japan are room, package, and mobile air conditioners, with respective totals of 90.1 million, 0.8 million, and 5 million being exported in 2013. The potential for replacement of the conventional refrigerant in mobile air conditioners with the low-GWP refrigerant R1234yf is very high. Further, studies have been conducted over the past several years on the use of lower-GWP refrigerants for stationary air conditioners. Additionally, in recognition of the urgent need to reduce global warming, regulations have been imposed in Japan and overseas regarding the use of high-GWP refrigerants such as HFCs.

1.1 Trends in Refrigerant Regulation

The EU protocol 2006/40/EC for mobile air-conditioning refrigerants, effective from January 1, 2011, prohibits the release of late-model cars using refrigerants with a GWP over 150. Furthermore, starting January 1, 2017, it will prohibit the release of any new car using such refrigerants. In 2009, the automobile industry decided to replace the conventional refrigerant, R134a, with the low-GWP refrigerant, R1234yf. However, in April 2012, the EU Commission temporarily permitted the continued use of R134a owing to a supply shortage of R1234yf. The sale of late-model cars using refrigerants with a GWP over 150 has been prohibited since January 1, 2013.

The regulation regarding the use of stationary air conditioners is known as F-gas Regulation (EC) No. 842/2006. The present regulation focuses on reducing refrigerant leakage from air conditioners and requires proper management, instructional courses for operators, labeling of equipment containing F-gas, and reports by producers, importers, and exporters of F-gas. In January 2015, the EU enhanced the existing regulations (see Table 1.1.1). The new amendment aims to reduce the leakage of F-gas to two-thirds of the present level and prohibits the release of equipment using F-gas in fields where an environmentally friendly refrigerant has been developed. To achieve this, a phase-down schedule has been determined that stipulates that the annual amount of HFCs sold in the EU be reduced to one-fifth by 2030. Consequently, refrigeration and air-conditioning equipment manufacturers who plan to sell products containing refrigerants from factories in out of the EU areas will have to get quotas of refrigerants after January 2017. The equipment with high-GWP refrigerant on which selling restrictions have been placed are listed in Table 1.1.2. F-gases with GWPs above 2500 will be banned in stationary refrigeration systems from 2020, and those with GWPs above 750 will be banned in stationary air conditioners from 2022.

At the Conference of Parties, which was held with the aim of abolishing practices that damage the ozone layer, three North American countries (US, Canada, and Mexico) submitted a proposal to revise the Montreal Protocol to restrict the production and sale of HFCs. However, HFCs do not damage the ozone layer. The global warming issue was caused by the replacement of prohibited CFCs and HCFCs, which damage the ozone layer, with HFCs, which have high GWPs. The proposal suggests restricting the distribution of HFCs in the framework of the Montreal Protocol. Table 1.1.1 and Fig. 1.1.1 compare the proposals and schedules of the three North American countries with the EU regulation.

Table 1.1.1 Summary of proposed and effective HFC regulations

	Proposal by three North American countries	EU regulation
Date of proposal or effect	Twenty-sixth meeting of the High Contracting Parties, November 2014	December 2013
Evidential law	Montreal Protocol	Amendment of Regulation (EC) No. 842/2006
Target refrigerants	Nineteen types of HFCs (R1234yf and R1234ze not included)	HFCs (R1234yf and R1234ze not included)
Baselines of HFC phase-down	Developed countries: HFCs and 85% of HCFCs (average value between 2008 and 2012) Developing countries: HFCs and 90% of HCFCs (average value between 2011 and 2012)	Average value between 2009 and 2012
Final values of HFC phase-down	Developed countries: 15% of the baseline in 2035 Developing countries: 15% of the baseline in 2045	Twenty-one percent (21%) of the baseline in 2030
Other restrictions		(1) Single split air-conditioning systems containing less than 3 kg of fluorinated greenhouse gases with a GWP of 750 or more shall be prohibited from January 1, 2025. (2) The use of fluorinated greenhouse gases with a GWP of 2500 or more to service or maintain refrigeration equipment with a charge size of 40 tons of CO ₂ equivalent or more shall be prohibited from January 1, 2020. (3) From January 1, 2017 refrigeration, air-conditioning, and heat pump equipment charged with HFCs shall not be permitted on the market unless the HFCs charged into this equipment are accounted for within the quota system.

Table 1.1.2 Market prohibitions

Products and equipment	Date of prohibition
Domestic refrigerators and freezers that contain HFCs with GWP of 150 or more	January 1, 2015
Refrigerators and freezers for commercial use (hermetically sealed equipment) that contain HFCs with GWP of 2500 or more	January 1, 2020
Refrigerators and freezers for commercial use (hermetically sealed equipment) that contain HFCs with GWP of 150 or more	January 1, 2022
Stationary refrigeration equipment, that contains, or whose functioning relies upon, HFCs with GWP of 2500 or more, except equipment intended for application designed to cool products to temperatures below -50 °C	January 1, 2020
Multipack centralized refrigeration systems for commercial use with a rated capacity of 40 kW or more that contain, or whose functioning relies upon, fluorinated greenhouse gases with GWP of 150 or more	January 1, 2022
Movable room air-conditioning equipment (hermetically sealed equipment that is movable between rooms by the end user) that contain HFCs with GWP of 150 or more	January 1, 2020
Single split air-conditioning systems containing less than 3 kg of fluorinated greenhouse gases, that contain, or whose functioning relies upon, fluorinated greenhouse gases with GWP of 750 or more	January 1, 2025

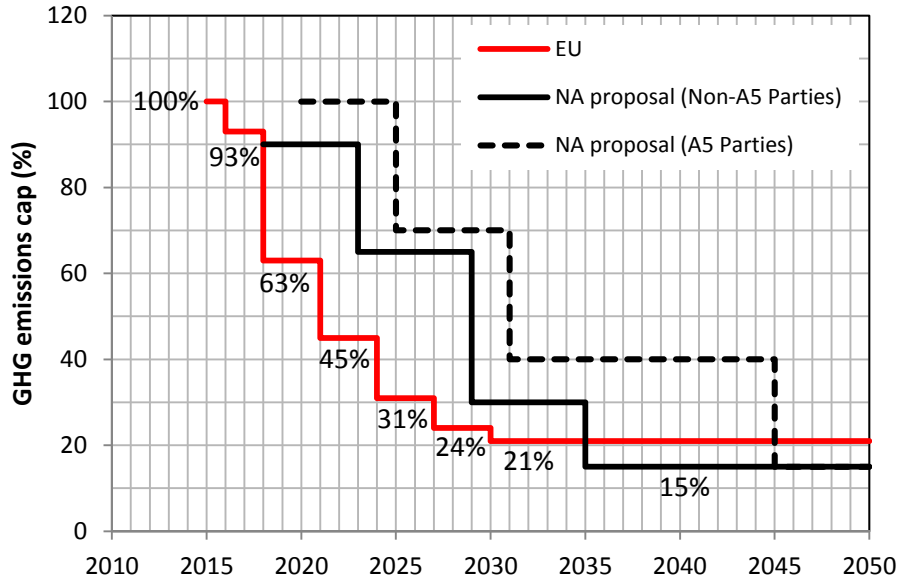


Fig. 1.1.1 Proposed HFC reduction stages

In Japan, the Global Environment Sub-Committee of the Central Environment Council and the Chemical and Biotechnology Sub-Committee of the Industrial Structure Council jointly created a task force and compiled an outline for the regulation of HFCs. The document released by the task force indicated that if no additional measures are taken, the emission of HFCs will double by 2020, with 80% of total HFC emissions coming from the air-conditioning sector. It highlighted the importance of integrating appropriate measures in the air-conditioning sector. Approximately 60% of leakages in the air-conditioning sector occur during operation; the remainder is from uncollected refrigerant from end-of-life equipment. Approximately 40% of all leakage during operation is from separate-type display cases. Conventionally, it is believed that the most important alleviatory measure is recovery of refrigerants from end-of-life refrigerators and air conditioners. However, this is inadequate.

On the basis of these discussions, the “Law on regulation of management and rational use of fluorocarbons” was established by the National Parliament on June 5, 2013, and took effect in April 2015. The name of the law was changed from the “Law for ensuring the implementation of the recovery and destruction of fluorocarbons concerning specific products.” The new law requires the replacement of high-GWP HFCs, refrigerant management and refrigerant recovery to reduce leakage of HFCs, and the following measures:

- (1) Fluorocarbon manufacturers should reduce their environmental impact through technology development and manufacturing of lower-GWP refrigerants.
- (2) Refrigeration and air-conditioning equipment manufacturers should achieve the goal of replacing high-GWP refrigerants with low-GWP refrigerants by the target year for each product sector. See Table 1.1.3.
- (3) For users of commercial refrigeration and air-conditioning equipment, proper management, installation, inspection, and repair is required.
- (4) For collection and destruction traders, a registration system for entities charging fluorocarbons for commercial refrigeration and air-conditioning equipment will be introduced, and a permit system for recovery of fluorocarbons will also be introduced.

Table 1.1.3 GWP cap and target year

Designated products and equipment	Currently used refrigerants and their GWP	GWP cap	Target year
Room air conditioner	R410A (2090), R32 (675)	750	2018
Commercial air conditioner	R410A (2090)	750	2020
Automobile air conditioner	R134a (1430)	150	2023
Condensing units and stationery freezing and refrigerating units	R404A (3920), R410A (2090), R407C (1774), CO2 (1)	1500	2025
Central freezing and refrigerating equipment	R404A (3920), Ammonia (<1)	100	2019
Rigid urethane foam insulation	R245fa (1030), R365mfc (795)	100	2020
Aerosol filled only with propellant	R134a (1430), R152a (124), CO2 (1), DME (1)	10	2019

1.2 Research trends on the Safety of Mildly Flammable Refrigerants

The development of environmentally friendly refrigerants for room and package air conditioners is imperative for the growth of air-conditioning technology. The low-GWP refrigerants R1234yf and R32 are promising candidates to replace conventional HFC refrigerants. However, these refrigerants are not very stable in air and are flammable. Therefore, it is essential to collect basic data about the flammability of low-GWP refrigerants and research their safety for practical use. The integration of basic information about refrigerant physical properties, cycle performance, life cycle climate performance (LCCP), flammability, and risk assessment will simplify their selection for practical use. These efforts are expected to contribute to the advancement of the global air-conditioning industry.

R1234yf and R32 are less flammable than propane and R152, and are therefore classified as mildly flammable refrigerants. In ASHRAE Standard 34, rank 2L was established for mildly flammable refrigerants with burning heats lower than 19 MJ/kg and burning velocities lower than 10 cm/s. Together with ammonia, R1234yf and R32 are classified as 2L. As illustrated in Fig. 1.2.1, the following conditions must be satisfied by an ignitable refrigerant that leaks from an appliance near an ignition source:

- (1) The refrigerant concentration must be within the required flammability range.
- (2) The energy of the ignition source must be higher than the MIE.
- (3) The air velocity adjacent to the ignition source must be lower than the BV.

If the air velocity adjacent to the ignition source is higher than the BV, burning will not occur because fire cannot propagate against the airflow.

Rank 2L on ASHRAE Standard 34 changed the restriction on refrigerants regarding their flammability and allows for the practical use of low-flammability refrigerants. However, in Japan, only the classifications “non-flammable” and “flammable” are recognized in the High Pressure Gas Safety Act and the Ordinance on the Security of Safety at Refrigeration. With the objective of gathering essential data for risk assessment of mildly flammable refrigerants, safety studies are being conducted by project teams from the Tokyo University of Science at Suwa, Kyushu University, University of Tokyo, and the National Institute of Advanced Industrial Science and Technology. Since 2011, they have been sponsored by the project “Development on Highly Efficient and Non-Freon Air Conditioning Systems” of the New Energy and Industrial Technology Development Organization (NEDO).

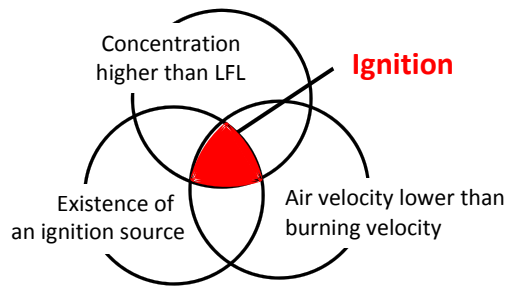


Fig. 1.2.1 Ignition mechanism

In addition, a research committee was organized by the Japan Society of Refrigerating and Air Conditioning Engineers to assess the risks associated with mildly flammable refrigerants. The Japan Refrigerating and Air Conditioning Industry Association and the Japan Automobile Manufacturers Association are presently undertaking risk assessments and the results are being discussed by the research committee. The 2014 activities of the committee to assess the risks associated with mildly flammable refrigerants are compiled in this report. The committee members would be pleased if this report proved helpful to persons working in associated fields.

References

- European Parliament, Directive 2006/40/EC of the European Parliament, May 17, 2006.
- European Parliament, Regulation (EC) No 842/2006 of the European Parliament, May 17, 2006.
- European Parliament, Regulation (EC) No 517/2014 of the European Parliament and of the Council, April 16, 2014.
- US Environmental Protection Agency, Summary: 2014 North American Amendment Proposal to Address HFCs under the Montreal Protocol, EPA, US, 2014.

2. Fundamental Flammability

2.1 Introduction

Because high-GWP compounds are stable in the atmosphere, less stable compounds are now being considered as lower-GWP alternatives. The properties that make these new compounds more reactive in the atmosphere also make them more flammable. Considering this tradeoff in risks, low-GWP compounds with mild flammability appear to provide the optimum balance of acceptable safety properties and environmental performance. Thus, risk assessments need to be performed on mildly flammable compounds before they are used in practical applications. (Hereafter, a compound with a maximum burning velocity of $S_{u, \max} \leq 10 \text{ cm s}^{-1}$ is called “mildly flammable” or “2L” compound).

According to ISO/IEC Guide 51 “Safety aspects: Guidelines for their inclusion in standards”, risk is defined as the “combination of the probability of occurrence of harm and the severity of that harm.” When assessing the risk of flammable refrigerants, we should consider the combination of the probability of fire occurring because of leakage of the refrigerant and the severity of that fire hazard. Accordingly, it is important to collect a set of such indices that appropriately expresses this risk.

In order to consider both the probability of potential fire incidents and the severity of fire hazards, ISO 817 (2014) uses the lower flammability limit (LFL), heat of combustion (H_c), and burning velocity ($S_{u, \max}$) to classify the flammability of refrigerants into four classes, which are summarized in Table 2.1.1. These properties must be evaluated in order to realize the use of new refrigerants in practical applications. ANSI/ASHRAE Standard 34 and ISO 817 recently introduced the new 2L flammability class to distinguish the lowest flammability class from the other flammability classes. ISO 5149 (2014) and IEC 60335-2-40 are considering relaxing restrictions on the use of the 2L refrigerants under the premise that the fire hazards caused by 2L refrigerants should be very low in both probability and severity.

According to ANSI/ASHRAE Standard 15 (2013), there shall be no hot surface over 427 °C permanently installed in a refrigerating machinery room. Thus, it is also important to understand the refrigerant’s thermal decomposition and thermal ignition on a hot surface.

Based on the above observations, if we are to export and import refrigerating systems using 2L refrigerants, correct evaluation of the fundamental flammability properties given above is a basic requirement.

On the other hand, in order to establish reliable risk assessments under practical conditions, performing risk assessments based on the flammability properties under unrealistic conditions is unhelpful and may actually be harmful. Instead, we should carry out risk assessments by considering the parameters that cover the worst case under practical conditions. From this viewpoint, the effect of humidity on flammability and thermal decomposition was within the scope of this research project.

Table 2.1.1: Refrigerant flammability classification in ISO 817 (2014) and representative refrigerants

Flammability class	Definition	Representative refrigerant
Class 3 (Higher flammability)	$LFL \leq 3.5 \text{ vol\%}$ or $H_c \geq 19,000 \text{ kJ kg}^{-1}$	R290, R600a
Class 2 (Flammable)	$LFL > 3.5 \text{ vol\%}$ and $H_c < 19,000 \text{ kJ kg}^{-1}$	R152a
Class 2L (Lower flammability)	In class 2, $S_{u, \max} \leq 10 \text{ cm s}^{-1}$	R717, R32 R1234yf, R1234ze(E)
Class 1 (No flame propagation)	No flame propagation at 60 °C	R134a, R410A, R22

In this progress report, we first present an interim report on these fundamental flammability properties of 2L refrigerants. A detailed practical risk assessment is presented in the following chapters.

As described previously, refrigerants are classified on the basis of the LFL, H_c , and $S_{u,max}$. In Section 2.2, we report on the measured flammability limits for 2L and 1 refrigerants, including the humidity issue. In Section 2.3, the burning velocity measurements for HFO-1234ze(Z) are reported.

To judge whether a refrigerant is flammable or not in practice, information is needed on the ignition energy of the refrigerant and the ignition source in the surrounding environment. Section 2.4 presents an evaluation of the ignition energy and quenching distance, including the dependence on concentration.

In this research project, an index called the extinction diameter was newly introduced to evaluate the flammability characteristics of 2L refrigerants. This index is expected to be used for judging whether or not an enclosure of electrical parts with openings such as a magnetic contactor and socket can become an ignition source for refrigerants. In Section 2.5, we add new data and discuss the extinction diameter.

Section 2.6 is on the thermal decomposition of refrigerants, and 2L refrigerants and typical non-flammable refrigerants are compared. As described earlier, the use of flammable refrigerants near a hot surface with a temperature of over 427 °C is forbidden in some applications. Thus, information on the onset of thermal decomposition is important. In addition, from the viewpoint of toxicity, knowing the toxicity level and concentration of thermal decomposition products and whether there is a significant difference between 2L and existing non-flammable refrigerants is of significant importance. Table 2.1.2 lists flammability characteristics obtained in this study. The values in the ISO 817 (2014) are also listed. The fundamental flammability data used in this report are basically quoted from this table.

Figure 2.1.1 illustrates an example comparison between the fundamental flammabilities of class 2L refrigerants (R32 and R1234yf) and a class 3 refrigerant (R290). Most of the data were obtained in this project. In this figure, the numbers 1, 2, and 3 are indices representing the flammability classification in ISO 817(2014). The numbers 1, 4, and 5 are indices relevant to the probability of fire, and the numbers 2 and 3 are indices that represent the severity of fire. The figure quantitatively demonstrates the following points:

- 2L refrigerants have significantly lower H_c and $S_{u,max}$ than R290 and exhibit weak flame propagation if they burn.
- 2L refrigerants have a higher LFL than R290, which indicates the lower probability for the occurrence of fire.
- 2L refrigerants have an E_{min} that is more than an order of magnitude greater than that of R290. Igniting them with a spark generated from the static electricity of a human body (approximately 10 mJ) is very difficult.
- 2L refrigerants have a quenching distance that is more than three times greater than that of R290. Thus, when a spark is generated between a pair of electrodes, the gap between them is often within the quenching distance of 2L refrigerants. In this case, a spark energy much greater than E_{min} is required to overcome the quenching effect of the electrode material.

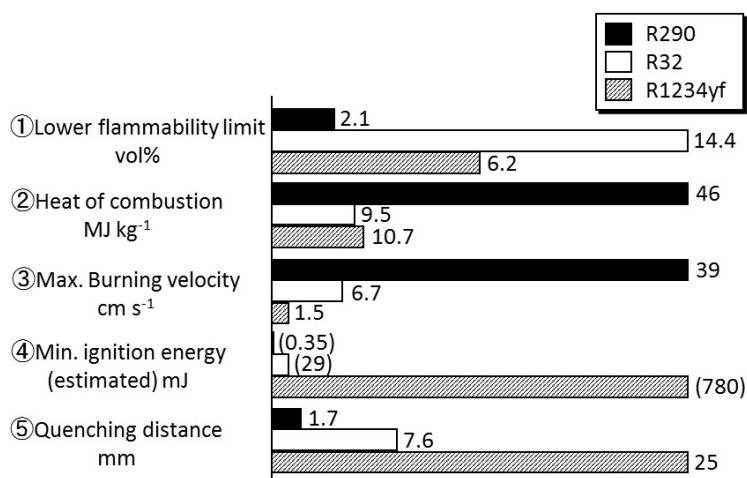


Figure 2.1.1: Comparison between flammability characteristics of 2L and 3 refrigerants

Table 2.1.2: Flammability characteristics of typical refrigerants

Compound	Chemical formula	C_{st} vol%	ISO817 (2014)			This work											
			$S_{u0,max}$ cm s ⁻¹	LFL vol%	H_c MJ kg ⁻¹	$S_{u0,max}$ cm s ⁻¹	Flammability limits ^a , vol%				H_c MJ kg ⁻¹	E_{min} mJ estimated	d_q mm				
							23 °C, 50%RH		35 °C, 0%RH					35 °C, 50%RH corrected for 23 °C		60 °C, 50%RH	
							LFL	UFL	LFL	UFL				LFL	UFL	LFL	UFL
R290	C ₃ H ₈	4.02	46 ^b	2.1	46.3	38.7 ^c	2.02 ^d	9.81 ^d	---	---	---	---	0.35 ^e	1.70 ^e			
R152a	CH ₃ CHF ₂	7.73	23	4.8	16.3	23.6 ^c	4.3 ^f	17.3 ^f	---	---	4.36 ^f	14.8 ^f	0.90 ^e	2.33 ^e			
HFC-254fb	CH ₂ FCH ₂ CF ₃	6.53	---	---	---	9.5 ^e	4.3 ^g	14.5 ^g	---	---	---	---	11.4	12 ^e	5.23 ^e		
R143a	CH ₃ CF ₃	9.48	7.1	8.2	10.3	ISO	7.3 ^h	17.9 ^h	7.3 ^f	17.7 ^f	7.4 ^f	15.0 ^f	27 ^e	7.03 ^e			
R32	CH ₂ F ₂	17.3	6.7	14.4	9.5	ISO	13.5 ^h	28.0 ^h	13.5 ^f	26.9 ^f	13.5 ^f	23.6 ^f	29 ^e	7.55 ^e			
R717	R717	21.8	7.2	16.7	18.6	ISO	15.3 ^h	30.4 ^h	15.8 ^f	29.2 ^f	18.0 ^f	24.5 ^f	45 ^e	8.95 ^e			
R1234yf	CH ₂ =CF ₂ CF ₃	7.73	1.5	6.2	10.7	ISO	6.7 ^h	12.0 ^h	5.4 ^h	13.5 ^h	4.8 ^f	15.0 ^f	780 ^e	24.8 ^e			
R1234ze(E)	(Z)-CHF=CHCF ₃	7.73	1.2	6.5	10.1	ISO	n.f.	n.f.	5.95 ^h	12.7 ^h	5.05 ^f	15.5 ^f	n.a.	n.a.			

$S_{u0,max}$: maximum burning velocity at 25 °C and 0%RH (relative humidity); LFL: lower flammability limit; UFL: upper flammability limit, H_c : heat of combustion at 25 °C and 0%RH; E_{min} : minimum ignition energy at 25 °C and 0%RH; d_q : quenching distance at 25 °C and 0%RH.

n.f.: nonflammable.

n.a.: not applicable because this compound is nonflammable under the test conditions.

^a Experiments were done by the ASTM E681 (2004) method, unless otherwise specified.

^b NFPA 68-2000 Annex C (informative), which quotes the highest $S_{u0,max}$ value in NACA report 1300 (1959), which was measured not in accordance with ISO 817 but done by the Bunsen burner method. The other $S_{u0,max}$ values were determined in accordance with ISO 817 (2014).

^c Takizawa et al. (2005).

^d Kondo et al. (2011). The test method is similar to but not exactly the same as ASTM E681 method.

^e Takizawa et al. (2015).

^f Kondo et al. (2014).

^g Kondo et al. (2006). The test method is similar to but not exactly the same as ASTM E681 method.

^h Kondo et al. (2012).

2.2 Effect of Humidity on Flammability Limits of Refrigerants

Many of the alternative refrigerants are multi-fluorinated compounds. In addition, some of them contain more fluorine atoms than hydrogen atoms. Such compounds usually have wider flammable ranges in moist air than in dry air. Knowing how the humidity affects the flammability of such compounds and others is important. In this context, a question arises as to what happens when a non-flammable compound having more fluorine atoms than hydrogen atoms is subjected to high humidity conditions.

In this study, the flammability limits were measured with the ASHRAE method (ASHRAE 34, 2013). The explosion vessel was a 12-l spherical glass flask, and the vessel flange was held on top by spring-loaded clamps. The flask was placed in a temperature-controlled air bath. In order to adjust the humidity condition of the air, pure water was injected into the vessel with a syringe. Two kinds of syringes were used. One was a 0.2 ml full scale, and the relationship between the injected water q mL and resulting water vapor pressure p mmHg (1 mmHg = 133.32 Pa), corrected for 23 °C, is given by $p = 80.06q - 0.078$. The other was a 1.0 ml full scale, and the relationship between the injected water and water vapor pressure is given by $p = 90.90q$.

2.2.1 Effect of laboratory level humidity on flammability limits of some flammable compounds

The effect of humidity on the flammability limits was measured for R717, R32, R143a, R1234yf, and R1234ze(E). All measurements were done at 35 °C. The results showed that the flammable ranges of R717, R32, and R143a remained almost constant regardless of the humidity, although they tended to slightly decrease as the humidity increased (Figure 2.2.1).

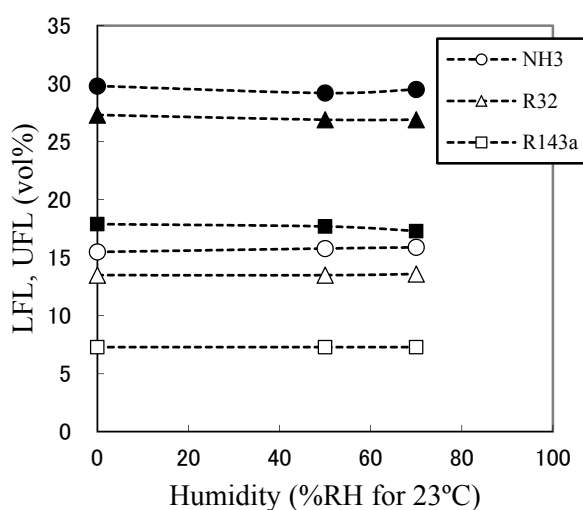


Figure 2.2.1: Effect of humidity on flammability limits of R717, R32, and R143a Measured at 35 °C. Open symbols: LFL; solid symbols: UFL.

On the other hand, the flammability limits of both R1234yf and R1234ze(E) were found to be quite sensitive to the humidity, as shown in Figure 2.2.2. Remarkably, R1234ze(E) was non-flammable in dry air but became flammable as the relative humidity was increased to 10%RH. For both compounds, increasing the humidity decreased the LFL and increased the upper flammability limit (UFL), which broadened the flammable range. The changes to the flammability limits were very steep at first and then became moderate.

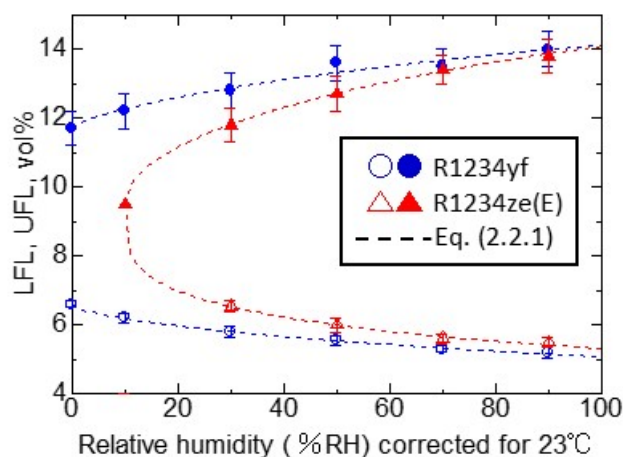


Figure 2.2.2: Effect of humidity on flammability limits of R1234yf and R1234ze(E) Measured at 35°C. Broken curves are fitting functions expressed by Eq. (2.2.1).

Because the changes in the flammability limits were very steep at first, expressing them by a simple power series function is very difficult. In this study, using an ellipse function was found to adequately express the changes:

$$y = y_0 + a [2q(x - x_0) - (x - x_0)^2]^b \quad (2.2.1)$$

Here, y is the flammability limit (vol%), and x is the relative humidity corrected for 23 °C and divided by 100. x_0 and y_0 denote the origin of the function; if the compound changes from non-flammable to flammable at a certain point, they show that border. q denotes the position of the maximum of the ellipse function; we usually used a value of 1.00. Table 2.2.1 lists the values of the parameters a and b determined for R1234yf and R1234ze(E).

Table 2.2.1: Effect of humidity on flammability limits of R1234yf and R1234ze(E) at 35 °C, where the humidity was corrected for 23 °C.

Refrigerant	Flammability limit	Origin of function		Position of maximum	Parameter	
		x_0	y_0		a	b
R1234yf	LFL	0.00	6.6	2.80	-0.600 ± 0.124	0.610 ± 0.173
	UFL	0.00	11.7	2.80	0.856 ± 0.071	0.681 ± 0.073
R1234ze(E)	LFL	0.10	9.5	2.80	-2.92 ± 0.18	0.25 ± 0.06
	UFL	0.10	9.5	2.80	2.23 ± 0.03	0.50 ± 0.07

2.2.2 Effect of high humidity on flammability properties of non-flammable refrigerants

As stated earlier, the flammability property of multi-fluorinated compounds is often strongly dependent on humidity. If it is a non-flammable compound whose molecule has more fluorine atoms than hydrogen atoms, it can become flammable under high humidity conditions. Refrigerant materials such as R410A, R410B, R134a (CH_2FCF_3), and R125 (CHF_2CF_3) are multi-fluorinated compounds and/or mixtures and are non-flammable. R410A is a 50/50 wt% mixture of R32 (CH_2F_2) and R125, and R410B is a 45/55 wt% mixture of R32 and R125. The following is the result of an investigation into whether or not the gases of R410A, R410B, R134a, and R125 become flammable under humid conditions.

Figure 2.2.3 shows the measured flammability limits. R410A became flammable when the relative humidity was higher than 19% at 60 °C. At a relative humidity of 19%, the UFL and LFL converged to 18.7 vol%. As the humidity increased,

the flammable range gradually increased and became 15.6 ± 0.2 – 21.8 ± 0.4 vol% at the relative humidity of 50%. The numbers after the plus-minus symbol are the estimation uncertainties considering the gradient and stability of the plot for the maximum flame propagation angle versus the sample concentration in air.

R410B was also found to be non-flammable at normal temperature and humidity. Figure 2.2.3 shows the effect of humidity on the flammability of R410B. R410B became flammable when the humidity was higher than 25%. The flammability limits converged to 18.6 vol% at a humidity of 25%. The flammable range gradually increased with the humidity and became 16.3 ± 0.3 – 20.9 ± 0.4 vol% at 50%.

Figure 2.2.3 also shows effect of humidity on the flammability of R134a when measured at 60 °C. R134a became flammable when the relative humidity became greater than 38% at this temperature. Under a humidity of 50%, the flammability limits became 11.5 ± 0.3 – 15.9 ± 0.4 vol%. On the other hand, both the UFL and LFL converged to 13.8 vol% at a relative humidity of 38%. Table 2.2.2 presents the results of least-squares fitting the data given in Figure 2.2.3 and Equation (2.2.1) for the three non-flammable refrigerants.

Finally, the effect of humidity on the flammability of R125 was measured up to a relative humidity of 50% at 60 °C. However, this compound remained non-flammable under this condition.

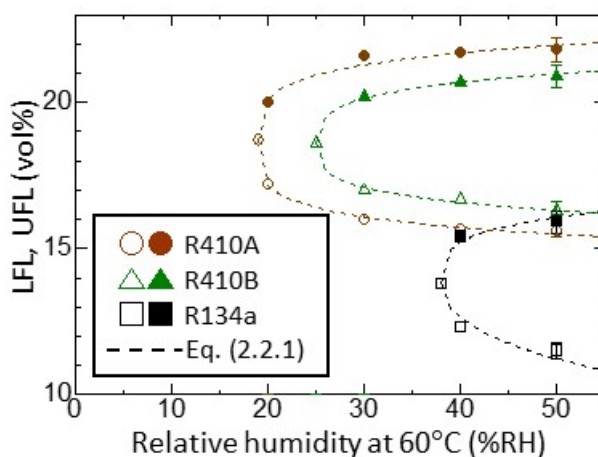


Figure 2.2.3: Effect of high humidity on flammability of non-flammable compounds. Measured at 60°C. Broken curves are fitting functions expressed by Eq. (2.2.1).

Table 2.2.2: Effect of high humidity on flammability limits of non-flammable compounds R410A, R410B, and R143a at 60 °C.

Refrigerant	Flammability limit	Origin of function		Position of maximum	Parameter	
		x_0	y_0	q	a	b
R410A	LFL	0.19	18.7	1.00	-3.70 ± 0.53	0.22 ± 0.09
	UFL	0.19	18.7	1.00	3.83 ± 0.59	0.25 ± 0.11
R410B	LFL	0.25	18.6	1.00	-2.90 ± 0.02	0.28 ± 0.11
	UFL	0.25	18.6	1.00	3.03 ± 0.02	0.29 ± 0.10
R134a	LFL	0.38	13.8	1.00	-5.04 ± 0.01	0.45 ± 0.13
	UFL	0.38	13.8	1.00	3.39 ± 0.01	0.27 ± 0.10

2.2.3 Effect of high humidity on flammability limits of mildly flammable refrigerants

The effect of high humidity on the flammability limits of mildly flammable refrigerants was examined for comparison with non-flammable refrigerants. R1234yf, R1234ze(E), R32, R143a, R152a, and R717 were measured. Table 2.2.3 summarizes the measurement results. The obtained values were compared with the ones obtained under the relatively low humidity of 50% corrected for 23 °C.

The flammable ranges of R1234yf and R1234ze(E) were found to be greatly affected by the humidity of the air. Indeed, increasing the humidity widened the flammable ranges of these compounds. Other than these two, water vapor acted as an inert gas against the other refrigerants. The flammable ranges of these compounds narrowed when the partial pressure of water vapor was increased in the air. This effect was particularly apparent on the flammability limits of R717.

Table 2.2.3: Effect of high humidity on flammability limits of some flammable compounds.

Refrigerant	35°C/50%RH for 23°C		60°C/50%RH	
	LFL, vol%	UFL, vol%	LFL, vol%	UFL, vol%
R1234ze(E)	5.95±0.15	12.7±0.4	5.05±0.1	15.5±0.7
R1234yf	5.4±0.15	13.5±0.5	4.8±0.1	15.0±0.6
R32	13.5±0.2	26.9±0.5	13.5±0.2	23.6±0.6
R717	15.8±0.4	29.2±0.4	18.0±0.7	24.5±0.5
R143a	7.3±0.15	17.7±0.5	7.4±0.1	15.0±1.0
R152a	(4.3±0.1)	(17.3±0.5)	4.36±0.05	14.8±0.5

^aNumbers in parentheses are the values measured in dry air.

2.2.4 Adiabatic flame temperatures

To understand the effect of humidity on the flammability properties of various compounds from another point of view, the adiabatic flame temperatures T_{ad} for the oxidation reactions were calculated. The chemical equilibrium was calculated for LFL and UFL mixtures of nine refrigerant materials, and the limit flame temperature (LFT) was obtained. Figure 2.2.4 show the LFT results, where the refrigerant numbers on the horizontal axis represent R410A, R410B, R134a, R1234yf, R1234ze(E), R32, R143a, R152a, and R717 in this order. The results demonstrated several points.

- (1) The LFT was always higher for the LFL than for the UFL. This may be because the chemical reactions were more complex at the UFL than at the LFL.
- (2) The LFT tended to be higher for the three non-flammable refrigerants than for the flammable refrigerants. This may be because the non-flammable compounds may require higher temperatures to chemically react than flammable compounds.
- (3) Although the flammability limits usually greatly varied between the humidity conditions of 50% at 60 °C and 50% corrected for 23 °C, the LFT did not greatly change between the two humidity conditions. Exceptions to this trend were R1234yf and R1234ze(E), for which LFT became quite low when the humidity condition was greatly increased. This may be because the extra fluorine atoms in these molecules tend to react with hydrogen atoms in the water vapor, which makes it possible for the flame to take reaction routes having lower barriers.

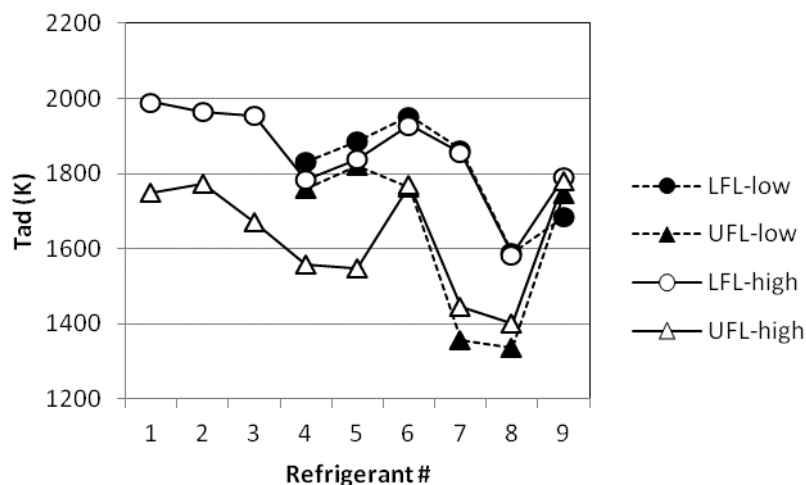


Figure 2.2.4: Adiabatic flame temperatures at flammability limits (LFTs) of various compounds

●, ▲: At flammability limits obtained at 35 °C at 50% RH corrected for 23 °C; ○, △: At flammability limits obtained at 60 °C and 50% RH. Refrigerants #1–9 on the horizontal axis represent R410A, R410B, R134a, R1234yf, R1234ze(E), R32, R143a, R152a, and R717 in this order.

2.3 Burning Velocity

The burning velocity of HFO-1234ze(Z) (*cis*-CHF=CHCF₃) was studied to elucidate the fundamental flammability properties of this new alternative low-GWP refrigerant. This compound was found to be non-flammable in dry air according to flammability limit measurements following the ASHRAE test method (ASHRAE 34, 2013). The burning velocity of HFO-1234ze(Z) was measured independently with normal gravity (1G) schlieren photography (SP) and the microgravity (μ g) spherical-vessel (SV) method.

First, we measured S_u using the 1G SP method (Takizawa et al., 2005). Because the density of gas is less when burned than unburned, buoyancy acts upon the flame. This phenomenon can clearly be observed in the case of slow-burning gases. In the early stage of combustion, the expanding flame of HFO-1234ze(Z) was nearly spherical. As the combustion proceeded, the flame propagated upwards because of buoyancy, and the flame sphere gradually became distorted to form a dimple at the bottom of the flame as a result of buoyancy-induced natural convection. When the mushroom-like flame contacted the ceiling of the combustion vessel, it was extinguished without propagating downwards. Thus, it was difficult to evaluate its burning velocity or even judge whether or not it was flammable.

Second, we used the SV method to measure the pressure–time development and obtained S_u by employing a spherical flame propagation model (Takizawa et al., 2005). The model was originally established for small hydrocarbons; we applied the model to hydrofluorocarbons. However, for mildly flammable compounds, the flame was distorted by buoyancy, which made application of the SV method very difficult. Therefore, we performed experiments in a μ g environment, where buoyancy does not work and S_u can be obtained from the spherically propagating flame without conductive heat loss to the wall.

The μ g experiments were performed using a 10-m drop tower at the AIST Hokkaido Center. This facility can achieve a gravity level of 10^{-3} G for 1.37 s, which was sufficient for our purpose. We carried out the μ g experiment using the same ignition system and recording system as in the 1G experiment. All of the power, timing, and recording systems were controlled from outside of the dropping capsule through 25-m length cables. Thus, the differences in the results were all due to the effects of gravity. All of the experimental procedures in μ g were the same as the 1G schlieren method except for the visualization of the flame front. In the μ g experiment, a direct image of the flame propagation was recorded with a high-speed video camera at a frame rate of 1000 fps, and the time profile of the flame radius was obtained by measuring

the rim of the most luminous zone of the flame front. To reduce the effects of the ignition spark and curvature (stretch) on the flame propagation, a relatively large cylindrical vessel with an inner diameter of 200 mm and volume of 6.28 L was used.

Figure 2.3.1 shows the pressure–time development together with direct images of the spherically propagating flame of HFO-1234ze(Z)/dry air in μg . As shown in this figure, the flame front was smooth and spherical except in the vicinity of the electrode, where a small dimple was formed because of conductive heat loss to the electrode. In contrast to 1G, the gas mixture in the vessel was burned completely in μg . The data in μg abstracts the intrinsic nature of flammability when not perturbed by the effect of the gravity. Unfortunately, because of the low flammability, we only observed flame propagation at 11.0, 11.5 and 12.0 vol% and at an initial pressure of 101.3 kPa or greater.

Although the measured $P(t)$ data were quite limited, $S_{u0, \max}$ was tentatively determined to be 1.9 cm s^{-1} by the μg SV method. This value is slightly higher than that of R1234yf (1.5 cm s^{-1}). However, this result does not seem reasonable because HFO-1234ze(Z) was non-flammable according to the ASHRAE flammability limit test (ASHRAE 34, 2013) in dry air, whereas R1234yf was flammable according to the same test.

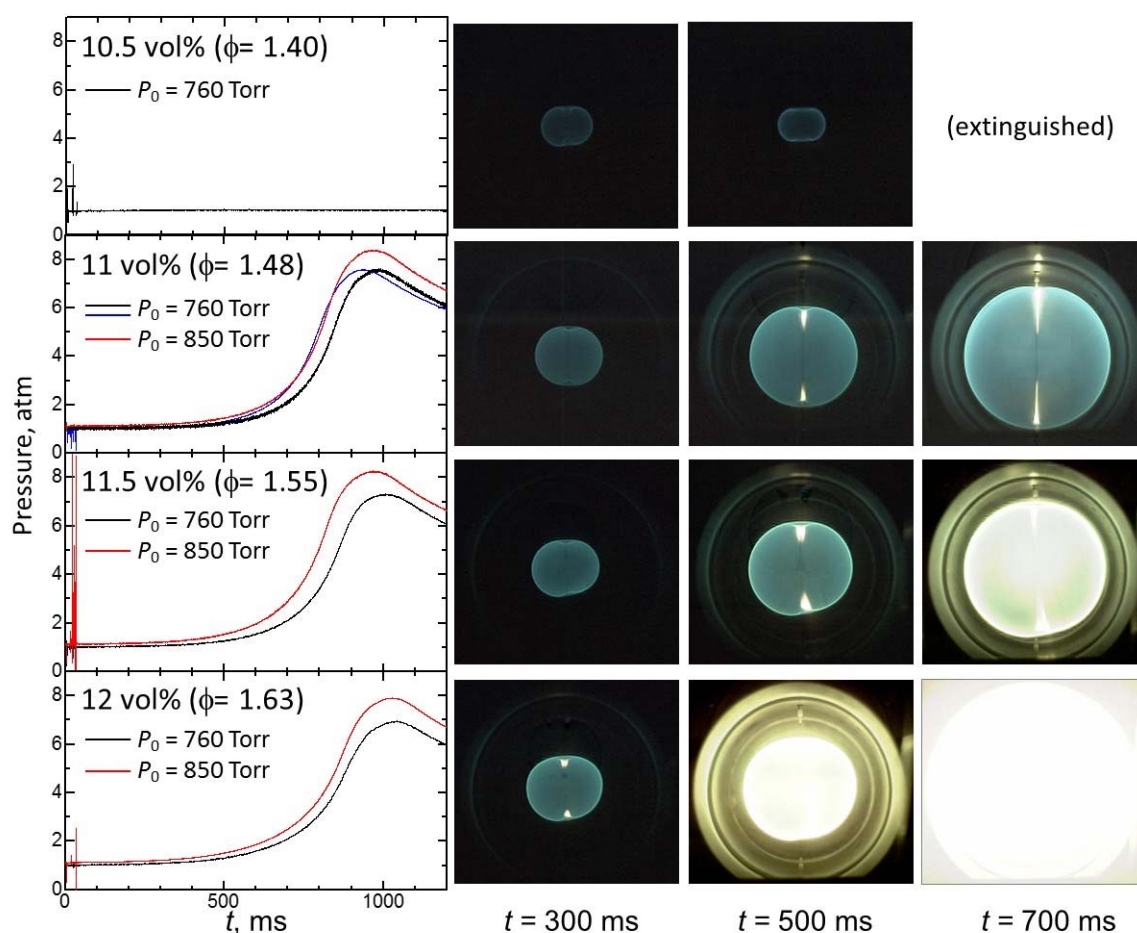


Figure 2.3.1: Flame propagation and pressure time profile of HFO-1234ze(Z)/dry air in microgravity

To confirm the above results, we first observed the combustion behavior of the R32/HFO-1234ze(Z) blend and compared the pressure rise data with R32/R1234yf and R32/R1234ze(E) blends at various mixing ratios. R32 was selected because it has a $S_{u0, \max}$ value that is slightly higher than these three R1234s, which facilitates ignition of these samples under unified ignition conditions. Also, R32 has a hydrogen-to-fluorine ratio of unity, so it would not provide either reactive or deactivating species in the reaction system.

Figure 2.3.2 shows the pressure–time profiles of R32/R1234 = 80/20, 60/40, and 40/60 vol% blends measured in μg . As shown in Figure 2.3.2(a), it was difficult to determine which of the three R32/R1234 = 80/20 blends showed the fastest pressure rise. Accordingly, we reduced the mixing ratio of R32 in the blend. As shown in Figure 2.3.2(b), the R32/R1234yf blend showed the fastest pressure rise among the R32/R1234 = 60/40 blends. Further reducing the R32 mixing ratio to 40 vol% resulted in the R32/HFO-1234ze(Z) blend having a slightly faster pressure rise than R32/R1234ze(E), as shown in Figure 2.3.2(c). The measured S_{u0} value of the R32/R1234ze(Z) (40/60 vol%) blend was 0.1 cm s^{-1} higher than that of the R32/R1234ze(E) (40/60 vol%) blend.

Secondly, we obtained the burning velocities of HFO-1234ze(Z) mixed with O_2 enriched air. O_2 enriched air increases flammability and gives stable flames of mildly flammable compounds. Changing the O_2 concentration ratio in the air is synonymous with changing the N_2 concentration ratio. So, the difference from the ambient air is difference with inerting effect by N_2 , without changing chemical effects.

Figure 2.3.3 shows the dependence of O_2 concentration ratio in the air on the stoichiometric S_{u0} for HFO-1234ze(Z), together with R1234yf and R1234ze(E) for comparison. From this figure, it was found that HFO-1234ze(Z) has a smaller S_{u0} than R1234yf and almost the same S_{u0} as R1234ze(E) in all the O_2 concentration ratio ranges tested.

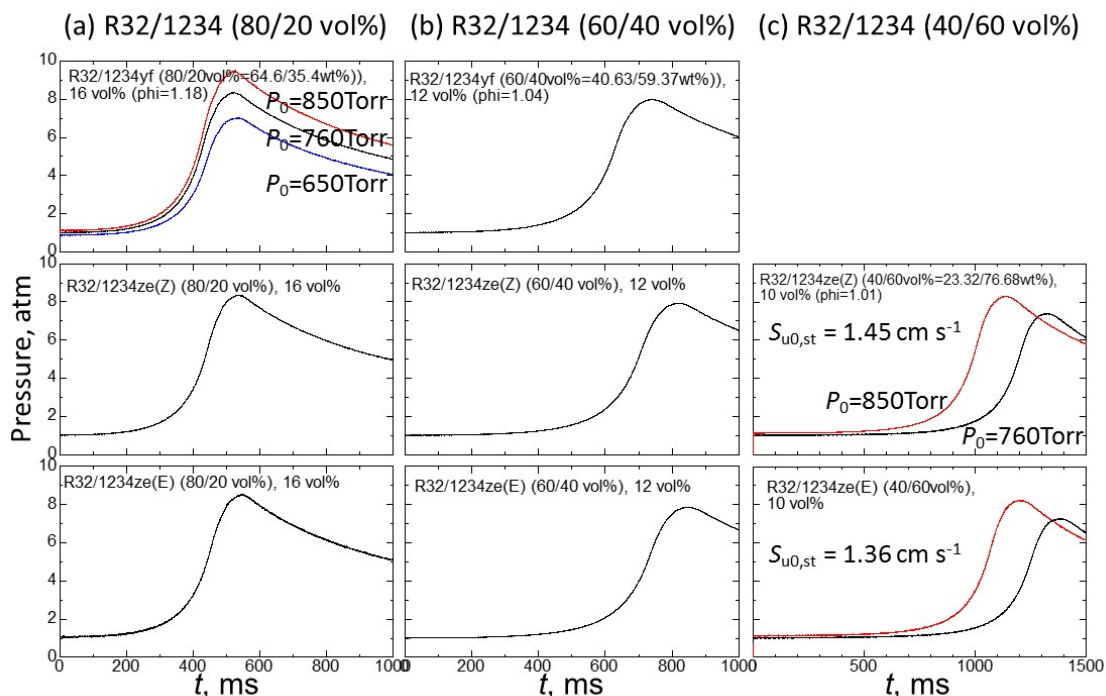


Figure 2.3.2: Dependence of pressure rise on R32/R1234 blend composition when measured in microgravity

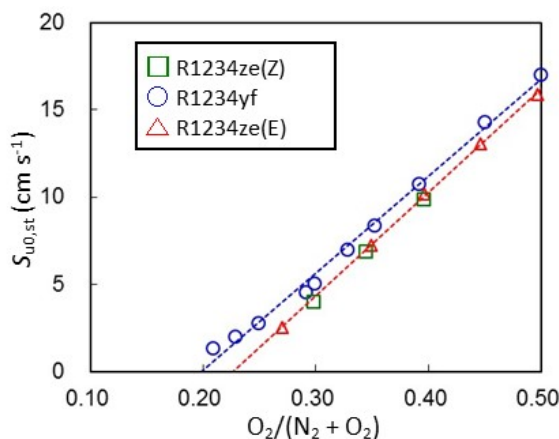


Figure 2.3.3: Dependence of O_2 concentration ratio in air on the stoichiometric S_{u0} for R1234 isomers

Based on the above observations of blend combustion, the burning velocity of pure HFO-1234ze(Z) was lower than that of pure R1234yf, which is inconsistent with the results of the pure compounds. The reason why S_u of pure HFO-1234ze(Z) was slightly higher than that of pure R1234yf may be because an overdrive due to an extremely strong ignition spark accelerated the flame propagation of HFO-1234ze(Z). As described earlier, the spark energy for ignition of HFO-1234ze(Z) is five times that for R1234yf, which makes S_u of HFO-1234ze(Z) slightly higher than that of R1234yf. Another reason may be the very limited data for HFO-1234ze(Z); the data were all obtained at an initial pressure of 101.3 kPa or higher. To correct this inconsistency, the temperature and pressure dependences of S_u for this compound should be examined.

Table 2.3.1 lists the $S_{u0,max}$ values and parameters relevant to the following section for eleven compounds. By developing the relationships between the burning velocity, which is the index for defining 2L refrigerants, and other parameters, we can better understand the fundamental flammability characteristics of 2L refrigerants.

Table 2.3.1: Burning velocities and flammability parameters for 11 compounds

Compound	Formula	T_{ad} , K	$S_{u0,max}$, cm s ⁻¹	ρ_u , kg m ⁻³	ρ_b , kg m ⁻³	c_p , J (g K) ⁻¹	λ_{av} , 10 ⁻³ W (m K) ⁻¹	δ , mm	α , 10 ⁻¹ cm ² s ⁻¹	t_c , ms
R290	C ₃ H ₈	2278	38.7	1.21	0.15	1.36	87.9	0.26	5.1	0.34
R600a	(CH ₃) ₂ CHCH ₃	2268	34.2	1.22	0.15	1.39	87.3	0.29	5.0	0.43
R152a	CH ₃ CHF ₂	2222	23.6	1.32	0.16	1.36	79.1	0.37	4.3	0.78
1243zf	CH ₂ =CHCF ₃	2312	14.1	1.40	0.16	1.33	80.4	0.59	4.2	2.1
HFC-143	CH ₂ FCHF ₂	2249	13.1	1.45	0.16	1.34	78.5	0.61	4.0	2.3
R152a/134a (50/50 vol%)		2179	11.7	1.45	0.14	1.34	76.6	0.67	3.9	2.8
HFC-254fb	CH ₂ FCH ₂ CF ₃	2183	9.5	1.49	0.18	1.35	75.7	0.78	3.7	4.1
R143a	CH ₃ CF ₃	2118	7.1	1.46	0.18	1.34	75.1	1.06	3.8	7.5
R32	CH ₂ F ₂	2207	6.7	1.38	0.16	1.33	77.7	1.22	4.1	9.1
R717	R717	2076	7.2	1.08	0.15	1.49	85.4	1.46	5.2	10
R1234yf	CH ₂ =CF ₃	2083	1.5	1.53	0.18	1.28	72.6	4.83	3.6	160

T_{ad} : adiabatic flame temperature, $S_{u0,max}$: maximum burning velocity at 25 °C and 101.3 kPa, ρ_u : unburned gas density, ρ_b : burned gas density, c_p : average isobaric heat capacity, λ_{av} : average thermal conductivity, δ : flame thickness, α : thermal diffusivity, t_c : characteristic time for chemical reaction.

2.4 Minimum Ignition Energy and Quenching Distance

When considering the probability of the occurrence of a fire hazard due to flammable gases, the flammability limits, minimum ignition energy (MIE), and quenching distance are some of the most important indices. Experimentally, the minimum ignition energy (E_{min}) is the lowest spark discharge energy that can ignite a flammable gas mixture at the most ignitable concentration. The parallel plate quenching distance (d_q) is the minimum distance between two surfaces above which flame propagation becomes self-sustaining. A standard test method for determining E_{min} and d_q is specified in ASTM E582-07 (2007). These parameters, if obtained appropriately, are useful for designing the electrical equipment that may be deployed in areas with a potentially flammable gas atmosphere. At present, however, there exists no appropriate test method that is suitable for evaluating the MIE of 2L compounds.

Figure 2.4.1 summarizes the published E_{min} data of compounds relevant to this study. For R290, E_{min} has been reported to be 0.247–0.48 mJ. For mildly flammable compounds, the reported E_{min} values vary widely from <10 mJ to >10 J. Even for R717, which has been studied extensively, NFPA 77 (2000) uses an E_{min} value of 680 mJ, while the High Pressure Gas

Safety Institute of Japan (KHK) uses 14 mJ. Such a wide variation makes assessing the fire risk based on E_{\min} very difficult. The difficulty with determining E_{\min} reliably is that it is very dependent on the electrode size, gap between electrodes, and ignition spark density and duration.

To improve the current situation, an ignition energy evaluation method is being developed to provide a reliable index for the fire risk.

Compared to E_{\min} , d_q seems to be much easier to measure and provides reliable data on mildly flammable compounds. In addition, E_{\min} is related to d_q and S_u through an equation of heat loss theory. Therefore, we first measured d_q and then estimated E_{\min} by using the measured d_q and S_u . Table 2.3.1 lists S_u and relevant parameters, and Table 2.4.1 lists d_q and relevant parameters.

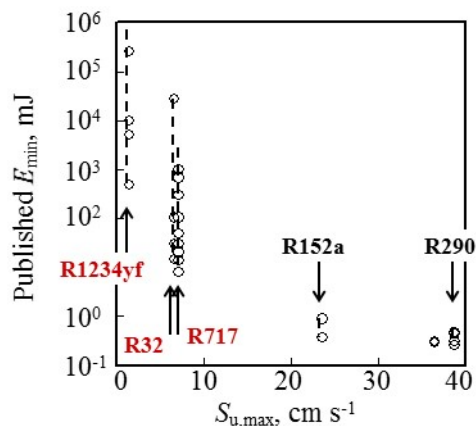


Figure 2.4.1: Wide variation in published experimental E_{\min} values for typical refrigerants

2.4.1 Quenching distance measurement

Figure 2.4.2 shows the apparatus for the parallel plate quenching distance measurement. The experimental setup and procedure were similar to ASTM E582 (2007). The apparatus was turned at an angle of 90° to the position of the ASTM E582 test apparatus. We tested both this geometry and the geometry of ASTM E582. Because a slowly propagating flame is significantly affected by the buoyancy, we measured d_q in both the vertical position $d_{q,v}$ (i.e., same position as the ASTM E582 apparatus) and horizontal position $d_{q,h}$ of the parallel plates. The cathode electrode was fixed, while the anode electrode could be moved with a micrometer to provide an adjustable gap width of less than 0.001 mm. The plane plate was made of machineable glass ceramic (Macor). The plates could be removed from the electrodes; we tested plates with diameters (D) of 5, 25, 50, 75, and 100 mm to examine the effect of the plate size on d_q . The flat-ended electrode wires were made of stainless steel with a diameter of 1.0 mm, and their ends were flush to the surface of the plane plate. For R1234yf (measured in the horizontal position of the parallel plates and in μg), which had a d_q value that was too large for our spark generator to make the breakdown, a thin tungsten wire electrode with a diameter of 0.3 mm was used with its tip projecting ca. 5 mm beyond the surface of each plate to facilitate the breakdown. To reduce the heat loss to the electrodes, the wire was burned and oxidized in air with a butane gas burner for at least 5 min before setting. A constant spark energy of 1.3 J with a duration of 3.0 ms was used to determine d_q .

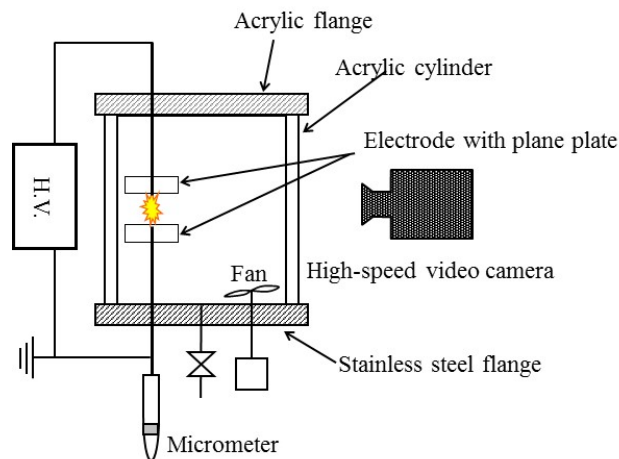


Figure 2.4.2: Experimental apparatus of parallel plate quenching distance ($d_{q,h}$) measurement

We judged whether ignition was achieved between the parallel plates. We obtained d_q by changing the gap width between the plates. The d_q value was determined as the average value over 10 tests between the maximum gap width at which ignition could not be observed and the minimum gap width at which ignition could be observed.

Figure 2.4.3 shows the converged $d_{q,v}$ and $d_{q,h}$ values plotted against the reciprocal of the mass burning rate ($\rho_u S_{u0,max}$) for all of the compounds except R1234yf. For R1234yf, d_q with $D = 100$ mm in μg was plotted instead of $d_{q,h}$. A converged value of d_q for R1234yf was not obtained because the 100 mm plates were not large enough for determining d_q of R1234yf. The d_q data for all of the compounds except R1234yf were fitted to an exponential fitting curve. The relative deviation of

the calculated values from the experimental values was 4.9% on average for all of the compounds except R1234yf. Thus, we obtained a good relationship between S_u and $d_{q,h}$ for highly to only mildly flammable compounds.

This figure also shows that $d_{q,h}$ of approximately 5 mm corresponds to $S_{u,max}$ of ca. 10 cm s^{-1} , i.e., the class 2/2L boundary. Figure 2.4.4 shows $d_{q,h}$ as a function of the equivalence ratio (ϕ) for all of the compounds except R1234yf. d_q widened rapidly as the refrigerant concentration decreased from the optimum value.

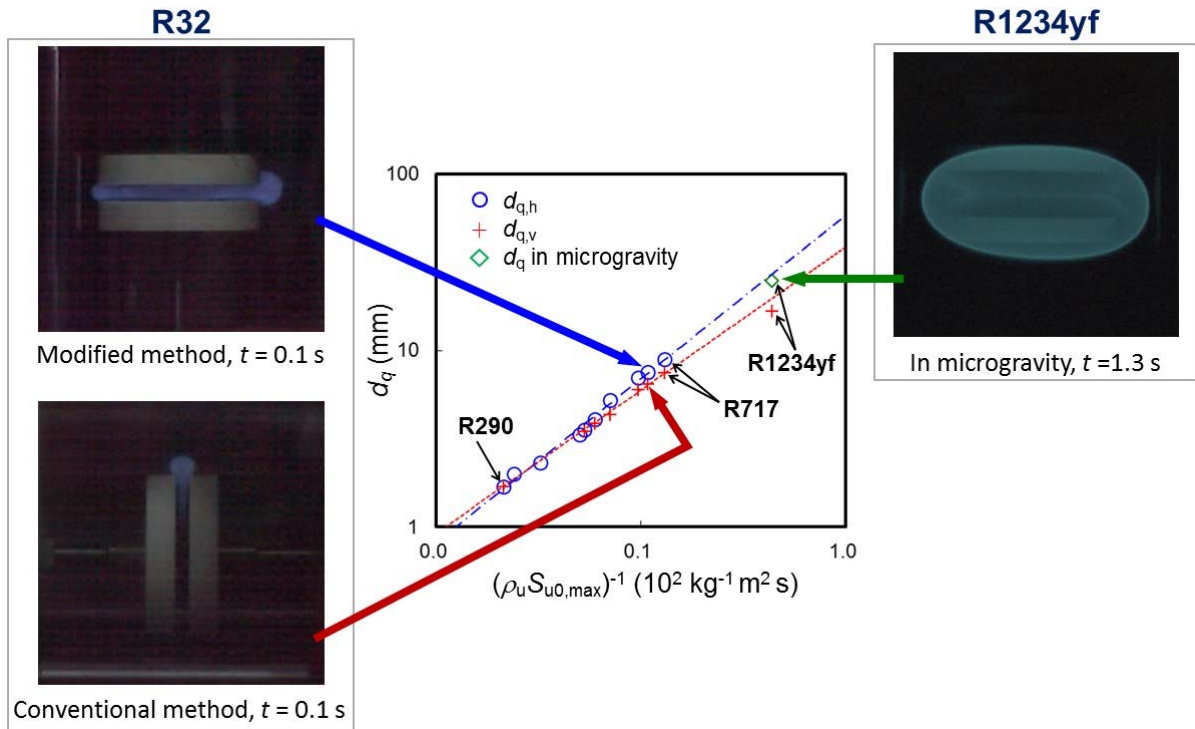


Figure 2.4.3: Quenching distances of 11 compounds as function of mass burning rate ($\rho_u S_u$)

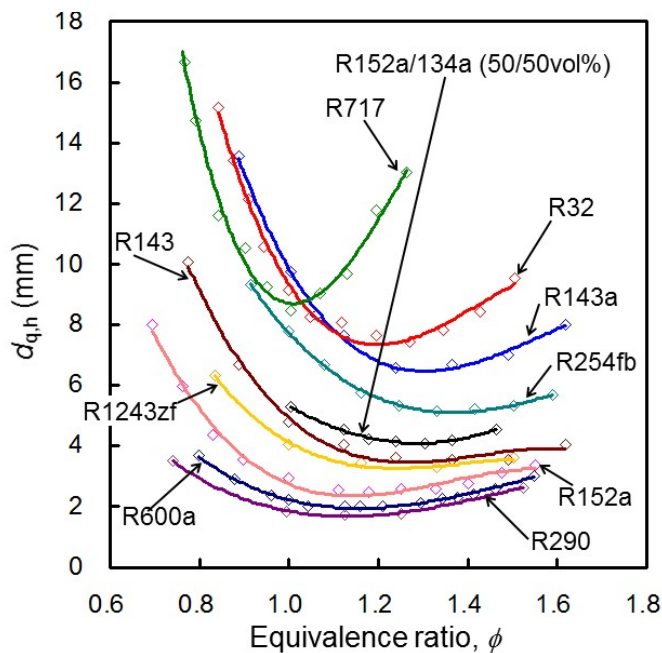


Figure 2.4.4: Concentration dependence of quenching distances for 10 compounds; ϕ is refrigerant/air equivalence ratio.

Table 2.4.1: Experimental quenching distances and estimated E_{\min} for 11 compounds

Compound	Exp. d_q				a	Calc. E_{\min} , mJ by Eq. (2.4.2) and $d_{q,h}$	Calib. E_{\min} , mJ ^c	Calc. E_{\min} , mJ by Eq. (2.4.2) and $d_{q,v}$
	$d_{q,h}$, mm	$d_{q,v}$, mm	Conc. vol%	ϕ				
R290	1.70	1.70	4.5	1.13	6.4	0.35	0.25	0.35
R600a	2.00	-	3.6	1.16	6.8	0.62	0.44	0.62
R152a	2.33	-	9.0	1.18	6.3	0.90	0.63	0.90
1243zf	3.33	-	8.5	1.33	5.6	2.2	1.5	2.2
HFC-143	3.58	3.48	11.5	1.24	5.9	2.9	2.0	2.6
R152a/134a (50/50 vol%)	4.08	3.88	11.5	1.24	6.1	3.8	2.7	3.0
HFC-254fb	5.23	4.35	8.5	1.33	6.7	12	8.4	5.3
R143a	7.03	6.00	12.5	1.36	6.6	27	19	13
R32	7.55	6.45	21.0	1.27	6.2	29	20	14
R717	8.95	7.45	21.9	1.00	6.1	45	32	19
R1234yf	24.8 ^{a, b}	16.6 ^b	10.0	1.33	5.1	780	550	76

^a Measured in microgravity. ^bThe value was not confirmed as converged. ^c11% reduction in adiabatic flame zone diameter $d_{q,h} - 2\delta$ to make E_{\min} of R290 equal to 0.247 mJ, which is reported by Lewis and von Elbe (1987).

2.4.2 Estimation of minimum ignition energy

The minimum ignition energy is the energy that is just sufficient to establish the flame sphere having the minimum radius necessary for self-sustained propagation. According to the simple heat loss theory, E_{\min} is given by

$$E_{\min} = (1/6) \pi d_{\min}^3 \rho_b c_p (T_b - T_u) \quad (2.4.1)$$

Here, d_{\min} is the diameter of the minimum flame sphere in a free space, and T_b and T_u are the burned and unburned gas temperatures.

Solving Equation (2.4.1) requires T_b and d_{\min} to be determined. Lewis and von Elbe (1987) postulated that the minimum flame has a diameter equal to the parallel plate quenching distance d_q and the same temperature as the adiabatic flame temperature T_{ad} . We observed the minimum flame diameter of R32 with the SP method and confirmed that d_q contained the flame thickness δ and d_{\min} (Takizawa et al, 2015). Therefore, we modified Equation (2.4.1) as follows:

$$E_{\min} = (1/6) \pi (d_q - 2\delta)^3 \rho_b c_p (T_b - T_u) \quad (2.4.2)$$

$$\delta = 2\lambda_{av}/(c_p \rho_u S_{u,max}) \quad (2.4.3)$$

E_{\min} estimated by Equation (2.4.2) and $d_{q,h}$ and $d_{q,v}$ are listed in the seventh and ninth columns of Table 2.4.1. For R290, the estimated E_{\min} value of 0.35 mJ was approximately 40% higher than the lowest experimental value of 0.247 mJ as reported by Lewis and von Elbe (1987). We calibrated the estimated E_{\min} by decreasing the flame kernel diameter ($d_q - 2\delta$) in Equation (2.4.2) by 11% so that E_{\min} of R290 would become 0.247 mJ; these values are listed in the eighth column of Table 2.4.1. Such calibration was justified considering the similarity in the structure of the minimum flame for all of the compounds. The agreement between the calibrated and experimental E_{\min} was somewhat improved. The reported E_{\min} values of R1234yf and R32 measured by the ASTM E582 method were higher than the calculated E_{\min} . The reason why the ASTM E582 method provided significantly large E_{\min} values for 2L refrigerants may be because the gap between the electrodes was narrower than d_q . To overcome the quenching effect on the plates, a much greater spark energy is necessary. Figure 2.4.5 shows the estimated E_{\min} vs. $d_{q,h}$ of R717 in this study together with the experimental E_{\min} values in the literature plotted against the electrode gap width at which E_{\min} was measured (Takizawa, 2015). Here, the size of the electrodes was not considered because of the limited data available. From this graph, considering E_{\min} of R717 to be some

10 mJ or less seems to be a reasonable proposition because all of the E_{\min} values higher than 100 mJ were measured with the electrode gap within the d_q value of R717.

As another example, Smith et al. (2003) reported experimental values for E_{\min} and d_q of flammable refrigerants using electrodes with 25-mm diameter parallel plates in the vertical position as follows: 0.30 mJ and 1.7 mm for R290, 0.89 mJ and 3.2 mm for R152a, 18,421 mJ and 4.3 mm for R143a, and 26,300 mJ and 5.2 mm for R32. Compared to our results given in Table 2.4.1, they ignited R143a and R32 with an electrode gap narrower than our d_q value but used a spark energy that was three orders of magnitude greater than our estimated E_{\min} for these compounds. The 25-mm parallel plates were not large enough to obtain the converged d_q value for R32. In other words, if very high energy is discharged between electrodes with small parallel plates, the incipient flame penetrates a narrower gap than d_q , and ignition can occur. For R290 and R152a, they measured E_{\min} with an electrode gap wider than our d_q , and their results agreed well with our estimated E_{\min} listed in Table 2.4.1. Thus, when considering E_{\min} of mildly flammable compounds, we should verify whether the ignition occurred with the electrode gap wider than the quenching distance. Otherwise, the flame heat loss to the electrodes may significantly increase the ignition energy, which would result in an overestimation of E_{\min} and undervaluation of the flammability of these compounds.

According to Equation (2.4.2), E_{\min} is substantially proportional to the cube of d_q . As expected from the concentration dependence of d_q in Figure 2.4.4, E_{\min} should dramatically increase if the refrigerant concentration becomes leaner or richer than the optimum concentration. This is one of the reasons for the difficulty with measuring E_{\min} ; this value can only be obtained in the immediate vicinity of the optimum concentration.

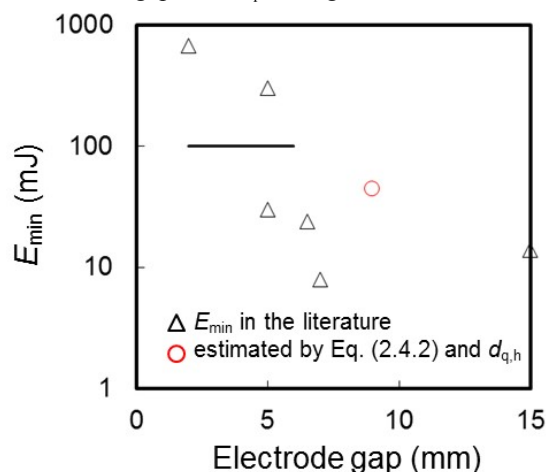


Figure 2.4.5: Published E_{\min} values for R717 as function of electrode gap at E_{\min}

2.4.3 Comparison with ignition energy under practical conditions

The estimated E_{\min} in the present study was compared with the magnitude of the spark energy that can be generated from static electricity due to the human body. With normal activity, a human body can generate an electric charge of 10–15 kV, and the stored charge energy can reach 20–30 mJ (NFPA 77, 2000). To ignite a compound with a given E_{\min} by static electricity, the amount of energy needs to be three times E_{\min} via a metallic material and 60 times E_{\min} via human skin (Davies, 1992, Tolson, 1980, Wilson, 1977). If this factor is applied to flammable refrigerants, R290 can be ignited by a spark from static electricity due to the human body. However, 2L refrigerants are very difficult to ignite via a spark between human skin and metallic materials.

Considering the practical conditions, the spark energy necessary to ignite a compound is usually far greater than its E_{\min} . The practical conditions are very different from those in the laboratory, where researchers carefully prepare the optimum concentration (see Figure 2.4.4), spark conditions, optimum gap between electrodes, etc. E_{\min} is obtained only under such conditions, and even a slight change may dramatically increase the measured E_{\min} , as shown in Figure 2.4.5. For 2L refrigerants, which have a quenching distance of more than 5 mm, E_{\min} can be obtained with a spark that is isolated from any objects within their quenching distances. Therefore, to ignite 2L refrigerants with practical electrical parts, the spark energy must be much greater than E_{\min} .

2.5 Extinction Diameter

When electrical parts with an opening such as a circuit breaker and a magnetic contactor are in a flammable gas atmosphere, the electric spark they generate can be an ignition source. Even though ignition occurs at the electrode gaps inside the enclosure, combustion is not transmitted to the flammable gas atmosphere outside the enclosure unless the diameter of the opening of the enclosure exceeds the critical value d^* , which we define as the “extinction diameter”. We first introduced the extinction diameter in this project. In earlier works, this parameter was not distinguished from the quenching distance. This is because the extinction diameter is generally equal to d_q for highly flammable fuel compounds. For 2L compounds, however, this parameter is several millimeters smaller than d_q , and we should understand this property for the safe use of electrical parts that are surrounded by flammable refrigerants.

Figure 2.5.1 shows a schematic drawing and picture of the apparatus for measuring the extinction diameter. A thin PTFE plate with an opening was set at the distance h from the ignition point. The plate was 70 mm square with a thickness of 1 mm. We observed whether or not the flame could pass through the opening.

For R1234yf, we carried out the experiment in μg . In 1G, d^* in the upward direction is not the most conservative case but probably the most optimistic case. Buoyant burned gas, which reduces the flame temperature, is very close to the top of the flame but far from the side of the flame. Accordingly, d^* shows the largest value in the upward direction and the smallest value in the horizontal direction in 1G. For this reason, we should know the d^* value that is obtained from the flame front that is well distant from the burned gas and free from cooling effects of the burned gas. Thus, we measured d^* of R1234yf in μg .

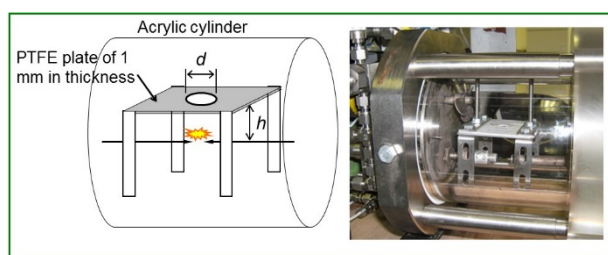


Figure 2.5.1: Apparatus of extinction diameter measurement.

Figure 2.5.2 shows the measured d^* for R32, R717, and HFC-254fb as a function of h . The plots at $h = 0$ indicate d_q values from Table 2.4.1. At a certain h value, when the diameter of the opening was smaller than d^* of this graph, the flame did not go through the opening. In the small h region, d^* decreased rapidly with increasing h . As h increased further, d^* decreased gradually and finally reached an almost constant value. This tendency may reflect the formation process of stable flames. The smaller the flame sphere, the more easily the flame propagation can be arrested.

Figure 2.5.3 shows d^* as a function of h when normalized by d_q . All of the refrigerants except R1234yf showed quite similar tendencies in terms of the flame growth and extinction. As h increased, d^* decreased and converged to less than 40% of d_q . In other words, in order to prevent the well-developed flame from going through the opening, the opening should have a diameter smaller than 40% of d_q .

For R1234yf, d^*/d_q decreased more rapidly with increasing h/d_q compared to the other three 2L compounds. One of the reasons was the difficulty in measuring $d^*(h = \infty)$ at room temperature. When measuring $d^*(h = \infty)$ of R1234yf, the temperature of the unburned gas was no longer the room temperature but increased significantly, which made the measured $d^*(h = \infty)$ smaller than at room temperature. To obtain $d^*(h = \infty)$ of R1234yf at room temperature, a much larger vessel is needed.

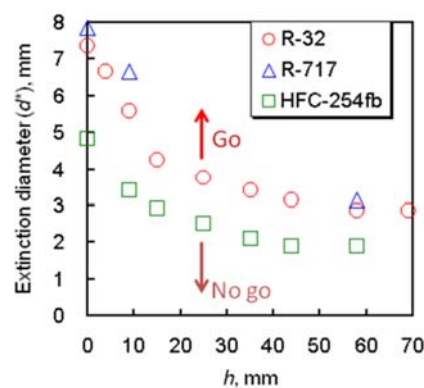


Figure 2.5.2: d^* of R32, R717, and HFC-254fb as function of h

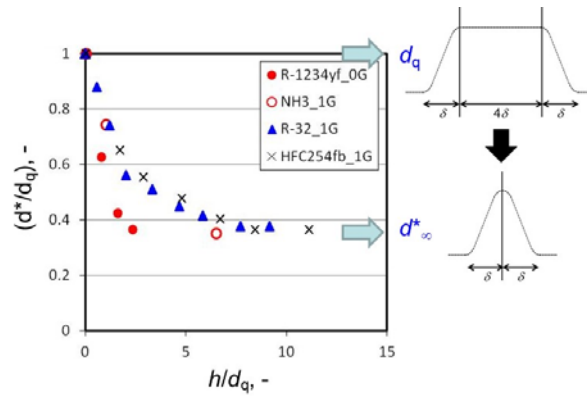


Figure 2.5.3: d^* as a function of h normalized by d_q for R1234yf, R717, R32, and HFC-254fb

For the application of d^* to practical risk assessment, the effect of the opening shape on d^* is important. We measured the extinction size of rectangular openings with length-to-width (l/w) ratios of 3 and 5 and those of conventional magnetic contactors. We can generalize the extinction diameter of openings by introducing the effective diameter (d_{eff}), which may be taken as the hydraulic diameter:

$$d_{\text{eff}} = 4A/P \quad (2.5.1)$$

Here, A is the cross-sectional area of the opening, and P is the perimeter of the opening. For a circle, $d_{\text{eff}} = d$.

Figure 2.5.4 shows a photograph of the openings of d^* at $h = 9$ mm for four refrigerants in comparison with the openings of a magnetic contactor (MC) and socket. For R290, because d^* is much smaller than the diameter of the opening of the MC and socket, they will become ignition sources. For R32, because d^* is larger than the diameter of the opening of the MC, the MC will not become an ignition source.

To make practical use of this index, we may first measure the distance between the ignition point and opening (h) and d_{eff} of electrical parts. If the combination of h and d_{eff} lies below the d^* curve of HFC-254fb in Figure 2.5.2, the flame of the 2L refrigerant will not go through the opening. Otherwise, it may be necessary to change h and/or d_{eff} of the equipment until the combination falls below the d^* curve in Figure 2.5.2.

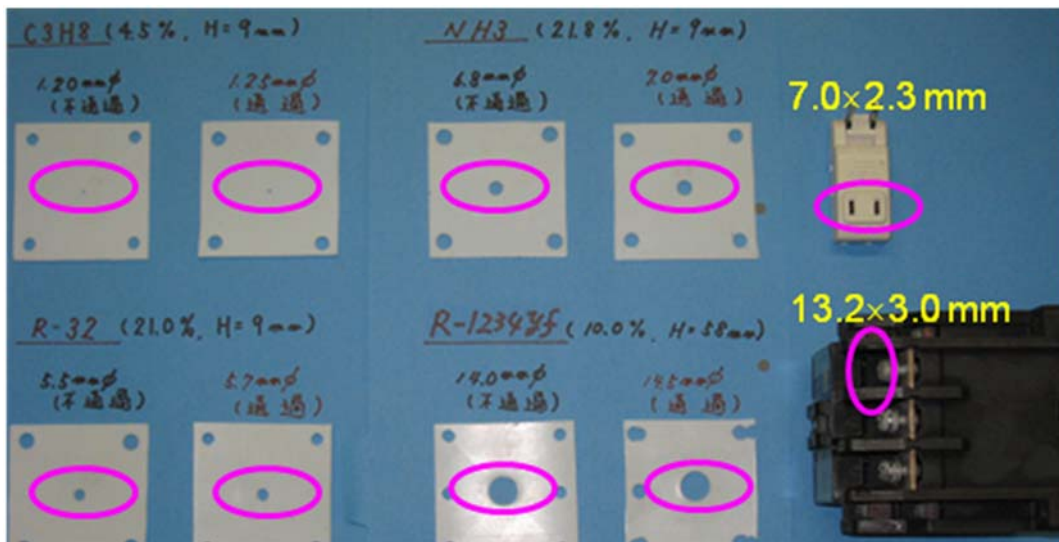


Figure 2.5.4: Comparison between d^* of four refrigerants and opening of magnetic contactor and socket. On the right-hand side of each pair of PTFE plates, we show the opening of “go.” The left-hand side shows “no go.”

2.6 Thermal Decomposition of Lower-GWP Refrigerants

2.6.1 Introduction

To analyze the risks of using lower-GWP refrigerants, it is necessary to clarify their decomposability and products. However, the high reactivities of products such as hydrogen fluoride (HF) make this quantification difficult. Moreover, Takizawa et al. (2011) has suggested that the reactivity of a molecule with more fluorine atoms than hydrogen atoms, such as R1234yf, is affected by humidity. Thus, its flammability limits and product composition depend on the relative humidity of the surrounding air.

The experiment described in this section was carried out to quantify the amount of HF, the main toxic product, and to analyze the effects of different wall materials.

2.6.2 Experimental methods and results

2.6.2.1 Experimental apparatus

There are two causes of HF generation from refrigerants: thermal decomposition by heating and combustion. In this research, only thermal decomposition was studied. A schematic diagram of the experimental apparatus fabricated to study thermal decomposition by heating is shown in Fig. 2.6.1. This experimental apparatus consisted of four parts: gas-mixing, heating, measuring, and detoxification parts.

The gas-mixing part was used to mix refrigerant and air at a specified concentration and humidity. The concentration was controlled by mass flow controllers, and the humidity was controlled by a dehumidifier and humidifier. The heating part was used to heat a gas sample and cause it to react in a straight pipe (inner diameter: 10.7 mm), and a 550-mm-long electric furnace was included around the pipe. The measuring part consisted of gas cells for Fourier transform infrared spectroscopy (FT-IR). To broaden the concentration measurement range, two cells with different path lengths were used. The detoxification part consisted of an absorbance tube that exhausted into a fume hood.

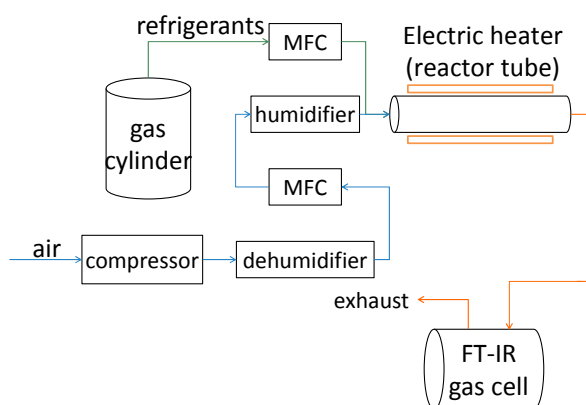


Fig. 2.6.1 Schematic diagram of the experimental apparatus

2.6.2.2 Materials tested and parameters

The experimental parameters are shown in Table 2.6.1. The refrigerants tested were mixtures of refrigerants (R32, R1234yf, R134a, and R22) and air. Inconel 600 and stainless steel (SUS304 and SUS316) were used as heating tube materials to compare the effect of corrosion between commonly used metals like stainless steel and corrosion-resistant ones.

Table 2.6.1 Experimental parameters

Refrigerants tested	Lower-GWP refrigerants: R32, R1234yf Conventional refrigerants: R134a, R22
Heating tube material	Inconel 600, Stainless steel (SUS304 and SUS316)
Refrigerant concentration [vol. %]	2.5–10
Temperature of the heater [°C]	400–700
Humidity [g-water / kg-dry air]	0–16
Total flow rate [ml/min]	100–200
Inner diameter of heating tube [mm]	10.7
Cross-sectional area of heating tube [cm ²]	0.90
Length of heating tube [mm]	550
Heating time [s] (in case of 200 ml/min)	5–15 (depends on factors such as heating temperature)

2.6.2.3 Effects of temperature and humidity

The effects of temperature and humidity were tested with Inconel tubes. The concentrations of the refrigerant and HF after heating versus the heater temperature are shown in Figs. 2.6.2–2.6.9 for each refrigerant. The summary is shown in Table 2. The variable parameter is absolute humidity [g-water / kg-dry air], and the fixed parameters are the refrigerant concentration (2.5 vol. %) and the total flow rate (200 ml/min).

In Figs. 2.6.2 and 2.6.3, the absolute humidity (AH) that is labeled “2” refers to values such that $0 \leq AH [g/kg] < 2$, and a label of “4” means that $2 \leq AH [g/kg] < 4$. Other figures are also labeled similarly. In these tests, the temperature at which the refrigerant concentration starts to decrease was not affected by the humidity. However, only in case of R1234yf, as humidity is higher, decreased refrigerant is less when heater temperature is around 600°C, where the around 50% of refrigerant is decomposed, as shown in Fig. 2.6.4. It is inferred the reaction rate decreased by higher humidity.

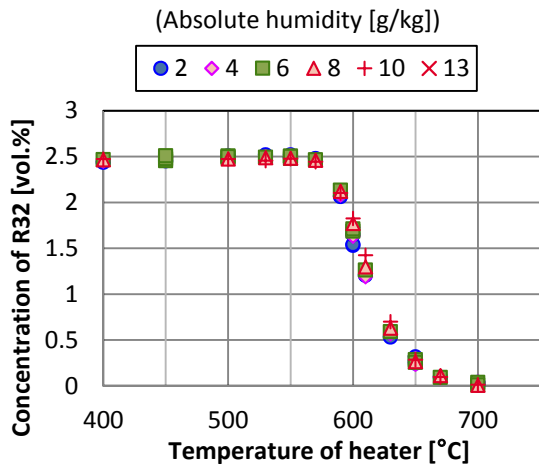


Fig. 2.6.2 Concentration of R32 versus heater temperature
(Total flow rate of 200 ml/min;
2.5 vol. % R32 with air; Inconel 600 tube)

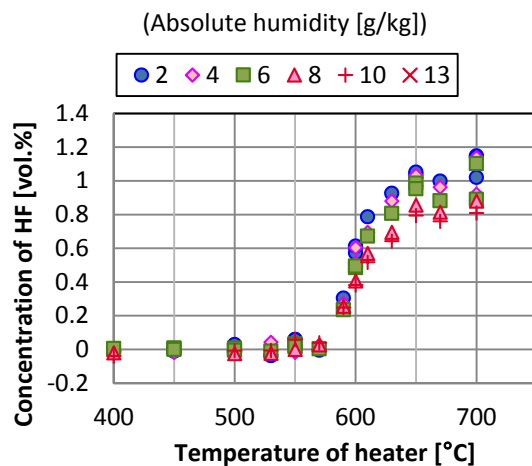


Fig. 2.6.3 Concentration of HF versus heater temperature
(Total flow rate of 200 ml/min;
2.5 vol. % R32 with air; Inconel 600 tube)

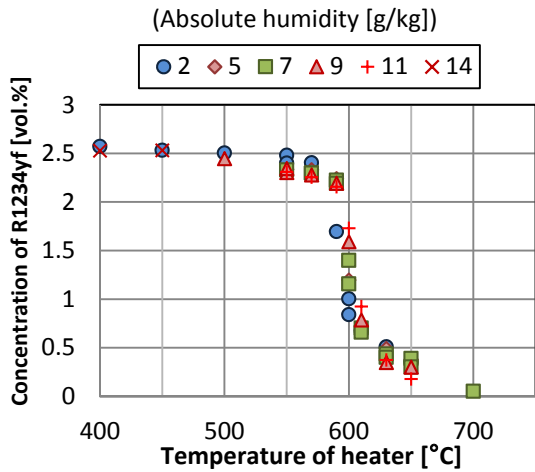


Fig. 2.6.4 Concentration of R1234yf versus heater temperature (Total flow rate of 200 ml/min; 2.5 vol. % R1234yf with air; Inconel 600 tube)

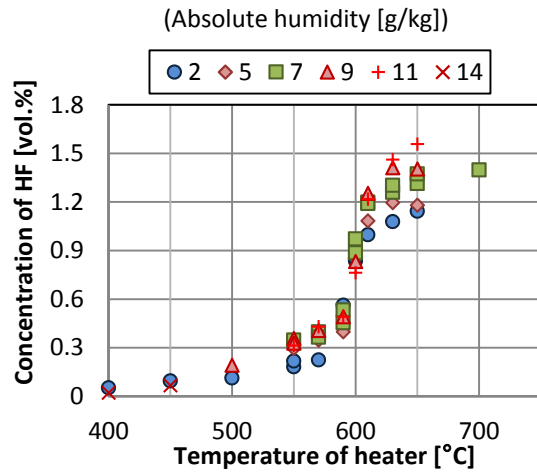


Fig. 2.6.5 Concentration of HF versus heater temperature (Total flow rate of 200 ml/min; 2.5 vol. % R1234yf with air; Inconel 600 tube)

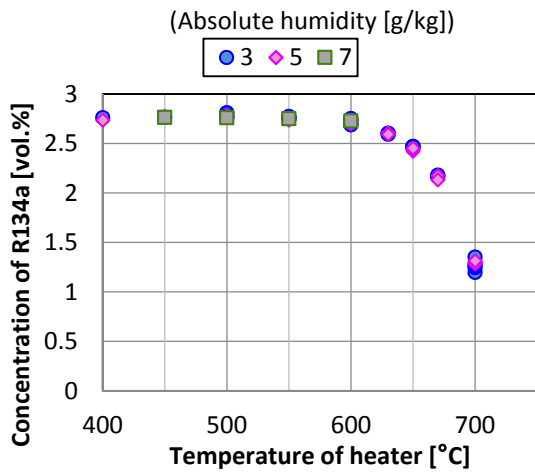


Fig. 2.6.6 Concentration of R134a versus heater temperature (Total flow rate of 200 ml/min; 2.5 vol. % R134a with air; Inconel 600 tube)

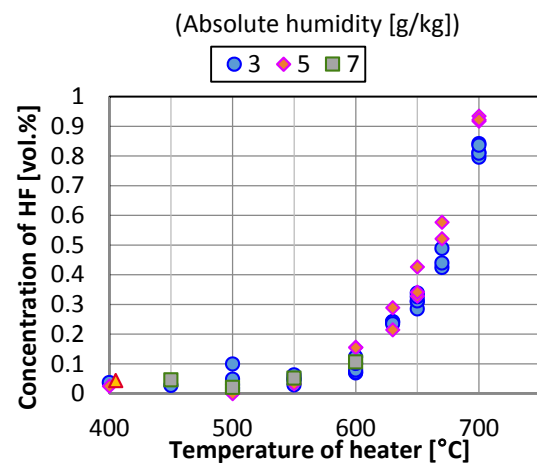


Fig. 2.6.7 Concentration of HF versus heater temperature (Total flow rate of 200 ml/min; 2.5 vol. % R134a with air; Inconel 600 tube)

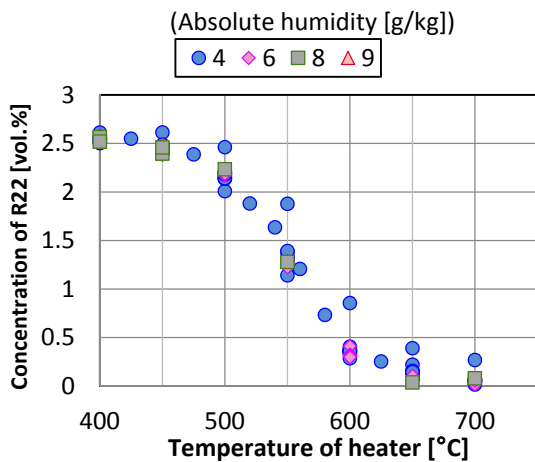


Fig. 2.6.8 Concentration of R22 versus heater temperature (Total flow rate of 200 ml/min; 2.5 vol. % R22 with air; Inconel 600 tube)

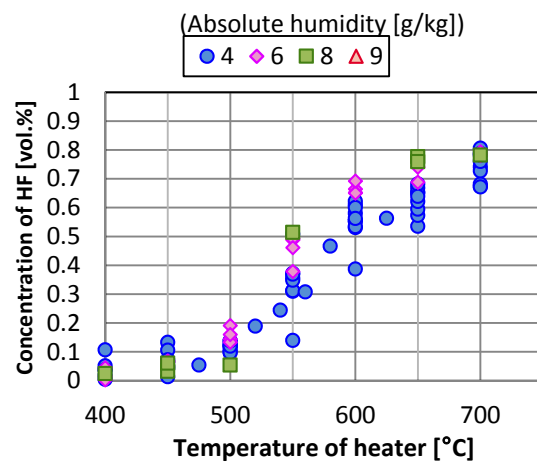


Fig. 2.6.9 Concentration of HF versus heater temperature (Total flow rate of 200 ml/min; 2.5 vol. % R22 with air; Inconel 600 tube)

Table 2.6.2 Effect of temperature and humidity

Refrigerant	Lower limit temperature limit for refrigerant decomposition [°C]	Effect of humidity on refrigerant decomposition
R32	550–570	Very little
R1234yf	570–590	Less decomposition in higher humidity
R134a	600–630	Very little
R22	450–500	Very little

2.6.2.4 Effects of using stainless steel

With stainless steel (SUS304 and 316) tubes, the effects of corrosion were tested. In this test, the temperature was increased in steps of 50°C to 700°C, and this process was repeated after the tube had time to naturally cool.

Some of the results are shown in Figs. 2.6.10 and 2.6.11, and a summary of these results including experiments with Inconel tubes is given in Table 3. The labels (e.g., “1st,” “2nd,” etc.) in the figures indicate the number of cycles of the temperature increase.

Almost the same results were obtained with Inconel tubes in the 1st test. However, as the tubes became corroded, the concentrations of the refrigerants started to decrease at lower temperatures.

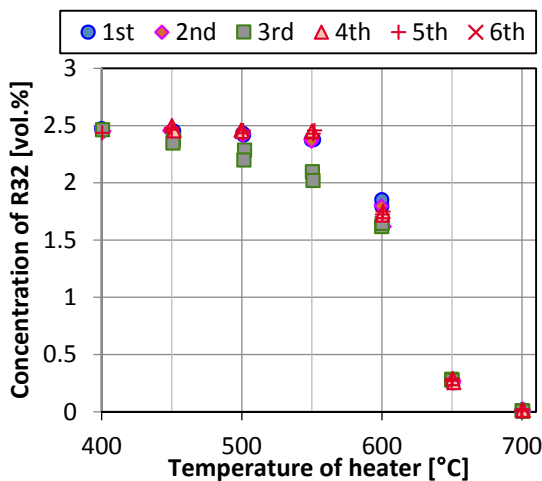


Fig. 2.6.10 Concentration of R32 versus heater temperature (Total flow rate of 200ml/min, 2.5vol. % R32 with humid air, SUS316 tube)

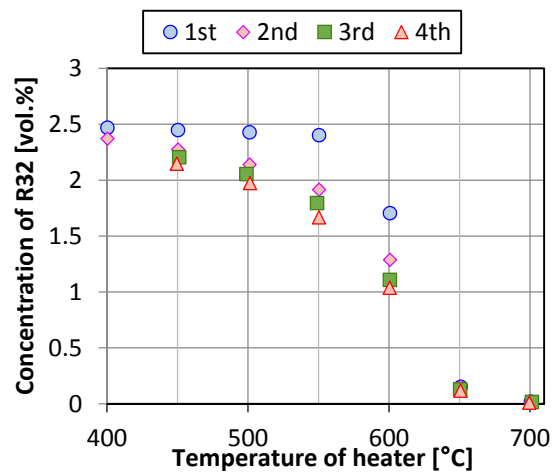


Fig. 2.6.11 Concentration of R32 versus heater temperature (Total 200ml/min, 2.5vol. % R32 with dry air, SUS304 tube)

Table 2.6.3 Difference in the lower temperature limit of decomposition between SUS and Inconel tubes [°C]

Refrigerant	Tube material	SUS316		SUS304
	Inconel 600	Dry	Wet (about 6[g/kg])	Dry
R32	570–590	Dry	450–500	400–450
R1234yf	550–570	Not measured	400–450	400–450
R134a	600–630	Not measured	600–630	450–500
R22	450–500	300–350	300–350	300–350

2.6.2.5 Effect of soot

We found that, in the experiments with R1234yf, the results gradually changed when the experiment was repeated using the same tube. The concentration of R1234yf after heating in this case is shown in Fig. 2.6.12. In this case, soot dust was

found in the tube, and the decrease in the R1234yf concentration started at a lower temperature comparing to the result in Fig. 2.6.4.

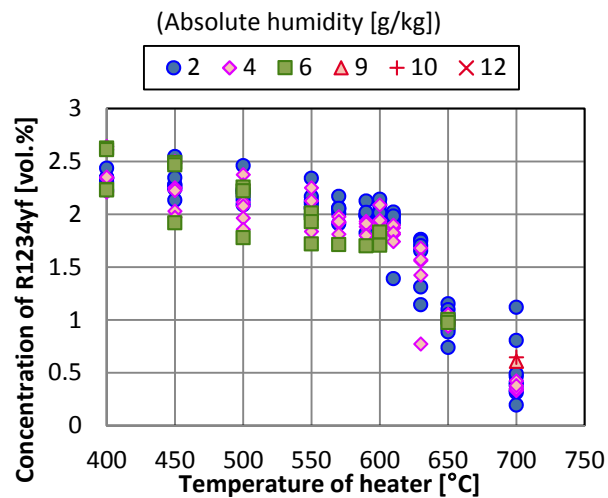


Fig. 2.6.12 Concentration of R1234yf versus heater temperature (Total flow rate of 200 ml/min; 2.5 vol. % R1234yf with dry air; Inconel 600 tube with soot)

2.6.3 Conclusion

To analyze the risks of using lower-GWP refrigerants, decomposition of refrigerants on a hot surface was tested, and we obtained the following results.

- 1) The respective temperatures at which the refrigerants began to decrease when heated for about 10 seconds were: R32: 570–590°C, R1234yf: 550–570°C, R134a: 600–630°C, R22: 450–500°C
- 2) For the refrigerants tested in this study, the temperature at which the refrigerant concentration started to decrease was not affected by the humidity. Only in the amount of decrease of R1234yf an effect of the humidity was obtained.
- 3) Either by the corrosion of the wall materials a result of the generation of , all tested refrigerants were decomposed at lower temperatures, and the amounts of the product and the decomposed refrigerant were increased.
- 4) By generated soot, R1234yf were decomposed in lower temperature and the amount of product and decomposed refrigerant are increased.

References

References

ASHRAE. 2013. ANSI/ASHRAE Standard 34-2013, Designation and safety classification of refrigerants. Atlanta: American Society of Heating, Refrigerating and Air-conditioning Engineers, Inc.

ASHRAE. 2013. ANSI/ASHRAE Standard 15-2013, Safety Standard for Refrigeration Systems. Atlanta: American Society of Heating, Refrigerating and Air-conditioning Engineers, Inc.

ASTM. 2004. ASTM E681-04, Standard test method for concentration limits of flammability of chemicals., ASTM International.

ASTM. 2007. ASTM E582-07, Standard Test Method for Minimum Ignition Energy and Quenching Distance in Gaseous Mixtures., ASTM International.

Davies D. K., 1992, The incendivity of sparks and brush discharges, *J. Electrostat.*, **27**: pp. 175-178.

- ISO. 1999. ISO/IEC Guide 51, Safety aspects— Guidelines for their inclusion in standards. International Organization for Standardization.
- ISO. 2014. ISO 817, Refrigerants— Designation and safety classification. International Organization for Standardization.
- ISO. 2014. ISO 5149, Refrigerating systems and heat pumps— Safety and environmental requirements. International Organization for Standardization.
- Ito, M., Dang, C., Hihara, E., 2014, “Thermal decomposition of lower-GWP refrigerants,” 2014 JSRAE Annual Conference, A343-1–4.
- Kondo S., Urano Y., Takizawa, K., Takahashi A., Tokuhashi K., Sekiya A., 2006, Flammability limits of multi-fluorinated compounds, *Fire Safety J.*, **41**: pp. 46-56.
- Kondo S., Takizawa, K., Takahashi A., Tokuhashi K., 2011, On the temperature dependence of flammability limits of gases, *J. Hazard. Mater.* **187**: pp. 585-590.
- Kondo S., Takizawa, K., Tokuhashi K., 2012, Effects of temperature and humidity on the flammability limits of several 2L refrigerants, *J. Fluor. Chem.*, **144**: pp. 130–136.
- Kondo S., Takizawa, K., Tokuhashi K., 2014, Effect of high humidity on flammability property of a few non-flammable refrigerants, *J. Fluor. Chem.*, **161**: pp. 29-33.
- Lewis B., Von Elbe G., 1987., Combustion, Flames and Explosions of Gases, third ed., Academic Press, New York: pp. 333-361.
- NFPA. 2000. NFPA 77, Recommended Practice on Static Electricity 2000 Edition., 2000NFPA.
- NFPA. 2002. NFPA 68, Guide for Venting of deflagrations 2002 Edition., 2002, National Fire Protection Association.
- Smith N. D., Mitchell W. A., Tufts M. W., 2003, Determining Minimum Ignition Energies and Quenching Distances of Difficult-To-Ignite Compounds, *J. Testing Eval.* **31**: pp. 178-182.
- Takizawa, K., Takahashi A., Tokuhashi K., Kondo S., Sekiya A., 2005. Burning velocity measurement of fluorinated compounds by spherical-vessel method. *Combust. Flame*, **141**: pp. 298-307.
- Takizawa, K., Tokuhashi, K., Kondo, S., and Nagai, H., 2011, “Flammability evaluation of R-1234yf and R-1234ze(E)”, Proceedings of the 49th Combustion Symposium, 146–147, Yokohama, Japan (in Japanese).
- Takizawa, K., Tokuhashi K., Kondo S., Mamiya M., Nagai H., 2012 “RP-1583 Assessment of Burning Velocity Test Methods”, pp. 44-49, http://www.techstreet.com/ashrae/cgi-bin/detail?product_id=1840089.
- Takizawa K., Tokuhashi K., Kondo S., 2015, Quenching distance measurement of highly to mildly flammable compounds, *Fire Safety J.* **71**: pp. 58-68.
- Tolson, P., 1980, The stored energy needed to ignite methane by discharges from a charged person, *J. Electrostat.*, **8**: pp. 289-293.
- Wilson, N., 1977, The risk of fire or explosion due to static charges on textile clothing, *J. Electrostat.*, **4**: pp. 67-84.

3. Physical Hazard Evaluation of A2L Refrigerants Based on Several Conceivable Handling Situations

3.1 Introduction

Recently, there has been a trend toward the development and use of alternative refrigerants that have no ozone-depleting potential and low global-warming potential. For example, there are strong expectations that difluoromethane (R32), 2,3,3,3.tetrafluoroprop-1-ene (R1234yf), and (E)-1,3,3,3.tetrafluoroprop-1-ene [R1234ze(E)] will be used as alternative refrigerants, and several pieces of equipment containing these refrigerants have already been commercialized in Japan. However, these alternative refrigerants have a degree of flammability, although the risk is less than that of most flammable gases. The fundamental combustion behaviors of the alternative refrigerants, such as their flammability limits, their minimum ignition energies, their burning velocities, and their quenching distances, have been examined and reported by several researchers (for example, Takizawa et al., 2015, 2009, Saburi et al., 2014, Spatz & Minor, 2008). In order to utilize A2L refrigerants in air conditioning systems, it is necessary to reconsider their classification and to relax standards for their handling on the basis of risk management for foreseeable actual handling situations and occasional accident scenarios.

We have therefore conducted a series of experimental evaluations of the physical hazards associated with A2L refrigerants, assuming various accident scenarios in situations in which A2L refrigerants are likely to be handled, based on discussions with developers and associations dealing with air conditioning systems in Japan (for example, Takaichi et al., 2014, Yajima, 2014). The three major handling situations shown in Fig. 3.1.1 have been assumed.

- (1) **Handling situation #1:** A wall-mount type room air conditioning system containing an A2L refrigerant is simultaneously used with a fossil-fuel heating system inside a general living space.
- (2) **Handling situation #2:** An air conditioning system containing an A2L refrigerant is handled at the factory for service and maintenance.

In this scenario, we focus on the following four accident scenarios:

- (a) *Accident scenario (a):* A service operative uses a portable lighter to smoke in a space in which an A2L refrigerant has leaked and accumulated.

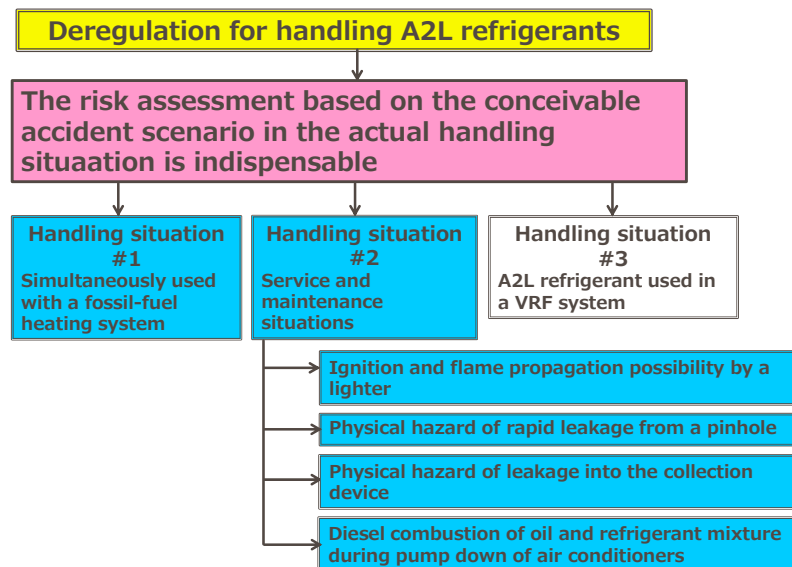


Fig. 3.1.1 Assumed handling situations and accident scenarios of A2L refrigerants.

- (b) *Accident scenario (b):* An A2L refrigerant leaks from a fracture or pinhole in the pipes or hoses such as that used to connect a car's air conditioning system to a collection device.
- (c) *Accident scenario (c):* An A2L refrigerant leaks inside a model device used for service and maintenance

such as a collection device.

(d) *Accident scenario (d)*: Diesel combustion of the compressor of an air conditioner containing an A2L refrigerant during pump-down.

(3) **Handling situation #3**: An A2L refrigerant is used in the Variable Refrigerant Flow (VRF) system.

In this report, we present digests of the results of experimental evaluation of A2L refrigerants in handling situations #1 and #2 above. The details of the work presented in this report have been published as reviewed papers (Imamura et al., 2012, 2013, 2014, 2015, Higashi et al., 2014).

3.2 Hazard Evaluation of Handling Situation #1: -Use with Fossil-Fuel Heating System-

3.2.1 Outline

In this situation, scenarios involving ignition, flame propagation, and concentration of combustion product (hydrogen fluoride, HF) were intensively investigated. We focused on two different types of accident cases: an A2L refrigerant leaking from an air conditioning system into a general living space in which a fossil-fuel heating system is already operating (*Case (i)*), and a fossil-fuel heating system operating in a general living space in which the leaked A2L refrigerant has already leaked and accumulated (*Case (ii)*).

An article describing the details of this topic was published in 2012 (Imamura et al., 2012, in Japanese).

3.2.2 Experiment

Figure 3.2.1 shows the schematic diagram of the experimental setup. A commercial room air conditioning system for an area comprising six Tatami mats (about 11 m²) was installed on the wall of an experimental facility (cube, 2800 mm each side) in which the center of the ventilation outlet was located 700 mm beneath the ceiling and at the center in the horizontal direction. Refrigerant was leaked in the downward vertical direction from the ventilation outlet. In *Case (i)*, a radiative oil stove (power: 2.4 kW, designed to heat 13 m²) and an oil fan heater (power: 3.2 kW, designed to heat 16 m²) were employed as representative fossil-fuel heating systems already operating inside the general living space. In *Case (ii)*, a ceramic heater (FPS1, Yarkar Ceramic Co., Ltd., Osaka) was employed as the heating source instead of the fossil-fuel heating system because the heating source had to be controlled remotely.

R1234yf, R32, and R410A were employed as the test refrigerants. The amount of leaked refrigerant was 800 g, which was designed based on the amount of refrigerant contained in most commercial air conditioning systems (NITE, 2010).

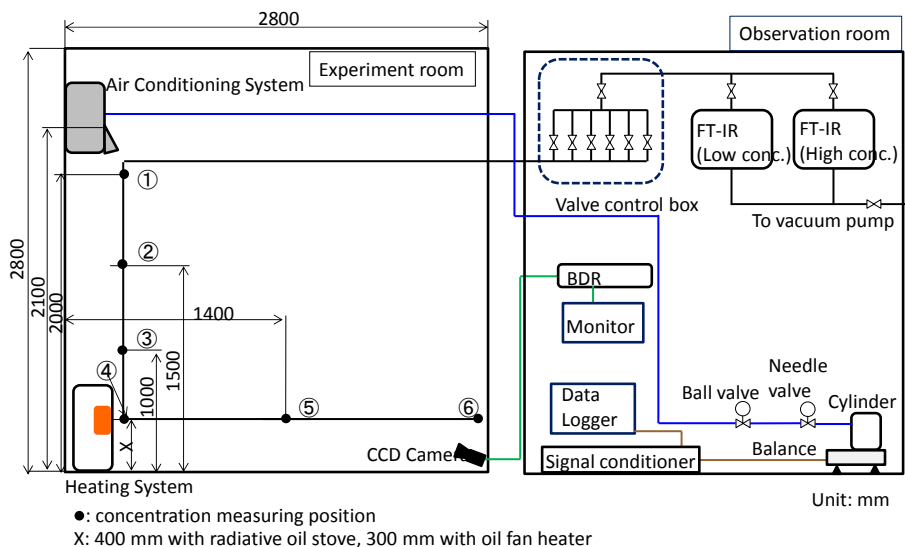


Fig. 3.2.1 Schematic diagram of experimental setup in the experimental evaluation for the handling situation #1.

In addition, two leak rates were used as the set value: 10 g/min and 60 g/min.

In this experiment, concentrations of the refrigerant and the HF that was produced by combustion or thermal decomposition were measured using Fourier transform infrared spectroscopy (FT-IR, JASCO, FT-IR4200, Tokyo).

3.2.3 Results and discussions

3.2.3.1 Case (i)

In all of the present experimental cases, no flame propagation to the leaked and accumulated A2L refrigerants in the experimental room was observed, and the situation in the experimental room was not changed before or after the experiment.

Figure 3.2.2 shows the time history of the leaked refrigerant and HF concentration at position 4 in Figure 3.2.1 for the case in which the fan heater is the representative fossil-fuel heating system that is simultaneously used. The time history of refrigerant concentration is similar to that of HF concentration regardless of the operation of the air conditioner. The maximum concentration of the refrigerant was approximately 2 vol%, which is much less than the lower flammable limit (LFL) of R32. More specifically, even when all of the R32 installed in the wall-mount type room air conditioner on the market was leaked to the general living space (approximately 8 m²), the R32 concentration did not exceed the LFL; thus, flame propagation to the room did not occur. These behaviors were also confirmed in the case of R1234yf.

Figure 3.2.3 shows the HF concentration in each refrigerant. Approximately 50–1500 ppm of HF was produced, which is much greater than the permissible value designated by the Japan Society for Occupation and Health (JSOH, 2014). The amount of HF produced in the case where the oil fan heater was used was much greater than that of the radiative stove.

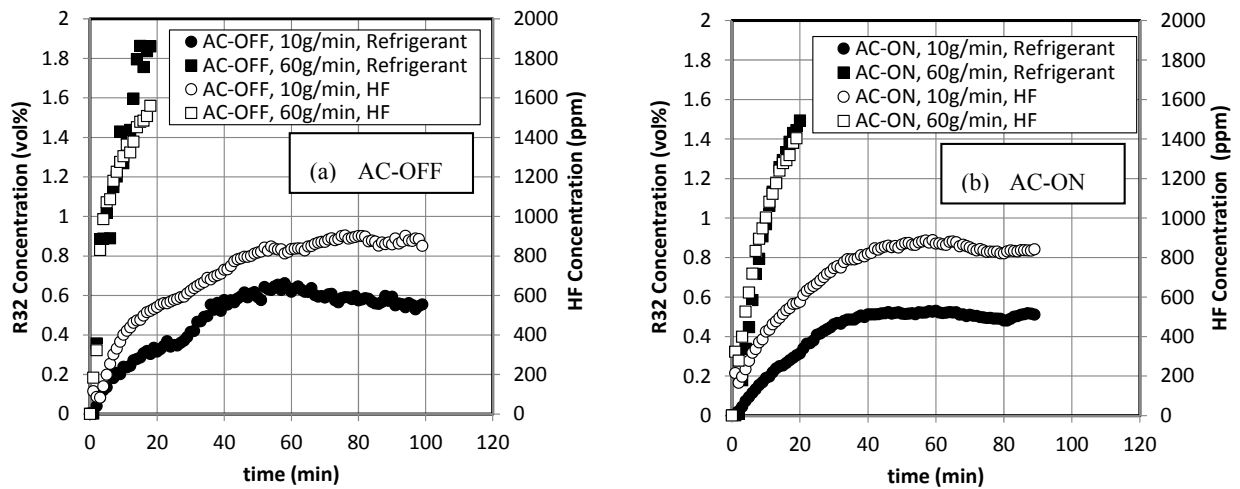


Fig. 3.2.2: Time history of the concentrations of refrigerant and HF at the front of the heating system. Heating system: Oil fan heater, Refrigerant: R32, Capacity of the experiment room: 22 m³
(a) Air conditioning system not in operation (b) Air conditioning system in operation

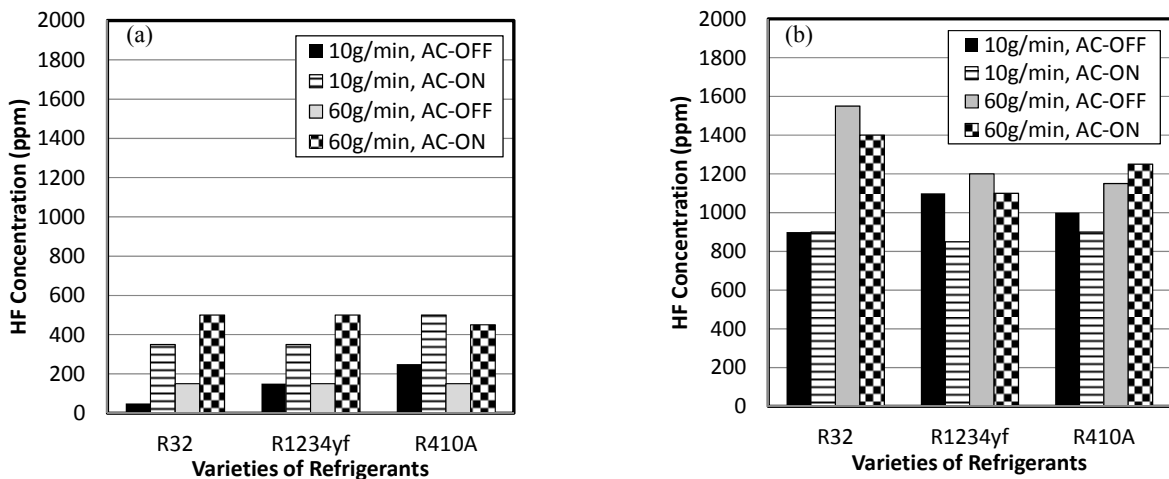


Fig. 3.2.3 Comparison of HF concentration with the leak rate and operation of air conditioning system:
(a) using a radiative oil stove (b) using an oil fan heater

This is because the refrigerant that was sucked into the fan heater was completely burned, whereas in the case of the radiative oil heater, a portion of the refrigerants that made contact with the heating body might not have burned, but only decomposed.

In the case of the radiative oil stove (Fig. 3.2.3(a)), the HF concentration when the air conditioner was in operation was apparently greater than the amount when the air conditioner was not in operation, regardless of the varieties of refrigerants; however, this trend was not always the same in the case of the oil fan heater (Fig. 3.2.3(b)). The reason for this may be

that the flow in the experimental room became complex as a result of the interaction of the circular flow by the fan heater and the air conditioner. In addition, although the HF generation by R32 was slightly higher than that by R1234yf and R410A, the HF generation ability of A2L refrigerants is similar to that of R410A.

3.2.3.2 Case (ii)

The concentration of refrigerant in the experimental room was at most 2 vol%, which is much lower than the LFL of R32. Flame propagation to the unburned refrigerant did not occur and not much HF was produced (less than 50 ppm, which is the guaranteed limit of the data).

3.3 Hazard Evaluation of Handling Situation #2-(a): -Ignition and Flame Propagation Possibility by a Lighter -

3.3.1 Outline

In this scenario, we evaluated the physical hazard for the case in which a commercial portable cigarette lighter is used inside a space in which an A2L refrigerant leaked and accumulated at the service and maintenance factory. A piezo-type gas lighter, a fuel-premixed turbo gas lighter, and a kerosene cigarette lighter were each used as the target gas lighter. The possibility of ignition and flame propagation to the accumulated A2L refrigerants located around the portable lighter were examined. The possibility of ignition from the heat of the cigarette tip was ignored because this type of ignition rarely occurs even for methane gas, which is well-known for being a highly flammable gas (Holleyhead, 1996).

Articles describing some of the details of this topic were published (Imamura et al., 2013, 2014 (in Japanese)).

3.3.2 Details of experimental evaluation of the possibility of ignition and flame propagation using piezo-type gas lighter and fuel-premixed turbo lighter

3.3.2.1 Determination of composition of test mixture

We assumed n-butane as the fuel in the gas lighter. We also assumed that the mixture comprising the fuel of the gas lighter, air, and an A2L refrigerant was formed very close to the outlet of the gas lighter, and we regarded the mixtures of the fuel gas and A2L refrigerant as a single component. In this report, we call the mixture of n-butane and A2L refrigerant “*fuel gas*,” and the mixture of this “*fuel gas*” and air as “*fuel mixture*.” The flammable zone of this “*fuel mixture*” in air was estimated simply using Le Chatelier’s relation (Eq. 3.3.1). In addition, strictly speaking, this estimation is only approximate because, in general, Le Chatelier’s relation is only approved for a mixture of saturated hydrocarbon which Burgess-Wheeler’s relation that multiple values of LFL at 25°C and combustion heat are constant is approved.

$$\frac{1}{LFL} = \frac{n_1}{LFL_1} + \frac{n_2}{LFL_2}, \quad \frac{1}{UFL} = \frac{n_1}{UFL_1} + \frac{n_2}{UFL_2} \quad (3.3.1)$$

where LFL is the lower flammable limit (vol%), UFL is the upper flammable limit (vol%), n is the volumetric fraction of the component (-), subscript 1 is n-butane, and subscript 2 is the A2L refrigerant.

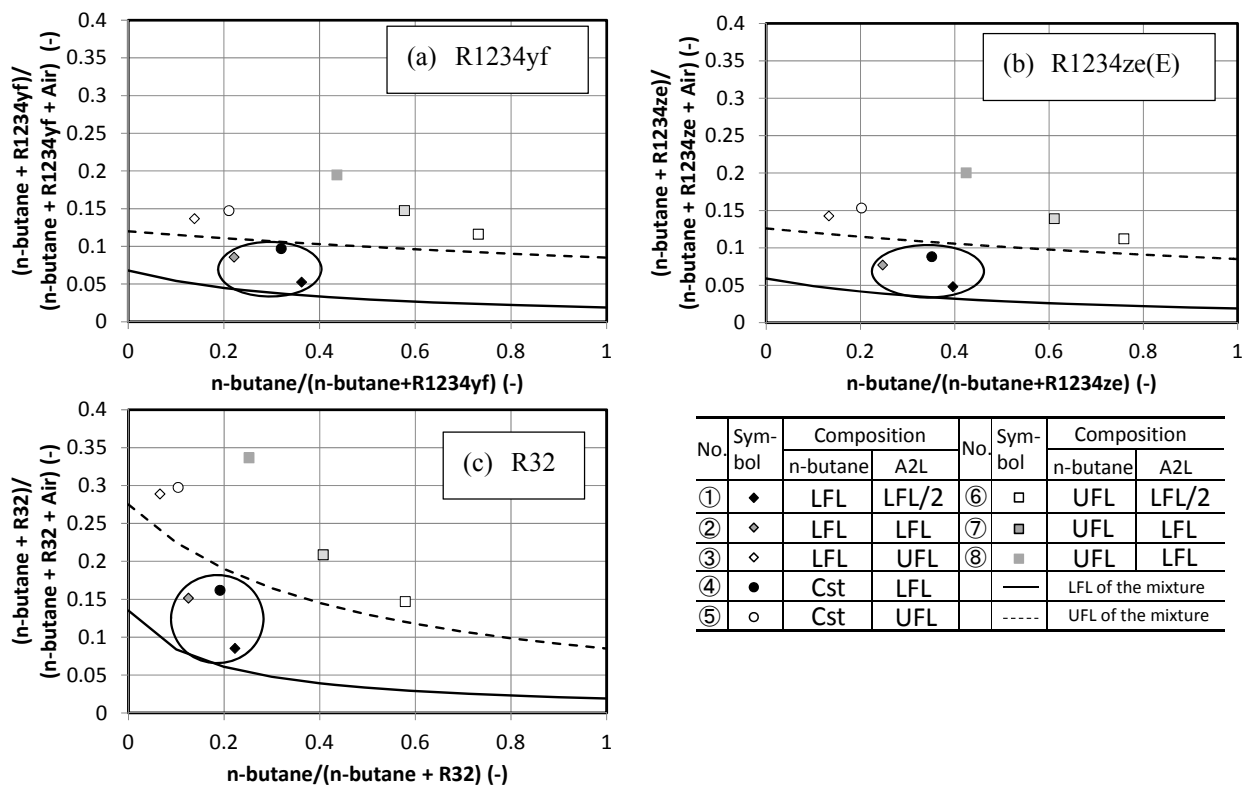


Fig. 3.3.1 Estimation of flammable range and concentration of “fuel mixture” (n-butane+A2L refrigerants) in the air with various compositions of “fuel gas” (n-butane/A2L refrigerant).

The concentration of n-butane very close to the outlet of the lighter ought to exceed the LFL. The examples in Fig. 3.3.1 show the relation between the composition ratio of “fuel gas” in the “fuel mixture” and also that of n-butane against the “fuel gas.” These composition ratios were estimated assuming that the concentration of n-butane was always greater than that of LFL. Thus, we considered the combinations of three concentrations of n-butane (LFL, C_{st} : stoichiometric concentration, and UFL) and of A2L refrigerant (LFL/2, LFL, UFL). The solid curve indicates the variation of LFL estimated from Eq. (3.3.1) with various composition ratios of “fuel gas” in the “fuel mixture,” and the dotted curve indicates that of UFL, respectively. As a result, the concentration of the “fuel mixture” was within the estimated flammable zone when the A2L refrigerant with concentration less than LFL was mixed with n-butane and air. We focused on the mixture having this composition, as shown in the closed circle in Fig. 3.3.1.

The ignition energy of n-butane with the same equivalent ratio as the above composition mixture was within the range of 0.25–2.40 mJ, which is as great as (or less than) the energy from the piezoelectric spark because it is a few millijoules (Matsui, 2012). Therefore, the “fuel gas” the composition of which was between the LFL and UFL curves has some ignition possibility. In addition, the ignition energies of R1234yf and R32, for example, are at least greater than a few dozen millijoules; that is, one figure larger than that of n-butane, hence the ignition energy of “fuel gas” will be much greater than that of n-butane. Therefore, actual ignition possibility is very small. The ignition possibility in the above composition is conceivably a very severe case.

3.3.2.2 Experiment

The operating device for a portable gas lighter comprising a pneumatic cylinder (SSD-X, CKD Corp.) and jig was located 300 mm above the bottom of an acrylic pool of volume 1000 mm³ at the center of the horizontal plane. Air to operate this device was supplied remotely using a solenoid valve at a pressure of 0.15 MPa. A piezo gas lighter and a commercial turbo gas lighter were employed as the ignition sources.

R1234yf, R1234ze(E), and R32 were employed in the evaluation. The A2L refrigerant was leaked in a downward direction from a height of 750 mm above the bottom of the pool. The target leakage rate was 10 g/min for all refrigerants. The refrigerant concentrations at the six vertical positions (0, 100, 300, 500, 750, and 1000 mm in height from the bottom of the acrylic pool) were measured using FT-IR before pushing the button of the piezo gas lighter. The vertical distribution of the refrigerant concentration was constant for heights less than 500 mm.

The operation to push the button of the lighter was maintained for 2 or 10 s per cycle. This operation was repeated for five or nine cycles at intervals of 5 s per cycle. The situation at the lighter outlet was observed using a digital video camera (Xacti, 30 fps, SANYO Electric Co., Ltd., Osaka).

3.3.2.3 Results and discussions

3.3.2.3.1 Piezo gas lighter

Figure 3.3.2 shows photographs of the piezo gas lighter and its surroundings. In the case of the accumulated A2L refrigerant with LFL concentration, a pale quick emission was observed near the outlet of the lighter, but this pale emission was quenched 1/30 s later. Flame propagation to the entire refrigerant in the surroundings was not observed. In the case

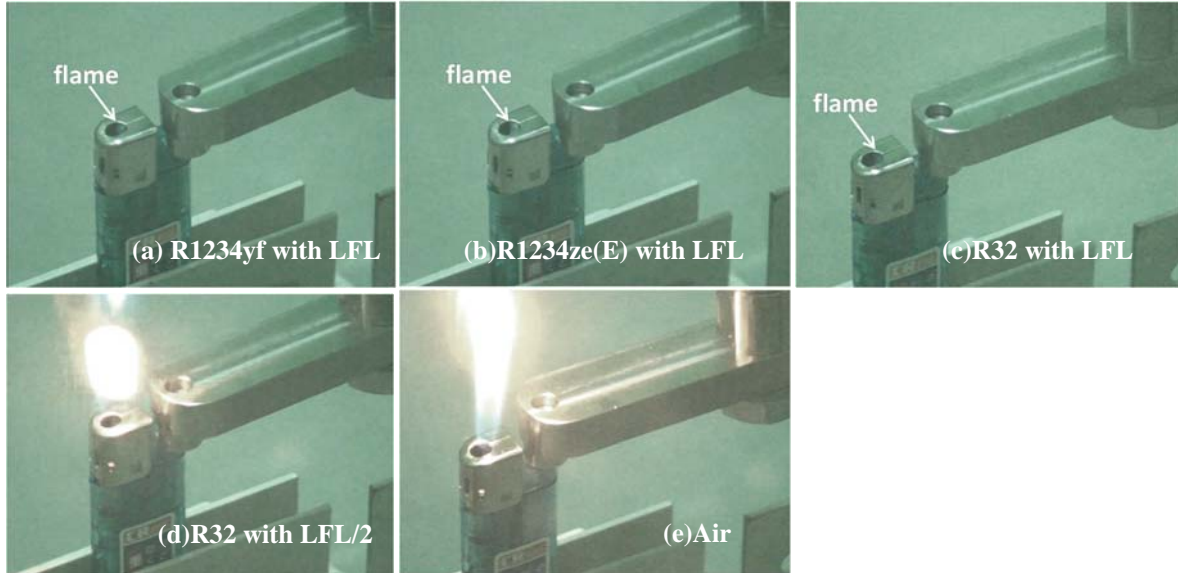


Fig. 3.3.2 Photos of the electronic piezo lighter and the surroundings near its outlet in the accumulated A2L refrigerant.

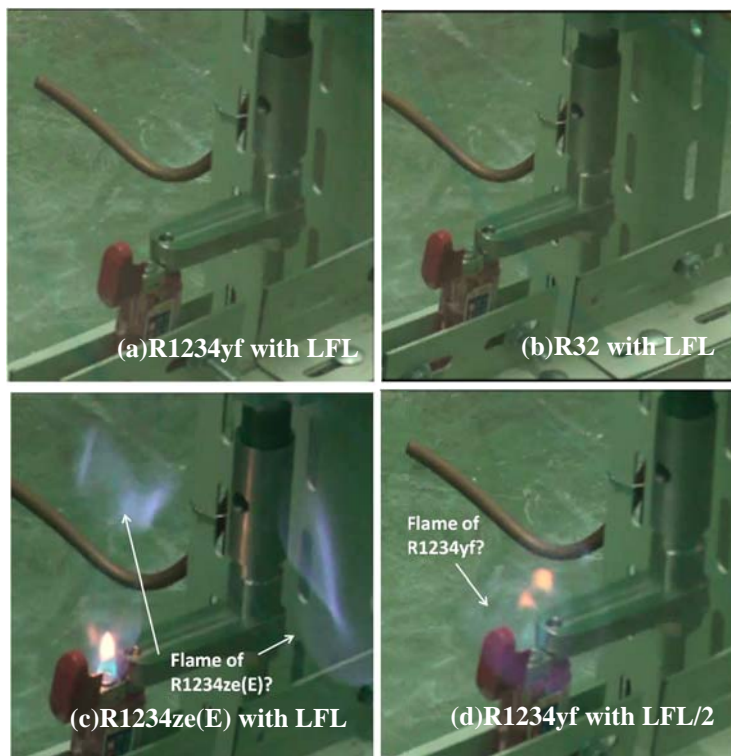


Fig. 3.3.3 Photos of the premixed turbo lighter and the surroundings near its outlet in the accumulated A2L refrigerant.

of the accumulated A2L refrigerant with a concentration of LFL/2, an open flame was generated at the gas lighter for several cases. However, the flame also failed to propagate to the entire refrigerant. These trends were also confirmed for the other refrigerants.

3.3.2.3.2 Premixed turbo gas lighter

Figure 3.3.3 show photographs of the fuel-premixed turbo gas lighter and its surroundings. For R1234yf and R32, the ignition property was nearly identical to the case using the piezo gas lighter. However, for R1234ze(E), with a low LFL and 71% R.H., a small flame propagation to the refrigerant in the surroundings was confirmed in several cases. Afterwards, the experiment was performed using identical conditions, but flame propagation was not confirmed. Although the apparent reason for this trend has not been verified, we considered the cause to be that mixing of the refrigerant and air proceeded as a result of the repeated operation of pushing the button, such that the flame generated at the outlet of the lighter propagated to the refrigerant. However, the flame did not propagate to the entire refrigerant in the surroundings; it was quenched 1–2 s afterwards.

3.3.3 Details of experimental evaluation of the possibility of ignition and flame propagation using kerosene cigarette lighter

3.3.3.1 Outline

In the situation of service and maintenance of air conditioning systems with A2L refrigerants installed, a kerosene cigarette lighter was assumed as the ignition source. The fuel of the kerosene cigarette lighter always vaporized into the windbreak when the cap was open. This point is the major difference to the piezo gas lighter and premixed turbo gas lighter. Further, the size of the open flame was larger than that of the piezo gas lighter and the premixed turbo gas lighter. We experimentally evaluated the possibility of ignition and flame propagation to the accumulated A2L refrigerant using a commercial kerosene cigarette lighter. An article describing the details of this topic has been submitted to an international journal for publication; consequently, we present only the key points of this topic in this report.

3.3.3.2 Experiment

Figure 3.3.4 is a schematic diagram of the experimental setup. Difluoromethane (called “R32” in this report) was used as the test A2L refrigerant. R32 was leaked downwards into an acrylic pool with dimensions 1000 mm × 1000 mm × 1000 mm. A commercial-use kerosene cigarette lighter was located 300 mm above the center base of the pool. To ignite the kerosene cigarette lighter remotely, an AC electric spark was generated at the gap of the electrodes (2-mm-diameter, stainless steel) which was oriented near the wick in the windbreak by an inverter-type neon transformer (CR-N16, Kodera Electronics, Co., Ltd., Gifu). A solid-state electrical relay (GSR-20L-D32Z, Misumi Group, Inc., Tokyo) was inserted into the power supply circuit. Switching by turning the electrical supply to the solid-state relay was controlled by means of a rectangular wave signal of 5 V p-p DC, generated by a function generator (33120A, Agilent Technologies, Santa Clara, CA). The electricity was supplied to the solid-state electric relay for 50, 100, and 500 ms (referred to as the “energization time”). In each ignition test, the switching action to energize the relay was repeated ten times at intervals of 5 s. The generated voltage between the gap of the electrodes was measured by means of a high-voltage probe (P6015A,

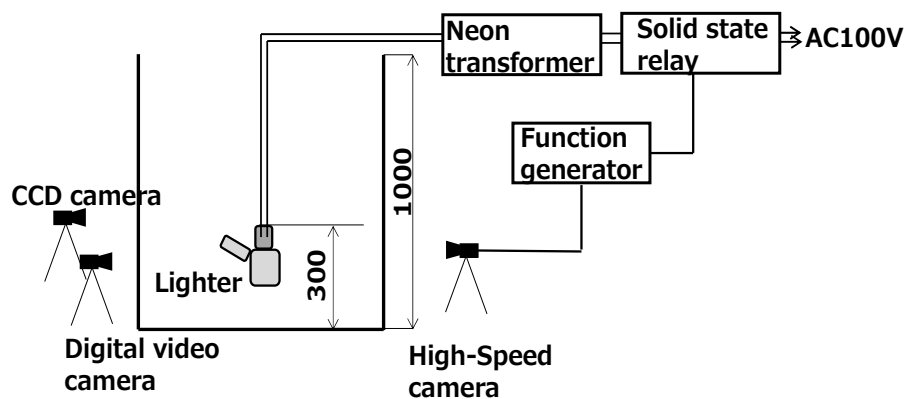


Fig. 3.3.4 Schematic diagram of the experimental setup for ignition test by a kerosene cigarette lighter. Unit: mm.

Tektronix Inc., Beaverton, OR), and the generated current was measured by means of a current transformer (Model 2100, Pearson Electronics Inc., Palo Alto, CA).

Video recordings of the kerosene lighter and its surroundings, containing R32, were made using a high-speed camera (FASTCAM SA-X; Photron Ltd., Tokyo), a digital video camera (HC-V520M, Panasonic Corporation, Osaka), and a

CCD camera (MTV-53KM21H, Mintron Enterprise, Co., Ltd., Taipei). The timing of the beginning of energization of the solid-state relay and that of commencement of the video recording by the high-speed camera were synchronized by means of a trigger signal generated by a function generator.

R32 in the amount of 220 g was leaked from a position 750 mm above the base of the pool at a leakage rate of 10 g/min. Before the ignition test, the concentrations of the accumulated R32 were measured by means of Fourier transform infrared spectroscopy with an FT-IR4200 spectrometer (JASCO Corporation, Tokyo). Concentrations were measured at heights of 0, 100, 300, 500, 750, and 1000 mm above the center of the base of the pool.

The composition of the mixture in the windbreak of the lighter in an atmosphere of accumulated R32 was analyzed by gas chromatography/mass spectrometry (GC/MS; GC-17A, Shimadzu Corporation, Kyoto). A 2.0-m-long vinyl tube with an internal diameter of 4 mm (total volume, 25.12 mL) was inserted into the windbreak. A 26 mL gas sample, which included air from the extraction tube and the gaseous mixture from the windbreak, was extracted, and a 200 μ L portion was analyzed by GC/MS in a single run. The GC/MS analysis was repeated four times.

3.3.3.3 Results and discussions

3.3.3.3.1 Evaluation of the ability of the supplied spark energy to ignite the wick of the kerosene lighter

Before performing the ignition test of the accumulated R32 by the kerosene cigarette lighter, validation of the supply energy by comparison with the actual spark energy generated by rubbing a flint was necessary. The energy of the actual spark by rubbing is mainly due to the formation heat of the worn-down flint particle. It is known that the general composition of a flint alloy is 70 wt% of cerium and 30 wt% of iron (Japan Smoking Articles Corporate Association, 2008). Therefore, we estimated the actual spark energy generated by rubbing the flint, assuming that the composition of flint alloy is also the same as the above general composition, and compared it with the supplied electrical energy, which is calculated by integration of the generated voltage and current over the energization time.

We measured the mass of the worn-down flint particles per rubbing by measuring the decrease in mass of the flint after 500 repeated rubbings, and obtained the mass of worn-down particles of the flint per rubbing as 1.2×10^{-4} g. The heat of oxidation of this flint particle was estimated at 1.2 J. On the other hand, the energies of the electric AC sparks were estimated approximately in the range 0.2–2.3 J under the present energized times (50–500 ms). These values for energies were hardly different from the spark energy generated by rubbing the flint. Therefore, the experiment in which the fuel of a kerosene lighter is ignited by an electric spark was deemed capable of simulating the actual situation of ignition of kerosene lighter by direct rubbing of the flint.

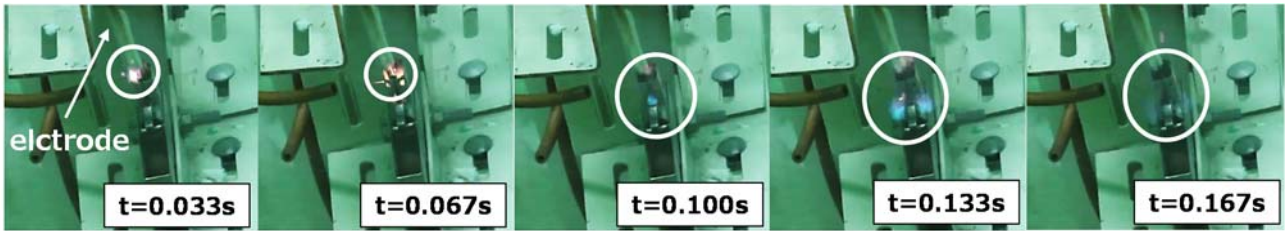
3.3.3.3.2 Results of experiments on the ignition of R32 by a kerosene lighter

Figure 3.3.5(a) shows photographs of the lighter and its surroundings containing R32 for sparks with an energization time of 50 ms. Although the wick of the lighter in the windbreak ignited for an instant, no steady open flame formed, and no flame propagation to the rest of the accumulated R32 occurred in any instance of the switching action.

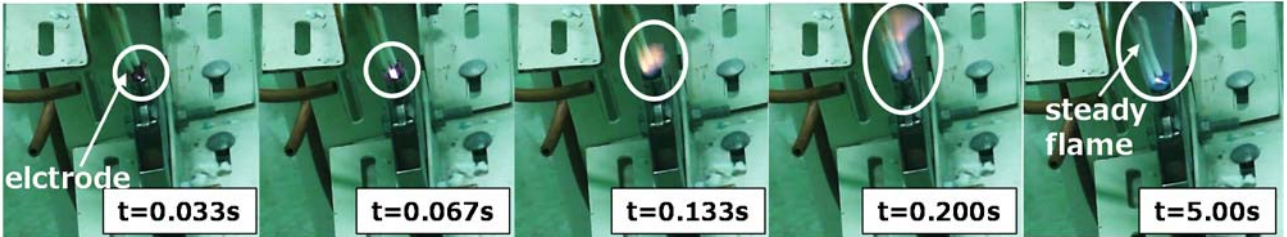
Figure 3.3.5(b) similarly shows photographs for sparks with an energization time of 500 ms. A steady open flame formed at the wick in the third cycle of the switching action, and the generated open flame propagated smoothly to the surrounding R32.

Figure 3.3.5(c) similarly shows photographs for sparks with an energization time of 500 ms. A steady open flame formed at the first switching action. Flame propagation occurred more immediately than was the case for an energization time of 100 ms.

When an AC electric spark was generated in isolation at a position 300 mm above the bottom of the acrylic pool in the accumulated R32, no ignition or flame propagation to the entire volume of R32 was observed, regardless of the energization time. This confirmed that ignition of the R32 and flame propagation in the gas were not caused directly by the electric spark, but were instead, caused by the open flame in the windbreak of the lighter. In addition, in some cases, no AC electric spark was observed in the accumulated R32. This suggests that the voltage required to produce electrical breakdown might differ between that in the mixture present in the windbreak of the lighter and that in the accumulated R32 in the absence of the lighter. In other words, it is possible that the mixture in the windbreak of the lighter did not contain any R32. In the present experiments, the rate of R32 was very slow (10 g/min); thus, it is likely that there was little mixing between the R32 and the gas in the windbreak.



(a) Energized time: 50 ms



(b) Energized time: 100 ms



(c) Energized time: 500 ms

Fig. 3.3.5 Photos of the kerosene cigarette lighter and its surroundings in the accumulated R32 before and after operation of the electricity supply to the electrode located in the windbreak. Concentration at the location of the lighter: approximately 16 vol%.

We analyzed the composition of the gas in the windbreak by means of GC/MS. Although some scatter occurred, similar significant peaks for the fuel alone were generally observed, whereas those for R32 alone were barely visible in any of the sample gases. This indicates that the gas mixture in the windbreak consisted of vaporized kerosene and air even when the lighter was positioned in the accumulated R32. It is therefore reasonable that an open flame was produced at the wick of the lighter by an electric spark of a similar energy to that produced by rubbing the flint, and that this flame propagated to the entire volume of R32. On the basis of the above results and discussions, the use of a kerosene cigarette lighter in accumulated R32 might be capable of causing ignition of and flame propagation to R32.

3.4 Hazard Evaluation of Situation #2-(b): -Physical Hazard of Rapid Leakage from a Pinhole-

3.4.1 Outline

In this situation, we assumed that an accident occurred in which an A2L refrigerant leaked from a fracture or pinhole formed in pipes or hoses during the factory service and maintenance. We evaluated the possibility for ignition of the entire refrigerant jet when there is an ignition source such as an electric spark near the refrigerant jet. We also evaluated the magnitudes of physical damage by the refrigerant jet igniting. An article describing the details of this topic was published in 2015 (Imamura et al., 2015).

3.4.2 Experiment

3.4.2.1 Refrigerant leakage system

The model leakage system consisted of a refrigerant cylinder, a balance, a regulator, a pressure gage, and a pinhole unit.

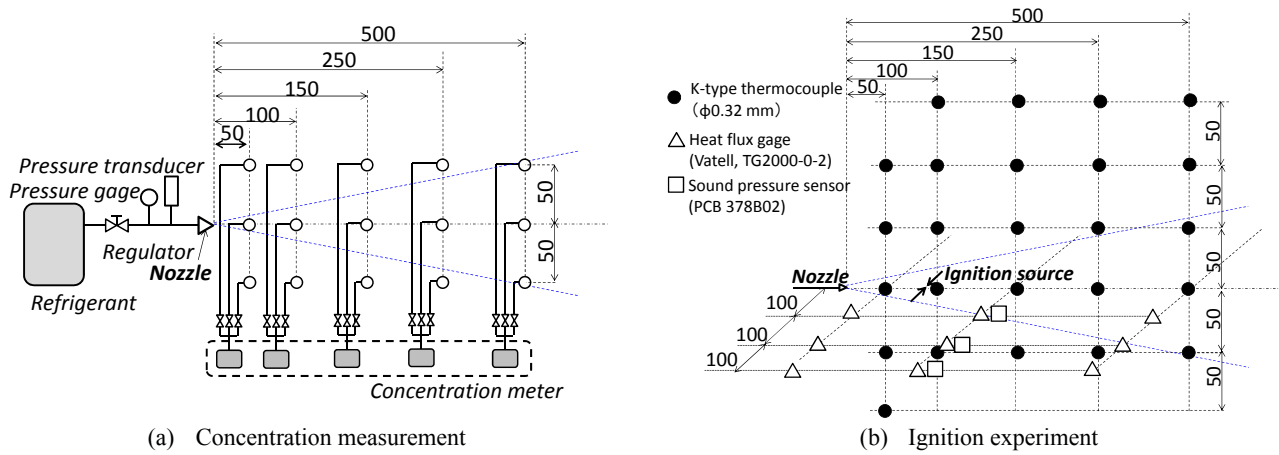


Fig. 3.4.1 Schematic diagram of experimental setup and measurement positions of concentrations, temperatures, heat flux, and sound pressures. Unit: mm

Table 3.4.1 List of experimental conditions for concentration measurement for situation #2-(b).

Experiment No.	Refrigerant	Pinhole diameter (mm)	Mass flow rate (g/min)
J20-38	R32	0.2	47.5
J20-08		1	82.5
J19-01		1	66.7
J20-03		3	116.7
J20-04			126.7
J20-09		3	297.5
J20-05		4	110.0
J20-10			195.0
J20-11		4	540.0
J20-07		1x4hor	82.5
J20-13		1x4hor	187.5
J20-06		1x4ver	97.5
J20-12	1x4ver	245.0	
J20-24	R1234yf	0.2	5.0
J20-25		0.2	17.5
J20-14		1	107.5
J20-19		1	122.5
J20-15		3	140.0
J20-20			542.5
J20-16		4	115.0
J20-21		4	472.5
J20-18		1x4hor	130.0
J20-23		1x4hor	335.0
J20-17		1x4ver	137.5
J20-22		1x4ver	320.0
J20-31	R1234ze (E)	0.2	5.0
J20-32		0.2	22.5
J20-26		1	82.5
J20-33		1	97.5
J20-27		3	97.5
J20-34			272.5
J20-28		4	87.5
J20-35		4	192.5
J20-30		1x4hor	85.0
J20-37		1x4hor	92.5
J20-29		1x4ver	85.0
J20-36		1x4ver	102.5

Table 3.4.2 List of experimental conditions for ignition measurement for situation #2-(b).

Experiment No.	Refrigerant	Pinhole diameter (mm)	Ignition Source	Mass flow rate (g/min)	
J22-21	R32	1	Ne-TR	260.0	
J22-27			Spark	172.5	
J22-22		3	Ne-TR	726.7	
J22-28			Spark	600.0	
J21-01		4	Spark	285.0	
J21-02				250.0	
J21-03			N.D.		
J21-04			Ne-TR	670.0	
J21-05			Openflame	N.D.(*)	
J22-25			Ne-TR	413.3	
J22-26		Spark	847.5		
J22-24		1x4 hor	Ne-TR	386.7	
J22-23	1x4 ver	Ne-TR	433.3		
J22-29		Spark	367.5		
J22-11	R1234yf	1	Ne-TR	106.7	
J22-12		3	Ne-TR	400.0	
J21-07		4	Spark	580.0	
J21-08			Ne-TR	500.0	
J21-09				500.0	
J21-10			650.0		
J22-14		1x4 hor	Ne-TR	346.7	
J22-13		1x4 ver	Ne-TR	353.3	
J22-15		R1234ze (E)	1	Ne-TR	120.0
J22-16			3	Ne-TR	260.0
J22-17			4	Ne-TR	220.0
J22-20			1x4 hor	Ne-TR	260.0
J22-18	1x4 ver		Ne-TR	140.0	
J22-19				213.3	

These components were connected by copper and stainless tubes. The outside diameter of these tubes was 6.35 mm ϕ (1/4"). Leak pressure was monitored by means of a pressure gage (PGI63B-MG2.5-LAQX, Swagelok Company, Solon, OH) and strain gage type pressure transmitter (PGS-20KA, Kyowa Electric Instruments, Co., Ltd., Tokyo). The pinhole was modeled using a cap-type coupling (1/4", SS-400-C, Swagelok Company) with a hole in the center. Two patterns were used for the shape of the hole: a circular pinhole and a rectangular slit. The diameter of the pinhole ranged over the values 0.2, 1.0, 3.0, and 4.0 mm, whereas the size of the rectangular slit was 1.0 mm \times 4.0 mm.

3.4.2.2 Concentration measuring system

Before conducting the ignition experiment, concentrations of the leaked refrigerant jet were measured using five ultrasonic gas analyzers (US-II-T-S, Daiichi Nekken Co., Ltd., Hyogo). The concentration was estimated from the average molecular weight, specific heat ratio, gas constant, and temperature. Concentrations were measured at 50, 100, 150, 250, and 500 mm in the downstream direction and -50, 0, 50 mm in the vertical direction from the center of the pinhole, i.e., the concentrations of refrigerant were measured at 15 positions, as shown in Figure 3.4.1(a). Because the refrigerant concentrations could only be measured at five positions at any given time, the refrigerant concentrations at the 15 positions were measured in groups of five by switching the valves. Positive height values indicate distances above the center of a pinhole, whereas negative values indicate distances below it. Refrigerant concentrations were measured for 30 s at each position because the refrigerant concentration approximately attained a uniform value within a period of less than 30 s after the opening of the valve.

3.4.2.3 Ignition experiment

In the ignition experiment, a single spark (DC), a continuous spark (AC), and an open flame were used as the ignition source. The single spark was generated using a high-voltage system (MEL1140B, Genesis Co., Ltd., Ibaraki). The designed energy of the spark was approximately 10 J. The continuous spark was generated using an inverter-type neon transformer (CR-N16, Kodera Electronics, Co., Ltd., Gifu). In the case where the continuous AC spark was used, the discharge time was varied over the range 15–30 s, so the total supply energy was more than the approximate order of 100 J. The length of the open flame was about 100 mm. These ignition sources were located 90 mm downstream from the center of the pinhole at the same height as the center of the pinhole.

In the ignition experiments, temperatures were measured at 25 points by means of 0.32 mm ϕ K-type thermocouples, heat fluxes were measured using nine heat flux sensors (TG2000-2, Vatell Co., Ltd., Christiansburg, VA), and sound pressures were measured using three microphones (378B02, PCB Piezotronics Inc., Depew, NY). The measured positions of these parameters are shown in Figure 3.4.1(b). The response time of the thermocouple was approximately 1–2 s, and that of the heat flux sensor was 1.5 ms.

3.4.2.4 Experimental conditions

The effects of various refrigerants, pinhole diameters, refrigerant mass flow rates, and varieties of ignition sources on the formation of flame and damage by combustion were examined experimentally. R1234yf, R1234ze(E), and R32 were used as test refrigerants. Leakages of these refrigerants were in the gas phase state. A list of experimental conditions for the concentration measurement is given in Table 3.4.1 and a list for the ignition experiment is given in Table 3.4.2. A 4-mm-diameter pinhole was chosen to correspond with a case in which the pipe or hose was broken completely, and a 0.2-mm-diameter pinhole was chosen to correspond to a case where a slight crack formed in the pipe or hose. In the cases shown by shading in Table 3.4.1, the refrigerant was leaked directly from a cylinder without passing through a regulator. Although the vapor pressure of the refrigerant is comparatively lower than the maximum operating pressure of a refrigerant in an air conditioning system, the air conditioning system would not be operational during service and maintenance. In addition, leakage from a hole with a 4-mm-diameter hardly occurs except when there is a complete fracture of the pipe or hose. On the basis of these considerations, the case of a refrigerant leaking at its vapor pressure from a 4-mm-diameter pinhole was assumed to correspond to the case of a very severe accident. In all the ignition experiments, the refrigerant was leaked directly from a pinhole without passage through the regulator, as shown in Table 3.4.2.

3.4.3 Results and discussions

3.4.3.1 Formation of flammable zone

Figures 3.4.2 show contour maps of concentrations of the refrigerant under various conditions. The iso-concentration curves are plotted at 2.5 vol% intervals, except for Figure 3.4.2(d), where the interval is 1.0 vol%. Figure 3.4.2(a), (b),

(e), and (f) show the result for R32, whereas Figures 3.4.2(c) and (d) show the results for R1234yf. The concentration

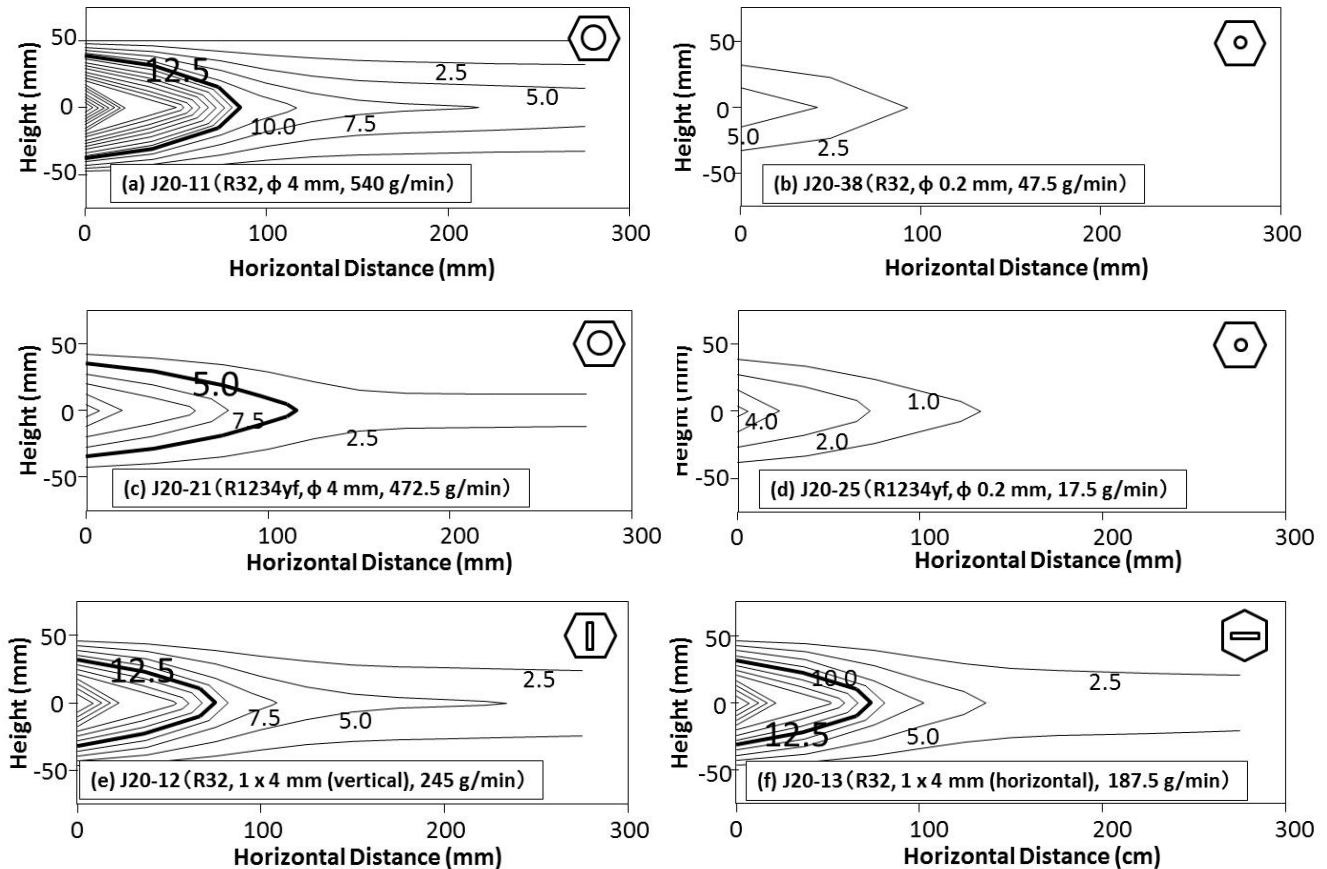


Fig. 3.4.2 Contour maps of averaged concentrations of leaking refrigerant jets under various leakage conditions.

curve at 12.5 vol% for Figures 3.4.2(a), (b), (e), and (f) and at 5.0 vol% for Figures 3.4.2(c) and (d) are shown as bold curves that correspond to concentrations slightly below the lower flammability limit [13.5 vol% for R32; 6.7 vol% for R1234yf (Kondo et al, 2012)].

In the cases shown in Figures 3.4.2(a) and (c), where the refrigerant leaked directly from a cylinder without passage through a regulator, the tip of the bold curve reached a position only 100 mm downstream from the pinhole, and the end of the bold curve in the vertical direction reached less than ± 50 mm. In other words, although the initial leak pressure was identical to the vapor pressure and part of the pipe was completely broken (the pinhole diameter was similar to the internal diameter of the pipe), corresponding to a very severe situation—a flammable zone was formed only locally. In the case of 0.2-mm-diameter pinhole (Figure 3.4.2(b) and (d)), no flammable zone was formed. The direction of the rectangular slit had barely any effect on the formation of the flammable zone, as shown in Figures 3.4.2(e) and (f).

3.4.3.2 Ignition and flame propagation

Figures 3.4.3 to 3.4.5 show photographs of a jet of leaking refrigerant in the presence of various sources of ignition. Figure 3.4.3(a) shows a leaking jet of R32 making contact with a single DC spark. In this case, although spark ignition was confirmed, as shown in the white closed circle in Figure 3.4.3(a), no flame propagation occurred in the leaking R32 (Figure 3.4.3(b)). Neither ignition nor flame propagation to the refrigerant was observed with R1234yf or R1234ze(E). In the case shown in Figure 3.4.4, the jet of leaking R32 made contact with a continuous spark. At the start of the refrigerant leak, a pale-violet emission was observed around the electrode (Figure 3.4.4(a)). This grew with time, although it was pushed away in the downstream direction (Figures 3.4.4(b) and (c)). However, as the temperature of the leaking refrigerant decreased with time and the leaking refrigerant produced a fog, a pale-violet emission became weakly visible (Figures 3.4.4(d) and (e)). With further passage of time and the formation of a steady jet of leaking refrigerant, the pale-violet emission was again observed, but only locally (around the electrode), and flame propagation to the entire refrigerant jet was not observed (Figure 3.4.4(f)). In Figure 3.4.5, the jet of leaking R32 made contact with an open flame. When the leak started, although an open flame was formed vertically at first (Figure 3.4.5(a)), it was gradually pushed away in the downstream direction and a pale-violet emission appeared at the bottom of the open flame (Figure 3.4.5(b)). The pale-

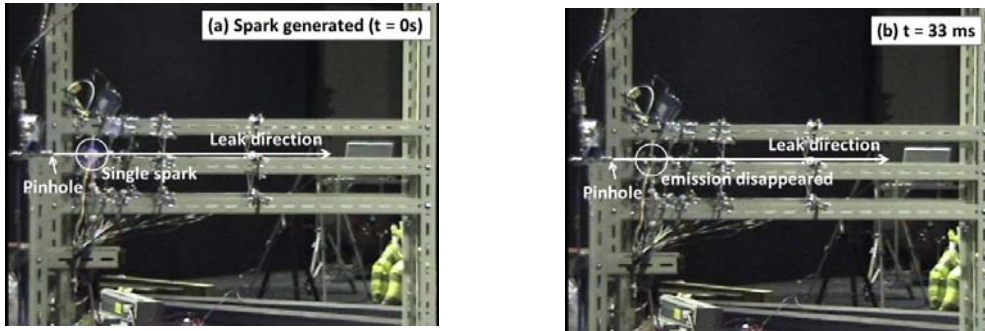


Fig. 3.4.3 Photographs of leaking refrigerant jet in contact with a single spark.
Refrigerant: R32; Pinhole: 4 mm ϕ ; Leak pressure: 0.81 MPa.

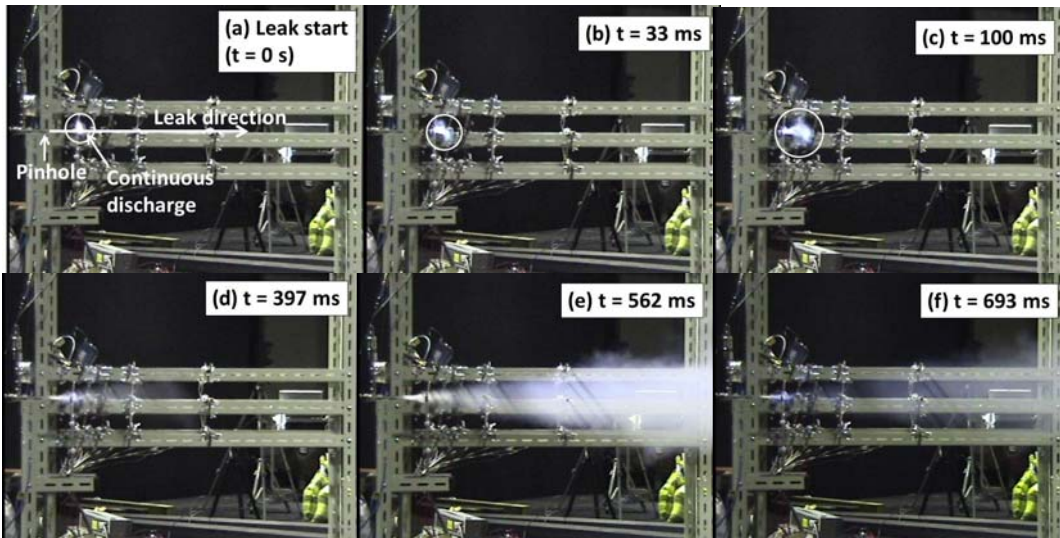


Fig. 3.4.4 Photographs of leaking refrigerant jet in contact with a continuous spark.
Refrigerant: R32; Pinhole: 4 mm ϕ ; Leak pressure: 0.66 MPa.

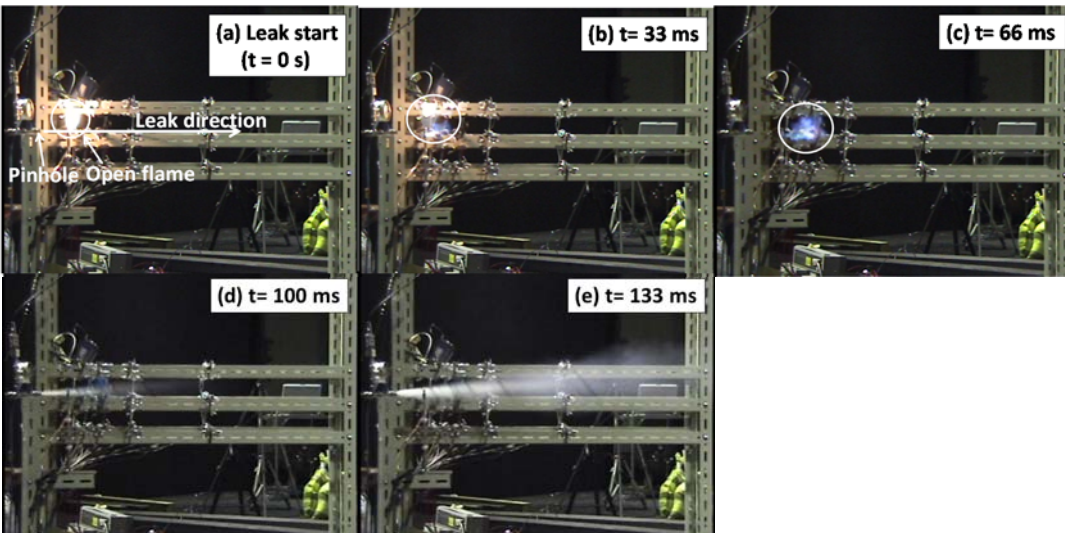


Fig. 3.4.5 Photographs of leaking refrigerant jet in contact with an open flame.
Refrigerant: R32; Pinhole: 4 mm ϕ ; Leak pressure: 1.16 MPa.

violet emission, which is characteristic of burning R32, then appeared and the bright emission of the open flame disappeared (Figure 3.4.5(c)). However, immediately afterwards, the pale-violet emission disappeared and no flame propagation to the bulk of refrigerant was observed. The open flame was therefore blown off.

3.4.3.3 Physical effects-temperature, heat flux, and combustion products

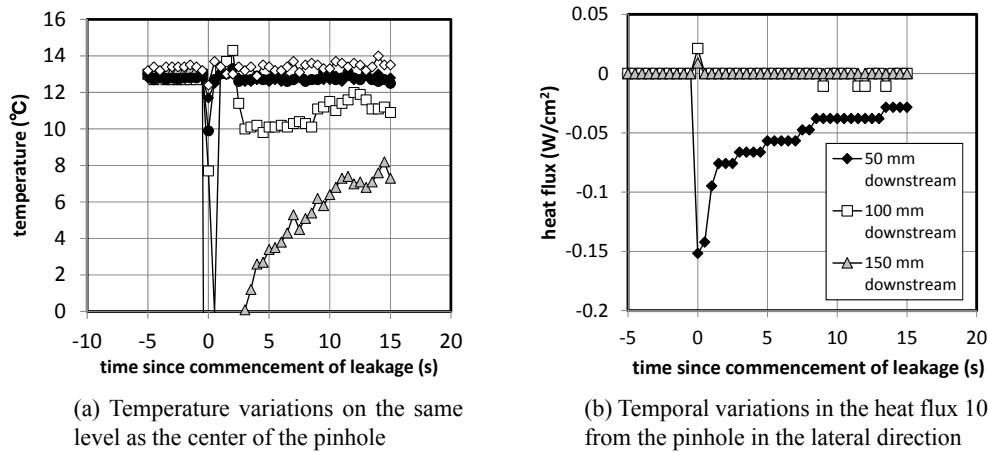


Fig. 3.4.6 Temporal variations in the temperature and heat flux around a leaking refrigerant jet. Refrigerant: R32; Pinhole: 4 mm ϕ ; Leak pressure: 1.06 MPa; Ignition source: continuous AC spark

Figure 3.4.6(a) shows the temporal history of the temperature at the same height as the center of the pinhole when R32 was leaked at a pressure of 1.06 MPa from a 4-mm-diameter pinhole. The ignition source was a continuous AC spark. Because the diameter of the thermocouple was 0.3.2mm, its response might not have been capable of following sudden temperature variations. Therefore, temperature data for the time immediately following the start of the leakage are not always reliable. However, if the leaked refrigerant was ignited by the continuous AC spark and a flame propagated to the entire leaked refrigerant jet, the temperature at the same height as the center of the pinhole should show a significant increase; but this was not observed in the present experiment, as can be seen in Figure 3.4.6(a).

Figure 3.4.6(b) shows the variation in the heat flux 100 mm from the central axis in the lateral direction. The surroundings around the leaked refrigerant jet were cooled as a result of the temperature decrease of the leaked refrigerant jet, resulting in the appearance of negative heat flux values. However, no significant increase in the heat flux was observed at either this or at other measurement positions.

The concentration of the combustion product (hydrogen fluoride, HF) was monitored by means of a portable gas analyzer (SC-70, Riken Keiki Co., Ltd., Tokyo). HF was generated at concentrations below the alarm concentration (3 ppm). Similar properties were observed under all the experimental conditions examined.

3.5 Hazard Evaluation of Situation #2-(c): - Physical Hazard of Leakage into the Collection Device -

3.5.1 Outline

In this scenario, we assumed that an A2L refrigerant leaked into the interior of a piece of equipment used for service and maintenance, such as a collection device. The leakage and ignition behaviors of the A2L refrigerant in the model collection

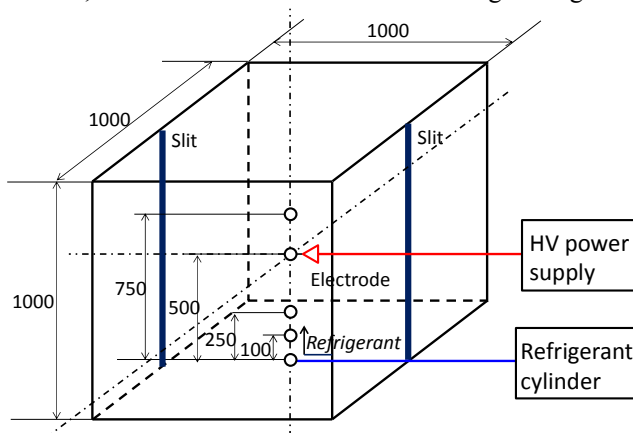


Fig. 3.5.1 Schematic representation of the experimental setup for Situation #2-(c).

○: positions for measurements of the concentration.

Table 3.5.1 List of experimental conditions for the situation #2-(c).

Experiment No.	Refrigerant	Slit width (mm)	Mass flow rate (g/min)
J26-01	R1234yf	0	390.0
J26-02		1	390.0
J26-03		5	390.0
J26-04		10	410.0
J26-05			380.0
J26-07			20
J26-08		R1234yf (Liquid)	20

device were examined for this situation. In particular, the effect of slits in the collection device designed to prevent accumulation and ignition of leaked refrigerant within the device was investigated. An article describing the details of this topic was published in 2015 (Imamura et al., 2015).

3.5.2 Experiment

3.5.2.1 Experimental setup

A 1000 mm × 1000 mm × 1000 mm acrylic pool was used as a model for the collection device. One plane of this model was covered with a vinyl sheet. The model collection device was provided with slits having several varieties of widths to permit diffusion of the refrigerant. Although this model collection device was larger than the ones in general use, we considered that the results of evaluations made using it would show more severe results than that posed by collection devices currently in use, because the amount of leaking refrigerant was greater than that which would be present in an actual situation.

Concentrations of the refrigerant in the model collection device were measured at five positions, located 0, 100, 250, 500, and 750 mm above the bottom and center of the model collection device, as shown in Figure 3.5.1. Concentrations of refrigerant were measured simultaneously using five ultrasonic gas analyzers of the same type as those used in the experiment for Situation #2-(b) (see section 3.4).

In the ignition experiment, a DC spark from a 16 J apparatus (Yokogawa Denshikiki Co., Ltd., Tokyo) was used as the ignition source. This ignition source was located at the center of the model collection device (500 mm above the bottom of the collection device). The DC spark was generated 30 s after the refrigerant leakage had stopped.

3.5.2.2 Experimental conditions

Experimental conditions were changed by selecting the width of the slits in the facing to be 0, 1, 5, 10, or 20 mm. In this experiment, R1234yf was the only test refrigerant used. Refrigerant in the gas phase state was leaked from a copper tube with a 6.35-mm-outside diameter without passage through a regulator, so that the mass flow rate was approximately 400 g/min. The leakage time was 60 s. The refrigerant was discharged in the upper vertical direction from the center bottom of the model collection device. The experimental cases are shown in Table 3.5.1. Only in the case of J26-08 was R1234yf leaked in the liquid-phase state.

3.5.3 Results and discussions

3.5.3.1 Concentration distribution in the model collection device

Figure 3.5.2 shows the changes in the concentration of the refrigerant in the model collection device over time. When the slit width w_s was 0 mm (Figure 3.5.2(a)), the concentration of the refrigerant increased immediately after commencement of the discharge. When the refrigerant discharge was stopped ($t = 60$ s), the concentration reached a uniform value that showed barely any change with time. When $w_s = 1$ mm (Figure 3.5.2(b)), the concentration was uniform for a comparatively long time after the refrigerant leakage was stopped, and it then decreased slowly. For example, at a height (z) of 500 mm above the bottom of the model collection device, where the ignition source was located, the time taken for the concentration to exceed the LFL (called the persistence time in this paper) was approximately 480 s. On the other hand, for $w_s = 20$ mm (Figure 3.5.2(c)), the concentration decreased immediately on cessation of the refrigerant discharge. At $z = 50$ cm, the persistence time was approximately 60 s.

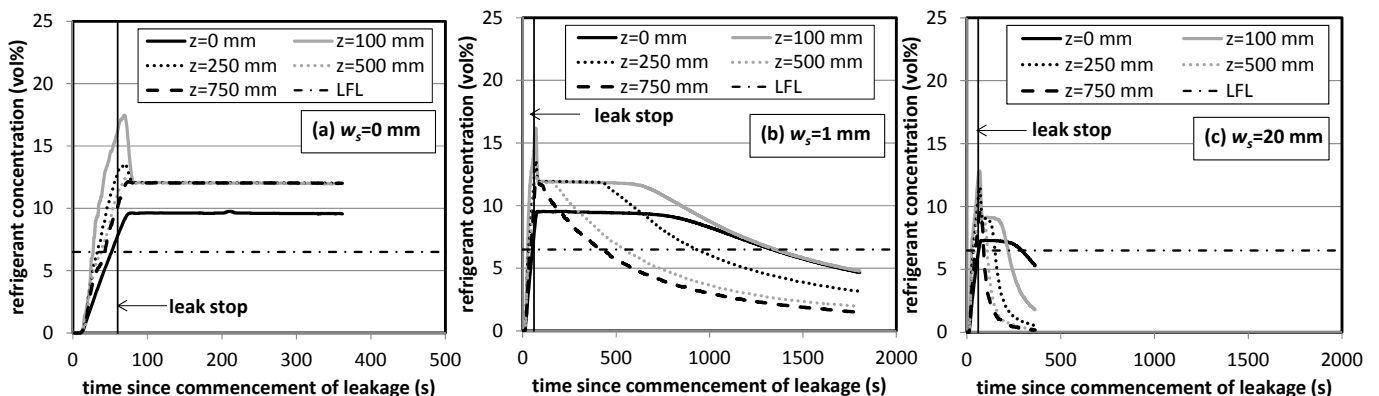


Fig. 3.5.2 Temporal variations in refrigerant concentrations leaking into the model collection device with several slit widths.

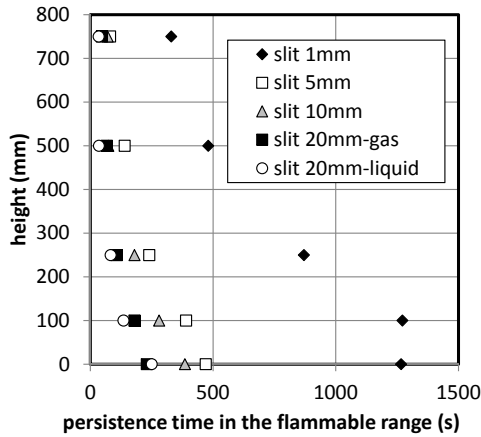


Fig. 3.5.3 Relationship between the height and the persistence time when the refrigerant concentration exceeded the flammable range.

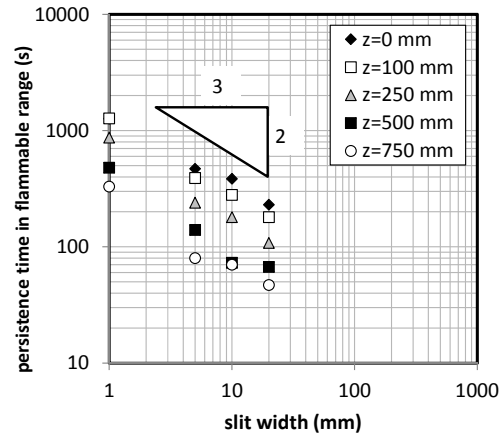


Fig. 3.5.4 Relationship between the persistence time and the slit width at various heights.

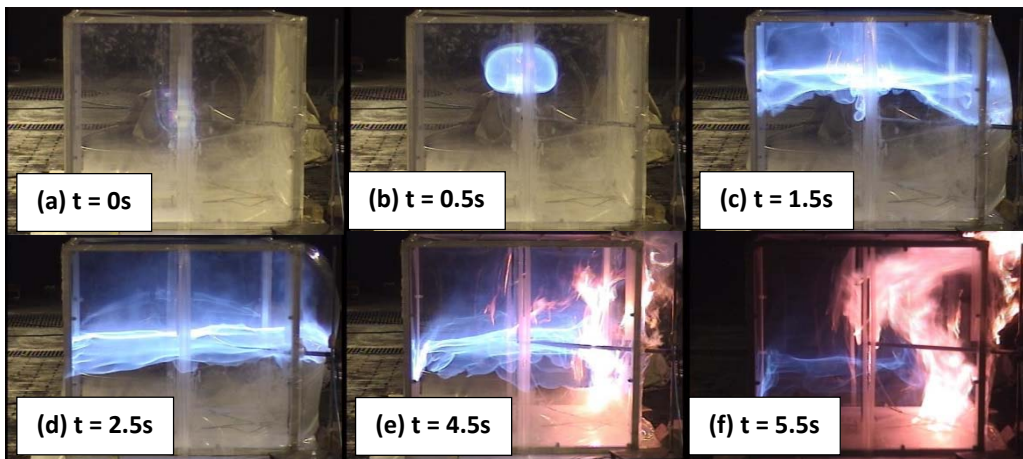


Fig. 3.5.5 Photographs of the model collection device with no slit after generation of a spark. Refrigerant: R1234yf; Leak rate: 380 g/min; Energy of the ignition spark: ~16 J. Variable t is the time after generation of the ignition spark.

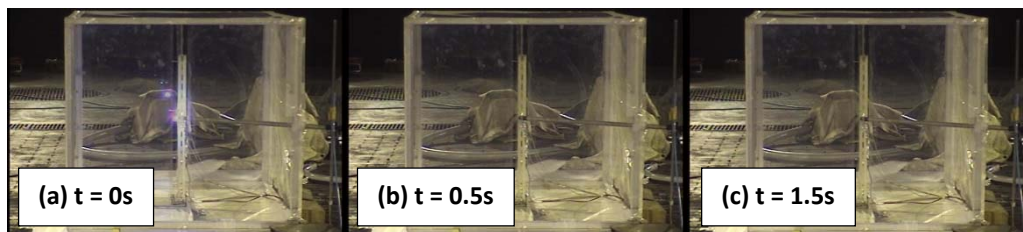


Fig. 3.5.6 Photographs of the model collection device with a 20-mm slit after generation of a spark. Refrigerant: R1234yf; Leak rate: 380 g/min; Energy of ignition spark: ~16 J.

Figure 3.5.3 shows the relation between the persistence time and the height. The persistence time decreased with increasing slit width at all heights. It was longer in the lower region because the refrigerant discharged into the model collection device from the bottom. Figure 3.5.4 shows the relation between the persistence time and the slit width at all heights. The profile for the decrease in the persistence time with increasing slit width was similar, regardless of the height, and the persistence time decreased approximately in proportion to $w_s^{2/3}$.

3.5.3.2 Ignition and flame propagation

Figure 3.5.5 shows photographs of the model collection device with no slit ($w_s = 0$ mm) and Figure 3.5.6 shows photographs of the model collection device with a 20-mm-wide slit ($w_s = 20$ mm). In the case of $w_s = 0$ mm, R1234yf near the ignition source ignited and a pale-violet flame propagated in the upward vertical direction as a result of buoyancy generated by the R1234yf flame. When the R1234yf flame made contact with the roof of the model collection device, the

pale-violet flame propagated horizontally and downward, but the flame did not propagate immediately to the unburned R1234yf because the burning velocity of R1234yf is very small and the supply of oxygen needed for combustion was limited. As a result, the pale-violet flame and unburned R1234yf reached equilibrium at a certain height. Later, the vinyl sheet covering a side plane burned, allowing fresh air to flow into the model collection device; at this stage, the flame propagated throughout the model collection device.

In the case of $w_s = 20$ mm, however, ignition and flame propagation were not observed, although an ignition spark was generated during a period when the refrigerant concentration exceeded the LFL. The reason for this might be the limited flow of R1234yf into the model collection device. The burning velocity of R1234yf is very low (1.5 cm/s, ISO, 2014), so the flame cannot propagate throughout the R1234yf present in the model collection device.

3.6 Hazard Evaluation of Situation #2-(d) - Diesel Combustion of Oil and Refrigerant Mixture during Pump-Down of Air Conditioners-

3.6.1 Outline

During the pump-down of the refrigerant (refrigerant collection) in heat pumps, the lubricating oil and refrigerant may reach a point at which they self-ignite as a result of the temperature rise due to the adiabatic compression of the gaseous mixture of the flammable refrigerant, lubricating oil, and air. This phenomenon has led to instances of accidental destruction of outdoor air conditioning units (Tokyo Metropolitan Government, 2012). Because R1234yf and R32 are slightly flammable, and are regarded as being low-GWP refrigerants, it is necessary to estimate their safety in comparison with R410A—a non-flammable refrigerant. Our study set out to examine the differences in the combustion conditions for each refrigerant, by conducting experiments with an apparatus capable of reproducing diesel explosions.

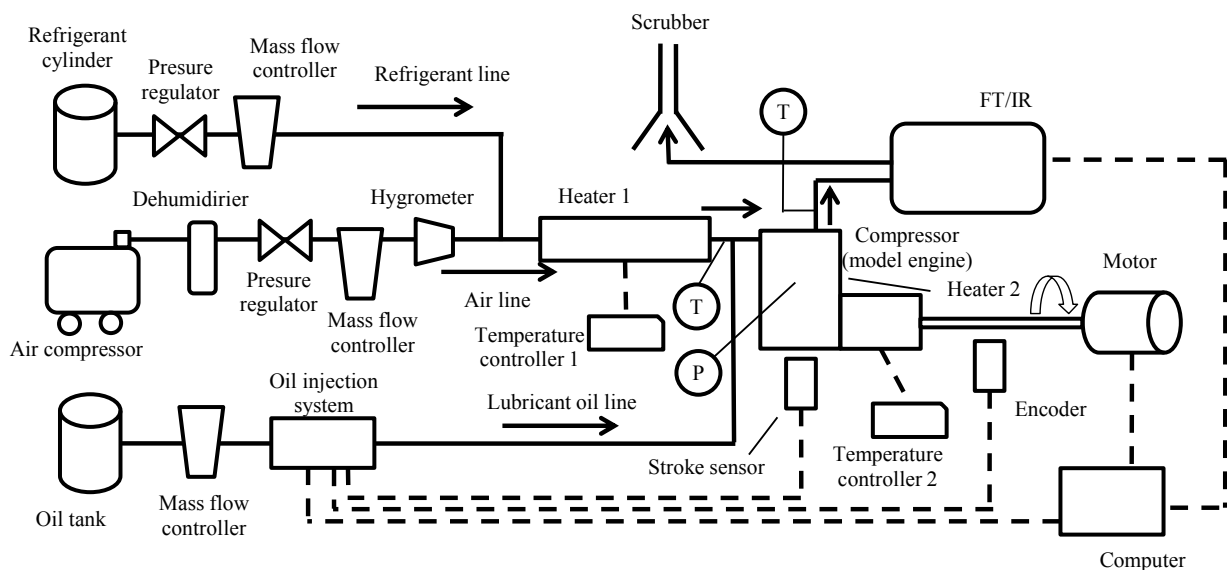
It should be noted that the results presented here do not indicate that the tested refrigerants pose a high combustion risk. Rather, it is the nature of the equipment being used and the prevailing conditions that induce the diesel combustion.

3.6.2 Materials and methods

3.6.2.1 Experimental apparatus

Figure 3.6.1 is a schematic diagram of the equipment used for the experiment. The equipment's main components are an air supply system, a refrigerant supply system, a temperature control system, a lubricating oil supply system, and a model engine (which acts as the compressor) driven by a motor. The flow rates of the air, refrigerant, and lubricating oil are all controlled and the three components are mixed. The resulting gaseous mixture then enters the engine and is compressed after being heated. The model engine, which acts as the compressor, is driven by a motor. The pressure in the engine is measured using a pressure gage. The exhaust gas is examined using Fourier transform infrared (FT/IR) analysis.

Fig. 3.6.1 schematic diagram of the equipment



(a) Air supply system

The air is compressed to 0.7 MPa by a compressor, passes through a dehumidifier, and the pressure is reduced to 0.3 MPa by a pressure regulator. The flow rate is controlled by the mass flow controller (MODEL8550MC-0-1-1, made by Kofloc).

(b) Refrigerant supply system

The vapor refrigerant from the refrigerant cylinder is reduced to a pressure of 0.3 MPa by a pressure regulator. The flow rate is controlled by the mass flow controller (FCST1050LC-4F2-F50L-N2, made by Fujikin). The refrigerant mixes with the air.

(c) Temperature control system

The temperature of the gaseous mixture of the air and the refrigerant is measured by a sheathed thermocouple and is controlled by heater 1 and the temperature controller (FHP-201, made by Tokyo Garasu Kiki; TC-1000, made by As one). Heater 2 controls the temperature of the model engine to equalize the temperature of the engine intake gas and that of the engine surface. These heaters are used to establish experimental conditions that make it easy to induce an explosion.

(d) Lubricant oil supply system

The lubricant oil exits the oil tank and passes through the flow meter (micro-flow meter MODEL213-311/295, made by TOYO CONTROL). The oil is then raised to a pressure of 180 MPa by the oil injection system (a common rail electric control fuel injection system, made by FC DESIGN) and is injected in the form of a spray. The timing of the injection is determined using an encoder and a stroke sensor fitted to the engine.

(e) Compressor

The model engine (R155-4C, made by ENYA, 4 cycle, 25.42-cc stroke volume, 16.0 compression ratio) is used as a compressor and is driven by a motor (MELSERVO-J3, made by Mitsubishi Electric) that is directly connected to its stroke shaft. A computer controls the rotational speed.

Figure 3.6.2 shows the cut model of the engine. The pressure sensor was connected to the place where the plug was placed originally. Figure 3.6.3 shows the connection of the motor and the engine. The shaft with the gear for the encoder connects the engine and the motor.



Fig. 3.6.2 Cut model of engine

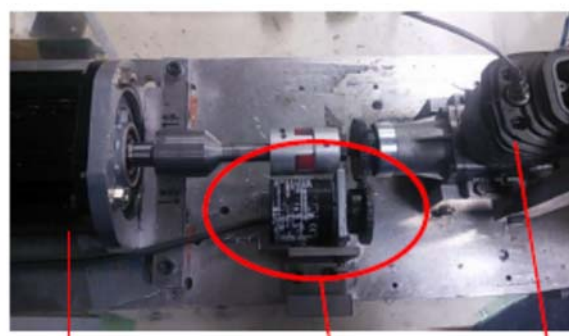


Fig. 3.6.3 Connection of motor and engine

(f) Measuring system

The temperatures of the intake and exhaust gas of the engine were measured using sheathed thermocouples. The pressure in the engine was measured using a pressure gage (6045A, made by KISTLER). The engine crank angle was measured using an encoder. These measurements, along with the flow rate of the oil and an injecting signal, were recorded by a data logger (data logger system NR-2000, made by KEYENCE). The sampling ratio was set to 40 kHz. The exhaust gas was analyzed using an FT/IR (Fourier transform infrared spectrometer FT/IR-4700, made by JASCO). The FT/IR used a single beam system, which carries out measuring by comparing the spectrum of the sample to that of the background.

3.6.2.2 Experimental method

Table 3.6.1 lists the conditions under which the experiment was conducted. Table 3.6.2 lists the refrigerants and the lubricating oil that were used. In addition to R410A (conventional refrigerant), R1234yf and R32 (new refrigerants), as well as R134a, R22, R125 (pure non-flammable refrigerants), and nitrogen gas (inert gas), were used for comparison.

The flow rate of the oil was determined from the theoretical air/fuel ratio, which is calculated from the air flow ratio, as determined by the number of revolutions per minute and the stroke volume of the engine. The calculated theoretical air/fuel ratio was 9.5, according to the results of a CHO analysis of the oil conducted by SVC Tokyo. The experimental parameters were determined according to the type and concentration of the refrigerant being used.

Table 3.6.1 Experimental conditions

Rotational speed, rpm	1500
Mixture flow rate, l/min	18.8

Inlet gas temperature, °C	260
Oil flow rate, l/min	2.295×10^{-4}
Refrigerant concentration, vol%	0 to 100

Table 3.6.2: Refrigerants and lubricating oil

Item	Type
Refrigerant	R1234yf, R32, R410A, R134a, R22, R125, N ₂
Lubricating oil	PAG (VG46)

(a) Experiment 1

In experiment 1, we investigated the self-ignition of a gaseous mixture of air and lubricating oil. The flow rate of the oil was set to the theoretical air/fuel ratio. We measured the changes in the pressure in the engine caused by the injection of the air–oil mixture.

(b) Experiment 2

In experiment 2, we measured the pressure inside the engine as we changed the refrigerant concentration.

(c) Experiment 3

In experiment 3, we investigated the self-ignition of gaseous mixtures of air, refrigerant, and lubricating oil by changing the refrigerant concentrations. The flow rate of the oil was fixed for all of the refrigerant concentrations.

In experiments 2 and 3, we analyzed the exhaust gas resulting from combustion of the gaseous mixture of air, refrigerant, and lubricating oil by using FTIR. Data obtained from Northwest-Infrared were applied to identify the combustion products. We used a spectrum of 4039 cm^{-1} for the quantitative analysis of the HF to avoid noise caused by H₂O and CO₂.

3.6.3 Results

In experiment 1, we examined the change in the pressure in the engine due to the presence of the lubricating oil. In experiment 3, we reproduced the mixing of the air during pump-down by varying the refrigerant concentration. We measured the effect of changing the refrigerant on the increase in the pressure by measuring the pressure inside the engine and analyzing the exhaust gas. We also investigated the effect of the lubricating oil on the changes in the pressure by comparing the results of experiments 2 and 3.

3.6.3.1 Result of experiment 1

Figure 3.6.4 shows the representative pressure changes in the engine when the gaseous mixture of air and lubricating oil was compressed. The horizontal axis shows the crank angle, which reached top dead center at 360°. The plots of the pressure are in 0.5 degree increments. The engine ran smoothly when no oil was injected, indicating that no combustion occurred. The pressure rose significantly with the injection of the oil, however. The exhaust gas changed to white and a loud noise and strong vibration were observed. In this case, we assumed that the lubricating oil self-ignited as a result of the temperature increase induced by adiabatic compression.

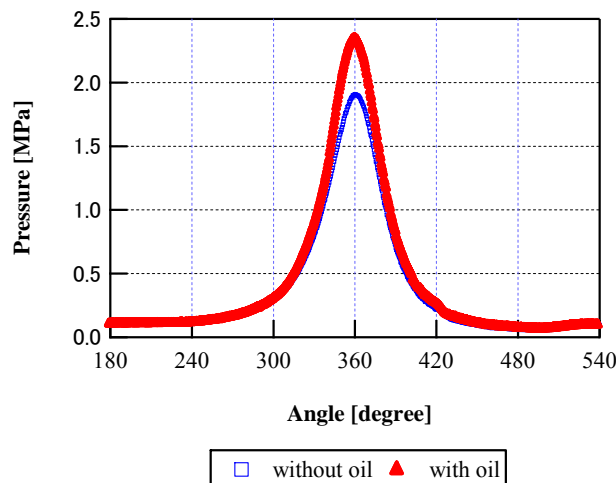


Fig. 3.6.4 Pressure in the engine

3.6.3.2 Result of experiment 2

Figure 3.6.5 shows the representative pressure changes in the engine when the gaseous mixture of air and refrigerant was compressed. The refrigerant used was R1234yf. The maximum pressure increased as the refrigerant concentration

decreased, presumably because of the difference between the specific heat ratio of the air and that of the refrigerant. Combustion did not occur and the rotation of the engine was smooth irrespective of the refrigerant concentration. These tendencies were similar in all of the other refrigerants. These results show that the refrigerants do not self-ignite without the lubricating oil.

3.6.3.3 Result of experiment 3

(a) Pressure in the engine

Figure 3.6.6 shows the representative pressure changes in the engine when the gaseous mixture of air, refrigerant, and lubricating oil was compressed. The refrigerant used was R1234yf.

In the case of R1234yf, when the refrigerant concentration was high, no significant increase in the pressure was observed. The maximum pressure decreased as the refrigerant concentration increased. Upon decreasing the refrigerant concentration, however, the pressure in the engine rose significantly and both intense noise and vibration were observed. The color of the exhaust gas was black at this point. We assumed that the refrigerant itself had combusted. As the refrigerant concentration further decreased, the maximum pressure also decreased. Similar results were obtained with R32, R410A, R134a, and R22, although the range of the refrigerant concentration at which combustion occurred and the maximum pressure differed depending on the refrigerant being used.

With R125, when the refrigerant concentration was high, no significant rise in the pressure was observed. This was the same for the other refrigerants. When the refrigerant concentration was decreased, however, there was no violent combustion like that observed with the other refrigerants. In addition, the maximum pressure was relatively low.

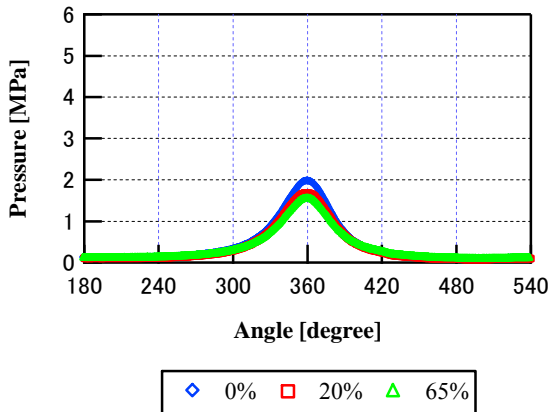


Fig. 3.6.5 Pressure in the engine without oil

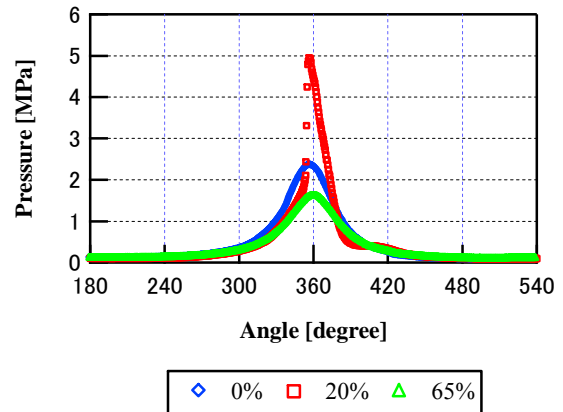


Fig 3.6.6 Pressure in the engine with oil

(b) Analysis of exhaust gas

For each refrigerant, we analyzed the resulting exhaust gas. Figures 3-6-6 and 3-6-7 show typical exhaust gas spectra. The refrigerant used was R1234yf, and the refrigerant concentration was 60% for Fig. 3.6.7 and 10% for Fig. 3.6.8. For Figure 3.6.7, typical R1234yf spectra were observed between 1800 and 1000 cm^{-1} . No combustion occurred at this time. For Figure 3.6.8, where combustion occurred, we observed the HF spectra at 4200 to 3600 cm^{-1} , that of COF_2 at 1980 to 1880 cm^{-1} , and that of CO at 2250 to 2000 cm^{-1} . We assumed that the HF and COF_2 were products of the combustion of the refrigerant.

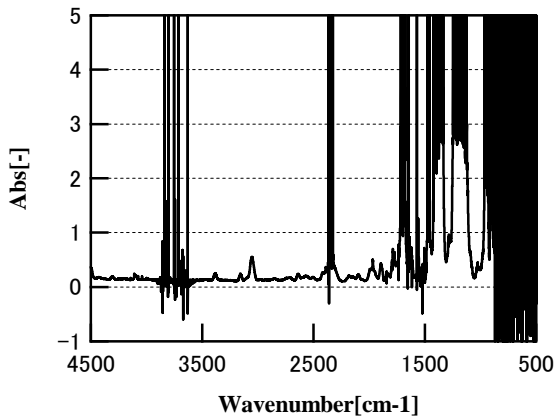


Fig. 3.6.7: Infrared absorption spectrum of exhaust for high R1234yf concentration

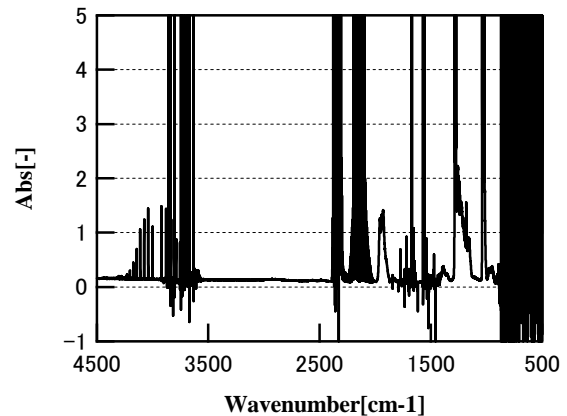


Fig. 3.6.8 Infrared absorption spectrum for low R1234yf concentration

3.6.3.4 Relationship between Pressure and Refrigerant Concentration

Figure 3.6.9 summarizes the results of experiments 2 and 3. The horizontal axis shows the volume concentration of the refrigerant, while the vertical axis shows the maximum pressure during the cycle, which was normalized with respect to the pressure at a refrigerant concentration of 0%. The theoretical value was calculated using Poisson's law based on the specific heat ratio of mixture of the air and that of the refrigerant.

(a) R1234yf

Combustion did not occur when the refrigerant concentration was higher than 30%. The maximum pressure with the lubricating oil was virtually the same as that without the oil. Combustion was observed when the refrigerant concentration was less than 20%. Within this range, the shape of the graph was convex and exhibited around 5 MPa at the maximum at a concentration of 10%. HF was produced when combustion occurred. The concentration of the HF increased with the maximum pressure and reached approximately 3.5 vol% at the maximum.

(b) R32

Combustion did not occur when the refrigerant concentration was higher than 30%. Combustion did occur, however, when the concentration was less than 30% and the maximum pressure increased with the refrigerant concentration, which reached approximately 5 MPa at the maximum. The borderline between the range of burning and non-burning was very clear. The concentration of HF increased as the maximum pressure increased.

(c) R410A

Combustion occurred when the concentration was less than 20%. In this range, the maximum pressure increased with that of the refrigerant. The borderline between the range of burning and non-burning was fairly clear. The concentration of HF increased together with the maximum pressure. We assumed that the real-world accidents would have occurred with air conditioners using R410A, so this result reflects the actual accidents well.

(d) R134a

Although combustion occurred when the concentration was less than 30%, the maximum pressure was lower than that obtained with the other refrigerants. The pressure was virtually equal to the result obtained with 0% of the refrigerant. Within this range, it appears that the refrigerant did not burn, but the lubricating oil did. By further decreasing the refrigerant concentration to less than 7.5%, the maximum pressure increased to approximately 4 MPa, which suggests that the refrigerant was also burning. The HF concentration was high around this range.

(e) R22

Combustion occurred when the concentration was less than 50%, giving a large range relative to the other refrigerants. The pressure reached approximately 5 MPa at the maximum and a concentration of 22.5%. The HF concentration exhibited a similar tendency to that of the pressure. When the refrigerant burned, HCl was also observed with the R22. Figure 3.6.10 shows the spectrum of the exhaust gas as measured by FTIR, while Figure 3-6-10 shows the relationship between the refrigerant concentration and that of HCl in the exhaust gas. The FTIR spectrum includes typical HCl spectra in the range between 3100 and 2600 cm^{-1} . We used the spectrum for 2844 cm^{-1} to perform a quantitative analysis of the HCl. The concentrations of both the HF and HCl exhibited similar tendencies, which suggests that the HCl was also produced by the burning of the refrigerant.

(f) R125

Combustion did not occur when the refrigerant concentration was higher than 10%. Further, although combustion occurred when the concentration was lower than 5%, intense combustion like that observed with the other refrigerants was not observed and the maximum pressure was lower. Only small amounts of HF were detected.

(g) Nitrogen gas

Because the properties of nitrogen are similar to those of air, the theoretical value for the maximum pressure appears virtually constant. Combustion occurred when the concentration of the nitrogen was lower than 70%, and the maximum pressure changed very little when the concentration was lower than 50%.

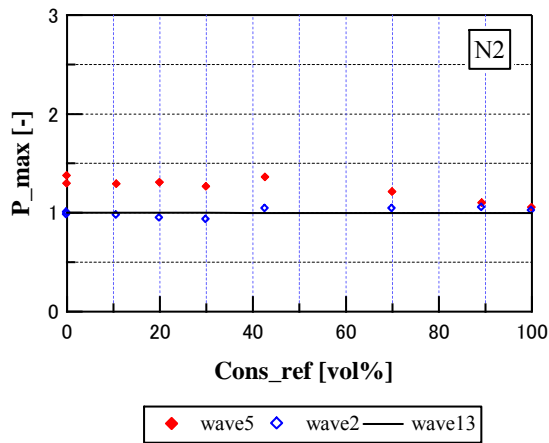
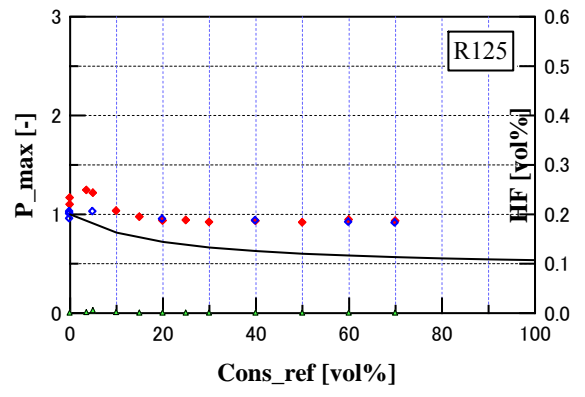
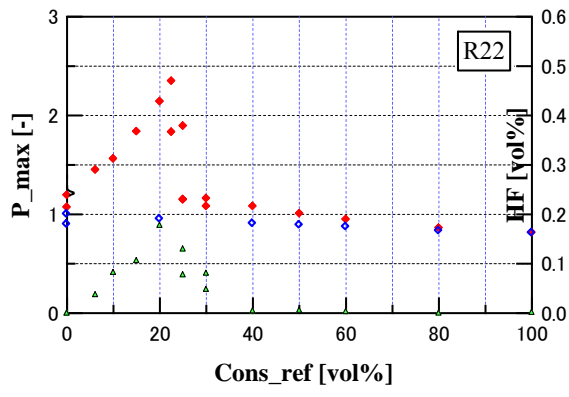
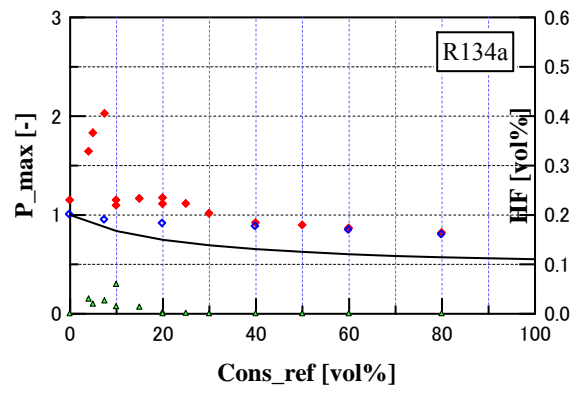
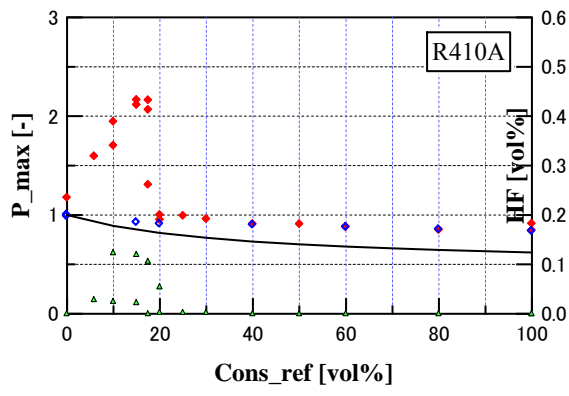
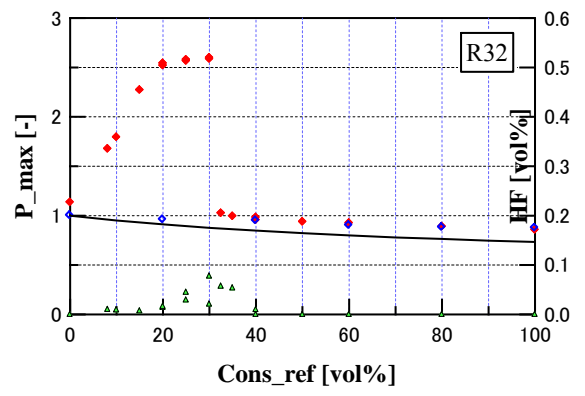
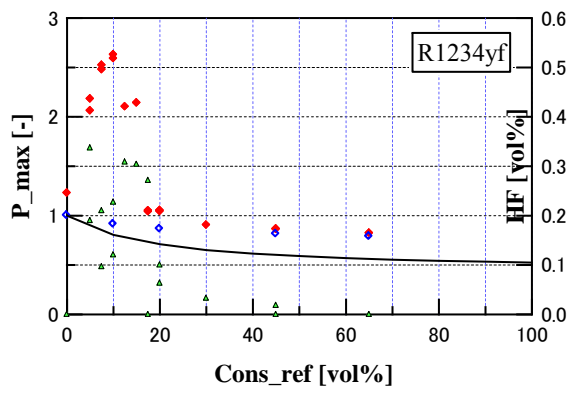


Fig. 3.6.9: Relationship between refrigerant concentration, pressure, and HF concentration

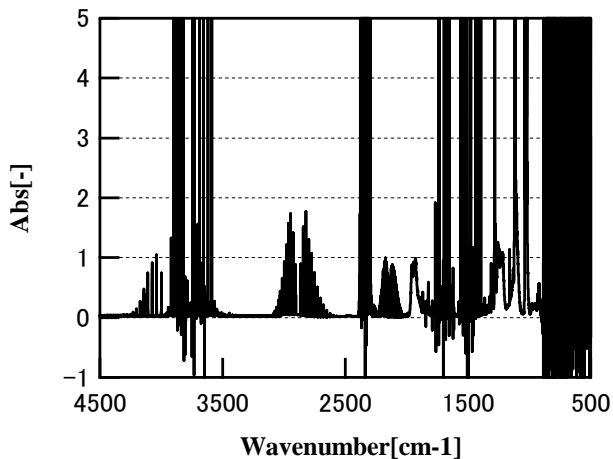


Fig. 3.6.10 Infrared absorption spectrum of R22 exhaust gas

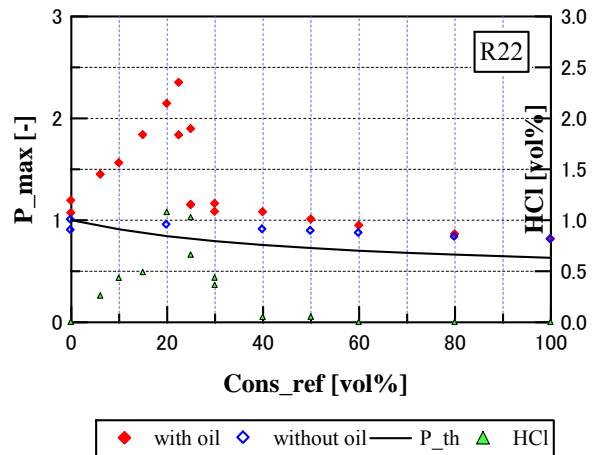


Fig. 3.6.11 Pressure and HCl concentration for R22

3.6.3.5 Discussion

For all the refrigerants except R125, no combustion occurred at high refrigerant concentrations, which corresponds to a pump-down being successfully accomplished in a real-world scenario. As the refrigerant concentration was reduced, however—as would occur if there were to be a leak from a refrigerant pipe that allowed air to mix with the refrigerant—the lubricating oil would self-ignite, leading to burning of the refrigerant at lower concentrations, regardless of the type of refrigerant being used. The pressure inside the compressor increases with the addition of refrigerant. By further decreasing the refrigerant concentration, the pressure changes and reaches a maximum at a certain concentration. The HF, which results from the burning of the refrigerant, arises within that range of concentrations in which the pressure rises rapidly. This implies that not only the lubricating oil but also the refrigerant itself is burning. Although the range of flammability differs slightly depending on the refrigerant, the range is wider than that for a general case. Furthermore, even those refrigerants that are categorized as being non-flammable burned in our experiments.

For R125, on the other hand, no intense combustion occurred at any concentration of the refrigerant and only very small amounts of HF were detected.

3.6.3.6 Flammability of refrigerants

For a refrigerant to combust, however, the following conditions must be satisfied: the refrigerant concentration must be within the required flammability range; the energy of the ignition source must be higher than the MIE; and the air velocity adjacent to the ignition source must be lower than the BV (JSRAE, 2014). According to the list of refrigerants in the previous section, R410A, R134a, R22, and R125 do not exhibit any flammability concentration range, while R1234yf and R32 exhibit different flammability ranges from those observed in our experiments. However, some investigations suggest that the presence of high-humidity air will lead to the range of flammability becoming wider, to the point where even some refrigerants that are categorized as being non-flammable will actually burn, which is mentioned in the previous section. This is caused by the water in the air reacting with the fluorine in the refrigerant, thus causing the refrigerant to burn more easily.

Although we used dried air in our experiments, water was produced by the burning of the lubricating oil. Moreover, other research has found that the flammability range becomes wider as the pressure is increased (Kondo *et al.*, 2011). Given this data, we can speculate that the environment inside the compressor, specifically, the humidity and high pressure, makes it easier for the refrigerants to burn.

3.7 Conclusions

3.7.1 Simultaneously used with a fossil-fuel heating system

Both the cases of R1234yf and R32, the concentration of refrigerant in the room was not more than the LFL of refrigerants even when all the refrigerants leaked from a wall-mounted type air conditioning system to the room, and so the flame propagation of refrigerants was not confirmed. However, generation of HF over the permissive concentration (3 ppm) was confirmed to be irrespective of the varieties of refrigerants including R410A because of the contact between refrigerants and the heating part in the fossil-fuel heating systems. It was experimentally confirmed that productivity of HF from R32 per unit time and mass was comparatively larger than that of R1234yf and R410A.

3.7.2 Ignition and flame propagation possibility by a lighter

- (1) It was verified that there are several possibilities in which the mixture composition of a lighter fuel/A2L

refrigerant/air exceeds the LFL. However, although the ignition experiment using a commercial piezo gas lighter was conducted above the estimated mixture composition, no ignition and flame propagation were observed in any of the tested refrigerants (R1234yf, R1234ze(E), R32).

- (2) For a premixed turbo gas lighter, ignition and flame propagation near the outlet of the lighter was observed for the R1234ze(E) case. The relative humidity in this case was 71% R.H. and room temperature was 19°C. However, the flame quickly went out, and a blast wave pressure capable of breaking an acrylic pool was not confirmed.
- (3) Ignition experiment was performed for a kerosene cigarette lighter using an AC spark to ignite the fuel of the lighter instead of rubbing the flint wheel directly. Ignition and flame propagation occurred in experiments in which we used AC electric sparks as a surrogate source of ignition for the usual generation of sparks by rubbing of the flint wheel. GC/MS analysis showed that the mixture in the windbreak of the kerosene cigarette lighter consisted mainly of vaporized lighter fuel and air, even when the lighter was located in accumulated R32. These results confirm that use of a kerosene cigarette lighter in accumulated R32 may cause ignition and flame propagation to the R32.

3.7.3 Physical hazard of rapid leakage from a pinhole

Even when the refrigerant leaked from a 4-mm-diameter pinhole, which is conceivable in the case of a very severe accident, a flammable zone was only formed locally around the pinhole for all test refrigerants. Even when the energy was much greater than that of an electrostatic and spark discharge, which are possible in actual situations, flame propagation to the entire refrigerant jet was not observed, and significant increases in blast wave pressure, heat flux, temperature, and HF concentration were not confirmed. Therefore, even if the A2L refrigerant leaked from the pipe fracture, the possibility of ignition and flame propagation of the A2L refrigerant by the conceivable ignition sources in the actual situation is extremely low.

3.7.4 Physical hazard evaluation of leakage into the collection device

When there was no structure to diffuse the leaked and accumulated refrigerant, it accumulated and remained in the device for a long time. This could be ignited, and the flame could propagate the entire device by a strong spark of 16 J. However, the possibility of ignition and flame propagation of the accumulated refrigerant is extremely low because generation of that much energy is not common in actual situations. In addition, the minimum ignition energy of the A2L refrigerant is much greater than the spark discharge energy generated from the electrical device in the collection device. If there was a slit with a width greater than 20 mm, the accumulation of refrigerant inside the device could be immediately prevented, and most of the ignition and flame propagation would be averted.

3.7.5 Diesel combustion of oil and refrigerant mixture during pump-down of air conditioners

This research has revealed that the accidents that may occur during the pump-down of air conditioners are caused by the diesel combustion of a mixture of air, refrigerant, and lubricating oil. Although an air/oil mixture could burn under experimental conditions, a higher pressure results when refrigerant is added to the mixture. We believe that the refrigerant itself burns and thus leads to a sudden and significant increase in the pressure. Compared to R410A and R22, which are conventional refrigerants, the new low-GWP refrigerants (R1234yf and R32) exhibit no major difference in terms of their flammable range and pressure.

REFERENCES

- Higashi, T., Saitoh, S., Dang, C., and Hihara, E., 2014, "Diesel combustion of oil and refrigerant mixture during pump down of air conditioners," Proc. of the International Symposium on New Refrigerants and Environmental Technology 2014, pp. 91–96.
- Holleyhead, R., 1996, "Ignition of flammable gases and liquids by cigarettes: A review," Science and Justice, Vol. 36, No. 4, pp. 257–266.
- Imamura, T., Kamiya, K., and Sugawa, O., 2015, "Ignition hazard evaluation on A2L refrigerants in situations of service and maintenance," International Journal of Loss Prevention in the Process Industries, in press, Available online at Jan. 6, 2015.

- Imamura, T. and Sugawa, O., 2014, "Experimental evaluation of physical hazard of A2L refrigerant assuming actual handling situations," Proc. of the International Symposium on New Refrigerants and Environmental Technology 2014, pp. 73–78.
- Imamura, T., Miyashita, T., Kamiya, K., and Sugawa, O., 2013, "Ignition hazard evaluation on leaked A2L refrigerants by commercial-use electronic piezo lighter," Journal of Japan Society for Safety Engineering, Vol. 52, No. 2, pp. 91–98, in Japanese.
- Imamura, T., Miyashita, T., Kamiya, K., Morimoto, T., and Sugawa, O., 2012, "Physical hazard evaluation for using air conditioning systems having low-flammable refrigerants with the fossil-fuel heating system at the same time," Transactions of the Japan Society of Refrigerating and Air Conditioning Engineers, Vol. 29, No. 4, pp. 401–411, in Japanese.
- Incorporated Administrative Agency National Institute of Technology and Evaluation (NITE), 2010, <http://www.nite.go.jp/data/000008482.pdf>, in Japanese [Last accessed Mar 10, 2015].
- International Organization for Standards, 2014, "ISO817: Refrigerants: Designation and Safety Classification", Third edition. [ONLINE] Available at: <https://www.iso.org/obp/ui/#iso:std:iso:817:ed-3:v1:en>. [Last Accessed Jan 19, 2015].
- Japan Society for Occupational Health, 2014, "Recommendation of occupational exposure limits," Vol. 56, p. 404. Available online at: http://joh.sanei.or.jp/pdf/E56/E56_5_14.pdf
- Kondo, S., Takizawa, K., and Tokuhashi, K., 2012, "Effects of temperature and humidity on the flammability limits of several 2L refrigerants", Journal of Fluorine Chemistry, Vol.144, pp.130-136.
- Kondo, S., Takizawa, K., and Tokuhashi, K., 2011, "On the pressure dependence of flammability limits of CH₂=CFCF₃, CH₂F₂ and methane," *Fire Safety Journal*, Vol. 46, No. 5, pp. 289–293
- Matsui, H., 2012, "Minimum ignition energy," TIIS News, No. 247, pp. 4–6, Available online at: http://www.tiis.or.jp/pdf/TIISNEWS_2012247.pdf, in Japanese [Last Accessed Mar 9, 2015].
- Saburi, T., Matsugi, A., Shiina, H., Takahashi, A., and Wada, Y., 2014, "Flammable behavior of A2L refrigerants in the presence of moisture," Proc. of the Tenth International Symposium on Hazards, Prevention and Mitigation of Industrial Explosions. Bergen: GexCon AS., pp. 327–334.
- Spatz, M. and Minor, B., 2008, "HFO-1234yf: A low GWP refrigerant For MAC," Honeywell/DuPont joint collaboration, SAE World Congress, Detroit, Michigan. [ONLINE] Available at: http://www2.dupont.com/Refrigerants/en_US/assets/downloads/SmartAutoAC/MAC_SAE_HFO_1234yf.pdf. [Last accessed Jan 19, 2015].
- Takaichi, K., Taira, S., and Watanabe, T., 2014, "Efforts of the Japan refrigeration and air conditioning industry association (JRAIA): Progress by mini-split risk assessment SWG," Japan Society of Refrigeration and Air Conditioning Engineers, Risk assessment of mildly flammable refrigerants: 2013 progress report. Chap. 8.1, 82–94 [ONLINE] Available at: http://www.jsrae.or.jp/info/2012progress_report_e.pdf. [Last accessed Jan 19, 2015].
- Takizawa, K., Igarashi, N., Takagi, S., Tokuhashi, K., and Kondo, S., 2015, Quenching distance measurement of highly to mildly flammable compounds, *Fire Safety Journal*, Vol. 71, pp. 58–64.
- Takizawa, K., Tokuhashi, K., and Kondo, S., 2009, "Flammability assessment of CH₂=CFCF₃: Comparison with fluoroalkenes and fluoroalkanes," *Journal of Hazardous Materials*, Vol. 172, pp. 1329–1338.
- Yajima, R., 2014, "Efforts of the Japan Refrigeration and Air Conditioning Industry Association (JRAIA), Progress of SWG for VRF system risk assessment," Japan Society of Refrigeration and Air Conditioning Engineers, Risk assessment of mildly flammable refrigerants: 2013 progress report. Chap. 8.2, 95–106 [ONLINE] Available at: http://www.jsrae.or.jp/info/2012progress_report_e.pdf. [Last accessed Jan 19, 2015].

4. Physical Hazard Assessment

4.1 Introduction

Refrigerants such as difluoromethane (R32, CH_2F_2), 2,3,3,3-tetrafluoropropene (R1234yf, $\text{CH}_2=\text{CFCF}_3$) and trans-1,3,3,3-tetrafluoropropylene (R1234ze(E), $\text{CHF}=\text{CHCF}_3$) have zero ozone depletion potential (ODP) and low global-warming potential (GWP). In particular, R1234yf and R1234ze have GWP lower than the regulation value of 150 for new mobile air conditioning (EC, 2012); thus, these compounds are considered to show great potential as next-generation refrigerants. Although these refrigerants perform better than existing refrigerants in terms of lower ODP and GWP, they are mildly flammable. It is important to evaluate the combustion safety of A2L refrigerants in the event of leakage into the atmosphere owing to installing and operating accidents. To address the issue of global warming due to conventional refrigerants, ASHRAE (2010) defined the optional Class 2L to classify refrigerants with lower flammability, and it is preparing to promote the conversion of air-conditioning equipment from conventional refrigerants to next-generation refrigerants. In this study, the fundamental flammability characteristics of A2L refrigerants were experimentally evaluated using a large spherical combustion vessel, and their safety was assessed. Flammability was investigated in terms of parameters such as the flame speed, burning velocity, and deflagration index K_G under the influence of elevated temperature and moisture and the uplift behavior due to buoyancy arising from the slow burning velocity.

4.2 Combustion Test

4.2.1 Introduction

To utilize these mildly flammable gases safely, ASHRAE (2010) added the optional 2L subclass to the existing Class 2 (lower flammability) to classify the safety of refrigerants. R32, R1234yf, and R1234ze are classified as A2L refrigerants, which are defined as having low toxicity and low flammability with a maximum burning velocity of ≤ 10 cm/s. A2L refrigerants have such a low burning velocity that a lifting of the flame front due to buoyancy significantly affects their combustion behavior. In terms of safety, investigating the fundamental flammable properties of these alternative refrigerants is important. In this study, a large-volume spherical vessel was prepared to observe and evaluate the effect of buoyancy on the flammable properties of R32 and R1234yf; the flame propagation behaviors of these two refrigerants were observed using a high-speed video camera, and the internal pressure in the vessel was measured using a pressure sensor. The flame propagation velocity was estimated by image analysis of the high-speed video images. The burning velocity was estimated from the flame speed and the pressure profile; the latter was measured using the spherical vessel method under the assumption of spherical flame front expansion (Takizawa *et al.*, 2009). The maximum peak pressure (i.e., maximum overpressure relative to the pressure in the vessel during combustion) and deflagration index (i.e., constant that defines the maximum rate of pressure increase with combustion time as defined by ISO 6184-2 (1985) and NFPA68 (2007)) were evaluated. Ignition tests using mixture gases with an electric discharge were conducted for a varying equivalent ratio ϕ , which is the ratio of the fuel–oxygen ratio to the stoichiometric fuel–oxygen ratio: $\phi = 0.8$ – 1.2 for R32 and $\phi = 1.2$ – 1.4 for R1234yf. In the current fiscal year, the flammability in the presence of elevated temperature and moisture was experimentally investigated in consideration of such conditions in summer, and the burning behavior at ignition was investigated. An evaluation scheme for the potential risk of combustion and explosion in actual situations was developed based on the experimentally obtained K_G values.

4.2.2 Experiment

Figure 4.2.1 shows the experimental apparatus with the spherical vessel. The spherical vessel had a diameter of 1 m and volume of 0.524 m^3 . A pressure transducer was placed on top in the vessel and the pressure signal during combustion was recorded on a data logger. The burning behavior was observed using a high-speed video camera through a PMMA viewing port. The R32 burning behavior was investigated at equivalent ratios of $\phi = 0.8$ – 1.2 . The R1234yf burning behavior was evaluated at equivalent ratios of $\phi = 1.2$ – 1.4 against a reference ratio of $\phi = 1.325$ (mixing ratio of 10 vol%, which Takizawa *et al.* (2009) reported as giving the maximum burning velocity for R1234yf when using the spherical vessel method (Metghalchi and Kech, 1980 and Hill and Hung, 1988)). Pressure transducers were used to introduce fuel gas into the vessel up to a certain partial pressure (BGs in Figure 4.2.1). Air was then introduced into the vessel until the total pressure in the vessel was conditioned at an atmospheric pressure of 101,325 Pa. During the gas introduction and mixing procedure, gas circulation was maintained using a diaphragm pump (DP in Figure 4.2.1). The electrode for the electric spark was a set of horizontally opposed tungsten wires with 7-mm gap length, and the wires were 0.3 mm in diameter to avoid heat loss and structural disturbance. The vessel was equipped with a jacketed mantle heater that covered the entire area of the vessel to maintain the initial temperature at a constant (Figure 4.2.1, right picture). The electrode provided a spark upon the application of a high-voltage power supply to ignite the mixture gas. The discharge voltage and current were recorded on an oscilloscope, and the discharge energy was estimated. The

expansion behavior of the flame front was recorded using the high-speed camera, and the recorded video image sequences were visually analyzed; the flame velocities in the side and upper directions were evaluated.

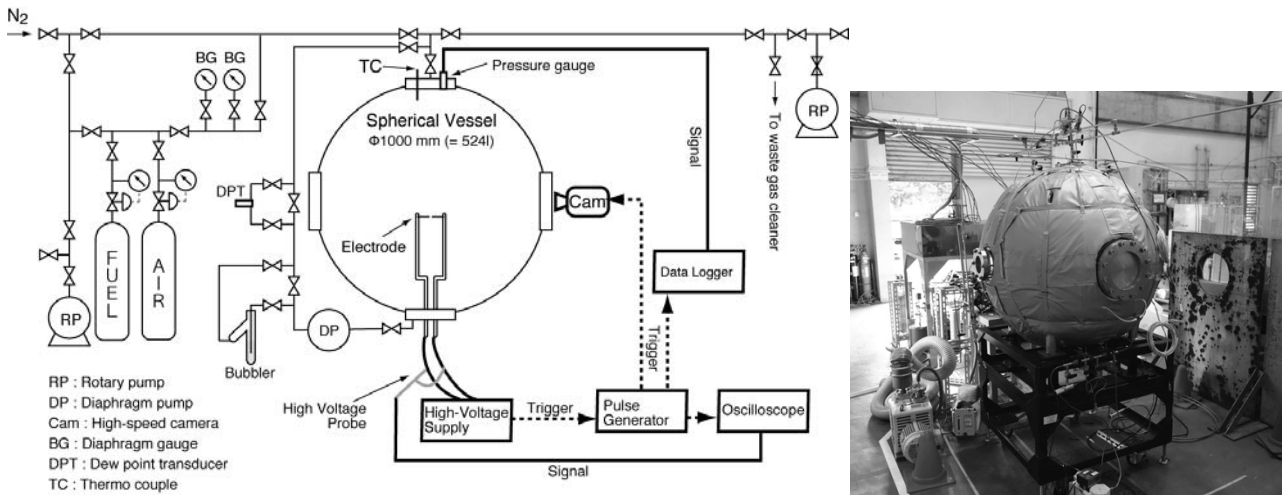


Figure 4.2.1 Schematic drawing (left) and photograph (right) of experimental apparatus.

4.2.3 Flame velocity and burning velocity

(a) Image observation

Figure 4.2.2 shows an example of the high-speed video images of the flame front propagation behaviors for R32 for $\phi = 0.9$ and 1.2. The flame expanded while slowly climbing upward. The shape of the flame front, which is the interface between the unburned and the burned gas, was distorted under the influence of buoyancy and viscosity. The expansion behaviors between $\phi = 0.9$ and 1.2 were almost the same except for their temporal responses. The left-hand-side picture in Figure 4.2.3 shows the high-speed video images of the flame front propagation behavior of R1234yf for $\phi = 1.35$. No clear and smooth flame front was observed; the flame front was convoluted without symmetry and floated upward. Furthermore, the ignition characteristics of R1234yf were unstable and depended on not only its flammability but also experimental conditions such as the discharge conditions including electrode geometry and heat loss and the vessel size and shape. Because it was difficult to examine the possibility of these effects, alternatives such as a small spherical vessel ($\phi 15$ cm, 15 L) and compact elongated cylindrical vessel (inner diameter: 10 cm, and length: 20 cm) were prepared to investigate the flammable behavior at ignition. The bottom picture in Figure 4.2.3 shows the test results for the compact elongated vessel. A smooth and clear flame front was observed that could not be seen in the large and small spherical vessels. The relation between the fluid dynamics from the high temperature produced by the burned gas and buoyancy and the slow burning velocity at the bottom of the flame resulted in the squeezed flame front shape. The flammability of the mixture gas in the closed vessel was affected not only by the fuel/air mixture ratio, initial pressure, and initial temperature but also by the vessel size and shape, ignition source, and other factors. These results suggest the influence of the small vessel volume and shape; thus, the effect of the fluid dynamic behavior on the flammability must be considered in scaled-up situations.

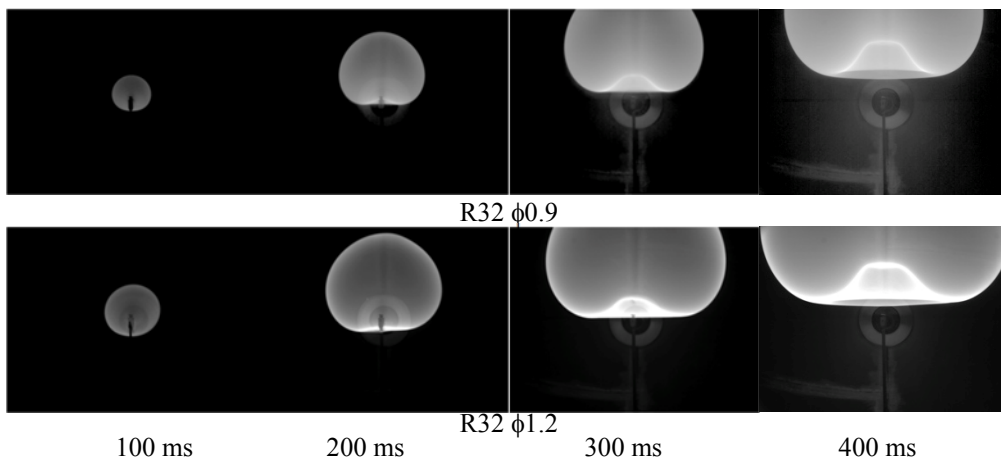


Figure 4.2.2 Images of flame front propagation for R32 (top: $\phi = 0.9$, bottom: $\phi = 1.2$)

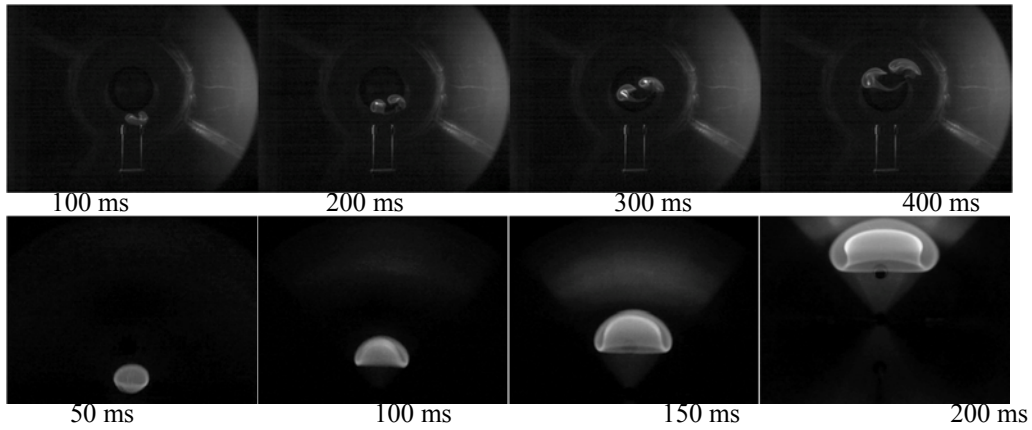


Figure 4.2.3 Images of flame propagation for R1234yf ($\phi = 1.325$, top: large spherical vessel, bottom: compact elongated vessel).

Figure 4.2.4 shows the pressure profiles for R32 for $\phi = 0.8–1.2$ as measured by the pressure transducer. The profiles all seemed to show that the pressure increased in a few stages. One possible cause for the same may be the influence of the reflected flame front from the top wall. The arrival time of the upper direction flame front to the top of the vessel could be predicted from image analysis: ~ 0.5 s for $\phi = 0.9$ and $0.46–0.47$ s for $\phi = 1.0–1.2$. Thus, the pressure reached a peak maximum far behind the arrival time of the flame front. The flame front rose in the upper direction owing to buoyancy, whereas the unburned gas remained in the lower part of the vessel. The underside of the flame front was accompanied by a complicated flow of unburned gas.

The pressure profiles for R1234yf were also measured; these are shown in Figure 4.2.5. The profile trends associated with the equivalent ratio were not simple. This seems to be due to the influence of the unstable ignition characteristics. The pressure increased to the peak maximum very gradually compared with R32 and took more than 6 s. The profile for the pressure increase at $\phi = 1.35$ was small, and no increase in pressure was observed at $\phi = 1.4$; therefore, most fuels seemed to remain unburned.

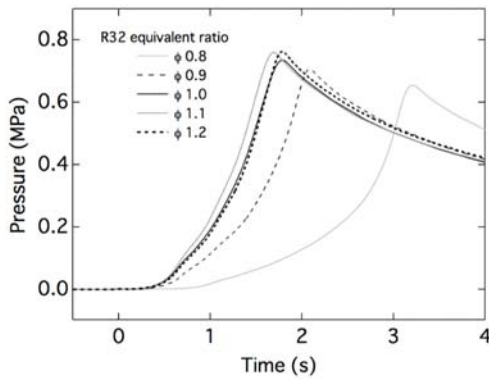


Figure 4.2.4 Pressure profile for R-32 ($\phi = 0.8–1.2$)

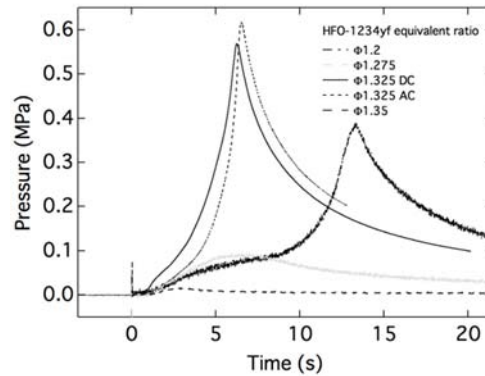


Figure 4.2.5 Pressure profile for R-1234yf ($\phi = 1.2–1.35$)

(b) Flame speed and burning velocity

The maximum flame width and flame top position from the ignition point were visualized for R32, and the flame speed S_f was estimated based on the temporal differentiation of the flame width and the flame top position. The flame speeds in the upper direction increased 1.2–2.0 times more than those in the side direction as time progressed, owing to buoyancy associated with the increase in volume of the burned side. For R1234yf, the proper evaluation of the maximum flame width and flame top position was difficult because a clear and smooth flame front was not observed.

The burning velocity S_u was evaluated from the flame speed S_f (Pfahl *et al.*, 2000) as follows:

$$S_u = \left(\frac{\rho_b}{\rho_u} \right) \cdot S_f \quad (4.2.1)$$

where ρ is the density ($\text{kg}\cdot\text{m}^{-3}$) and subscripts u and b denote unburned and burned gas, respectively. ρ_u is the density at the initial condition, and the unknown ρ_b density was estimated using the chemical equilibrium calculation developed by Gordon and McBride (1994) under the assumption of constant pressure during combustion. S_f is the flame speed ($\text{cm}\cdot\text{s}^{-1}$). In this study, the upward flame speed S_f was estimated from the rate of change in the flame top position (cm) with time along with the sideward flame speed S_{f_s} , which was estimated from the rate of broadening of the half-flame width r_f (cm) (Pfahl *et al.*, 2000). The sideward S_{f_s} minimizes the influence of buoyancy, whereas the upward S_f involves

the apparent speed due to buoyancy. The burning velocity S_u was also calculated by the spherical vessel method (Metghalchi and Keck, 1980, and Hill and Hung, 1988) under the assumption of spherical flame front expansion as follows:

$$S_u = \frac{R}{3} \left[1 - (1-x) \left(\frac{P_0}{P} \right)^{\frac{1}{\gamma_u}} \right]^{-2/3} \cdot \left(\frac{P_0}{P} \right)^{\frac{1}{\gamma_u}} \frac{dx}{dt} \quad (4.2.2)$$

where R is the inner radius of the chamber (m), x is the mass fraction of burned gas, P_0 is the initial pressure in the chamber (Pa), P is the instantaneous pressure during burning in the chamber (Pa), and γ_u is the specific heat ratio. The values of x and γ_u for each instantaneous pressure were estimated using the equilibrium code (Gordon and McBride, 1994). As shown in Figure 4.2.6, the burning velocity S_u was estimated by using the sideward flame speed S_f for R32. The burning velocity according to the spherical-vessel (SV) method was also estimated from the obtained pressure profiles and numerical computation under the assumption of spherical flame propagation for R32, as shown in Figure 4.2.6. Although the flame did not propagate with a spherical shape, as indicated by the high-speed video images shown in Figure 4.2.2, S_{u0} was estimated and used to investigate the deviation due to distortion from buoyancy. During analysis, the pressure increase profile did not depart from the scope of the spherical flame front expansion in an initial stage of burning. S_{u0} was compared with the reference S_{u0} values for R32 (Takizawa *et al.*, 2005). The burning velocities based on the flame speed and SV method show similar equivalent ratio dependencies; however, the SV method slightly underestimated S_{u0} . As shown in Figures 4.2.3 and 4.2.5, the flame front expansion was convoluted except for $\phi = 1.325$, and applying the SV method was difficult. Therefore, the burning velocity S_{u0} was estimated for R1234yf for $\phi = 1.325$ only; this is shown in Figure 4.2.7. For R1234yf, the buoyancy had a particular influence on the flame expansion behavior. Takizawa *et al.* (2010) estimated $S_{u0-\mu g}$ for R1234yf under a microgravity ($-\mu g$) environment, and it is shown as a reference in Figure 4.2.7. From the results of the hollowed-out shape of the flame front observed in the compact elongated vessel (Figure 4.2.3), we have to take account of the evaluation procedure of the flame speed by image analysis as well as the burning velocity by the SV method.

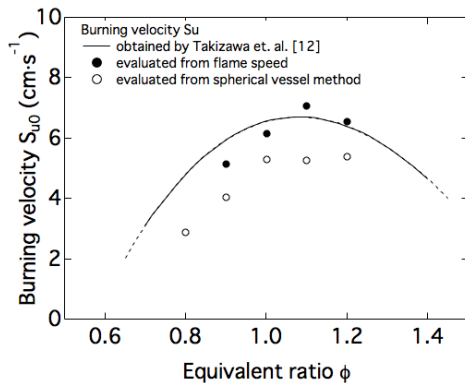


Figure 4.2.6 Estimated burning velocity for R32

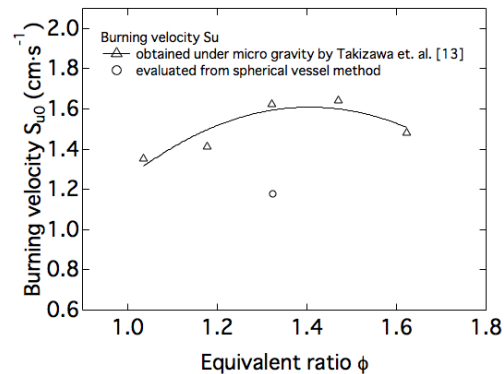


Figure 4.2.7 Estimated burning velocity for R1234yf

(c) Effect of moisture

Kondo *et al.* (2012) have reported the effects of temperature and humidity on the flammability limits of some A2L refrigerants; this is an important issue, especially with the hot and humid climate of Japan. Temperatures of over 30°C and 80% humidity are often recorded in the summer. In addition to R32 and R1234yf, R1234ze(E) was included in the assessment medium, and the flammability of these A2L refrigerants in the presence of elevated temperatures and moisture was experimentally investigated using the spherical vessel (Figure 4.2.1). The dew point measured by the dew-point transmitter in the middle of the circulation loop (shown in Figure 4.2.1) and the partial pressure were used to control the humidity in the mixture gas. The moisture was added to the mixture gas in the circulation loop by a bubbler. In the experiment, ~56% RH was attained at the given temperature of 30°C. Flammability tests were conducted under dry (10–30°C) and wet (60% RH at 30–35°C) conditions for R32 at $\phi = 1.1$ and for R1234yf at $\phi = 1.325$ (Saburi *et al.*, 2014). For R1234ze, the tests were conducted under dry and wet (above 50% RH) conditions at an elevated temperature of 35°C. With the addition of the moisture and elevated temperature, R32 exhibited flammability with almost the same flame front shape as under the dry condition, and R1234yf showed a relatively clear flame front shape compared with the dry condition. A blue flame was observed for R1234yf under the dry condition; however, a luminous flame was observed under the wet and elevated temperature conditions. R1234ze was not flammable under the dry condition even at elevated temperature; however, it became flammable under the wet condition. It was observed that the flame front formed a clear interface and floated up under buoyancy. The dependencies of the pressure profiles and P_{\max} and K_G on the equivalence ratio are shown in Figure 4.2.8. The evaluation results under elevated temperature and dry/wet conditions are briefly summarized in Table 4.2.1.

Research on the effect of buoyancy on the flammability behavior that considers humidity will continue to be conducted.

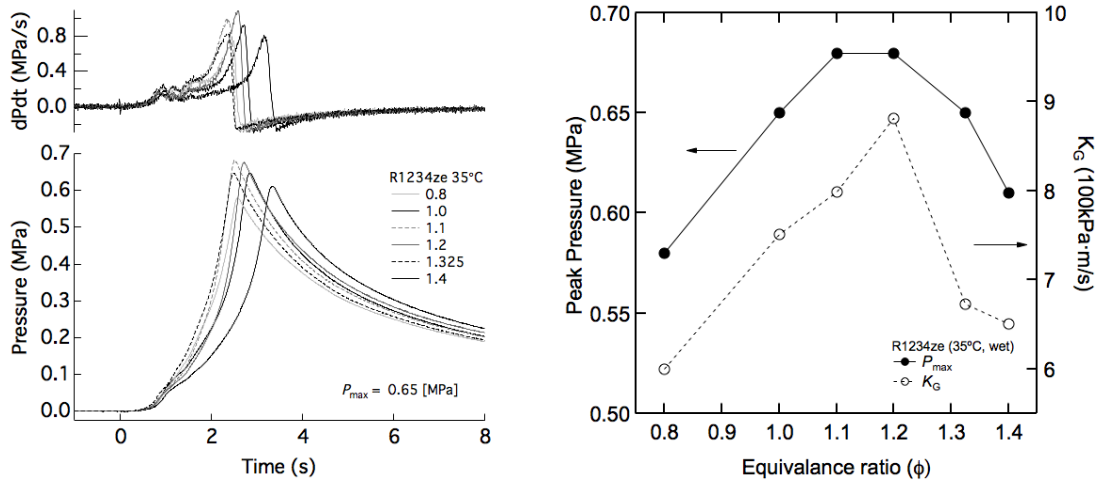


Figure 4.2.8 Example profiles of R1234ze at 35°C and wet condition (left: effect of equivalence ratio on pressure profile, right: effect of equivalence ratio on P_{max} and K_G).

Table 4.2.1 Brief summary of evaluated properties for refrigerants.

Refrigerant	Equivalence ratio (ϕ)	Temperature (°C)	Moisture (wet-dry condition)	P_{max} (100 kPa)	K_G (100 kPa · m · s ⁻¹)	Flame speed S_f (cm · s ⁻¹)	Burning velocity S_u (cm · s ⁻¹)
R32	1	35	Dry	7.5	7.6	62	7.3
	1.1	35	Dry	7.3	8	65	7.6
		35	Wet (64% RH)	7.2	10.6	71	8.5
R1234yf	1.325	30	Dry	6.2	5.72	–	–
	1.325	35	Wet (78% RH)	6.6	8.22	28	3.4
R1234ze	0.8–1.5		Dry		Not flammable		
	1.2	35	Wet (50%RH)	6.8	8.81	33	4.1
	1.325		Wet (55%RH)	6.5	6.73	37	4.5

4.3 Hazard Evaluation According to Deflagration Index

The deflagration index K_G was estimated to analyze the recorded pressure profiles. K_G is commonly used to estimate and design an area of the explosion vent of an enclosure to release the internal pressure and protect structures where internal explosion may occur. To evaluate the real-scale hazard, the relationship of the pressure behavior to the deflagration index K_G and the presence of an open region was studied based on the experimental results in section 4.2.

4.3.1 K_G value

K_G is defined by ISO6184-2 (1985) and NFPA68 (2007) and is described in the following equation,

$$K_G = \left(\frac{dP}{dt} \right)_{max} \cdot V_{vessel}^{\frac{1}{3}} \quad (4.3.1)$$

where P is the pressure (100 kPa), t is the time (s), and V_{vessel} is the vessel volume (m³). A larger K_G requires a larger venting area to prevent the enclosure from bursting. Table 4.2.1 summarizes the deflagration indices K_G for each refrigerant along with other properties such as P_{max} , S_f , and S_u . The physical interpretation must be considered carefully because K_G is determined after the reflection of the flame front at the top wall, as noted in subsection 4.2.3; however, the evaluated values may be useful for designing the venting area. The results of the evaluated fundamental flammability characteristics will be expanded in scale for application to flammable behavior at actual scales, and an evaluation scheme for the potential risk of combustion and explosion in actual situations will be considered.

4.3.2 Potential risk of combustion of A2L refrigerants compared to other flammable gases

To realize the practical application of A2L/2L refrigerants and enhance safety, the potential risk of explosion, including detonation, should be considered. At present, few studies have reported on this matter. As an implicit but useful reference, a comparison of explosion characteristics such as the minimum ignition energy (MIE), detonation limit, and K_G with other flammable gases should be very informative. Table 4.3.1 lists flammable parameters such as P_{max} , K_G ,

burning velocity, flammability limits, and detonation limits (Mannan, 2005) for mixtures with air. P_{\max} and the burning velocity appear to have the same tendency as K_G . A further comparison of the combustion and explosion risks of A2L/2L refrigerants with other flammable gases should be considered.

Table 4.3.1 Comparison of P_{\max} , K_G , and other parameters with other gases.

Flammable Material	P_{\max} (100 kPa)	K_G (100 kPa·m·s ⁻¹)	Burning velocity (cm·s ⁻¹)	Flammability limits(%)	Detonation limits(%) ^{*3}		Autoignition Temperature (°C) ^{*6}
					Confined tube	Unconfined	
Acetylene	10.6 ^{*1}	1415 ^{*1}	166 ^{*2}	2.5—80.0 ^{*3}	4.2—50.0		305
Hydrogen	6.8 ^{*1}	550 ^{*1}	312 ^{*2}	4.2—75.0 ^{*3}	18.3—58.9		400
Ethylene			80 ^{*2}	2.70—36.0 ^{*3}	3.32—14.70		490
Diethyl ether	8.1 ^{*1}	115 ^{*1}	47 ^{*2}				
Benzene			48 ^{*2}	1.3—7.9 ^{*3}	1.6-5.55		562
Ethane	7.8 ^{*1}	106 ^{*1}	47 ^{*2}	3.0—12.4 ^{*3}	2.87—12.20	4.0—9.2	515
Propane	7.9 ^{*1}	100 ^{*1}	46 ^{*2}	2.1—9.5 ^{*3}	2.57—7.37	3.0—7.0	450
Butane	8.0 ^{*1}	92 ^{*1}	45 ^{*2}	1.8—8.4 ^{*3}	1.98—6.18	2.5—5.2	405
Ethyl alcohol	7.0 ^{*1}	78 ^{*1}		3.3—19.0 ^{*3}	5.1—9.8		
Methanol	7.5 ^{*1}	75 ^{*1}	56 ^{*2}				
Methane	7.1 ^{*1}	55 ^{*1}	40 ^{*2}				
Ammonia	5.4 ^{*1}	10 ^{*1}	7.2 ^{*4}	15—28 ^{*5}			651
R32	7.6 [†]	11 [†]	9 [†]	13.5—26.9 ^{*7}			
R1234ze(E)	6.8 [†]	9 [†]	5 [†]	5.95—12.7 ^{*8}			
R1234yf	6.6 [†]	8 [†]	3 [†]	5.4—13.5 ^{*8}			

*1 Ref. (NFPA68, 2007), Table E.1 (0.005 ft³ sphere; E = 10 J, normal condition). *2 Ref. (NFPA68, 2007), Table D.1.
*3 Ref. (Mannan, 2005), Detonation limits obtained for confined tube. *4 Ref. (ISO/DIS 817, 2010)
*5 Ref. (NFPA325, 1994) *6 Ref. (Mannan, 2005), Table 16.4
*7 Ref. (Kondo, 2014), at 35°C and 50%RH condition *8 Ref. (Kondo, 2012), at 35°C and 50%RH condition
† This work. (at 35°C and wet condition).

4.3.3 Evaluation of reduced pressure based on K_G

To apply refrigerants safely to air-conditioning equipment, the potential risk of combustion and explosion in actual situations should be evaluated by using the results of the laboratory-level fundamental evaluation stated in section 4.2. The relationship between the deflagration index and the influence on humans and structures was considered using the concept of vent design using K_G values. For example, the reduced effect of pressure due to an opening in the room can be evaluated based on vent design. Figure 4.3.1 illustrates the concept of explosion venting. In contrast to the pressure profile P and maximum pressure P_{\max} in the closed vessel used in section 4.2, the pressure profile will be characterized by the reduced overpressure P_{red} , maximum reduced overpressure $P_{\text{red,max}}$, and static activation overpressure for vent P_{stat} . The vent area A versus the designated reduced pressure $P_{\text{red,max}}$ for K_G can be estimated from various models (VDI-3673, 2002; BS EN 14491, 2012; Siwek, 1996). On the other hand, the vent area A is usually supposed to be circular or square-shaped. If the square is rectangular, the desirable ratio of the long side (L) to the short side (D) is within 2 (NIIS-TR-No.38, 2005). In an actual situation in the room, L/D will exceed 2, and the effective venting area A_v was experimentally evaluated. A spherical closed vessel was used in section 4.2, whereas a cubic vessel of side 50 cm was prepared for the test to simulate a room. The schematic apparatus and photograph of the cubic vessel are shown in Figure 4.3.2. The vessel is made of 3-mm-thick stainless steel and is equipped with a viewing window made of 10-mm-thick PMMA in the front side of the vessel. A circular vent is mounted on the side of the vessel to evaluate the fundamental pressure reducing effect on the presence of the venting space. The venting area was sealed with plastic wrap. Tubes for fuel gas inlet, exhaust gas outlet, and fuel concentration analysis were arranged at the top of the vessel. The gas concentration can be adjusted and determined by the partial pressure in a closed vessel; however, this evaluation was not possible in this vessel, and the concentration was measured by FT-IR analysis. The fuel gas was leaked into the vessel through the gas inlet tube at a rate of 10 g/min. A stirring propeller mixes fuel and air in the vessel to the premix condition. The gas concentration was measured at 15 cm from the bottom. A discharging electrode was positioned at 15 cm from the bottom and was used for DC discharge ignition. Two breather valves are mounted on the top of the vessel to prevent the buildup of excess pressure and protect the vessel structure. The measurements of the discharging voltage and current, pressure, and temperature in the vessel and the observation of the flammable behavior using the high-speed video camera were conducted concurrently with ignition. Figure 4.3.3 shows an example of high-speed video images of the flame front propagation behaviors for R32 for $\phi = 1.54$ with a $\phi 212$ mm circle vent. Initially, the flame front was expanded spherically and slowly lifted up due to buoyancy and become distorted; however, the internal pressure was increased due to the production of high-temperature combustion gas. The gas in the vessel was

discharged through the vent hall, and the flame front was gradually affected by the exhausting flow. The flammable behavior and reduced pressure were observed under the presence of various vent shapes—circles, squares, and rectangles—with different ratios of long and short sides. The reduced pressure effect was summarized according to the vent area and aspect ratio of rectangles. The effect of decreasing explosion severity due to the presence of the venting will be assessed by determining the relationship between the reduced pressure and the vent area and vent shapes (L/D).

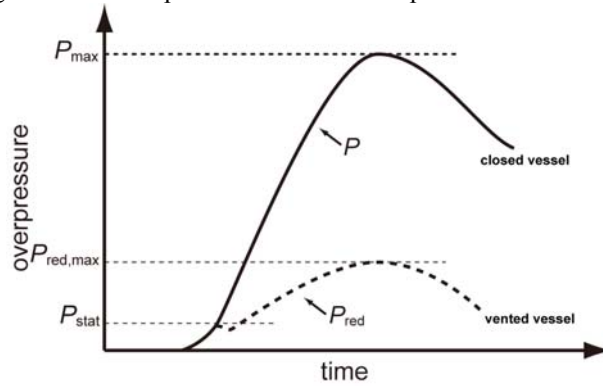


Figure 4.3.1 Reduced pressure behavior for venting.

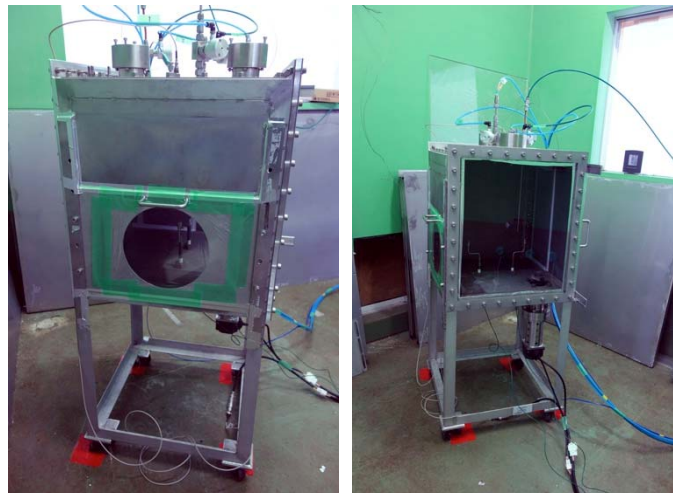
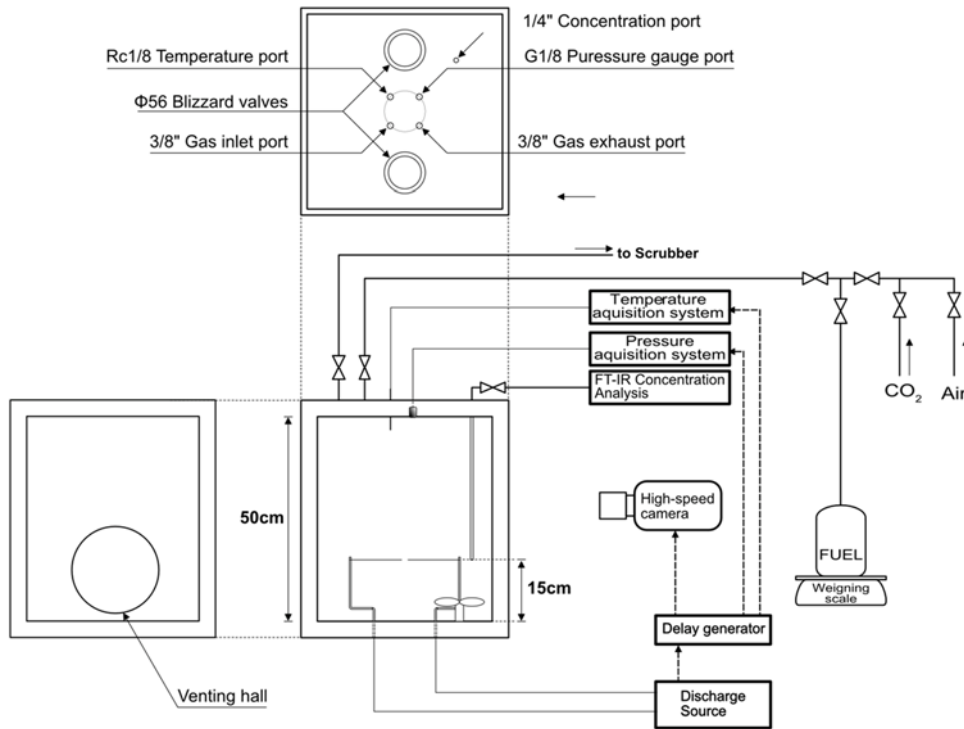


Figure 4.3.2 Schematic apparatus and photos of rectangular experimental vessel for vent effect.

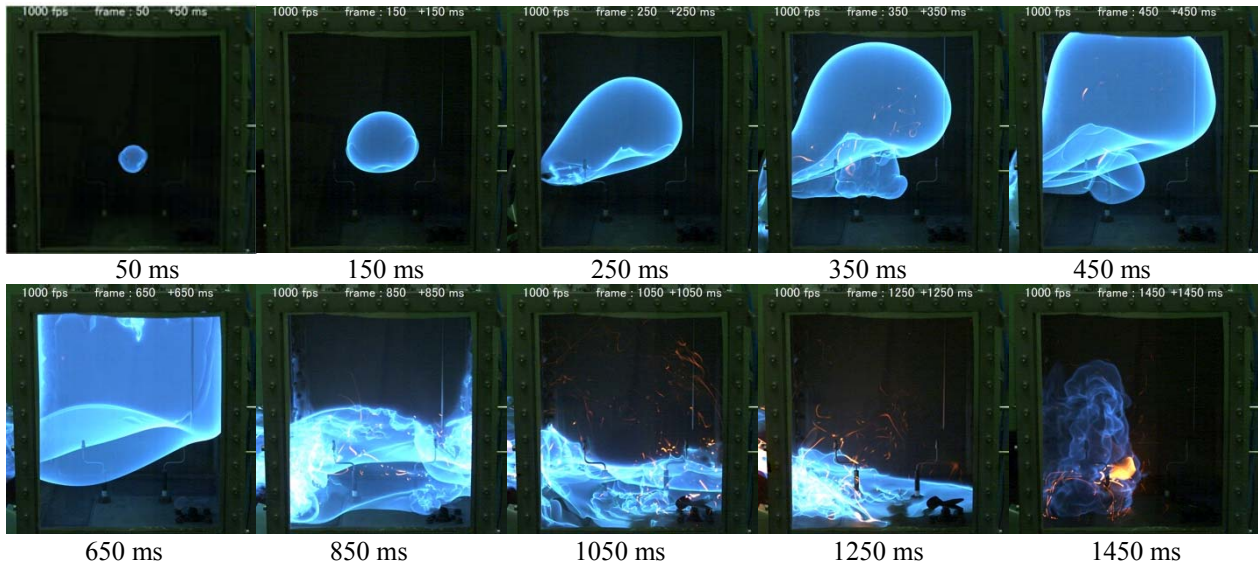


Figure 4.3.3 Images of flame propagation for R32 ($\phi = 1.54$) in rectangular vessel with $\phi 212$ mm circle vent.

4.4 Conclusion

To assess the physical hazard from the combustion and explosion of A2L refrigerants for ensuring safety, the fundamental flammability characteristics of A2L refrigerants were evaluated. The flammability was investigated in terms of parameters such as the flame speed, burning velocity, and K_G under the influence of elevated temperature and moisture and the uplift behavior due to buoyancy arising from slow burning velocity. To evaluate the explosion severity, the reduced pressure effect due to the presence of an opening in the room was studied, and the effective area of venting was experimentally evaluated according to the venting design for explosion protection. A cubic vessel with 50-cm side was prepared for the test. The flammable behavior and reduced pressure were observed under the presence of various vent shapes—circles, square, and rectangles—with different ratios of long and short sides. The reduced pressure effect was summarized according to the vent area and aspect ratio of the rectangles. To assess the explosion risk of A2L/2L refrigerants, the burning velocity and detonation limits were compared with those of other flammable gases. The evaluation results obtained in this chapter will be integrated with the outcomes from chapter 3.

Nomenclature

A_V	geometric vent area (m^2)
A_{eff}	effective vent area (m^2)
E_f	effective venting efficiency (%)
K_G	deflagration index for gases ($100 \text{ kPa}\cdot\text{m}/\text{s}^2$)
P	pressure (Pa)
P_{max}	maximum pressure (Pa)
P_{red}	reduced pressure (Pa)
dP/dt	rate of pressure rise ($100 \text{ kPa}/\text{s}$)
S_f	flame speed (cm/s)
S_u	fundamental burning velocity (cm/s)
S_{u0}	fundamental burning velocity at ambient condition (cm/s)
t	time (s)
T	temperature (K)
V_{vessel}	vessel volume (m^3)
ϕ	equivalence ratio
ρ	density (kg/m^3)

References

American Society for Testing and Materials, 2005, Standard Test Method for Autoignition Temperature of Liquid Chemicals, ASTM E 659–78.

- ASHRAE, 2010, Designation and Safety Classification of Refrigerants, ANSI/ASHRAE Standard 34-2007 Addendum ak.
- BS EN 14491, 2012, Dust Explosion Venting Protective Systems, British Standards Institution.
- European Commission, 2012, Proposal for a Regulation of the European Parliament and of the Council on Certain Fluorinated Greenhouse Gases, COM (2012) 643 Final.
- Gordon, S., and McBride, B. J., 1994, Computer Program for Calculation of Complex Chemical Equilibrium Compositions and Applications, I. Analysis, NASA RP-1311.
- Hill, P. G., and Hung, J., 1988, Laminar Burning Velocities of Stoichiometric Mixtures of Methane with Propane and Ethane Additives, *Combustion Science and Technology*, **60**, pp.7–30.
- ISO 6184-2, 1985, Explosion Protection Systems– Part 2: Determination of Explosion Indices of Combustible Gases in Air, (1985).
- ISO/DIS 817, 2010, Refrigerants: Designation and Safety Classification, International Organization for Standardization, Geneva, Switzerland, (current DRAFT DFS/ISO/FDIS 817:2012).
- Kondo, S., Takizawa, K., and Tokuhashi, K., 2012, Effects of Temperature and Humidity on the Flammability Limits of Several 2L Refrigerants, *Journal of Fluorine Chemistry*, **144**, pp. 130–136.
- Kondo, S., Takizawa, K., and Tokuhashi, K., 2014, Effects of High Humidity on Flammability Property of a Few Non-Flammable Refrigerants, *Journal of Fluorine Chemistry*, **161**, pp. 29–33.
- Mannan, S., 2005, *Lee's Loss Prevention in the Process Industries*, 3rd ed., Elsevier, **2**, p.1383.
- Metghalchi, M., and Keck, J. C., 1980, *Combustion and Flame*, **38**, pp. 143–154.
- NFPA, 1994, NFPA 325 Guide to Fire Hazard Properties of Flammable Liquids Gases, and Volatile Solids, NFPA.
- NFPA, 2007, Guide for Venting of Deflagrations 2007 Edition, NFPA **68**.
- NIIS-TR-No.38, 2005, Technical Recommendations of the National Institute of Industrial Safety, ISSN 0911-8063 (in Japanese).
- Pfahl, U. J., Ross, M. C., and Shepherd, J. E., 2000, Flammability Limits, Ignition Energy, and Flame Speeds in H₂–CH₄–NH₃–N₂O–O₂–N₂ Mixtures, *Combustion and Flame*, **123**, pp. 140–158.
- Saburi, T., *et al.*, 2014, Flammable Behaviour of A2L Refrigerants in the Presence of Moisture, *10th International Symposium on Hazards, Prevention, and Mitigation of Industrial Explosions*, Bergen, pp. 327–334.
- Siwek, R., 1996, Explosion Venting Technology, *J. Loss Prev. Process Ind.*, **9**, 81–90.
- Takizawa, K., *et al.*, 2009, Flammability Assessment of CH₂=CFCF₃: Comparison with Fluoroalkenes and Fluoroalkanes, *Journal of Hazardous Materials*, **172**, pp. 1329–1338.
- Takizawa, K., Takahashi, A., Tokuhashi, K. Kondo, S., and Sekiya, A., 2005, Burning Velocity Measurement of Fluorinated Compounds by the Spherical-Vessel Method, *Combustion and Flame*, **141**, pp. 298–307.
- Takizawa, K., Tokuhashi, K., Kondo, S., Mamiya, M., and Nagai, H., 2010, Flammability Assessment of CH₂=CFCF₃ (R-1234yf) and its Mixtures with CH₂F₂ (R-32), *2010 International Symposium on Next-generation Air Conditioning and Refrigeration Technology*, Tokyo, P 08.
- VDI-3673, 2002, Pressure Venting of Dust Explosions, Verein Deutscher Ingenieure.

5 Procedure for Risk Assessment of Mildly Flammable Refrigerant

5.1 Introduction

The risk assessment of mildly flammable refrigerants such as R32, R1234yf, and R1234ze(E) was promoted by SWGs of the Japan Refrigeration and Air Conditioning Industry Association (JRAIA). As shown in Fig. 5.1.1, the mini-split air-conditioner risk assessment SWG (I) compared a mildly flammable refrigerant with conventional refrigerant from the viewpoint of risk. The SWG tried to assess the risk of flammability caused by the ignition and inflammable properties of the NEDO project. In the risk assessment, the two hazards of burning harmful fluorine compounds and diesel explosion during service and disposal were not studied. This was because when we started the study on mildly flammable refrigerants, we had little scientific knowledge on these two hazards. We began an assessment on the two hazards to gain more scientific knowledge through a collaboration between the University of Tokyo and National Institute of Advanced Industrial Science and Technology (AIST). At present, the two hazards for mildly flammable refrigerants do not differ from the hazards of conventional refrigerants, so we did not start a risk assessment study on them. We believe these hazards are problematic but are accepted by society. The procedure for assessing the flammability risk of mildly flammable refrigerants is described below.

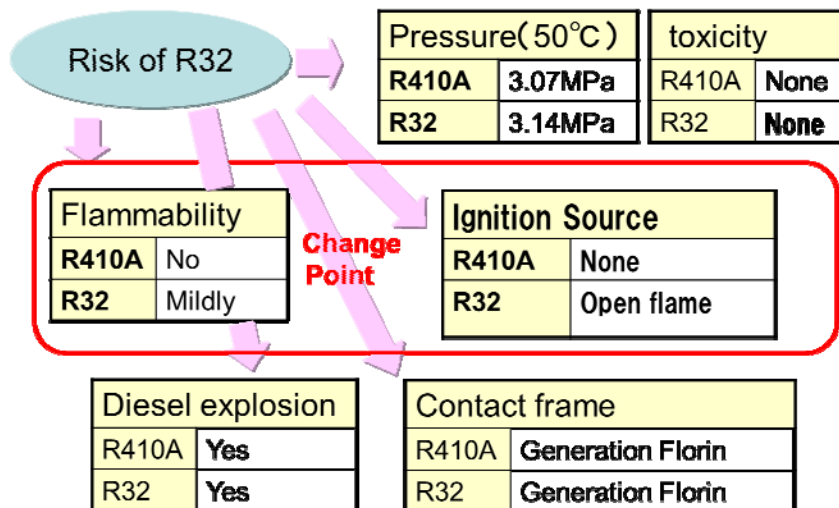


Fig. 5.1.1 Hazard comparison of mildly flammable and conventional refrigerants

5.2 Procedure of Risk Assessment

Figure 5.2.1 shows the procedure for the risk assessment of mildly flammable refrigerants, with steps added to IEC Guide 51.

The steps are as follows:

- Select risk assessment method
- Select evaluation region for the product
- Select stages of the air-conditioner's life cycle
- Investigate the air-conditioner's installation circumstances
- Determine severity of hazard
- Set tolerance levels
- Investigate refrigerant leak rate, speed, and amount of air-conditioner
- Use CFD or calculations to determine flammable time volume
- Consider ignition sources.

When these steps have been performed, the risk is specifically estimated in FTA.

The steps continue.

- j) Develop FTA and calculate probability followed by inspection
- k) Compare risk (consistency with the tolerance)
- l) Evaluate risk (consistency with the tolerance)

When the risk is below the risk tolerance, the risk assessment stopped. If the risk is above the tolerance, then the next steps must be performed.

- l) Reduce risk (Measures include the implementation of equipment, a manual, and regulations)
- m) Redevelop FTA and recalculate probability

The procedure then returns to the following step:

- k) Compare risk (consistency with the tolerance)

When the risk is below the tolerance, the procedure goes to

- n) Commercialize (confirm important topics) and release to market.

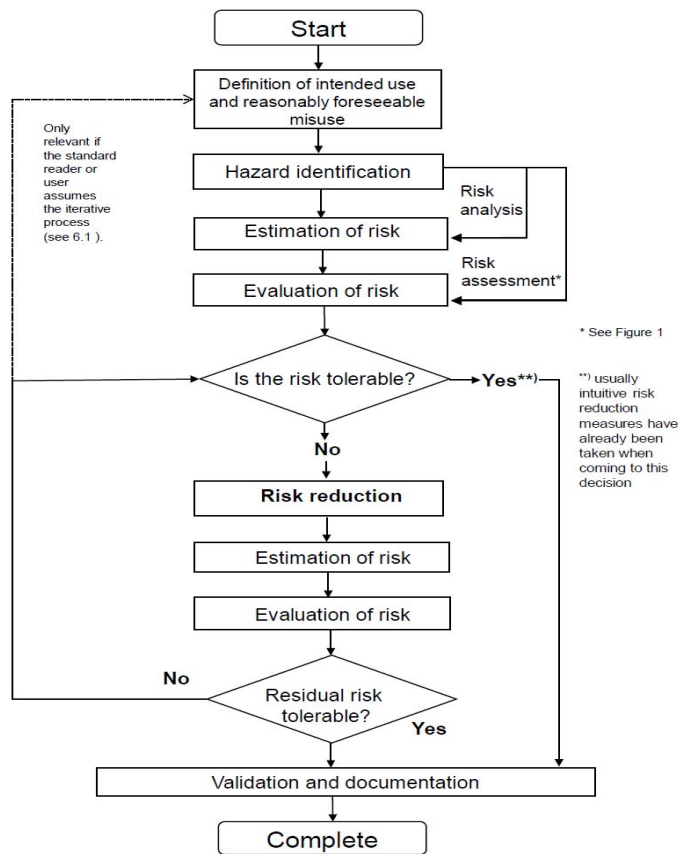


Fig. 5.2.1 Iterative process of risk assessment and risk reduction

In the NEDO project, the groups studying the flammable properties differ from the groups performing the risk assessment. Thus, it took time for the groups to perform tests. When an experimental result was obtained, later groups proceeded with the risk assessment and improved the accuracy.

This is described from the next clause in detail.

In general, the risk assessment was performed using methods such as FTA, ETA, FMEA, etc. The risk assessment of flammable

Strategy of Risk Evaluation		Risk				
Likelihood ↑	Frequently	10 ⁻²				Not acceptable
	Some time	10 ⁻³				Not acceptable
	Rare	10 ⁻⁴				Acceptable with conditions
	Usually not	10 ⁻⁵				Acceptable
	Very difficult	10 ⁻⁶				Acceptable
	Extremely difficult	10 ⁻⁷				Acceptable
	Near zero	10 ⁻⁸				Acceptable
	Possibility of incident:		0	I	II	III
		No damage	Minor damage (smoke from product)	Light damage (fire from product, light injury)	Major damage (fire, human injury)	Lethal damage (permanent injury, death, burn down house)
		→ Severity				

Fig. 5.2.2 Risk map

refrigerants considers two individual phenomena: the presence of an ignition source and the generation of a flammable volume. Thus, we choose FTA to determine the individual phenomena because it allows for easy calculation.

The 2001 risk assessment performed at JRAIA on the use of propane in air-conditioners was also based on FTA, but the concept of a risk map (R-map) had not yet been perfected, and the accident-generation probability (i.e., tolerance) is given in below. Figure 5.2.2 shows an R-map with a particular focus on safety.

For the target setting of the equipment in the risk assessment, the product committee in JRAIA considered a household air-conditioner, a building with multiple air-conditioners, and a chiller. There are many variations in air-conditioning equipment, and making clear divisions in the target equipment is difficult. However, although the products differ, the installation situation, usage state, installation persons, service persons and disposal method (considering regulations) generally show distinct features. It is necessary to divide air-conditioners into different groups and assess the individual risk of each group.

When air-conditioners are placed in very narrow classifications, the risk assessment needs to be performed on an individual basis. This complicates the risk assessment, and data common to different groups cannot be collected. In addition, the circulation number of the target product becomes low. Therefore, the tolerance value, which is described later, will be large, and there will be concern that the safety of the actual product has not been sufficiently secured.

5.3 Air-Conditioner Equipment and Risk Assessment Situation

Figure 5.3.1 shows the variety in air-conditioners, and Table 5.3.1 compares the household air-conditioner, commercial air-conditioner, building multi-air-conditioner, and chiller.

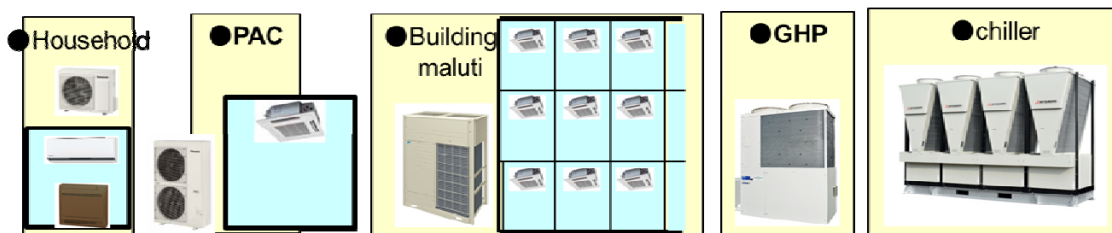


Fig. 5.3.1 Variety of air-conditioner

Table 5.3.1 Comparison of air-conditioner

Type	SWG	Horse power	Cooling Capacity	Refrigerant amount	Install form (outdoor/indoor)
Household A.C.	Mini-split SWG (I)	0.8~3HP	2.2~8.0kW	0.5~2kg	1set/1set
Housing Maluti A.C.		1.5~3HP	3.6~8.0kW	2~4kg	1set/2~4set
Commercial PAC	Mini-split SWG (II)	1.5~12HP	3.6~30kW	2~19kg	1set/1~4set Indoor unit installed in same room
Building Maluti A.C.	Building maluti SWG	5~60HP	14.0~168kW	5~100kg	1~3set/2~64set Indoor unit installed in individual room
GHP	GHP SWG	↑	↑	3~200kg	↑ (By engine drive)
Chiller	Chiller SWG	3~500HP	7kw~	1~7000kg	1~120set : water cooling unit

Figure 5.3.2 shows the evaluated risk of each air-conditioner. The leak rate, leak speed, flammable space volume, and ignition sources were selected for a wall-mounted air-conditioner for household use. Then, the first FTA was performed, and the ignition sources and flammable volume time were reexamined based on the new information gained by the NEDO project. After the SWG considered the

new information, the obtained risk of the wall-mounted air-conditioner was below the tolerance permitted by the R-map. Thus, the risk assessment was stopped. For the floor-type air-conditioner for household use, the first risk value was not below the tolerance value. Therefore, we reconsidered its actual use, and the structures of houses in Japan were investigated again. Fan agitation measures were also performed. The risk assessment was repeated, and the risk was found to be lower than the tolerance in the R-map.

The leak rate, leak speed, flammable time volume, and ignition sources were selected for the commercial air-conditioner and building multi-air-conditioner in the same manner and evaluated in the first FTA. However, the risks of installation when semi-underground, in a narrow place, and a karaoke shop did not meet the tolerance values allowed in the R-map. Therefore, measures were taken to develop a manual and standards to ensure that the risk was below the tolerance.

A chiller contains a large amount of refrigerant, so the flammable time volume in the event of a leak is large. Because there are multiple ignition sources on the side, such as electromagnetic switches with a large capacitance, the risk will be above the permitted tolerance according to the R-map. Therefore, an exhaust device needs to be developed so that a flammable volume will not form. The SWG is considering regulations to enforce such a measure.

Because the equipment means a large refrigerant amount, many ignition sources, and large flammable time volume, measures are needed to ensure warnings of gas and dispersal methods such as a spread fan, exhaust fan, and external equipment. Manuals and industry association standards need to be incorporated to enforce standards.

Hereinafter, the household air-conditioner and chiller are differentiated in terms of the FTA for the equipment and measures. However, a basic risk assessment does not greatly differ for a household air-conditioner, commercial air-conditioner, building multi-air-conditioner, and chiller.

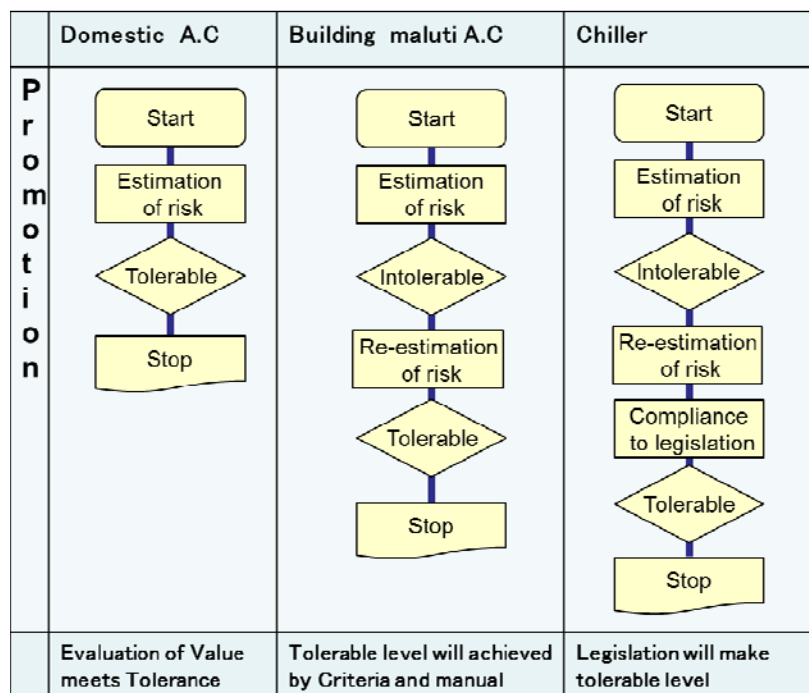


Fig. 5.2.3 Risk assessment

The steps for the risk assessment of a household air-conditioner are described below. Content was excerpted from the risk assessment method described in the previous progress report, so there is some overlap. After the risk assessment procedure for a household air-conditioner is described, the differences between a building multi-air-conditioner, commercial air-conditioner, and chiller are detailed. The risk assessments for a building multi air-conditioner, commercial air-conditioner, and chiller are described afterward.

5.4 Risk Assessment Procedure for Household Air-Conditioner

5.4.1 Tolerance level of risk assessment

The presentation of the National Institute of Technology and Evaluation (NITE) is referred to in order to describe the risk assessment of the accident probability. Figure 5.4.1 outlines the risk levels.

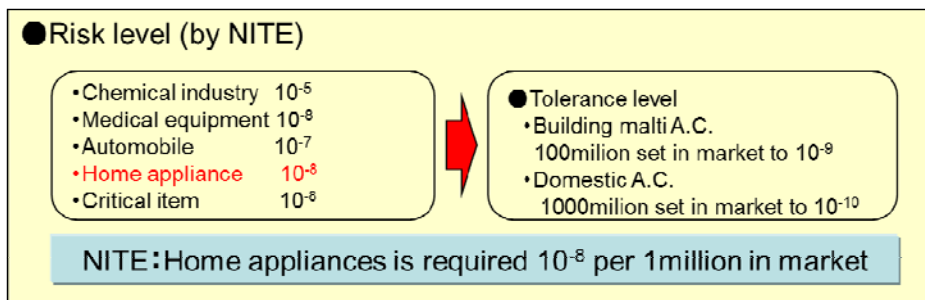


Fig. 5.4.1 Risk level

Large-scale facilities such as chemical plants are managed by various regulations and have a risk tolerance of about 10^{-5} . However, the tolerance for a home electronics unit owned by an ordinary consumer, who does not generally consider maintenance, is 10^{-8} accidents/year (based on 1 million sets sold). In other words, a product is regarded as safe if a fatal accident occurs once in 100 years for 1 million sets in circulation. The total number of household air-conditioners in circulation is about 100 million, so the target probability for risk tolerance is 10^{-10} accidents/year.

An important relation between the circulation number and accident probability is when there are 100,000 products in circulation. At this point, the probability of a major accident should be below about 10^{-6} .

However, while the handbook of the Ministry of Economy, Trade and Industry considers fatal accidents, the probability of an important accident should be considered. When the tolerance was established in our risk assessment, the amount of harm was not considered; thus, when an ignition accident occurred, only the risk of the worst-case scenario (i.e., fatality) was assessed.

Heinrich's empirical rule says that there are 300 accidents for every serious accident. If this empirical rule holds true for the risk assessment, the risk may be 300 times the tolerance in the worst case. This risk assessment on the use of a mildly flammable refrigerant in a household air-conditioner calculated the risk of minor harm. However, the mini-split air-conditioner considered by SWG (I) set the tolerance value conservatively. This is because conventional refrigerants are not flammable, but the refrigerant under study is mildly flammable. The previous study considered the risk severity level of the mildly flammable refrigerant to be minor damage; thus, a more efficient and cost reasonable air-conditioner was developed.

For building multi-air-conditioners and commercial air-conditioners, the SWG adopted a risk tolerance of less than once per 100 years. On the other hand, the risk of a chiller can be reduced by maintenance, intervention by specialists, and regulations like those followed for use in industrial factories. Therefore, the SWG adopted a tolerance of once per 10 years for chillers. This tolerance is the value set in Japan; the tolerance differs for each country and area, where the custom and culture differ. The safety requirements for air-conditioners also differ, so the tolerance in each country should be established individually according to the social conditions and acceptable risk level.

5.4.2 Setting of leakage

The numerical values of the leak rates for each service company belonging to the JRAIA were weighted according to the market share of each company to determine the mean refrigerant leak rate for all products in the household air-conditioner market. Each household air-conditioner service company is affiliated with an equipment manufacturer, mostly in Japan, and the related service company receives a majority of the service work. Therefore, the leak rate data are highly reliable. In Japan, the leak rate for all of the household air-conditioners is 0.023% per year.

With regard to the leak speed, there are many forms of leakage. One takes place over several days and depend on pipe corrosion. Another form is a slight leakage over several months. In addition, rapid leakage can occur with a defective weld that leaks in several hours. In the first risk assessment, the leak speed was calculated under the last condition because of the high leak speed. According to IEC60335-2-24, the severest case would be all of the refrigerant leaking out in 4 min. This occurs when a plumbing pipe breaks and the household air-conditioner spouts its refrigerant. However, the leak rate is determined under the assumption of no decrease due to

temperature and no dissolution balance for the refrigeration oil of a refrigerant; thus, these conditions are not realistic. The leakage was set so that all of the refrigerant was leaked. The leak rate and leak amount of the household air-conditioner were not reconsidered because the tolerance value was mostly met. However, the results of the risk assessment for the air-conditioner calculated under such severe setting are described later.

An indoor leak speed of 10 kg/h, as prescribed by ISO5149, was adopted for the building multi-air-conditioner and commercial air-conditioner. The comparison to the market reliability data referred to this value, and the rates of slow leakage (10 kg/h), rapid leakage (100 kg/h), and high-speed leakage (750 kg/h) were determined for an indoor unit and outdoor unit. The chiller was assumed to spout refrigerant out at an audible speed when a leak forms.

5.4.3 Setting of flammable spaces

When estimating the flammability, setting the space volume is the most important step. When estimating a small space, harmful ignition is certain to occur in every case. In other words, when the space is set too small, a flammable refrigerant cannot be used. In Japan, household air-conditioners are generally installed in rooms with floor areas of about 9.9 m². This can be considered a suitable value, but the catalog specifies installation in rooms up to 7.43 m² in size (i.e., 4.5 *tatami* mats). Thus, the risk assessment performed in 2000 for air-conditioners using propane used an area of 7 m² (4 mats) as the severe condition. Therefore, the leak space was set to a floor area of 7 m² and height of 2.4 m for the risk assessment of a household air-conditioner installed at a height of 1.8 m. Figure 5.4.2 outlines the interior space of the room and the installation situation. For the outdoor unit, three sides were assumed to be walls, and the fourth was assumed to be a glass window opening up to an apartment.

For a building multi-air-conditioner, the office room was initially set to a 13 m² area and height of 2.7 m. In the following risk assessment, a karaoke room and eatery have small enclosed rooms. The outdoor unit was first set to have two surrounding walls. However, for the risk assessment of the interior, severe conditions such as the diffusion effect of wind on semi-underground installation and a machinery room were difficult to establish. For a specific chiller volume, the mean, minimum, and maximum values of the machinery room area are summarized in the List of Completed Facility Research of the Journal of Heating and Air-Conditioning Sanitary Engineering (2007–2010). In the analysis model, the area of the machinery room was defined as the average value, and the height of the machinery room was defined as 5 m.

The next hazard considered was a refrigerant leak during storage in a warehouse before physical distribution. Household air-conditioners are often kept in large-scale depots near the sales area, but a medium-scale depot of semi-fireproof construction as set by the Building Standards Law was considered in this risk assessment. This room was assumed to have a floor area of 1000 m² and store 10,000 sets. Under these conditions, the volume is small and the risk is high.

Because the circulation process would not change when a building multi-air-conditioner or commercial air air-conditioner are transported, a medium-scale depot of semi-fireproof construction was assumed, and the depot was assumed to contain 2300 sets because of the different equipment size. In a chiller filled with a refrigerant, when the pipes are laid in the building, there are no hazards from a mildly flammable refrigerant.

Even the conditions for the service and disposal steps were determined from an investigation of each company and consultation with the SWG. Rather severe conditions were established, and a risk assessment was performed for each step.

5.4.4 Simulation of flammable time volume

The generated volume and duration of the flammable region were determined based on the leak rate and space volume given above. The integrated value is referred to as the flammable time volume.

In short, the flammable time volume is the ratio of the flammable area generated in 1 year base to the assumed space and that is maintained. In the early stages of the risk assessment on the use of a propane air-conditioner, the flammable time volume was

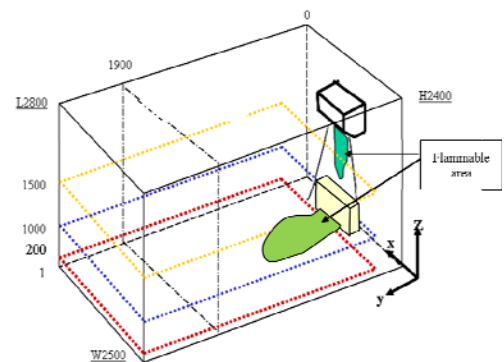


Fig. 5.4.2 Installation air-conditioner

determined by converting the calculated value into the equivalent R32. The interface of separation and reformation was established in 2012 by the University of Tokyo and calculated from simulation results to ensure that pressure does not eventually build up to cause a refrigerant leak. Figure 5.4.3 shows the simulation conditions for each air-conditioner considered by the University of Tokyo.

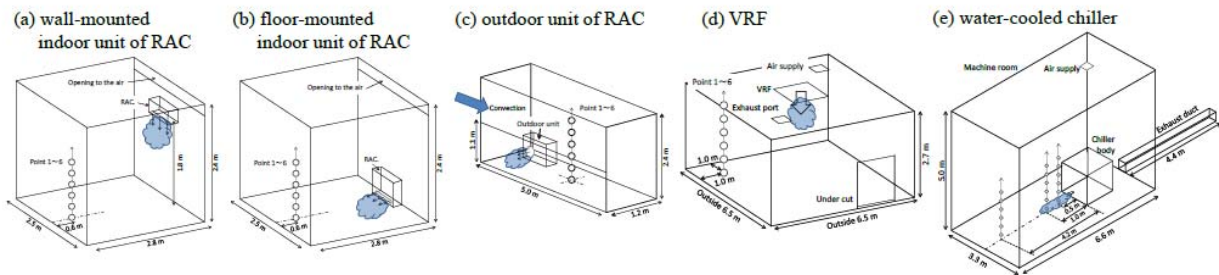


Fig. 5.4.3 Simulation conditions of each air-conditioner

The flammable time volume of each simulated air-conditioner is given in the figure from the University of Tokyo, and each SWG of JRAIA calculated the ignition probability using these values.

Table 5.4.1 gives the flammable time volumes of R32 and R1234yf used in a mini-split air-conditioner SWG(I). For R1234yf, each value was calculated by converting it to the equivalent simulated value of R32 under the same conditions.

Table 5.4.1 Flammable time volumes in leakage situations ($\text{m}^3 \cdot \text{min}$)

	R290	R32	R1234yf
1.1 Logistics	5.50×10^1	2.00×10^{-4}	2.20×10^{-4}
2.2 Installation	7.16×10^2	2.40×10^{-3}	2.50×10^{-4}
2.5 Mistakes	7.75×10^{-2}	9.00×10^{-3}	1.30×10^{-2}
2.10 Refrigerant charge	8.51×10^3	9.97×10^1	3.70×10^2
3.1 Indoor unit operation	1.41×10^1	5.00×10^{-4}	5.50×10^{-4}
3.5 Indoor unit stop	7.16×10^3	2.40×10^{-2}	2.50×10^{-2}
4.1 Outdoor unit	7.76×10^{-1}	9.00×10^{-2}	1.30×10^{-1}
5.1 Connecting pipe	8.51×10^3	9.97×10^2	3.70×10^3
7.8 Service/relief	7.75×10^{-2}	9.07×10^{-3}	1.30×10^{-2}
8 Disposal	Using similar situations and values		

The flammable time volume for a household air-conditioner excluding a full refrigerant leak was small at 10^{-4} to $10^{-2} \text{ m}^3/\text{min}$. On the other hand, it could become large for a building multi-air-conditioner and chiller at $0.6\text{--}314 \text{ m}^3/\text{min}$.

Note that the flammable time volume is obtained by CFD, if a value is based on CFD, it can be obtained by simplifying the equation changed by SWG according to Kataoka's reports. The flammable time volume can be obtained with the following equation:

$$V_{\text{tv}} = (\text{Rg}/(\text{H} \times \text{A})^{1/2})^3 \quad (5.4.1)$$

When using these values, the interior and height of the space can become large numbers, carefully judging the calculated values is necessary.

5.4.5 Setting of ignition sources

If the R32 refrigerant used in a household air-conditioner leaks to the environment, a flammable atmosphere can form in rare cases. In such a case, sparks from electrical equipment, metal collision, and static electricity or the open flame of combustion equipment such as oil stoves are assumed to be ignition sources. In addition, smoking objects can ignite oil and gas with sparks to produce an open flame. These ignition sources were examined in detail in the 2011 and 2012 progress reports of the Japan Society of Refrigerating and Air Conditioning Engineers. The SWG referenced the reports by Imamura et al. (2012), Takizawa (2011), and Goetzler et al. (1998) to describe the following items assumed to be ignition sources:

- (1) An electromagnetic contactor with no cover ignites at 7.2 kVA or more. However, if a contact is covered with a clearance of 3 mm or less, it does not ignite until 12 kVA or more. Low-voltage electrical equipment in Japanese homes almost never ignites.

- (2) Electronic lighter rarely ignites, and flame doesn't propagate.
- (3) Mildly flammable refrigerant is not ignited by burning tobacco that does not emit a flame.
- (4) Kerosene fan heater is not flame propagation under the influence of the flow.
- (5) Static electricity caused by humans in a living space almost never causes ignition.
- (6) To ignite by open flame with a weak flame, such as candles and matches.

Based on the above considerations, the ignition sources of outdoor and indoor household air-conditioner units using R32 or R1234y were assumed to be open flames in the risk assessment. Note that the ignition sources of store air-conditioners, which have a different environment, are described separately.

The capacitance increases with the size of the equipment, so the settings for the ignition sources in a household air-conditioner, building multi-air-conditioner, and chiller are different. Even if the household air-conditioner has a small refrigerant leak, and the refrigerant burns in the burning apparatuses, the flame does not propagate. Table 5.4.2 lists the ignition sources for each air-conditioner.

Table 5.4.2 Ignition sources of air-conditioners Y: ignited, NF: no flame propagation, N: not ignited

		Ignition source	Domestic A.C	Commercial P.A.C	Building-multi P.A.C	Chiller
Spark (in flammable region)	Electric parts	Appliance (cause of fire)	NF	Y	Y	Y
		Parts in unit (below 5 kVA)	—	NF	NF	Y
		Power outlet, 100 V	N	N	N	Y
		Light switch	N	N	N	N
	Smoking equipment	Match	Y	Y	Y	Y
		Oil lighter	NF	NF	NF	NF
		Electric gas lighter	N	N	N	N
	Work tool	Metal spark (forklift)	Y	Y	Y	Y
		Electric tool	N	N	N	N
		Recovery machine	N	N	N	N
Human body	Static electricity	N	N	N	N	
Open flame (contact with flammable region)	Smoking equipment	Match	Y	Y	Y	Y
		Oil or gas lighter	Y	Y	Y	Y
	Combustion equipment	Heater	NF	Y	Y	Y
		Water heater	NF	Y	Y	Y
		Boiler	NF	Y	Y	Y
		Cooker	NF	Y	Y	Y
	Work tool	Gas burner (Welding)	Y	Y	Y	—

In a mini-split air-conditioner SWG, such ignition sources were considered, and the years it would take for each ignition source to manifest in the home was determined. A fire accident from gas was specifically picked out from the statistics of the Japanese Fire-Deface Agency. The number of ignition sources that were open flame was extracted from the number of Japanese the dwelling area. This allowed the probability for an ignition source of presence in a dwelling area over a year in ordinary homes to be determined. The same probability is described in later sections for the building multi-air-conditioner, commercial air-conditioner, and chiller.

5.4.6 Human error probability

The human error of a worker is a factor for a refrigerant leak, and an accidental fire can occur in the operational stage, which comprises installation, repair, and disposal. Table 5.4.3 presents the event probability of a worker's human error considered by the

Table 5.4.3 Human error probability

Phase	Mode of conciuosness	Physiological state	Probability
0	Unconscious, Syncope	Sleeping	1
I	Blurring	Weary, Snoozing	> 1E-1
II	Normal, Relaxed	at rest, Usual working	1E-2 to 1E-4
III	Normal, Clear	Active state	< 1E-5
IV	Excited	in a hurry, panic	> 1E-1

SWG for a building multi-air-conditioner. Hashimoto (1984) reported on “safe human engineering,” and this table indicates the error probability according to the worker’s mode of consciousness. Normally, the error probability is 10^{-2} to 10^{-5} when the worker is relaxed. The worker’s human error probability was set to 10^{-3} for the household air-conditioner and commercial air-conditioner. Such workers who handle building multi-air-conditioners are considered to have received relatively good training. The human error probability was set to 10^{-4} in the FTA.

5.4.7 Consistency with tolerance value

After the requirements are set as above, the FTA is developed, and the ignition probability is determined. The FTA is constructed according to the probability that a refrigerant leaks, the flammable density and presence of the leaking refrigerant (flammable time volume), and the probability of ignition sources each year. This can be simply expressed as follows:

$$A_p > F_p = L_p \times V_p \times I_p \times D \quad (5.4.2)$$

where A_p is the tolerance, F_p is the ignition probability, L_p is the rapid refrigerant leak, V_p is the flammable time volume, I_p is the probability of an ignition source manifesting per year, and D is the duplicating rate.

The duplicating rate D is explained in section 5.5. The presence of V_p and I_p in an indoor space is not perfectly duplicated. For example, when a highly dense refrigerant leaks to diffuse about 15 cm above the indoor floor, the generated flammable region is at a height of 3–12 cm. Thus, if a person lights a cigarette with an oil lighter while sitting in a chair, ignition combustion will not occur. In order to represent a situation where it will occur, such as when the person is stooping down from the chair to light up a cigarette, D should be adjusted from 0 to 1. However, even in a complicated study, the effects on the final numbers of the FTA were small. Thus, in most cases the mini-split SWG (I) set $D = 1$. Based on the calculation results in the FTA of the initial risk assessment, D was set to 1 in the simplified equation (1). Therefore, the ignition probability was calculated even when the location of the flammable region and ignition sources did not match. The derived values thus actually contained a fairly large safety margin. The mini-split SWG (I) did not consider V_p for the current velocity when a refrigerant leaked.

Figure 5.4.4 shows the FTA based on the previous equation (5.4.2).

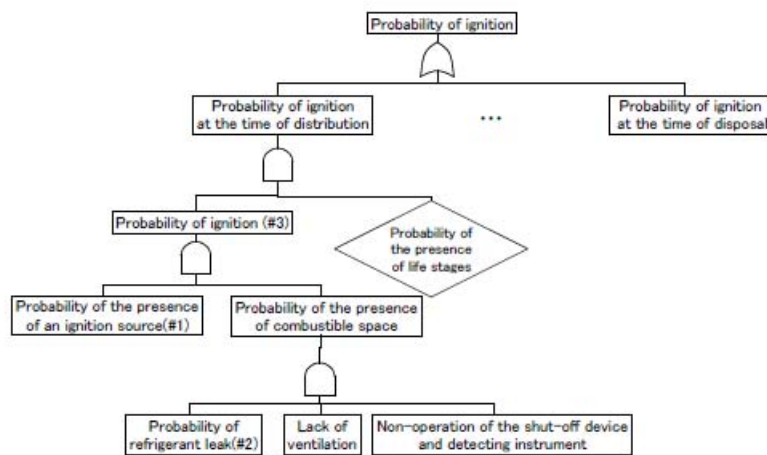


Fig. 5.4.4 Basic FTA of mildly flammable refrigerant

This FTA expanded in detail for each stage, and the calculated values for transport and storage, installation, usage, service, and disposal were obtained. If the obtained value was less than the tolerance value, the risk assessment generally ended and proceeded to step k (Commercialize and release to market). If the calculated risk was more than the tolerance value, the review took two paths. One was following steps h–j. That is, the measures to reduce the risk were reviewed. The second was to find an event in the critical path

that raises the risk value in the FTA. If the number of hypothesized events was not a rough number, more accurate numbers were obtained through analysis of the information or more detailed experiments. The calculated values from the review loop of this FTA were repeated until the tolerance value was met. Several measures can be considered to lower the risk below the tolerance value. Figure 5.4.5 shows the actual calculated ignition probability in the mini-split SWG (I) for the usage stages. Strict values were set in the logistics, installation, usage, service, and disposal stages to calculate the probability for the FTA. The value was lowered below the tolerance through a review of the probability calculation. Table 5.4.5 presents the tolerance values of the ignition probability and the R32 values of each stage.

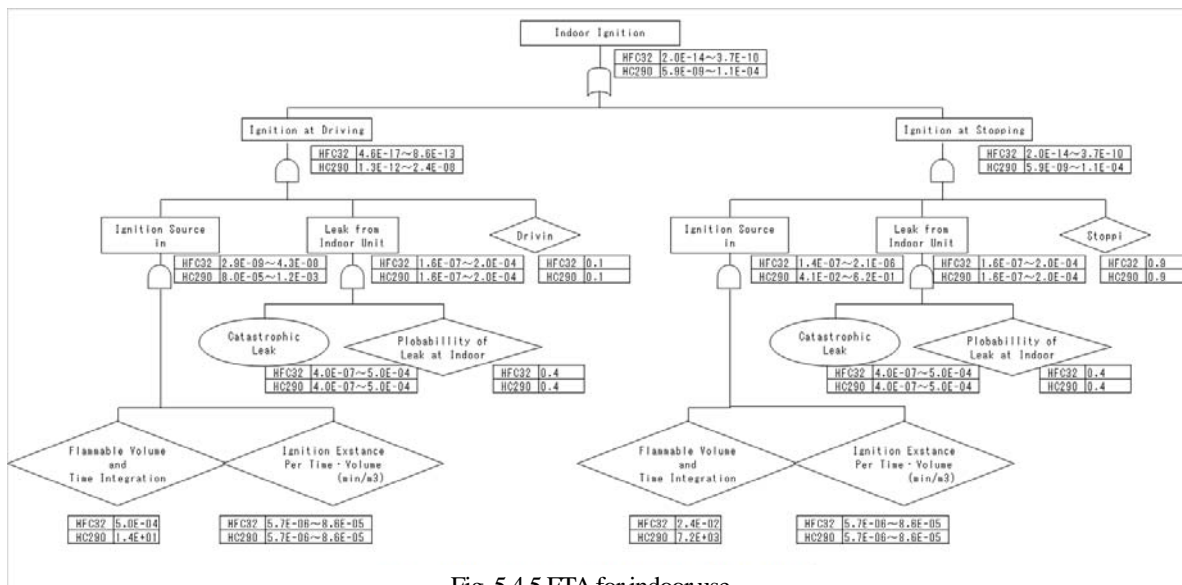


Fig. 5.4.5 FTA for indoor use

Since the tolerance showed almost no change, it was safe to perform more detailed analysis on the household air-conditioning. The SWG judged a safety manual to be necessary, and documentation was developed for work safety during installation and service. Note that the one-to-one connection of floor-type housing air-conditioners and multi-connection air-conditioners installed on floor as analyzed by the SWG did not be reach the tolerance values in the primary evaluation. This is explained in detail in Chapter 6.

Table 5.4.5 Results of risk assessment review

Risk: Ignition Probability			
	R290	R32	R1234yf
Logistic	9.2×10^{-11} – 1.4×10^{-7}	4.1×10^{-12}	4.5×10^{-12}
Installation	3.7×10^{-9} – 2.2×10^{-8}	2.7×10^{-10}	3.1×10^{-10}
Use (Indoor)	5.0×10^{-13} – 9.5×10^{-9}	3.9×10^{-15}	4.3×10^{-15}
(Outdoor)	4.9×10^{-13} – 9.3×10^{-9}	1.5×10^{-10}	2.1×10^{-10}
Service	2.8×10^{-7} – 8.1×10^{-7}	3.2×10^{-10}	3.6×10^{-10}
Disposal	4.1×10^{-7} – 5.1×10^{-7}	3.6×10^{-11}	5.3×10^{-11}

After the leak rate was selected, the leak speed, flammable time volume, and ignition sources were determined in the same way, and the initial FTA was performed for the commercial air-conditioner and building multi-air-conditioner. The risk for a refrigerant leak from these air-conditioners on the ceiling of an office was below the tolerance. However, in a secondary evaluation where the air-conditioners were semi-underground and in a narrow place (e.g., a karaoke shop), the risk was higher, and a manual was developed to lower the risk to below the tolerance according to the R-map.

A chiller has a large enclosed capacity. Therefore, the flammable time volume in the event of a leak is large. Because there are more ignition sources inside, such as an electromagnetic switch with a large capacitance, the possible risk was not below the tolerance according to the R-map in the first evaluation. Therefore, an exhaust device is necessary to prevent the formation of a flammable

region. To enforce such a measure, regulations are being considered.

5.4.8 Summary of household air-conditioner

The SWG(I) described above set a small volume of space and high leak rate. The flammable time volume did not become too large, and the ignition probability for sources other than an oil lighter was minimal at less than or equal to the tolerance value. Therefore, a second risk assessment was not performed, and the risks associated with flammability during the life cycle were evaluated again. When the risk was reconsidered in sequence, all of the members in the SWG(I) confirmed that there was no problem. Note that installation work on household air-conditioners in Japan is often carried out by local electrical shop or professionals. A plumbing manual should be developed in order to improve the accuracy of the work during installation and service. This content from JRAIA has been published to affiliated companies and related organizations, and the contents reflect the work manuals of each air-conditioner manufacturer and related organizations.

5.5 Differences of Building Multi-Air-Conditioner and Commercial Air-Conditioner

Compared to the risk assessment procedure given above for a household air-conditioner, the amount of refrigerant charge is much greater for a building multi-air-conditioner and commercial air-conditioner, and the installation conditions and usage environment are also quite different. The differences in the risk assessment procedure that were not given in the previous sections are itemized below.

(1) Risk level

Similar to the household air-conditioner, the risk tolerances of a building multi-air-conditioner and commercial air-conditioner were taken from the market circulation number with a target accident frequency of once per 100 years.

Building multi-air-conditioners and commercial air-conditioners have the same kind of cooling capacity, but a commercial air-conditioner indoor unit is attached to one outdoor unit, while a single outdoor unit is attached to multiple indoor units for a building multi-air-conditioner. Thus, the amounts of refrigerant significantly differ. Because of differences in the location, installation skill and equipment, the tolerance values for each were provided separately in the risk assessment.

Building multi-air-conditioners have a market distribution of 10 million units. Thus, the risk tolerance was 1×10^{-9} in use, while the risk tolerance for other services and installation was 1×10^{-8} . Commercial air conditioners have a market distribution of 7.8 million units; thus, the risk tolerance was 1.3×10^{-9} in use and 1.3×10^{-8} for other stages.

(2) Leakage

Building multi-air-conditioners and commercial air-conditioners were considered to have a standard leak rate of 10 kg/h as defined in ISO5149. This value was taken from market defect data that was collected for the SWG. Indoor units were compared for their risks of a slow leak (10 kg/h), rapid leak (1-10 kg/h), and high-speed leak (10-75 kg/h). For the indoor unit, SWG considered the risk of a high-speed leak was 0 because it was not observed in a leak rate test using nitrogen. On the other hand, the outdoor unit showed a rate of more than 10 kg/h; thus, it had a risk for rapid leaks and high-speed leaks.

(3) Ignition source

Table 5.4.2 presents the ignition sources for a building multi air-conditioner and commercial air-conditioner. The NITE statistics were used to determine the accident rate of fires with home electronics as the intermediary, and the ignition source were analyzed in detail. The SWG extracted the spread number and probability of ignition sources according to the kitchen model. The office model assumed many ignition sources. Table 5.5.1 presents the ignition probability of equipment based on the fire information.

Table 5.5.1 Ignition sources from NITE statistics (part of whole)

Ignition source		Office	Kitchen		
Spark	Indoor Unit	5.7×10^{-16}	4.5×10^{-16}	P=installed units*accident rate numbers on market space v Fire accident rate:3 time year(NITE), numbers on market	
	Appliances	Air cleaner	7.0×10^{-16}	-	Installed:0.2 units room, accident rate:3.6 year, numbers on
		Humidifier	5.6×10^{-16}	-	Installed:0.09 units, accident rate:3 year, numbers on site: :
		Mobile	7.6×10^{-16}	-	Installed:8.12, accident rate:23 17years (LT10year), numbe
		PC	1.2×10^{-14}	-	Installed:8.12, accident rate:174 17years(LT10year), numb
		Light	1.3×10^{-15}	1.6×10^{-15}	Installed:10 15, accident rate:227 17years(LT10year), numb
		Tracking	6.7×10^{-16}	1.1×10^{-15}	Installed: 10 15, accident rate:202 17years(LT10year), numb
		Refrigerator	-	1.6×10^{-12}	Installed:0 3, accident rate:267 17years(LT10year), numbe
		Freezer	-	3.8×10^{-15}	Installed:0 2, accident rate:16 17years(LT10year), number:
		Dishwashers	-	9.7×10^{-15}	Installed:0 2, accident rate:71 17years (LT10year), number:
		Phone	-	2.5×10^{-16}	Installed:0 1, accident rate:18 17years(LT10year), number:
	TV	-	1.1×10^{-15}	Installed:0 1, accident rate:355 17years(LT10year), numb	
Exhaust fan	-	5.5×10^{-15}	Installed:0 4, accident rate:105 17years(LT10year), numb		
Smoking Equipment (Match/Oil lighter)	8.8×10^{-07}	-	P=smoking rate in the room: 0.209 17.1 space volume (2- \$moking rate in the room: 0.1, smoking rate:0.209 (Japan Smoking numbers: 17.1 day person(2013-JT), using rate: ?		
Ignition Equipment (Match/Oil lighter)	-	1.2×10^{-06}	P=5 space volume (24*60)*0.05 Using rate for gas burner 5 times day, Using rate Match O		
Open flame	Combustion equipm	Water heater	8.3×10^{-03}	6.7×10^{-02}	[Office]inst:0.1, Using rate: 2h day, [Kitchen]2, 60min da
		Heater	-	2.7×10^{-03}	Installed:0.001 units, Using rate: 4h day, 60day year
		Kitchen burner	-	3.1×10^{-01}	Installed:15 units, Using rate: 0.023. Installed rate: 0.9
		Gas rice cooker	-	5.0×10^{-01}	Installed:2 units, Using rate: 2h day. Installed rate:0.3
		Gas Oven	-	5.8×10^{-02}	Installed:2 units, Installed rate: 2.9E-04

(4) Life stage and installation case

The air-conditioner installation was separated into different cases: in an office, in a restaurant, in a karaoke room, semi-underground, and in a machinery room. A model was developed, and the risk was assessed for each stage of the life cycle. Table 5.5.2 presents the results of the building multi SWG.

Table 5.5.2 Risk assessment of life stage and installation case (part of whole)

Exponent values show probability of fire accident (times/year/unit)

Installation Case (charge kg <floor area m ² *ceiling height m>		Life stage	Transport/ Storage		Installation		
			Allowable	<1E-08			
				N	Y		
Indoor unit	Ceiling (26.3)	Office <40.6*2.7>	1.1E-15 ~ 2.7E-15	-	1.9E-09	-	3
	Floored (52.8)	Restaurant <9.7*2.5>			1.9E-09	-	
	Ceiling (88.1)	Karaoke <4*2.4>			-	-	
Outdoor unit	Typical (26.3)	-	1.1E-15 ~ 2.7E-15	-	1.9E-09	-	
	Each floored (26.3)	<3.4*4.0>			1.9E-09	-	
	Semi-underground (26.3)	<15.3*3.5>			1.1E-08	1.9E09	

(5) Countermeasures

The improvements of the stage and installation cover for a building multi air-conditioner and commercial air-conditioner with a high ignition probability were comprehensively considered. The installation case with a high ignition probability was a tightly sealed karaoke room in use, and the tolerance could not be met. Therefore, the SWG considered acceptable security measures such as

connecting a ventilator with a refrigerant leak detection apparatus. The next situation considered was when a burner is used as an ignition source at the service stage. When a refrigerant leak is noticed during burner work, the burner will be put out immediately. To ensure that a leak is noticed, a refrigerant leak detector should be installed to measure the refrigerant density. This countermeasure requires a series of acts developed by education and training and practiced. The ignition probability can be suppressed to below the tolerance with this device. The safety guideline GL-13 of the JRAIA should be revised based on the risk assessment results and distributed.

5.6 Difference of Chiller

The differences in the risk assessment procedure for a building multi-air-conditioner and commercial air-conditioner were described in previous sections, but a chiller has a large amount of refrigerant and is installed in an underground machinery room, which is tightly sealed. For the establishment and use of a chiller in Japan, the most important and distinctive point is that various regulations and manuals already exist to ensure safety. When a new refrigerant is applied, the risk assessment assumes that all chillers are filled with safety regulations and manuals as important matter.

(1) Risk level

The tolerance of the chiller is near that for equipment in industrial use. The risk can be reduced by maintenance, specialist intervention, and regulations. The chiller SWG estimated the stock in the market over 6 years to be 134,000 units. The ignition probability was set to “once per 10 years.”

(2) Setting of life stages

An overhaul was added to the chiller, and six stages were estimated. After a seal check is performed upon installation, the refrigerant is sealed, so the transport was not evaluated.

(3) Condition of machinery room

The air was ventilated four times or more per hour by mechanical forced ventilation. The air supply and exhaust louver area were determined by referring to the Kagoshima Prefecture Building Standards. An air-supply port was installed above the equipment, and an exhaust port was located on the wall behind the equipment.

(4) Refrigerant leakage point

The refrigerant leakage point was assumed to be located 0.15 m from the floor at is the center of the front face of the equipment. The refrigerant leakage occurred through a 0.1-m cylindrical nozzle at sonic speed.

(5) Countermeasures and summary

A flammable area is not generated when the above mechanical compulsion ventilation is in effect. However, when there is no ventilation, a flammable area does not disappear for a long time. For a water-cooled chiller, sufficient ventilation and sensor installation in the vicinity of the floor surface are very important security measured. To lower the flammable density in the event of a rapid leak from the chiller, ventilation is indispensable and the most effective measure. Therefore, a manual and safety regulations should be developed. If mildly flammable refrigerant leaks under ventilation conditions, almost no flammable space is formed.

Because many manuals and regulations already exist for chillers, as given above, ensuring safety may require considering how much a person obeys the regulations with regard to work on the installation, use, and disposal.

5.7 FMEA and Other Hazards

To confirm whether or not high-risk items are not considered based on the situation by each company (quality information on the past), a hazard was selected for comprehensive FMEA, and there were clearly no refrigerants with great differences in the past. On the hazards of burning harmful fluorine compounds and diesel explosion, the differences in the hazards were judged to be socially acceptable by the University of Tokyo and AIST which performed a basic assessment. Because the risk assessment depends on the manufacturer, the specifications of the air-conditioner and compressor of each company differ, which affect the assessment of defective quality. Thus, some additional considerations may be necessary. Many pieces of equipment need to be considered. The

chiller SWG is performing an FMEA on items common to each company. Japanese electric appliance manufacturers often require an FMEA for air-conditioner commercialization as reference information.

5.8 Summary of Risk Assessment

This chapter presented a risk assessment procedure that was conducted by the mini-split risk assessment SWG (I) based on the risk assessment advanced at JRAIA through a collaboration between the University of Tokyo, Suwa Science University of Tokyo, and AIST Chemical Division. The differences between a building multi-air-conditioner, commercial air-conditioner, and chiller were also described.

A risk assessment is a preliminary evaluation of a product for future commercialization. It is only a tool to determine what hazards are present in the product. The hazard must be addressed if it is harmful. Product engineers master this tool well; it is mandatory to provide safe equipment with a reasonable social cost. Active disclosure of the residual risks and unexpected risk needs to be continued. Going along with the general opinion was not the aim, but because the risk of an air-conditioner increases with the refrigerant amount and the equipment size increases with the voltage source capacity, the risk tends to become high in FTA analysis. Some countermeasures include reducing the refrigerant leakage amount by providing a shutoff valve, diluting the concentration by adding a high-speed fan, including dispersal fans and an exhaust, eliminating the ignition source of power-off instrumentation located outside the installation compartment, and connecting humans to an alarm device. There are many choices to avoid risks. These include confirming a seal during installation, reporting safety checks, and regular inspections of equipment. Risk can also be avoided by enforcing regulations and standards. The characteristics, installation conditions, usage condition, convenience, and cost of each device should be chosen to determine the best approach.

In addition to being repeated many times, the risk assessment for building multi-air-conditioners, commercial air-conditioners, and chillers can be simply described by using excerpts from past reports. For detailed conditions and evaluation methods and results, the data can be confirmed from past progress reports. At last this progress report 2014 provides the latest published information as a reference.

6 Risk Assessment of Mini-Split Air Conditioners

6.1 Introduction

Risk assessment of mini-split air conditioners, which started in 2011, has been completed for all applicable products. Consequently, this progress report is scheduled to be the final one. For risk assessment of the flammability risks of mini-split air conditioners, please refer to refrigerant leak simulation, ignition source evaluation, FTA evaluation method, etc. summarized in Chapter 5.

The following is a brief summary of the FTA results for wall-mounted air conditioners, one-to-one connection floor-standing housing air conditioners, and multi-connection floor-standing housing air conditioners, and diesel explosion or combustion products, for which data were obtained in the risk assessment undertaken in this project.

In addition, please refer to the detailed risk assessment results for one-to-one connecting floor-standing housing air conditioners and multi-connection floor-standing housing air conditioners described in Sections 6.4 and 6.5, respectively.

To avoid lengthy terminology, this report uses the following abbreviations (except in case of captions): one-to-one connection wall-mounted air conditioners are referred to as “normal wall mounted air conditioners”; one-to-one connection floor-standing housing air conditioners are referred to as “single floor-standing air conditioners”; multi-connection floor-standing housing air conditioners are referred to as “multi floor-standing air conditioners”; and multi-connection wall mounted air conditioners are referred to as “multi-wall mounted air conditioners”.

6.2 Refrigerant Leak Simulation

The combustible space-time product of mini-split air conditioners was initially determined by using the values calculated in the document “Using propane room air conditioner of the risk assessment” and proportionally converting them for R32. It was subsequently re-calculated using the results of a new simulation carried out at the University of Tokyo in 2012, which set the boundary in order not to cause refrigerant leakage associated with pressure increase. Figure 6.2.1 shows the state of the wall mounted, floor-standing indoor and outdoor mini-split air conditioner units used in the simulation conducted by the University of Tokyo.

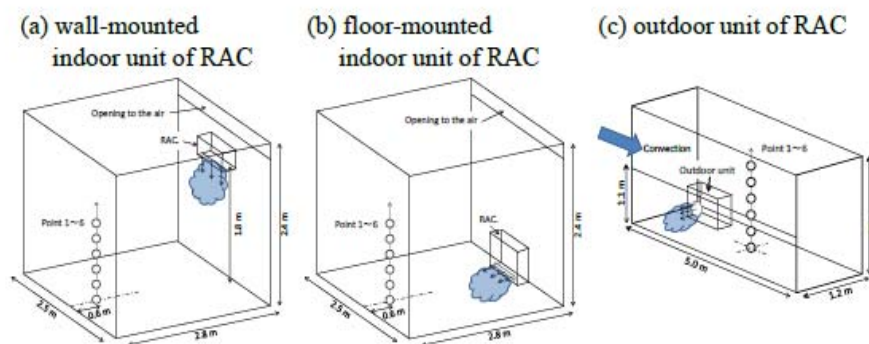


Fig. 6. 2. 1 Simulation conditions for each

Following determination of the combustible space-time product for each air conditioner simulated in the conditions shown in the figure by the University of Tokyo, we used the values obtained to re-calculate the ignition probability of mini-split SWG. Because no comprehensive simulation was carried out for R1234yf, we compared its simulation values to those of R32 under the same conditions, and calculated each value in proportional terms. The value of the combustible space-time product of mini-split air conditioners using R32 and R1234yf is as written in Chapter 5, and will therefore not be described here.

6.3 Ignition Source Evaluation

Evaluation and discussion of ignition sources in an environment where a mini-split air conditioner is used are detailed in the progress reports of the Japan Society of Refrigerating and Air Conditioning Engineers for the years 2011, 2012, and 2013. In addition, referring to the reports from Mr. Imamura (Tokyo University of Science, Suwa), Mr. Takizawa (National Institute of Advanced Industrial Science and Technology), and report No. DOE/CE/23810-92, written in 1998 by Arthur D. Little, Inc. (ADL), the assumed ignition sources of residential air conditioners are sparks and open flame.

For R32 and R1234yf, the assumed ignition sources around indoor and outdoor units are sparks from matches or oil lighters, the scraping of metal forklift nails, or open flame brought in from outside the flammable area such as matches, lighters, and welding torches.

In addition, the amount of refrigerant leakage is less for residential air conditioners. Thus, even if the refrigerant can ignite in the combustion chamber of any combustion facilities, water heaters or heating devices are not regarded as ignition sources, because flame propagation to the outside of the equipment is difficult.

6.4 Summary of FTA

The results of the risk assessment for mini-split air conditioners in the configuration outlined above are described again in Table 6.4.1. In the case of the one-to-one connection normal wall mounted air conditioners, the hazard occurrence probability (ignition rate) in the revised risk assessment was almost 10^{-10} during use, and was below 10^{-9} during transportation, installation, and operation. Because each value was below the tolerance value, no further risk assessment tests were carried out.

In order to achieve equivalent performance and efficiency for R1234yf when applying mildly flammable refrigerants to conventional R410A mini-split air conditioners, the heat exchanger has to be increased to approximately 1.4 times its size, and a new large-size compressor has to be developed and its reliability ensured. While looking at Table 6.4.2, it is necessary to keep in mind that the values have been slightly revised from the 2013 progress report.

Table 6.4.1 Ignition probability of various refrigerants (normal wall mounted air conditioner)

Risk: Ignition probability			
Life Stage	R32	R1234yf	R290
Logistic	4.1×10^{-17}	4.5×10^{-17}	$1.9 \times 10^{-8} \sim 5.0 \times 10^{-6}$
Installation	2.7×10^{-10}	3.1×10^{-10}	$1.5 \times 10^{-6} \sim 1.7 \times 10^{-5}$
Use (Indoor)	3.9×10^{-15}	4.3×10^{-15}	$5.9 \times 10^{-9} \sim 1.1 \times 10^{-4}$
(Outdoor)	1.5×10^{-10}	2.1×10^{-10}	$9.7 \times 10^{-13} \sim 1.9 \times 10^{-8}$
Service	3.2×10^{-10}	3.6×10^{-10}	$9.3 \times 10^{-6} \sim 1.7 \times 10^{-5}$
Disposal	3.6×10^{-11}	5.3×10^{-11}	$1.8 \times 10^{-5} \sim 1.3 \times 10^{-4}$

However, the values for single floor standing air conditioners and multi-floor standing air conditioners are larger than the tolerance value even in the reviewed risk assessment. Therefore, research into installation and actual service conditions, and investigation of door clearances was conducted, primarily in Japanese style houses, in order to achieve risk assessment closer to that of actual usage.

We also reviewed whether the same tolerance values could be applied for normal wall mounted air conditioners.

The measures above and those proposed are described in detail in Sections 6.4 and 6.5; however, the latest risk assessment results, which are very important, are as described in Table 6.4.2.

Table 6.4.2 Ignition probability of various mini-split air conditioners

Risk: Ignition probability			
Life Stage	Normal wall mounted R32	Single floor standing R32	Multi floor standing R32
Logistic	4.1×10^{-17}	3.6×10^{-11}	1.1×10^{-9}
Installation	2.7×10^{-10}	4.0×10^{-11}	9.0×10^{-9}
Use (Indoor)	3.9×10^{-15}	4.1×10^{-10}	4.7×10^{-10}
(Outdoor)	1.5×10^{-10}	8.6×10^{-11}	1.1×10^{-9}
Service	3.2×10^{-10}	2.6×10^{-10}	4.3×10^{-9}
Disposal	3.6×10^{-11}	2.5×10^{-11}	4.1×10^{-10}

The tolerance value for single floor-standing air conditioners was 10^{-9} during use, and 10^{-8} during transportation, installation, etc. which almost satisfies the allowable values.

6.5 Diesel Explosion and Combustion Products

In addition to the combustibility hazard, there is a possibility of toxic substance generation caused by diesel explosion or combustion. These are discussed briefly below. For details, please refer to past progress reports.

Diesel explosions can be caused by erroneous workflow when retrieving the refrigerant from the compressor upon installation, service, or disposal of the unit, which allows air to enter the system. Following the application of regulations to the releasing of fluorocarbons into the atmosphere, diesel explosions occurred only a few times within a decade. Injuries resulting from diesel explosions are typically blows or other harm caused by the fragments of the exploding compressor, and the stator or rotor inside the compressor or machine casing. Other heavy parts hitting persons will cause a level III serious injury. With a probability of occurrence of three times in 10 years, and factoring the number of residential air conditioners spread in the market, the probability of occurrence is estimated to be approximately 3×10^{-9} . This falls into Area-B of the R-Map, which means there is no direct risk for users, but certain countermeasures are necessary. Warnings regarding this hazard have been declared on the homepage of JRAIA and are also written in the operation manuals and other related documents of each company. However, as in the case of the diesel explosion accident that occurred in Osaka last year, such accidents occur upon relocation of air conditioners by personnel with insufficient knowledge and technology. A diesel explosion is a hazard that presents several problems, such as how to effectively appeal to persons who are not professional air conditioner installation and relocation technicians or to individuals who carry out relocation or dismantling on a DIY basis, in order to reduce such accidents. In the future it will be necessary to continue the education and training of professional technicians, and also to communicate the risks of a diesel explosion to individuals who are not professional technicians but who conduct related work, and devise some means of ensuring that the work is carried out correctly and safely.

Because evasive measures can be taken, the risk evaluation for hazards caused by combustion products is set at level II (moderate injury) within the R-Map. Further, on the basis of interviews conducted with JRAIA and each company, no such accidents have been reported for the past 20 years; thus, the estimated probability of occurrence is 5×10^{-10} . Consequently, risk assessment is now focused on Area-C within the R-Map, and there is high probability that this hazard has not been regarded as a problem even in the case of conventional refrigerants. Based on the results of analysis carried out by the University of Tokyo and the National Institute of Advanced Industrial Science and Technology, in the case of both R32 and R1234yf, there were no major differences in either the amount of toxic or chemical substances generated compared to conventional refrigerants. Therefore, even though detailed discussions might be necessary, the combustion products of mildly flammable refrigerants are thought to generally have acceptability similar to that of conventional refrigerants. Naturally, it goes without saying that, like conventional refrigerants, caution must be exercised upon concurrent use with fire.

6.6 Housing Air Conditioner Risk Assessment and Results

6.6.1 Housing air conditioner installation modes and problems

In addition to the wall mounted type, there are several types of other housing air conditioners, and separate risk assessments are necessary based on the method of installation or connection specifications. Figure 6.6.1 shows housing air conditioner installation types and conditions of analysis of multi-connection housing air conditioners in comparison with one-to-one connection air conditioners. In addition to the wall mounted type, other types of indoor housing air conditioner units include the floor standing type, the ceiling mounted cassette type, the wall-embedded type, and the built-in type. On the one hand, the mildly flammable refrigerant currently being evaluated is a CFC with a high relative air density, which leads to it tending to accumulate close to the ground.

The risk is highest in the case of refrigerant leakage by floor-standing type units, and it is assumed that in the case of multi-connection floor-standing housing air conditioners, which have a large amount of refrigerant loaded, the risk is even higher. To avoid complications, we first discuss the evaluation conducted of the one-to-one connection floor-standing type housing air conditioners, and then refer to the multi-connection floor-standing housing air conditioners. Finally, we present the ignition risk probabilities of multi-connection wall mounted air conditioners as a reference.

6.6.2 One-to-one connection floor-standing housing air conditioners (Single floor-standing air conditioners) Ignition sources and installation conditions

Ignition sources for single floor-standing air conditioners were assumed to be the same as that for conventional wall mounted type air conditioners. The indoor space was determined to be a small room with a floor space of 7 m² and room height 2.4 m, and the indoor unit was installed on the floor. Refer to Fig. 6.6.1 for an outline.

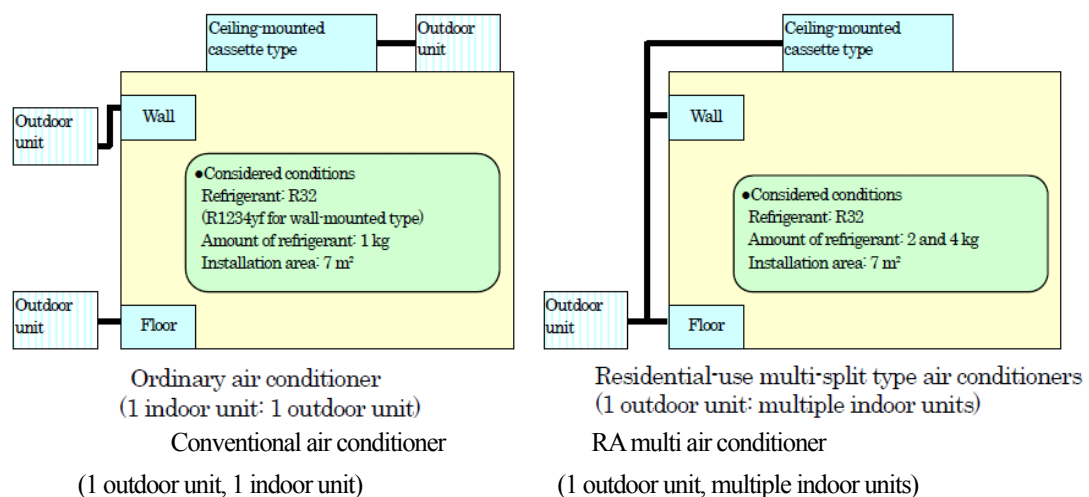


Fig. 6.6.1 Housing air conditioner installation types and conditions of analysis

6.6.3 Probability of accident occurrence and aims of single floor-standing air conditioner risk assessment

The tolerance values for the probability of accident occurrence within the risk assessment are based on the same National Institute of Technology and Evaluation (NITE) concept as for the wall mounted type. Housing air conditioners such as the floor-standing type are in some cases installed by service personnel for residential air conditioners, but usually the installation work is carried out by professionals who received adequate training. In the risk assessment evaluation of floor-standing type housing air conditioners, the tolerance value for the probability of accident occurrence during use was set below 10⁻⁹ considering the small amount of floor standing units in the market, less than 1%, compared to the wall mounted type, and because of specifications and usage similar to the package air conditioners or multi air conditioners for buildings.

In addition, assuming service providers engage in self-prevention during servicing work, the hazard level was considered to be one rank lower and was therefore set at 10⁻⁸ or below. In carrying out the risk assessment, the floor-standing type housing air conditioners were compared to wall mounted type room air conditioners and ceiling mounted cassette type package air conditioners in all life stages. The results of organizing the theories leading to the allowable risk values (probability of accident

occurrence), and the tolerance values (probability of accident occurrence) in each life stage during the risk assessment are shown in Table 6.6.1.

Table 6.6.1 Life stages and tolerance values of single floor-standing air conditioners (probability of accident occurrence)

Life stage		RAC (wall-mounted)	RAC (floor standing)	PAC (cassette-type)
Refrigerant		R32, R1234yf	R32	R32
Representative model		Wall-mounted Amount of refrigerant: 1.0 kg / 7 m ²	Floor standing Amount of refrigerant: 1.0 kg / 7 m ² In actual use (indoor): 10 m ²	Indoor unit: cassette, ceiling suspended Amount of refrigerant: 3 kg / 11 m ² Outdoor unit: Amount of refrigerant: 6 kg / 42 m ²
Transport, storage		10,000 units / 1,000 m ² (outdoor unit)	10,000 units / 1,000 m ² (outdoor unit)	2,300 units / 1,000 m ² (actual DAIKIN storehouse record)
Use	Indoor	<ul style="list-style-type: none"> Probability of a quick leak 4.0E-4~4.7E-4 Ventilation condition: no ventilation, no opening Ignition source: all in common Calculation method of the probability of a fire accident: → Subject: instantaneous ON operation 	<ul style="list-style-type: none"> Probability of a quick leak 1.5E-5 Ventilation condition: no ventilation, no opening Ignition source: common + set for every presumable room Calculation method of the probability of a fire accident: → Subject: instantaneous ON operation 	<ul style="list-style-type: none"> Probability of a quick leak (VRV × safety rate 3) 5.0E-6 × 3 Ventilation condition: 3 mm × 900 mm opening Ignition source: common + set for each industry Calculation method of the probability of a fire accident: → Instantaneous ON operation according to the ignition source Judge if the operation is continuous
	Outdoor	<ul style="list-style-type: none"> Probability of a quick leak 2.2E-7~2.8E-4 Wind velocity: 1.0 m/s 	<ul style="list-style-type: none"> Probability of a quick leak 2.2E-7~2.8E-4 Wind velocity: 1.0 m/s 	<ul style="list-style-type: none"> Probability of a quick leak (equivalent of VRV) Quick: 1.34E-3 Jet: 1.37E-4 Wind velocity: 0.0.5 m/s
Service & repairing		Probability of a human error occurring: 1.0E-3	Probability of a human error occurring: 1.0E-3	Probability of a human error occurring: 1.0E-3
Disposal (Recycling method)		Removed by volume seller (pump-down) Collect refrigerant form unit → recycle center (according to the Home Appliance Recycling Act)	Removed by volume seller (pump-down) Collect refrigerant form unit → recycle center (according to the Home Appliance Recycling Act)	Collect refrigerant from outdoor unit Place of installation Other than place of installation
Setting allowable risk value		Product diffusion: 100,000,000 units / 10 years. 1 accident in 100 years. Lower than 1E-10	Product diffusion: 200,000 units. 1 accident in 100 years. In use: Lower than 1E-08 During work: Lower than 1E-07 Equivalent risk tolerance level as for SWGII and VRV SWG types which are being discussed at the same time. In use: Lower than 1E-09 During work: 1E-08	Product diffusion: 6,000,000 units. 1 accident in 100 years. In use: Lower than 1E-09 During work: 1E-08 *1 *1 If the worker is working continuously, risk tolerance level will be considered 1 rank lower due to self-defense.

6.6.4 Single floor-standing air conditioner risk assessment analysis

In the above theory, the results of risk assessment carried out based on the FTA of the single floor-standing type air conditioner at a floor space of 7 m² did not satisfy the tolerance value. In measure S1, the (indoor) usage stage for single floor-standing air conditioners was reconsidered, restricting installation in rooms with a floor space smaller than 6-jo (approximately 10 m²). The results of ignition risk probability calculation, including those of other stages, are shown in Table 6.6.2. If measure S1 is taken, the ignition probability during usage becomes 9.9×10^{-10} , which is less than the tolerance value. For details, please refer to the progress report of 2013.

Table 6.6.2 Ignition risk probability of floor-standing type Housing air conditioner (with measure S1)

Type	Risk: Ignition Probability	
	Representative model	R32 (Measure 1)
Logistics (for each warehouse)	Middle-size warehouse	3.6×10^{-11}
Installation	3.24 m ² veranda	4.0×10^{-11}
Use (Indoor)	9.9 m ² room	9.9×10^{-10}
(Outdoor)	3.24 m ² veranda	8.6×10^{-11}
Service	3.24 m ² veranda	2.6×10^{-10}
Disposal	3.24 m ² veranda	2.5×10^{-11}

Table 6.6.3 Ignition risk probability of floor-standing type Housing air conditioner (with measure S2)

Type	Risk: Ignition Probability	
	Representative model	R32 (Measure 2)
Logistics (for each warehouse)	Middle-size warehouse	3.6×10^{-11}
Installation	3.24 m ² veranda	4.0×10^{-11}
Use (Indoor)	7 m ² room	4.1×10^{-10}
(Outdoor)	3.24 m ² veranda	8.6×10^{-11}
Service	3.24 m ² veranda	2.6×10^{-10}
Disposal	3.24 m ² veranda	2.5×10^{-11}

6.6.5 Single floor-standing air conditioner risk assessment analysis considering installation in 4.5-jo space [Measure S2]

Measures restricting the floor space for installation in a living room lead to heavy dependence on installation service providers. Accordingly, as the refrigerant density will become approximately 2.7% in a case where 1 kg of refrigerant is leaked and diffused throughout a room, we thought of Measure S2. Measure S2 considers achieving a refrigerant density below LFL by diffusing the refrigerant within the room using the indoor fan after a leakage has been detected. The possibility of being unable to diffuse the refrigerant using the indoor fan due to a power outage (※1), turned-off breaker (※2), or a malfunction of parts (※3) was also considered. Regarding turned-off breakers, it is possible that users will turn off the breaker outside the seasons for cooling or heating, so it is necessary to write a clear warning on the indoor unit itself. We considered the effect of warning signs on the units to decrease the probability of turned-off breakers to 1/10. While the actual combustible airspace is zero if the refrigerant is diffused by the indoor fan, when calculating the ignition risk probability without using Measure S2, we theoretically set the FTA at 1/10000 of the combustible space-time product value.

The ignition risk probability of floor-standing type housing air conditioners with Measure S2 is shown in Table 6.6.3.

When Measure S2 was carried out, the indoor (i.e., during usage) ignition risk probability of floor-standing type housing air conditioners reached an allowable risk value lower than that of conventional wall mounted air conditioners (below 10^{-9}), at the same conditions of a small room with a floor space of 7 m² and room height 2.4 m. The effects of diffusing leaked refrigerant using the indoor fan will be discussed in detail in the chapter on multi floor-standing air conditioners.

(※1) The annual average power outage time rate of 10 electric power companies throughout Japan.

(※2) Intermediate periods when air conditioners are not used total four months (April-May, October-November). Probability of users turning off the breaker during these periods. (Calculated based on the investigation results of research companies)

(※3) The altogether malfunction probability of the unit PCB, refrigerant leakage detector PCB, and the indoor fan motor. (Calculated based on the exchange rate of each part during market service.)

6.7 Multi-connection Housing Air Conditioner Risk Assessment and Results

The problem in case of multi-connection housing air conditioner installation is that up to four indoor units are connected to a single outdoor unit, which necessarily leads to a larger refrigerant charge amount. Accordingly, it is a combustible space-time product in the case of a refrigerant leakage and with it the risks become larger. In this chapter, we discuss the risk assessment prerequisites and results of floor-standing type air conditioners that have a high risk even among multi-connection type housing air conditioners, and finally we present the FTA results for multi-connection type wall mounted air conditioners.

The indoor unit installation types and usage itself of multi floor-standing air conditioners are exactly the same as for single floor-standing air conditioners, so the ignition sources can also be regarded as the same.

Table 6.7.1 shows the life stages and tolerance values (probability of accident occurrence) of multi-connection housing air conditioners. As shown in Table 6.7.1, the tolerance values for multi floor-standing air conditioners are the same as those for single floor-standing air conditioners; the tolerance value for the probability of accident occurrence during use was set below 10^{-9} , and below 10^{-8} during the work of service providers. The amount of refrigerant was set at 4 kg the supposable maximal amount for multi-connection housing air conditioners. Further, the two corrections below were made to the supposable room and refrigerant leakage conditions in order to achieve more realistic results.

- 1) All rooms within a residence definitely have doors (hinged or sliding) and door clearances. The upper and lower door clearance is considered to be 3 mm.
- 2) The initial refrigerant discharge density for floor-standing type air conditioners is considered to be 30%, based on the results of actual refrigerant leakage tests conducted by JRAIA in several companies.

Table 6.7.1 Multi-connection housing air conditioner life stages and tolerance values (RAC multi)

Life stage		RAC (wall-mounted)	③ Multi-split type RAC	VRV
Refrigerant		R32, R1234yf	R32	R32
Representative model		Wall-mounted type Amount of refrigerant: 1.0 kg / 7 m ²	Wall-mounted and floor-standing types Amount of refrigerant: 4.0 kg / 7 m ²	Four-way cassette / 3 HP / Amount of refrigerant: 26.3 kg / 42 m ² Floor-standing type
Transport, storage		10,000 units / 1,000 m ² (outdoor unit) →	10,000 units / 1,000 m ² (outdoor unit)	1,000 units / 1,000 m ²
Use	Indoor	<ul style="list-style-type: none"> Probability of a rapid leak occurrence 4.0E-4 - 4.7E-4 Ventilation conditions: no ventilation, no clearance Ignition source: all in common Calculation method of the probability of a fire accident → Subject: instantaneous ON operation 	<ul style="list-style-type: none"> Probability of a rapid leak occurrence 1.5E-5 (equivalent to SWG II) Ventilation conditions: no ventilation, no clearance Ignition source: common + set for each presumable room Calculation method of the probability of a fire accident → Subject: instantaneous ON operation 	<ul style="list-style-type: none"> Probability of a rapid leak occurrence 5.0E-6 Ventilation conditions: safety measures specified in ISO5149FDIS Ignition source: common + set for each industry Calculation method of the probability of a fire accident → Determine instantaneous ON operation or continuous operation depending on ignition source
	Outdoor	<ul style="list-style-type: none"> Probability of a rapid leak occurrence 2.2E-7 - 2.8E-4 Air velocity: 1.0 m/s 	<ul style="list-style-type: none"> Probability of a rapid leak occurrence 2.2E-7 - 2.8E-4 Air velocity: 1.0 m/s 	<ul style="list-style-type: none"> Probability of a rapid leak occurrence Rapid: 1.34E-3 Blow-out: 1.37E-4 Air velocity: 0.0,5 m/s
Service & repair		Probability of a human error occurrence: 1.0E-3	Probability of a human error occurrence: 1.0E-3	Probability of a human error occurrence: 1.0E-4
Disposal (Recycling law)		Removed by mass retailer (pump-down) Collect refrigerant from unit → recycle center (Specified in Home Appliance Recycling Law)	Removed by specialized company (pump-down) Collect refrigerant from unit → recycle center Mounted type → specialized scrapper Other than mounted-type → recycle center	Removed by specialized company (pump-down) Collect refrigerant from unit → specialized scrapper (Not specified in Home Appliance Recycling Law)
Setting allowable risk value		Product diffusion: 100 million units / 10 years, 1 accident in 100 years 1E-10 or lower	Product diffusion: 1 million units, 1 accident in 100 years In use: 1E-08 or lower During work: 1E-07 or lower Equivalent to allowable risk level for SWG II and VRV SWG types being discussed concurrently In use: 1E-09 or lower During work: 1E-08 or lower	Product diffusion: 10 million units, 1 accident in 100 years In use: 1E-09 or lower During work: 1E-08 or lower *1 *1 If a worker is working continuously, allowable risk level is considered to become lower due to self-defense.

6.7.1 Setting conditions of analysis based on realistic housing environment

Ventilation is different for residential and office buildings; thus, clearings were considered adjusted to housing environment. There are two types of residential ventilation: ventilation through clearings (i.e., door clearings) and machine ventilation. In order to achieve effective ventilation, it is necessary to provide an air supply route and an air discharge route. Figure 6.6.1 shows the air supply and discharge routes in an average residential building.

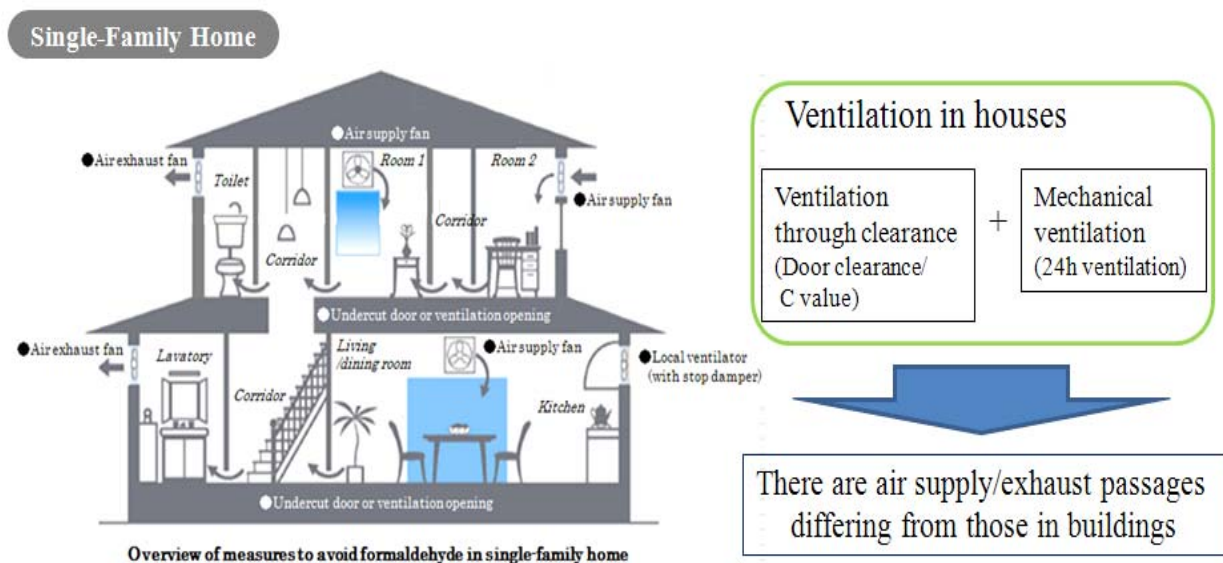


Fig. 6.7.1 Considered ventilation routes based on actual housing environment

6.7.2 Regarding door clearances based on housing environment: hinged doors and sliding doors

Let us now consider door clearances in residential buildings, based on housing environment.

Clearings in average residences can be considered as two scenarios: cases where doors are used as actual ventilation routes and cases where they are not. More precisely, if doors are used as actual ventilation routes the clearances are larger than 10 mm. However, even if they are not used as ventilation routes, there are clearances above and below the doors. Figure 6.7.2 show the clearance inspection results for hinged doors of various manufacturers. The results for each manufacturer show a clearance of 3 mm above and 4 mm below the door.

Similar investigation results for sliding doors are shown in Figure 6.7.3. In the case of sliding doors, the results show a clearance of 3 mm above and 3 below the door, and a 6.5 mm clearance at the door slit.

From the above results, actual testing and FTA were conducted with a strict condition of 3 mm clearances both above and below the doors (disregarding door slits). Regarding sliding doors such as fusuma and shouji (Japanese sliding/ paper screen doors), if the fittings are made separately there may be no clearing at the bottom, so the calculation conditions were changed to 0 mm below, 3 mm above and 6.5 mm slit clearing, and severe risk assessment was carried out separately.

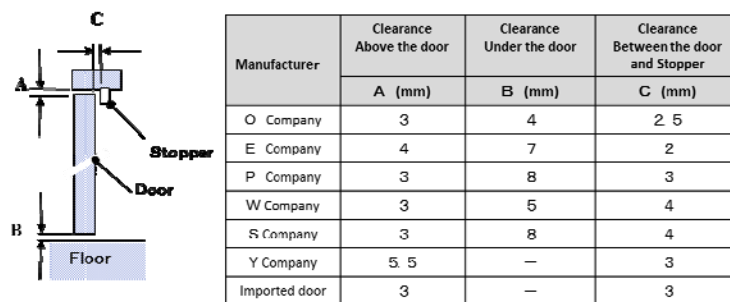


Fig. 6.7.2 Clearance of door

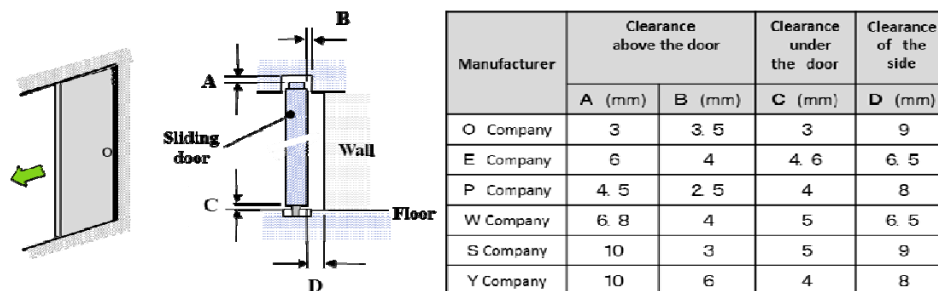


Fig. 6.7.3 Clearance of sliding door

6.7.3 Initial refrigerant density of an indoor leakage of multi-connection floor-standing air conditioners

The density of refrigerant leaking from the outlet of multi floor-standing air conditioners is the density of leakage from the air ducts of the product equipment into the room, and is thus a very important parameter as a condition for calculating ignition risks. The theoretical conditions stated in the progress report of the University of Tokyo (initial leakage density of 100%) were originally set to evaluate risks relatively higher. This time, in order to carry out simulation with more realistic conditions, we conducted analysis based on the operation test results of JRAIA for several companies (initial: 30%). Fig. 6.7.4 gives a comparison of the current analysis using more realistic conditions, and of the original simulation conditions of the University of Tokyo. Based on the market investigation results for refrigerant leakage, we also changed the speed of refrigerant leakage to 10 kg/h.

6.7.4 Combustible space-time product

In the simulation with realistic residential conditions, shown in Figure 6.7.4, we considered multi floor-standing air conditioners, and analyzed the combustible space-time product for the case of an indoor refrigerant leakage amount of 4 kg. The results are shown in Figure 6.7.5 and Table 6.7.1. If the refrigerant leaks into the room in the case of multi floor-standing air conditioners, because R32 is heavier than air, the refrigerant will gather close to the floor in high density and leak outside of the room through the clearances under

the doors of the room. As shown in Figure 6.7.2, in the case of hinged doors, when the leakage has stopped after 24 minutes, the amount of refrigerant remaining inside the room is 2.4 kg, and 40% of the overall leaked refrigerant is leaked to the outside of the room. Further, in the case of sliding doors, as with hinged doors, the refrigerant leaks to the outside of the room from the clearances at the sides of the door, and about 30% of the entire leaked refrigerant is leaked outside after 24 minutes. Table 6.7.1 shows the analysis results of combustible space-time product simulation in the case of hinged doors and sliding doors. Compared to hinged doors, the clearances that leak the high density refrigerant gathered close to the floor are narrower in the case of sliding doors, so a combustible space is present in the room for a slightly longer time. However, as there are vertical clearances at the sides of sliding doors, the combustible space-time product for sliding doors was 1.51 m³/h, which is virtually the same as the value of 1.43 m³/h in case of hinged doors. Thus, realistically considering the clearances of doors etc., inside residences, the effect of refrigerant leaking to the outside of the rooms is significant, and even if a leakage occurred inside the room, the refrigerant would not remain in one place for a long time.

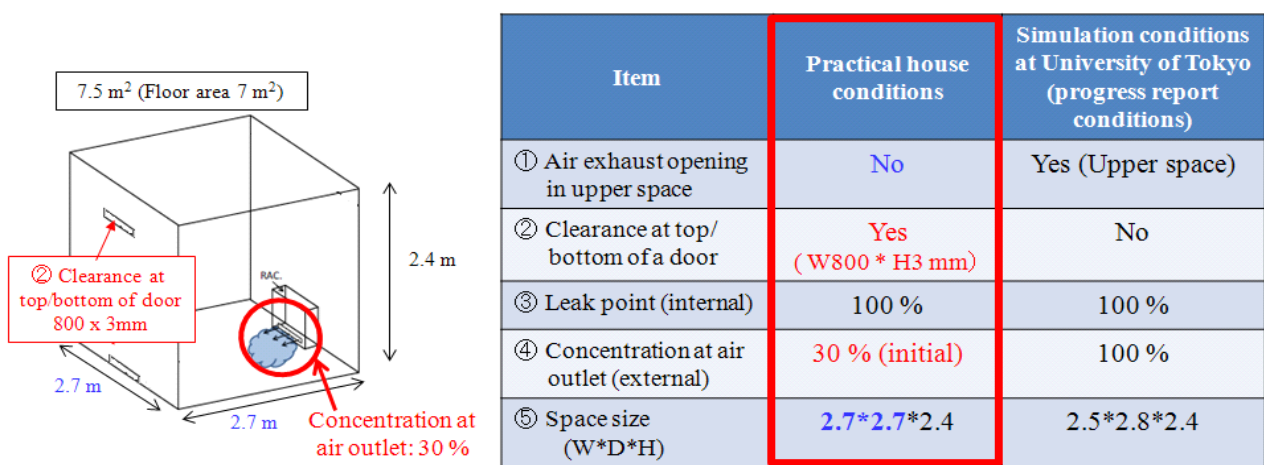


Fig. 6.7.4 Comparison of simulation conditions

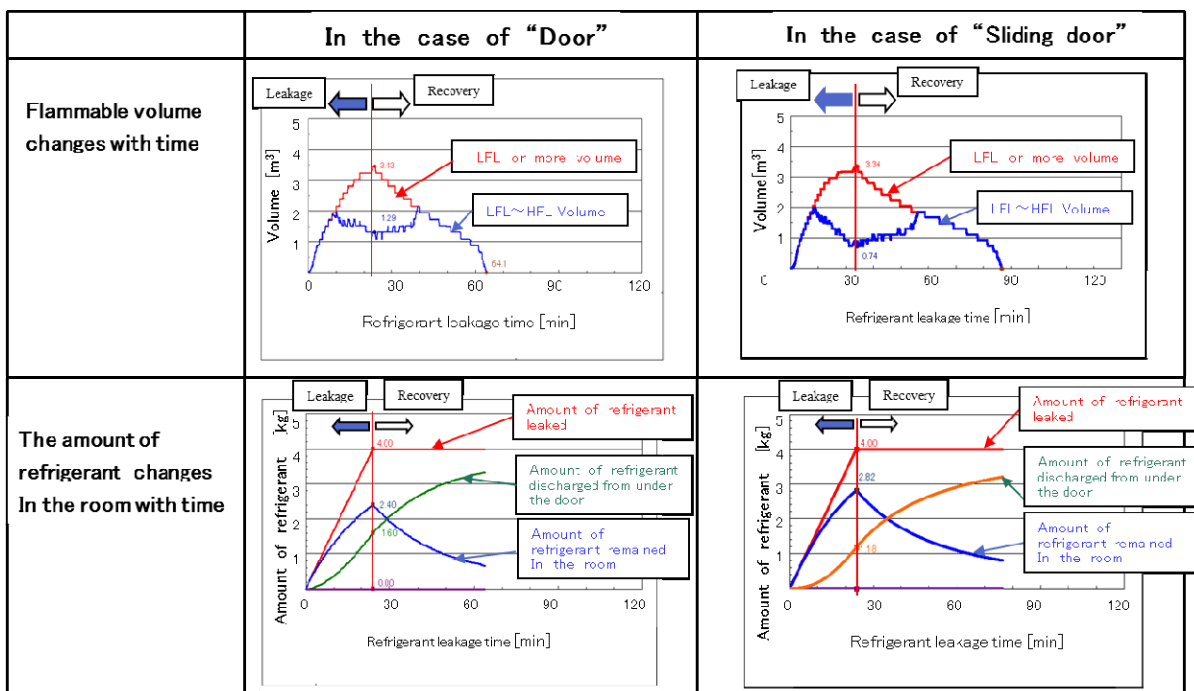


Fig. 6.7.5 Change in flammable volume and amount of refrigerant remaining in the room with time

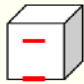
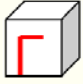
	Door 	Sliding door (No clearance under the door) 
Space-time product of flammable cloud [m ³ ·h]	1.43	1.51
Time the flammable volume remained in the room [min]	64	77

Table 6.7.1 Combustible space-time product in the case of hinged doors and sliding doors (in a 4.5-jo / approx. 7.5 m² room)

6.7.5 Multi-connection floor-standing housing air conditioner risk assessment analysis

As stated in Section 6.7.4, considering the actual door clearings in residences, if the refrigerant is leaked into a room, it will be discharged via door clearances, but there will still be some combustible air space remaining on the ground level. Accordingly, in order to lessen the risks of ignition, we also considered adding the use of an indoor unit fan to diffuse the refrigerant (Method M2) as done in the case of single floor-standing air conditioners.

6.7.6 Results of diffusion by the indoor unit fan

Figure 6.7.6 is the actual testing data of 4 kg R32 refrigerant leakage in a 4.5-jo (approx. 7.5 m²) room, showing the change in refrigerant density at various heights from the floor. The graph on the left shows the results in the case of no diffusion, while the graph right shows the results of using the indoor unit fan to diffuse refrigerant (Measure M2). In addition, the result of diffusion (Measure M2) shows the results of starting to use the indoor unit fan 20 seconds after the refrigerant started to leak. Using the indoor unit fan to diffuse the refrigerant was effective in the case of a refrigerant leakage amount smaller than [LFL density x room capacity], and in the case of a 4.5-jo (approx. 7.5 m²) room, even with 4 kg refrigerant leakage, LFL density was not reached.

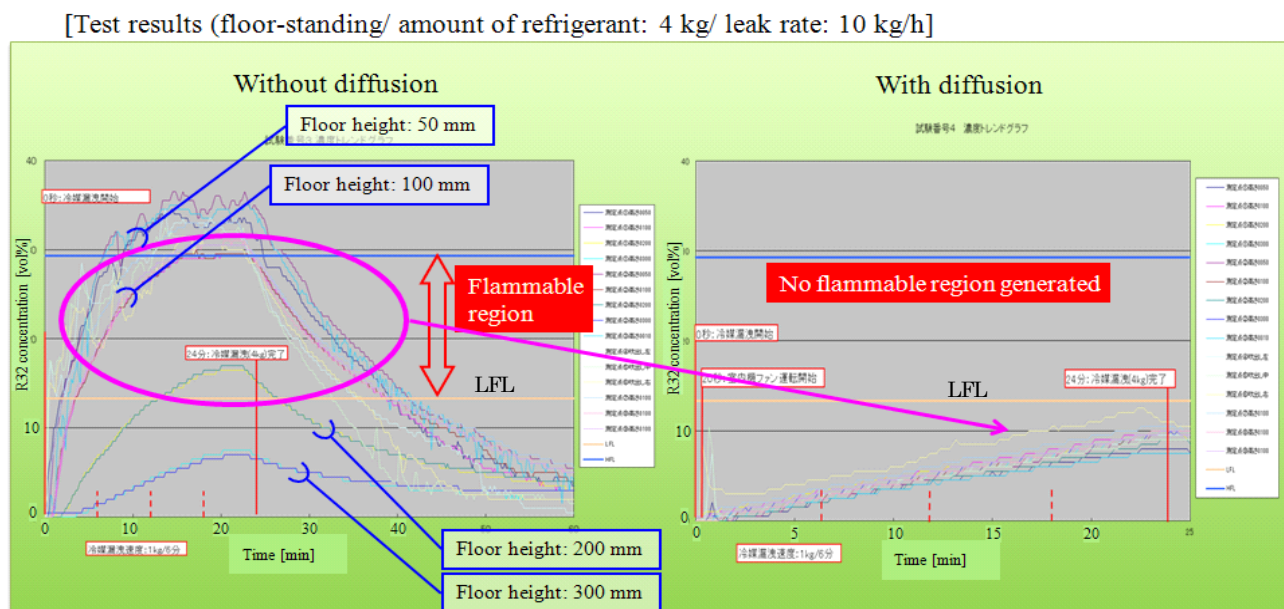


Fig. 6.7.6 Refrigerant density at various heights in case of a refrigerant leakage inside the room (4.5-jo / approx. 7.5 m² room)

6.7.7 Multi-connection floor-standing housing air conditioner (multi floor-standing air conditioner) risk assessment results

Table 6.7.2 shows the ignition risks at each life stage of the multi floor-standing air conditioner. The ignition risk at indoor (during use) stage is the result considering common hinged doors. Based on Table 6.7.2, no additional countermeasures are necessary in any stage

other than the indoor (during use) stage. On the one hand, in the indoor (during use) stage, adding the realistic factor of door clearances of residences and also the use of the indoor unit fan to diffuse refrigerant (Measure M2), the ignition probability becomes 4.7×10^{-10} , which is smaller than the tolerance value (below 10^{-9}). In addition, as in the case of sliding doors, the probability becomes 4.7×10^{-10} , which is less than the tolerance value.

Finally, based on the current risk evaluation, we will add comments regarding caution upon installation in a high air-tight room to the ‘R32 piping construction manual’ made by JRAIA.

Table 6.7.2 Ignition risk probability at each life stage (for multi floor-standing air conditioners)

Risk: Ignition Probability		
Type	Representative model	R 32
Logistics (for each warehouse)	Middle-size warehouse	1.1×10^{-09}
Installation	3.24 m ² veranda	9.0×10^{-09}
Use (indoor)	7 m ² room	4.7×10^{-10}
Use (outdoor)	3.24 m ² veranda	1.1×10^{-09}
Service	3.24 m ² veranda	4.3×10^{-09}
Disposal	3.24 m ² veranda	4.1×10^{-10}

Table 6.7.3 shows the occurrence rate in every supposable pattern applying FTA, and the ignition probability of each pattern in the indoor (during use) stage. In the table, Pattern 2 is the case where the indoor unit fan is used to diffuse refrigerant (Measure M2), which makes up 50.91% of all patterns. Adding it to Pattern 1 (air conditioner in operation), the fan is in operation in 99.7% of the occurrence of all patterns. The ignition risk is also 1.58×10^{-11} when Patterns 1 and 2 are combined, which is an extremely low value compared to the tolerance value (below 10^{-9}).

Table 6.7.3 Ratio of occurrence patterns applying FTA and their ignition risk probabilities in the indoor (during use) stage

Pattern	[Method 2]		Power	Operation / Stop	Part malfunction Yes/No	Occurrence ratio / all patterns	Ignition risk probability	
	Diffusion with I.U. fan	Breaker OFF countermeasure						
General risk	1	Diffusion possible	Breaker ON	Operating (indoor fan ON)	No	48.80%	7.7E-12	
	2			Stop → indoor fan ON	No	50.91%	8.1E-12	
Risk that does not occur in general	3	Diffusion not possible	Same as above	Stop	Yes	0.04%	5.6E-11	
	4				Power outage	No	0.002%	2.4E12
	5				Breaker OFF	No	0.25%	3.9E-10
Sum. ignition risk probability:							4.7E-10	

6.8 Multi-connection Wall Mounted Air Conditioners (Multi-Wall Mounted Air Conditioner) Risk Assessment

Finally, Table 6.8.1 shows the ignition probabilities at each life stage for multi-wall mounted air conditioners. Because only the indoor units are different, apart from the indoor (during use) stage, the values are the same as for the multi floor-standing air conditioner

shown in Table 6.7.2.

In the case of multi-wall mounted air conditioners, the ignition risk probability in the indoor (during use) stage is 1.0×10^{-9} even without countermeasures, which satisfies the tolerance value (below 10^{-9}). Accordingly, in the case of multi-wall mounted air conditioners, there is no need to consider Measure M2.

Table 6.8.1 Ignition risk probability in each life stage (multi-wall mounted air conditioners)

Type	Representative model	R32
Logistics (for each warehouse)	Middle-size warehouse	1.1×10^{-9}
Installation	3.24 m ² veranda	9.0×10^{-9}
Use (indoor)	7 m ² room	1.0×10^{-9}
(outdoor)	3.24 m ² veranda	1.1×10^{-9}
Service	3.24 m ² veranda	4.3×10^{-9}
Disposal	3.24 m ² veranda	4.1×10^{-10}

6.9 Summary of Housing Air Conditioners Risk Assessment

Risk assessment was carried out for mini-split SWG, focusing on conventional wall mounted air conditioners, in order to speed up global warming prevention, we widened the field of risk assessment to housing air conditioners. Among housing air conditioners, we analyzed the risk assessment of floor-standing type housing air conditioners, and confirmed that by adhering to Measure S1, they can be used without problems. In addition, the results of risk evaluation of multi-connection type housing air conditioners with a refrigerant load of 4 kg also showed that by taking Measure M2 the values will be lower than the tolerance value set as below 10^{-9} (below 10^{-8} during the work of service providers). Accordingly, even in the case of multi-connection floor-standing type housing air conditioners that have the highest risks, by confirming the clearances within a residence and applying the measure using the indoor unit fan to diffuse leaked refrigerant, it was proven that these air conditioners can also be used without problem. From the above, risk assessment for R32 was completed for all forms (wall mounted, ceiling mounted cassette, wall embedded, floor-standing, built-in [low ceiling installation]) of housing air conditioners (one-to one and multi-connection), and it has been confirmed that there are no problems upon use.

6.10 Summary

In the mini-split risk assessment SWG, we analyzed the risk assessment for R32 and R1234yf in wall mounted small-size commercial use air conditioners (substantially, the same as residential air conditioners), and confirmed that there are no problems upon use. We also analyzed the risk assessment for housing air conditioners using R32 and confirmed that they can be used without problem if certain measures are adhered to. In order to lessen the risks, we also revised the manuals used during installation or servicing for SWG. More precisely, as the ‘Piping construction manual for residential air conditioners using R32 refrigerant’ (industrial society internal material) issued by JRAIA, we added points of caution reminders to service manuals and installation manuals, etc., and made suggestions and manuals for the measures that can be carried out upon use of R32.

Finally, from the results of the analysis carried out at the Tokyo University of Science, Suwa and the National Institute of Advanced Industrial Science and Technology, which participated in the society of study for mildly flammable refrigerant risk assessment, revising the FTA facilitated significant improvements in the precision of risk evaluation, for which we express our gratitude. In the future, we expect that once the level of harm becomes clear, we will be able to use R32 and R1234yf air conditioners with even more safety, and to contribute to global warming prevention. This concludes our risk evaluation of mini-split air conditioners for the present.

References

- Tomohiko Imamura and Osami Sugawa: *Evaluation of Physical Hazards Upon Concurrent Use of Air Conditioners Using Mildly Flammable Refrigerant and Heating Equipment Using Fossil Fuels*; Japan Society of Refrigerating and Air Conditioning Engineers Collection of Papers, Vol. 29, No.4, pp. 401-411 (2012)
- Kenji Takaichi : *The International Symposium on New Refrigerants and Environmental Technology*; Kobe , pp. 90-94 (2012)
- Kenji Takaichi, *Research Project on Risk Assessment of Mildly Flammable Refrigerants, 2012 Progress Report*, Japan Society of Refrigerating and Air Conditioning Engineers, Ed.: March 2014, p. 78 (2014)
- Kenji Takaichi, *Study on Minimum Ignition Energy of Mildly Flammable Refrigerant*; (2011)
- Eiji Hihara , *Research Project on Risk Assessment of Mildly Flammable Refrigerants, 2013 Progress Report*, Japan Society of Refrigerating and Air Conditioning Engineers, Ed.: March 2014, p. 1 (2014)
- Eiji Hihara et al., *Research Project on Risk Assessment of Mildly Flammable Refrigerants, 2013 Progress Report*, Japan Society of Refrigerating and Air Conditioning Engineers, p. 16 (2014)
- Kenji Yao, *The International Symposium on New refrigerants and Environmental Technology*; Kobe, pp. 182-189 (2000)
- Ryuzaburo Yajima-, *Research Project on Risk Assessment of Mildly Flammable Refrigerants, 2011 Progress Report*, Japan Society of Refrigerating and Air Conditioning Engineers, Ed., March 2014, p. 90 (2013)
- Dean Smith et al., *Determining Minimum Ignition Energies and Quenching Distances of Difficult to Ignite Components*; Journal of Testing and Evaluation, Vol. 31, No. 3 (2003)
- Goetzler et al., *Risk Assessment of HFC-32 and HFC-32/134a (30/70 wt. %) in Split System Residential Heat Pumps*; DOE/CE/23810-92, Arthur D. Little, Inc. (1998)
- Tomohiko Imamura et al., *Evaluation of Fire Hazards of A2L Class Refrigerants*; The International Symposium on New Refrigerants and Environmental Technology, pp. 65-68 (2012)
- Minor et al., *Flammability Characteristics of HFO-1234yf*; AIChE Process Safety Progress Vol. 29, No. 2, pp. 150–154 (2010)
- Minor et al., *Next Generation Low GWP Refrigerant HFO-1234yf Part 2*; ASHRAE meeting, N.Y. (January 2008)
- Ministry of Economy, Trade and Industry of Japan, Commerce Distribution Group Product Safety Division: *Risk Assessment Handbook, Practical Edition*; Internet access, http://www.meti.go.jp/product_safety/recall/risk_assessment_practice.pdf (last accessed: 2015-03-20)

7. Risk Assessment for Split Air Conditioners (Commercial Package Air Conditioners)

7.1 Introduction

7.1.1 Progress of risk assessment for split air conditioners

A risk assessment for split air conditioners (commercial package air conditioners (C-PAC)) with A2L refrigerants was carried out in three steps. We assessed R32 refrigerant in this study, and plan to add other A2L refrigerants in near future. In the 1st step, as typical for normal C-PAC models, we selected a ceiling cassette indoor unit installed in an office, an outdoor unit installed at ground level without additional refrigerant charge on site, and storage at a warehouse that is somewhat protected from fire. In the 2nd step, we selected severe cases for various installations of C-PAC less than 14 kW, excluding floor-standing indoor units. In the 3rd step, we carried out risk assessment for all C-PAC systems less than 30 kW, including floor-standing indoor units.

We plan to introduce the necessary safety measures to reduce the risk of ignition, in the installation manuals of commercial package air conditioner with A2L refrigerants, in autumn 2015. Figure 7.1.1 presents the risk assessment schedule for C-PAC.

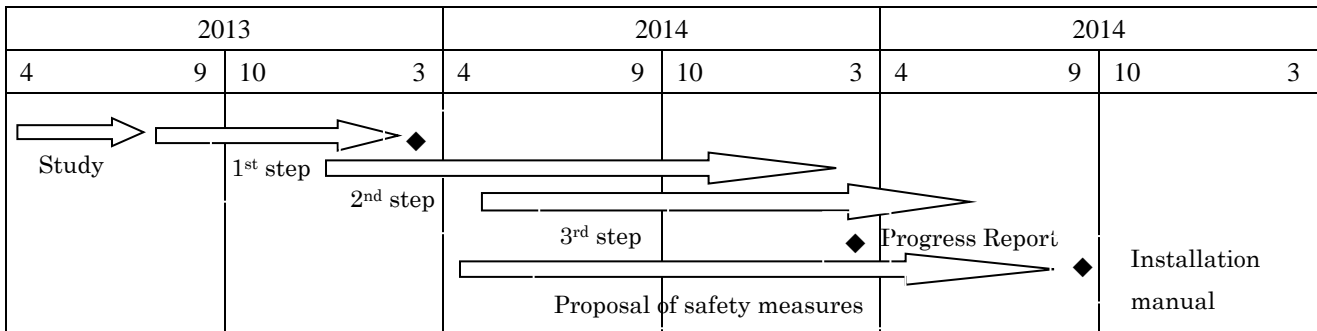


Figure 7.1.1: The risk assessment schedule for commercial package air conditioner

7.1.2 Features of C-PAC

Table 7.1.1 summarizes the main features of C-PAC compared with “mini split air conditioners (residential air conditioners (RAC))” and “multi air conditioners for building (VRF)” from a perspective of the risk assessment with A2L.

First, the cooling capacity range for C-PAC is 3.6–30 kW. Accordingly, the amount of refrigerant is also 2–19 kg. These values are relatively medium-scale compared to RAC and VRF. Regarding the amount of refrigerant, we assumed a system with the maximum amount with additional charge on site, which accounted for approximately 20% of all installations in Japan. Regarding installation, the all indoor units of C-PAC as one refrigeration circuit are installed in a single room, even if there are two indoor units or more. The risk of refrigerant leakage inside the room is relatively lower than VRF systems separated by several rooms.

Second, the type of indoor units is similar to VRF than RAC, because of commercial use. The conditions of the indoor unit’s installation are also similar to VRF, such as an office or a restaurant with openings for natural ventilation, and *karaoke*-rooms with mechanical ventilation (preventing sound leakage).

The outdoor conditions including the ice thermal storage systems are basically installation outside buildings because they all have air-cooled heat exchangers. Thus, the risk of refrigerant leakage is lower than the water-cooled outdoor units installed inside buildings. On the other hand, C-PAC outdoor units are sometimes installed in narrow spaces between buildings because of their compact slim body with side flow. We assessed such severe installation cases caused by bad ventilation.

Moreover, C-PAC can be installed in small spaces such as a minivan during transportation or small warehouses for

retailers. We added such severe cases. Table 7.1.2 summarizes the severe cases of C-PAC.

Table 7.1.1: Comparison of features of different air-conditioners

Type	Mini split (RAC)	Split (Commercial PAC)	VRF
Cooling Capacity	2.2–8.0 kW	3.6–30 kW	14.0–168 kW
Amount of Refrigerant	1–2 kg	2–19 kg	5–50 kg
Installation Outdoors:Indoors	1:1–5 (Indoors: Multiple rooms)	1:1–4 (Indoors: Single room)	1–3:1–64 (Indoors : Multiple rooms)
Type of Indoor Units	Wall-mount Floor-standing (low) Ceiling-cassette	Wall-mount Floor-standing (slim) Ceiling-cassette Ceiling-suspended Built-in duct	Wall-mount Floor-standing (perimeter) Ceiling-cassette Ceiling-suspended Built-in duct
Type of Outdoor Units	Air-cooling	Air-cooling Ice thermal storage	Air-cooling Ice thermal storage Water-cooling
Installation Location (Indoor Units)	Residence	Office Kitchen/Restaurant Factory <i>Karaoke-room (Tight)</i>	Office Kitchen/Restaurant Factory <i>Karaoke-room (Tight)</i>
Installation Location (Outdoor Units)	Ground Veranda	Ground Each floor Semi-underground Narrow space	Ground Each floor Semi-underground Machine room
Type of Logistics	Fire-protected warehouse Small warehouse	Fire-protected warehouse Small warehouse	Fire-protected warehouse
	Truck Mini van	Truck Mini van	Truck

Table 7.1.2: Severe cases of commercial package air-conditioners

Condition	Risk	Normal cases	Severe cases
Tubing length	Charge amount	Less than 30m : Charge less	Greater than 30m : Add charge
Installation height (IU)	Gas remaining at a high concentration	Ceiling : greater than 1.8m	Floor-standing : 0m
Installation location (IU)	Ignition sources	Office	Kitchen
	Ventilation		<i>Karaoke-room (Tight)</i>
Installation location (OU)	Gas remaining	Ground	Each floor
			Semi-underground
			Narrow space
Storage	Gas remaining	Fire-protected warehouse	Small warehouse
Logistics	Ignition sources	Truck	Minivan

7.1.3 Risk assessment methodology

The key to the risk assessment of C-PAC using an A2L refrigerant is fire accidents caused by gas leakage, which has a mild flammability than the current refrigerant (R410A). Figure 7.1.2 presents the mechanism of a fire accident by A2L refrigerants. The ignition probability is multiplied by these factors. It is important that the ignition probability satisfies the allowable risk level of the market. If not, safety measures are needed to reduce the risk.

Similar to the risk assessments for RAC and VRF SWG in JRAIA, we assessed the risk for C-PAC as follows.

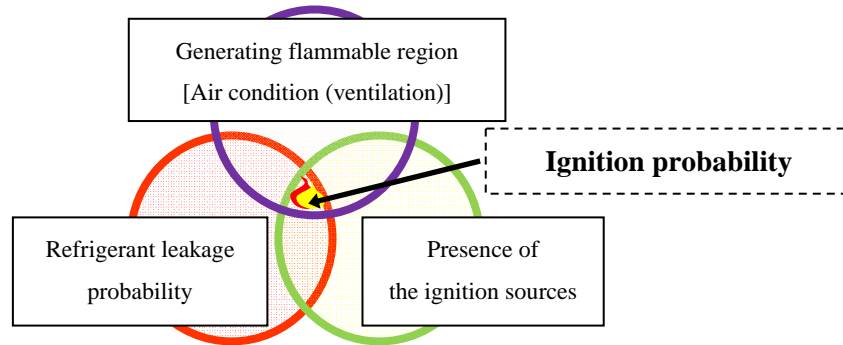


Figure 7.1.2: Mechanism of ignition with A2L refrigerants

7.1.4 Assumption of the allowable risk level

Because there are 7.8 million units of C-PAC on the market, the allowable levels are as follows if the allowable level of a serious accident occurring is once every 100 years. In practice, the hazards associated with an ignition accident should be assessed, but this has not yet been completed. Thus, all accidents were treated as serious. In each stage of the life cycle excluding usage, workers handle the equipment. The workers are trained to control the risk and reduce the severity even in the event of an accident. Thus, the allowable ignition probability was increased by an order of magnitude for these stages.

[Allowable risk levels for ignition accidents for C-PAC]

- Usage stage: 1.3×10^{-9}
- Excluding the usage stage (Logistics, Installation, Service, Disposal): 1.3×10^{-8}

7.1.5 Factors of ignition accidents for C-PAC with A2L refrigerants

Normally, refrigerant leakage from air conditioners does not occur. However, there is possibility of unexpected leakage. In this case, the ignition probability is calculated by multiplying “the probability of leakage,” “the probability of generating a flammable region” and “the probability of the presence of ignition sources,” as shown in Figure 7.1.2.

First, the probability of leakage from C-PAC was obtained from the values classified by the VRF SWG in JRAIA because the design specifications of C-PAC are similar to VRF. The probability of indoor unit leakage for a C-PAC was three times that for a VRF. We assumed that it depended on the level of leakage checked during installation.

[The probability of refrigerant leakage from a C-PAC]

- Indoor unit: 1.03×10^{-3} for slow leakage, 1.50×10^{-5} for rapid leakage
- Outdoor unit: 6.13×10^{-3} for slow leakage, 1.34×10^{-3} for rapid leakage, 1.37×10^{-4} for slow leakage

During the following life-cycle stages: “Installation,” “Service,” and “Disposal,” leakage sometimes occurs by human error such as improper operation. The probability of human error for a C-PAC was also assumed as 10^{-3} which was 10 times that for a VRF because the education level was relatively lower.

Second, the probability of generating a flammable region in the space was calculated by a three-dimensional concentration simulation analysis during refrigerant leakage for each installation model. Some simulation results are presented in Section 7.2.

Moreover, we researched the probability of presence of ignition sources for each installation model based on the results

of the ignition source assessment obtained by the Japan Society of Refrigerating and Air Conditioning Engineers. This topic is discussed in Section 7.3.

7.2 Refrigerant Leakage Simulation

For each installation model, the time for generating a flammable region and the volume of the flammable region generated were calculated by a CFD simulation considering the amount and velocity of refrigerant leakage, the installation space volume, and so on. The product of the time for generating a flammable region and the volume of the flammable region generated is called the “space-time product of flammable region (STPF)” in this report.

7.2.1 Simulation for indoor installation models

(a) Ceiling installation models

Because the indoor installation for C-PAC was similar to VRF, the STPF was obtained from the results of a simulation for VRF indoor units by Tokyo University, as shown in Figures 7.2.1-7.2.2. For some models, STPFs were simply calculated with Equation (7.2.1). Table 7.2.1 summarizes the STPFs for ceiling installation models.

$$STPF_1/STPF_2 = (M_1/(h_1 \times A_1^{0.5}))^3 / (M_2/(h_2 \times A_2^{0.5}))^3 \quad (7.2.1)$$

STPF: Space-time product of flammable region (m³min)

M: Amount of refrigerant (kg), h: Height of the leakage (m), A: Floor area (m²)

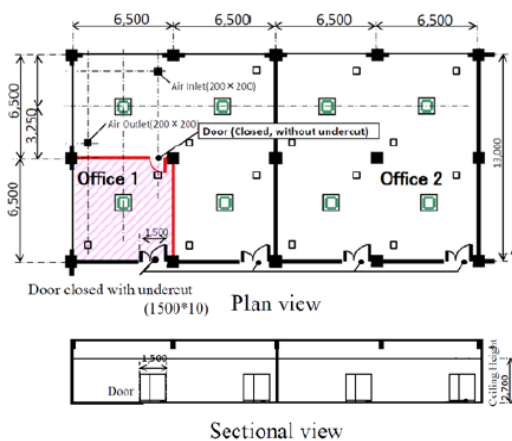


Figure 7.2.1: Simulation model for an office

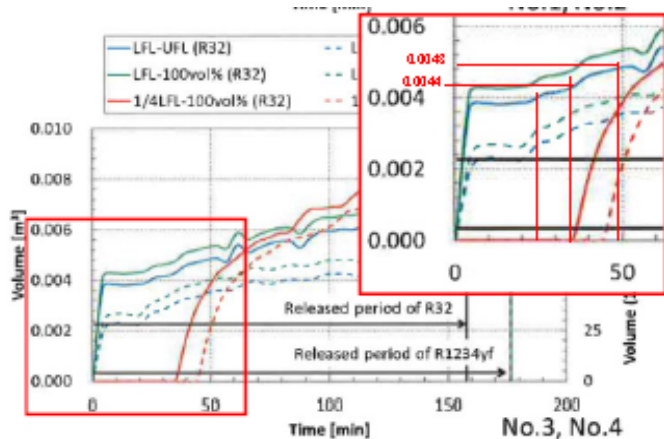


Figure 7.2.2: STPF simulation for the office model

Table 7.2.1: Space-time product of flammable region for ceiling installation models

Model (indoor)	Floor area	Height	Opening for natural ventilation	R32charge amount	Leak velocity	Time	STP of flammable region (the fan stop)
	m ²	m	mm	kg	kg/h	min	m ³ ·min
SIM (base)	42.3	2.7	1500×10	26.3	10	158	1.62×10 ⁰
7.1 kW Office	42.3	2.7	1500×10	3	10	18	6.40×10 ⁻²
14 kW Kitchen	57.2	2.5	1500×10	8	10	48	1.53×10 ⁻¹

(b) Floor installation model

For a floor installation model, refrigerant leakage tends to remain near the floor at a high concentration, as shown in the simulation in Figure 7.2.3. The leakage conditions were set as the following. Leak location: flare joint in an indoor unit, R32 concentration: 100%, and Velocity: 10.0 kg/h. In case of the fan stop, the flammable region remained near the floor for a long time, and the STPF was much higher than that for the ceiling installation model. Although the leakage gas

from the ceiling installation models diffused down into the room very well, the leakage gas from floor-standing installation models remained near the floor, even if there was an opening for natural ventilation under a wall. The results are presented in Figure 7.2.4 and Table 7.2.2. To check the validity of the simulation, we conducted a practical test under the same conditions, as shown Figure 7.2.5. The practical results at the fan stop are similar to those CFD. When the fan operated at 10m³/min after 1min from the start of leakage, a flammable region never developed because of the good diffusion throughout the room. Because floor-standing indoor units for C-PAC have a high air-discharge outlet (slim type), the diffusion due to the fan can be effective. We proposed forcible fan operation with a refrigerant leakage detector as a safety measure to reduce the ignition risk.

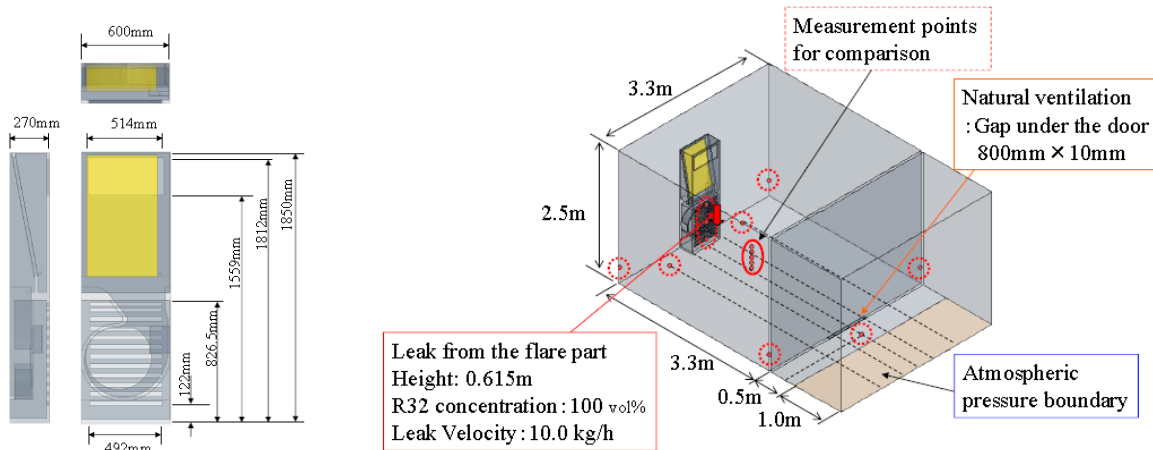


Figure 7.2.3: Simulation model for the floor-standing indoor unit

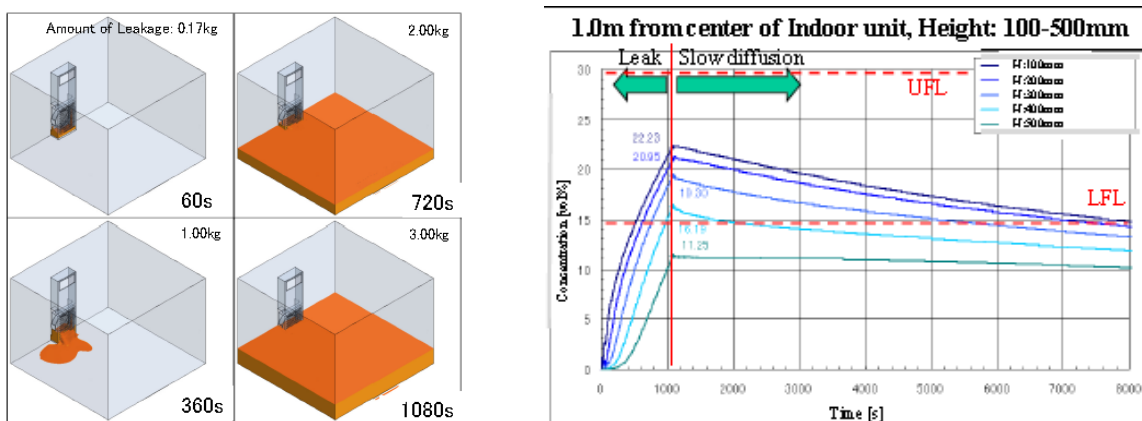


Figure 7.2.4: Flammable region simulation for the floor-standing indoor unit

Table 7.2.2: Space-time product of the flammable region for floor-standing models

Model (indoor)	Floor area	Height	Opening for natural ventilation	Charge amount	Leak velocity	Leak location	Time	STP of flammable region (the fan stop)
	m ²	m	mm	kg (R32)	kg/h	-	min	m ³ · min
SIM (base)	10.9	2.5	800×10	3	10	Flare	142	4.64×10 ²
Restaurant	14	2.5	800×10	3	10	Flare	142	3.23×10 ²

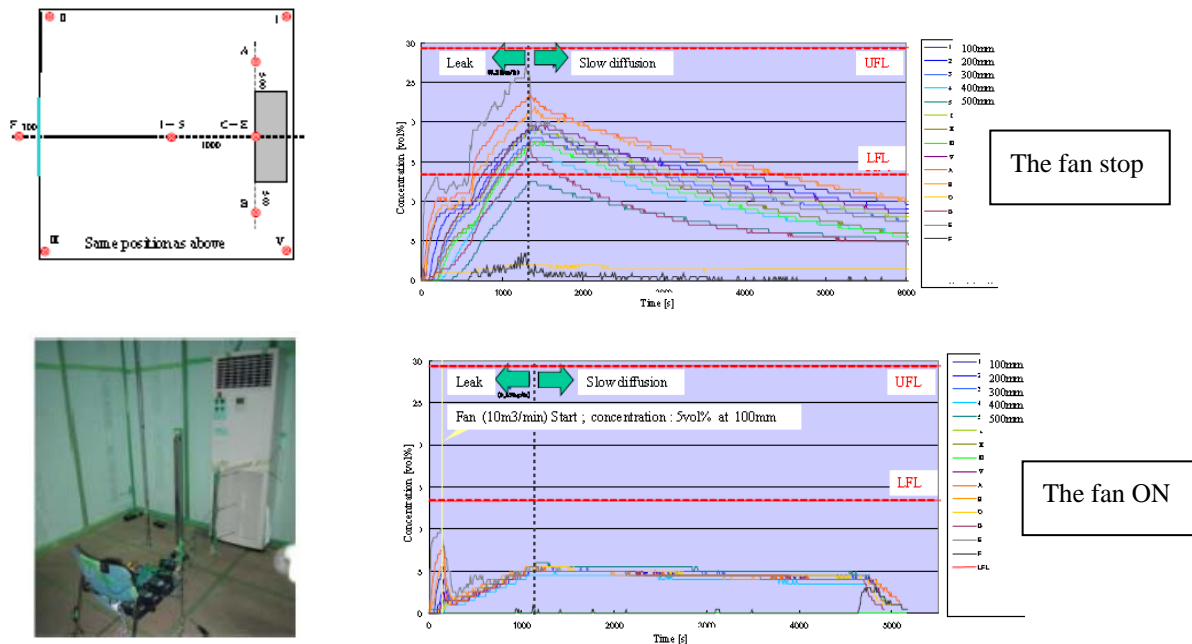


Figure 7.2.5: Practical test for a floor-standing C-PAC indoor unit with/without a fan

7.2.2 Simulation for outdoor installation models

(a) Ground installation model and semi-underground installation model

First, Figures 7.2.6-7.2.7 show a comparison of simulation results for outdoor units with “ground” and “semi-underground” installation models. Although the leakage gas did not remain for the “ground installation,” it tended to remain for the “semi-underground installation” because of the enclosure of all four sides of the unit by walls. For a semi-underground installation model, because the leakage gas remained around outdoor units for quite a long time, the time for generating a flammable region was approximately 10 h when the amount of leakage was 8 kg. The STPF for the “semi-underground installation” was 10000 times larger than that for the “ground installation.”

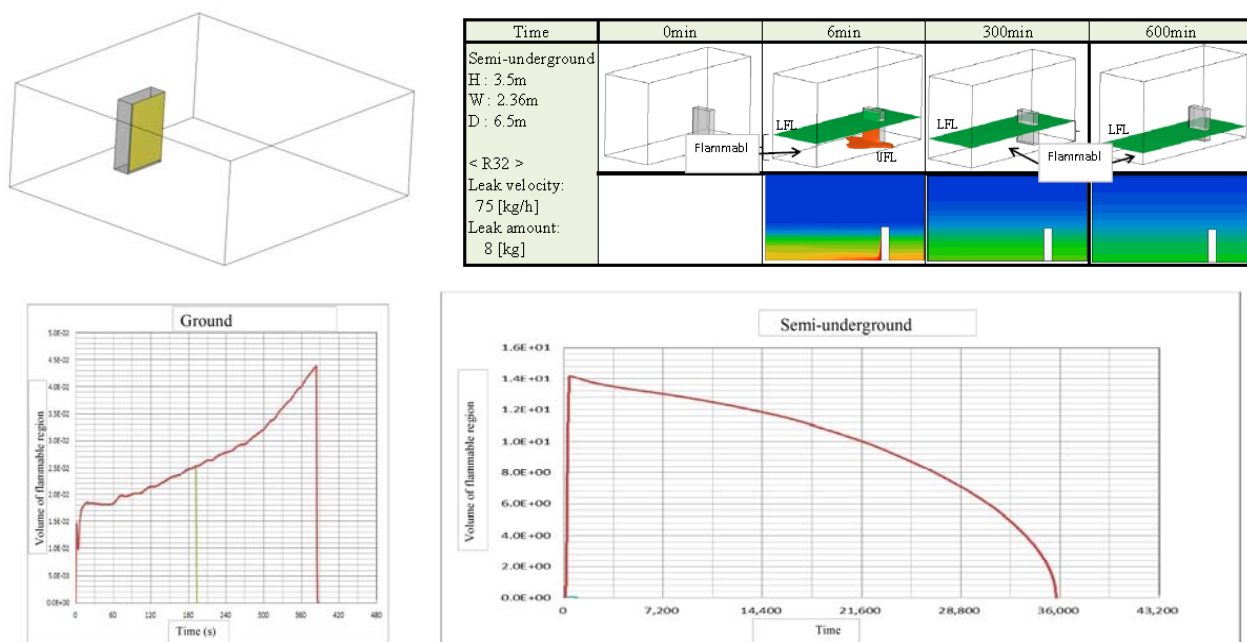


Figure 7.2.6: STPF simulation for the ground model Figure 7.2.7: STPF simulation for the semi-underground model

Table 7.2.3: Space-time product of the flammable region for “ground” and “semi-underground”

Model (outdoor)	Installation condition	Floor area	Height	Charge amount	Leak velocity	Leak location	Time	STP of flammable region (the fan stop)
	-	m ²	m	kg (R32)	kg/h	-	min	m ³ ·min
Ground	four walls _open	50	2	4	75	Heat exchanger	3.3	2.94×10 ⁻²
				8			6.5	2.80×10 ⁻¹
Semi-underground	four walls _close	15.34	3.5	4	75	Heat exchanger	15.9	2.08×10 ¹
				8			595.3	5.97×10 ³

(b) Narrow space installation model

“Narrow space installation” was a unique condition of a C-PAC. We assumed that an outdoor unit was installed at a very narrow space between buildings, and there were some obstacles on both sides. On one side, there was a small opening of 0.6 m which could be sufficient to walk through, or 0.3 m as the unrealistic worst case. These two conditions had a difference in the STPF, as summarized in Table 7.2.4.

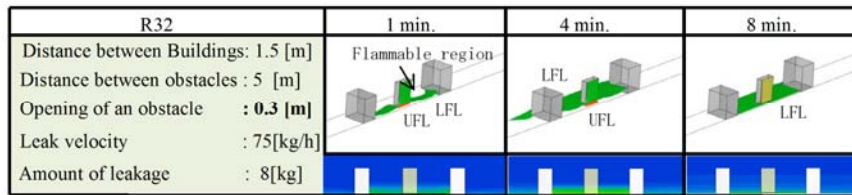


Figure 7.2.8: Simulation model for the narrow space outdoors

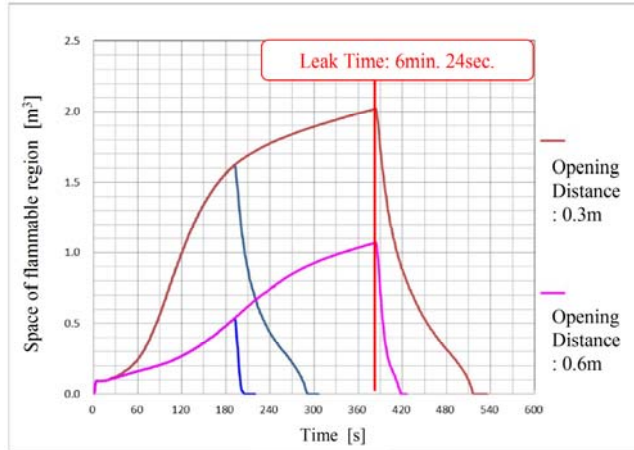


Figure 7.2.9: Flammable region simulation for the narrow space outdoors

Table 7.2.4: Space-time product of the flammable region for the “narrow space”

Model (outdoor)	Distance between buildings	Opening at one wall	Floor area	Height	Charge amount	Leak velocity	Time	STP of flammable region (the fan stop)
	m	m	m ²	m	kg (R32)	kg/h	min	m ³ ·min
Narrow space	1.5 (one side open partially)	0.3	7.5	2	4	75	4.9	3.24 x 10 ⁰
		0.6					3.5	8.30 x 10 ⁻¹
		0.3			8.6		9.75 x 10 ⁰	
		0.6			7.0		3.75 x 10 ⁰	

7.3 Ignition Source

7.3.1 Setting of the ignition source

There are two cases of ignition triggers. The first case is the action of the ignition source, such as a spark in a flammable space, and the other case is when the refrigerant at a flammable concentration comes into contact with an open flame. Because the factors of the ignition risk scenarios were different for each trigger case, we summarized the ignition sources in Table 7.3.1.

On the basis of the results of the ignition-source assessment obtained by the Japan Society of Refrigeration and Air Conditioning Engineers, we determined that ignition for R32 would not occur from sparks such as electrical sockets, electrical switches, electrical lighters among smoking devices (oil lighters and matches were made ignition sources), or static electricity generated by the human body. The ignition sources of sparks for R32 were very limited, compared to R290.

7.3.2 The Probability of the presence of ignition sources

For each installation model, we researched the probability of the presence of ignition sources according to the Japanese markets' statistics. Table 7.3.2 presents a comparison of indoor installation models between a normal "office" and a "kitchen" with many ignition sources. The probability of the presence of an open flame from appliances was calculated by the use rate from the market, and the spark probability was calculated by the probability of the occurrence of fire accidents due to appliances from the NITE reports.

For outdoor installation, Table 7.3.3 presents a comparison between "ground installation," "each floor installation," "semi-underground installation" and "narrow space installation."

We researched the probabilities of the presence of ignition sources for all installation models for each life stage, and used them for the calculation of the ignition probability accordingly.

Table 7.3.1: Ignition sources of R32 (Y: Ignited, N: not ignited)

		Ignition source	R32	R290(ref)
Spark (in flammable region)	Electric Parts	Appliance (cause of fire)	Y	Y
		Parts in Unit (less than 5kVA)	N	Y
		Power Outlet, 100V	N	Y
		Light Switch	N	Y
	Smoking Equipment	Match	Y	Y
		Oil lighter	Y	Y
		Electric Gas Lighter	N	Y
	Work Tool	Metal Spark (forklift)	Y	Y
		Electric Tool	N	Y
		Recovery Machine	N	Y
Human Body	Static Electricity	N	Y	
Open flame (contact with flammable region)	Smoking Equipment	Match	Y	Y
		Oil or Gas lighter	Y	Y
	Combustion Equipment	Heater	Y	Y
		Water Heater	Y	Y
		Boiler	Y	Y
		Cooker	Y	Y
	Work Tool	Gas Burner (Welding)	Y	Y

Table 7.3.2: Comparison of the probability of the presence of ignition sources for an office and a kitchen

Ignition source [Units]		Office	Kitchen		
Spark [times/ m ³ min]	Indoor Unit	5.7×10 ⁻¹⁶	4.5×10 ⁻¹⁶	P=installed units×accident rate/numbers on market/space volume/(365×24×60) Fire accident rate:3time/year(NITE), numbers on market:88.4mil. units	
	Appliances	Air Cleaner	7.0×10 ⁻¹⁶	-	Installed: 0.2units/room, accident rate:3.6/year, numbers on site: 17.3 mil
		Humidifier	5.6×10 ⁻¹⁶	-	Installed: 0.09 units, accident rate:3/year, numbers on site: 8.11 mil
		Mobile	7.6×10 ⁻¹⁶	-	Installed: 8.12, accident rate:23/17 years (LT10year), numbers: 23.9 mil.
		PC	1.2×10 ⁻¹⁴	-	Installed: 8.12, accident rate:174/17 years (LT10year), numbers on site: 11.8 mil
		Light	1.3×10 ⁻¹⁵	1.6×10 ⁻¹⁵	Installed: 10/15, accident rate:227/17 years (LT10year), numbers on site: 165 mil
		Tracking	6.7×10 ⁻¹⁶	1.1×10 ⁻¹⁵	Installed: 10/15, accident rate:202/17 years (LT10year), numbers on site: 298 mil
		Refrigerator	-	1.6×10 ⁻¹⁴	Installed: 0/3, accident rate:267/17 years (LT10year), numbers on site: 3.88 mil
		Freezer	-	3.8×10 ⁻¹⁵	Installed: 0/2, accident rate:16/17 years (LT10year), numbers on site: 0.658 mil
		Dishwashers	-	9.7×10 ⁻¹⁵	Installed: 0/2, accident rate:71/17 years (LT10year), numbers on site: 1.511 mil
		Phone	-	2.5×10 ⁻¹⁶	Installed: 0/1, accident rate:18/17 years (LT10year), numbers on site: 5.67 mil
TV	-	1.1×10 ⁻¹⁵	Installed: 0/1, accident rate:355/17 years (LT10year), numbers on site: 25.2 mil		
Exhaust Fan	-	5.5×10 ⁻¹⁵	Installed: 10/15, accident rate:105/17 years (LT10year), numbers on site: 5.96 mil		
Smoking Equipment (Match/Oil lighter)	8.8×10 ⁻⁷	-	P=smoking rate in the room×0.209×17.1/space volume/(24×60)×0.05 Smoking rate in the room: 0.1, smoking rate: 0.209 (Japanese Adult) Smoking numbers: 17.1/day/person(2013JT),use rate Match/Oil lighter: 0.05		
Ignition Equipment (Match/Oil lighter)	-	1.2×10 ⁻⁶	P=5/space volume/(24×60)×0.05 Using rate for gas burner 5times/day, Use rate Match/Oil lighter: 0.05		
Open flame [-]	Combustion equipment	Water Heater	8.3×10 ⁻³	6.7×10 ⁻²	[Office]inst.: 0.1, Use rate: 2h/day, [Kitchen]2, 60min/day. Installed rate: 0.8
		Heater	-	2.7×10 ⁻⁵	Installed: 0.001 units, Use rate: 4h/day, 60day/year
		Kitchen Burner	-	3.1×10 ⁻¹	Installed: 15 units, Use rate: 0.023. Installed rate: 0.9
		Gas Rice Cooker	-	5.0×10 ⁻²	Installed: 2 units, Use rate: 2h/day. Installed rate:0.3
		Gas Oven	-	5.8×10 ⁻⁴	Installed: 2 units, Installed rate: 2.9×10 ⁻⁴
		Coffee Siphon	-	8.7×10 ⁻⁴	Installed: 3 units, Installed rate: 2.9×10 ⁻⁴
		Gas Burner	-	6.9×10 ⁻⁴	Installed: 0.5 units, Use rate: 0.2min/time, 10times/day
		Gas Roaster	-	5.8×10 ⁻⁴	Installed: 2 units, Installed rate: 2.9×10 ⁻⁴

Table 7.3.3: Comparison of the probability of the presence of ignition sources for outdoor installations

Ignition Source [Units]		Ground	Each Floor	Semi-Underground	Narrow Space		
Spark [times/ m ³ min]	Outdoor Unit	1.4×10 ⁻¹⁴	9.5×10 ⁻¹⁴	2.5×10 ⁻¹⁴	9.1×10 ⁻¹⁴	P=5.6/7,800,000/space volume/(365×24×60) Fire accident rate: 5.6times/year, numbers:7.8mil. units	
	Smoking Equipment (Match/Oil lighter)	Worker	3.6×10 ⁻¹⁰	1.3×10 ⁻⁹	1.7×10 ⁻⁹	1.7×10 ⁻⁹	[Worker] P=Smoking space rate×service rate×0.322×16/space volume/(24×60)×0.05[spark]×0.01 Smoking rate near unit: G: 0.2, EF: 0.1, SU/NS: 0.5 Service rate: 0.1 Smoking rate for workers: 0.322(Japanese Male: JT) Smoking numbers for workers: 16/day (Japan) Use rate for match/oil lighter: 0.05 Rule disregarding rate during work: 0.01
		User	5.6×10 ⁻⁸	5.4×10 ⁻⁸	1.1×10 ⁻⁷	1.1×10 ⁻⁷	[User] P=Smoking rate near units×0.209×17.1/space volume/(24×60)×0.05[spark]×smoking area rate Smoking rate near units: G/SU/NS: 0.05, EF: 0.0125 Smoking rate: 0.209, Numbers: 17.1/day (Japanese Adult), Smoking area rate: EF: 0.5, others: 0.9
Open flame [-]	Smoking	Worker	6.0×10 ⁻⁸	3.0×10 ⁻⁸	1.5×10 ⁻⁷	1.5×10 ⁻⁷	[Worker] P=Smoking space rate×service rate×0.322×16×5/space volume/(24×60×60)×0.01 [User] P=Smoking rate near units×0.209×17.1×5/space volume/(24×60×60)×smoking area rate Open flame generating time: 5s
		User	9.3×10 ⁻⁶	1.3×10 ⁻⁶	9.3×10 ⁻⁶	9.3×10 ⁻⁶	
	Boiler	6.6×10 ⁻⁴	2.2×10 ⁻⁴	2.2×10 ⁻⁴	2.2×10 ⁻⁴	P=Use rate×Installed rate Installed rate: 0.1% Use rate...Ground: 0.66(24h/day, 20days/month) Others: 0.22(8h/day, 20days/month)	

7.4 FTA

For each life-cycle stage (Logistics, Installation, Usage, Service, and Disposal), the ignition probability was calculated by an FTA based on the assumed risk scenarios. We made FTAs with separate indoor and outdoor installations for each life-cycle stage. Basically, the ignition probability in the FTA was multiplied “the leak probability,” “the probability of generating flammable region,” and “the probability of the presence of ignition sources,” as mentioned before. We introduced the FTA of the “Service” stage as follows.

7.4.1 FTA of the service stage for outdoor installation

Figure 7.4.1 shows the FTA of the service stage. The values on this FTA sheet were used for the following model:

- Outdoor Ground installation, Max charge amount: 8 kg (R32) for 14 kW systems.

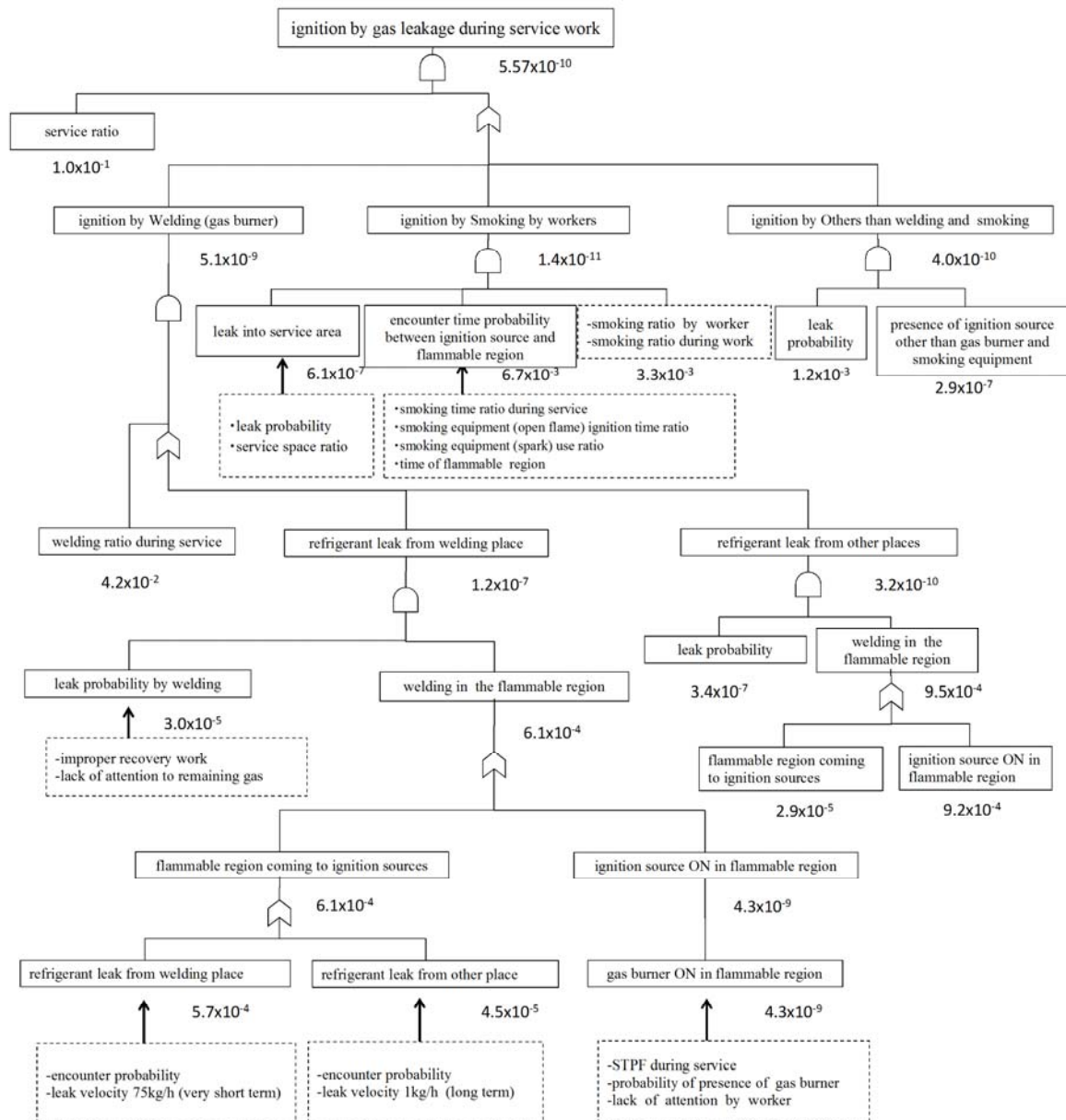


Figure 7.4.1: FTA of the service stage

The main ignition sources during Service were assumed to be a gas burner (welding) and smoking equipment (match/oil lighter). In particular, because the gas burner during welding was a dominant factor in the risk scenarios in the FTA, we

subdivided the risk scenarios due to gas burner. The cases in which a gas burner (welding) encountered a generated flammable region were subdivided precisely. The first case was the same location for welding and refrigerant leakage, and the other case was the different location for them. In the first case, the leakage occurred in a burst due to welding so that the leak velocity was assumed to be 75 kg/h. In other case, we assumed that the leak velocity was 1 kg/h, which is a slow leakage that a worker could not notice.

7.4.2 FTA of the service life stage for indoor installation

For indoor installation, we used the same FTA as the outdoor installation. The following probabilities were set to zero, because there is no chance of occurrence for an indoor installation during service:

- Refrigerant charge/recovery
- Smoking in the room during service

Although the risk of indoor service by improper work and smoking were lower than that of outdoor service, the effect of the STPF was larger.

7.5 Result of the Risk Assessment for Each Model

We carried out a risk assessment for C-PAC in three steps. These steps are as follows: 1st step: typical normal C-PAC models, 2nd step: severe cases for less than 14 kW systems excluding floor-standing indoor units, and 3rd step: severe cases for all C-PAC less than 30 kW including floor-standing indoor units. In this report we assessed for R32 refrigerant. We plan to add other A2L refrigerants to this risk assessment.

7.5.1 1st step models (Typical normal C-PAC models)

We set the typical normal C-PAC models as summarized in Table 7.5.1.

First, 80% of the C-PAC systems on market were installed according to piping length: less than 30 m, and no needed additional refrigerant charge on site. Thus, we set the amount of refrigerant charge to the initial factory value.

Second, an indoor unit was selected for its cooling capacity: a 7.1 kW four-way ceiling-cassette system, which was the best seller in the Japanese market. The installation location was set in an office, which had openings for natural ventilation. A 14 kW system was selected as the outdoor unit as the model with the largest amount of refrigerant between 7.1 kW and 14 kW, which had same installation floor area. The installation location was set as ground installation, in which any leakage gas did not remain because of openings on all four sides. The logistics was set to normal truck delivery and fire-protected warehouse storage. Because the luggage space of truck does not have an ignition source, truck delivery was omitted from the 1st step models. The ignition source of the warehouse was assumed to be a metal spark by a forklift bar.

Table 7.5.2 summarizes the results of the risk assessment for the 1st step models. The ignition probability was calculated for each life-cycle stage. Because the ignition probability satisfied the allowable risk level, safety measures were not needed under the current handling level.

Table 7.5.1: Parameters of the 1st step models

Condition	Type	Location	Feature	Installation space		Capacity (kW)	Piping length (m)	Charge amount (kg)
				Floor area(m ²)	Height (m)			
Indoors	Ceiling cassette	Office	Opening for natural ventilation	42.3	2.7	7.1	≤30	3
Outdoors	Side flow	Ground	Open all four sides	50	2	14.0	≤30	4
Storage	Bulk storage	Warehouse	2300 units	1000	—	14.0	—	4

Table 7.5.2: Results of the risk assessment for the 1st step models

Life stage [allowable level]	Logistics [$\leq 1.3 \times 10^{-8}$]		Installation [$\leq 1.3 \times 10^{-8}$]		Usage [$\leq 1.3 \times 10^{-9}$]		Service [$\leq 1.3 \times 10^{-8}$]		Disposal [$\leq 1.3 \times 10^{-8}$]	
	without	with	without	with	without	with	without	with	without	with
Office (Indoors)	—	—	6.61×10^{-10}	None	3.37×10^{-12}	None	1.19×10^{-10}	None	3.12×10^{-12}	None
Ground (Outdoors)	—	—	6.75×10^{-10}	None	6.35×10^{-11}	None	2.23×10^{-10}	None	6.05×10^{-11}	None
Warehouse	1.55×10^{-11}	None	-	-	-	-	-	-	-	-

7.5.2 2nd step models (Severe C-PAC models less than 14 kW excluding floor-standing indoor units)

In the 2nd step, we selected the severe C-PAC models less than 14 kW, excluding floor-standing indoor units, as summarized in Table 7.5.4. First, the amount of refrigerant charge was set at the maximum system value, in consideration of the longest piping length. Second, indoor installation models were selected from two cases as follows: kitchen with many ignition sources and *Karaoke* (tight)- room without openings for natural ventilation. The size of the C-PAC for the *Karaoke*- room was set to 3.6 kW because of the small indoor space volume.

For the *Karaoke*- room model, the leakage gas was assumed to accumulate at just the LFL concentration in the lower part of the room, owing to the malfunction of the mechanical ventilation, which should be operated usually. Although the leakage gas was expected to diffuse throughout the room entirely in practice, we calculated assuming the worst-case scenario because we have not performed a simulation for a tight- room yet. Moreover, the leak velocity was assumed to be 2 kg/h as a slow leakage because it was assumed that the users would not open the door of the *Karaoke*- room during a slow leak, rather than rapid leak (10 kg/h). We calculated the ignition probability for 3h of continuous use time for the room by one customer. Figures 7.5.1-7.5.2 show the assumed conditions, and Table 7.5.3 summarizes the STPF for *Karaoke*- room models.

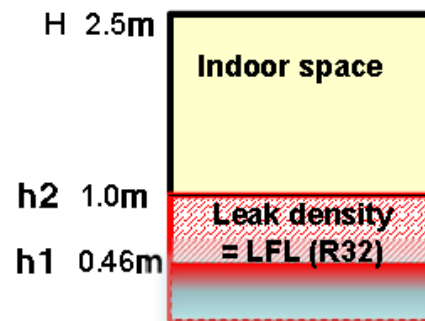
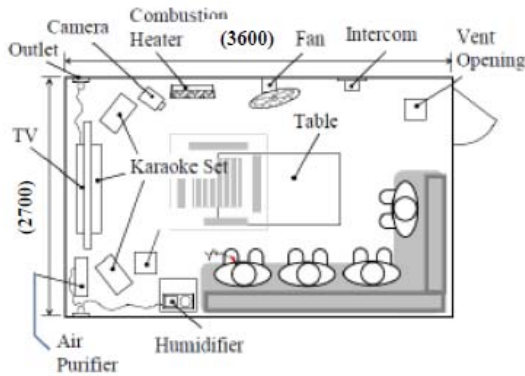


Figure 7.5.1: Simulation model for the *Karaoke*- room

Figure 7.5.2: Assumed accumulation of gas leakage for the *Karaoke*-room

Table 7.5.3: Space-time product of the flammable region for the “*Karaoke*- room”

Height of flammable limit	Accumulation height	Floor area	Height of room	R32charge amount	Leak velocity	Time	STP of flammable region (the fan stop)
	m	m ²	m	kg	kg/h	min	m ³ ·min
h1 : ULF	0.46	9.7	2.5	3	2	138	6.16×10^2
h2 : LFL	1.0	9.7				90	8.73×10^2

The outdoor installation models were selected as four cases, as mentioned before. The storage condition was an additional small warehouse for the retailer. Considering the delivery of small C-PAC outdoor units (less than 7.1 kW with a single fan), we selected a minivan delivery model, assuming a higher ignition risk than normal truck delivery due

to the same space for the driver seats and luggage space. The leak velocity during transport was assumed to be 75 kg/h as burst leakage due to vibration. Table 7.5.5 summarizes the results of the risk assessment for the 2nd step models.

For some stages of outdoor semi-underground installation and narrow space installation, the ignition probability did not satisfy the allowable level. We clarified the dominant risk factors and proposed safety measures to reduce the ignition probability to be lower than the target, as summarized in Table 7.5.6. The dominant risk factors during work were human errors such as improper refrigerant recovery that generated a flammable region and improper wiring of a power supply that cause a spark to occur, and the probability of the presence of an open flame such as a gas burner during welding. Thus, we proposed education for the worker and carrying a leak detector, as necessary safety measures.

For the usage stages, we proposed a reduction in the probabilities of the presence of ignition sources and generating a flammable region as follows: semi-underground: prohibit installation near a boiler and, mechanical ventilation or unit's fan operating with a leak detector. Narrow space: an opening of 0.6 m or more for one side, or prohibit installation near a boiler.

Table 7.5.4: Parameters of the 2nd step models

Condition	Type	Location	Feature	Installation space		Capacity (kW)	Piping length (m)	Charge amount (kg)
				Floor area(m ²)	Height (m)			
Indoors	Ceiling cassette	Office	Max charge	42.3	2.7	7.1	75	6
		Kitchen	Ignition sources	57.2	2.7	14.0	75	8
		Karaoke-room	Tightness	9.7	2.4	3.6	50	3
Outdoors	Side flow	Ground	Open all four sides	50	2	14.0	75	8
		Each floor	Close three sides	3.6	4	14.0	75	8
		Semi-underground	Close four sides	15.3	3.54	14.0	75	8
		Narrow space	Open one side(small)	7.5	2	14.0	75	8
Storage	Floor	Small warehouse	Small space	15	2.7	14.0	—*	8*
Logistics	Delivery	Minivan	Ignition sources	4.65	1.34	7.1	—*	6*

*Disposal stage: maximum amount of charge with additional charge on site

Table 7.5.5: Results of the risk assessment for 2nd the step models

Life stage [allowable level]		Logistics [≤ 1.3×10 ⁻⁸]		Installation [≤ 1.3×10 ⁻⁸]		Usage [≤ 1.3×10 ⁻⁹]		Service [≤ 1.3×10 ⁻⁸]		Disposal [≤ 1.3×10 ⁻⁸]	
Safety measures		without	with	without	with	without	with	without	with	without	with
Indoors	Office	—	—	6.65×10 ⁻¹⁰	None	4.20×10 ⁻¹²	None	1.21×10 ⁻¹⁰	None	3.37×10 ⁻¹²	None
	Kitchen	—	—	6.66×10 ⁻¹⁰	None	1.03×10 ⁻¹⁰	None	2.65×10 ⁻¹⁰	None	2.80×10 ⁻¹²	None
	Karaoke room	—	—	6.79×10 ⁻¹⁰	None	8.71×10 ⁻¹¹	None	1.04×10 ⁻⁹	None	2.04×10 ⁻¹¹	None
Outdoors	Ground	—	—	7.55×10 ⁻¹⁰	None	3.13×10 ⁻¹⁰	None	5.57×10 ⁻¹⁰	None	2.60×10 ⁻¹⁰	None
	Each floor	—	—	8.51×10 ⁻¹⁰	None	5.79×10 ⁻¹⁰	None	1.47×10 ⁻⁹	None	6.81×10 ⁻¹⁰	None
	Semi UG	—	—	3.60×10 ⁻⁷	4.89×10 ⁻⁹	7.14×10 ⁻⁷	1.13×10 ⁻⁹	1.12×10 ⁻⁷	2.33×10 ⁻⁹	8.68×10 ⁻⁸	9.46×10 ⁻⁹
	Narrow S	—	—	2.77×10 ⁻⁹	None	5.96×10 ⁻⁹	1.17×10 ⁻¹⁰	1.84×10 ⁻⁸	4.21×10 ⁻¹⁰	7.21×10 ⁻⁹	None
Logi	Small WH	1.26×10 ⁻¹¹	None	-	-	-	-	-	-	1.22×10 ⁻¹⁰	None
	Minivan	1.73×10 ⁻¹⁰	None	—	—	—	—	—	—	6.66×10 ⁻¹⁰	None

Table 7.5.6: The dominant risk factors and safety measures for the 2nd step models

Dominant risk factors		Usage stage		Installation/ Service stage	Disposal stage
Outdoor	Factor	Leakage gas	Presence of ignition sources	Human error	Human error
	Item	Diffusion/ Ventilation	Boiler	Refrigerant recovery Gas burner (Welding)	Refrigerant recovery Wiring for power supply
Semi-underground	Safety measures	“Prohibit installation near a boiler” and, “Unit’s fan operating with a leak detector” or “mechanical ventilation”		“Education for workers” and “Carrying a leak detector”	
Outdoor	Factor	Leakage gas	Presence of ignition sources	Human error	Human error
	Item	Diffusion/ Opening	Boiler	Refrigerant recovery Gas burner (Welding)	Refrigerant recovery Wiring for power supply
Narrow space	Safety measures	“Opening of 0.6 m or more for one side” or “prohibit installation near a boiler”		“Education for workers” and “Carrying a leak detector”	

7.5.3 3rd step models (Severe C-PAC models less than 30 kW including floor-standing indoor units)

In the 3rd step, we selected severe C-PAC models less than 30 kW including floor-standing indoor units, as listed in Table 7.5.7. The maximum piping length of a 30 kW system was set to 120m, and the amount of refrigerant charge was set at the maximum accordingly. Moreover, the number of indoor units was four, as higher values increased the leakage probability.

Floor-standing indoor unit models were selected as two cases. The first case was a 4.5 kW system as the minimum volume of the indoor installation space. The other case was a 30 kW (7.1 kW× four indoor units) system as the maximum amount of refrigerant. Moreover, we added a small ice thermal storage system for the C-PAC. The use rate of the amount of refrigerant versus the indoor space volume for ice thermal system was larger than the normal system owing to ice thermal storage tank installed outside. Because they are used for an office or a school, we set a ceiling installation for the indoor unit. Furthermore, the amount of refrigerant was set to 9 kg as the maximum piping length because the largest ice thermal storage system for a C-PAC was 14 kW.

For Logistics, we only evaluated for a normal warehouse because a large C-PAC cannot be delivered to a small warehouse and by minivan. The initial amount of refrigerant for a 30 kW system was set to 7 kg.

Table 7.5.8 summarizes the results of the risk assessment for the 3rd step models. For “floor-standing indoor units” and outdoor “semi-underground” and “narrow space” installations, the ignition probability did not satisfy the allowable level.

In the case of “floor-standing indoor unit,” as mentioned before, the STPF was too high because the leakage gas tended to remain near the floor at a high concentration. For safety measures during the usage stage, forcing the unit’s fan to be ON with a leak detector near the floor was effective. For the work stages (Service and Disposal), “education for workers” and “carrying a leak detector” were effective, same as the 2nd step models.

The ignition probability for the indoor installation models in the 3rd step, except for the floor-standing units was slightly lower than that for the 2nd step models, because of the large space volume of the indoor rooms, rather than the effect of the amount of refrigerant charge. For the outdoor installation models, the ignition probability was slightly increased compared to the 2nd step models, owing to the large amount of charge for the same installation space. However, the necessary safety measures were the same as the 2nd step, as summarized in Table 7.5.9.

Table 7.5.7: Parameters of the 3rd step models

Condition	Type	Location	Feature	Installation space		Capacity (kW)	Piping length (m)	Charge amount (kg)
				Floor area(m ²)	Height (m)			
Indoors	Ceiling	Office	Max charge	169	2.7	30.0	120	19
		Kitchen	Ignition sources	80	2.7	30.0	120	19
	Floor	Restaurant	Leakage gas remain	14	2.5	4.5	50	3
		Factory	Leakage gas remain	100	3	30.0	120	19
Indoors (Ice)	Ceiling	Office	Charge rate	50	2.7	14.0	75	9
Outdoors	Side flow	Ground	Open all four sides	50	2.5	30.0	120	19
		Each floor	Close three sides	3.6	4	30.0	120	19
		Semi-UG	Close four sides	15.3	3.54	30.0	120	19
		Narrow S	Open one side(small)	7.5	2.5	30.0	120	19
Storage	Bulk storage	Warehouse	2300units	1000	—	30.0	—	7

Table 7.5.8: Results of the risk assessment for the 3rd step models

Life stage [allowable level]	Logistics [$\leq 1.3 \times 10^{-8}$]		Installation [$\leq 1.3 \times 10^{-8}$]		Usage [$\leq 1.3 \times 10^{-9}$]		Service [$\leq 1.3 \times 10^{-8}$]		Disposal [$\leq 1.3 \times 10^{-8}$]		
	without	with	without	with	without	with	without	with	without	with	
Indoors	Office	—	—	6.63×10^{-10}	None	7.61×10^{-13}	None	4.82×10^{-12}	None	1.90×10^{-12}	None
	Kitchen	—	—	6.77×10^{-10}	None	7.97×10^{-11}	None	1.65×10^{-10}	None	7.33×10^{-12}	None
	Restaurant	—	—	1.70×10^{-8}	2.45×10^{-10}	9.39×10^{-9}	1.20×10^{-11}	9.28×10^{-9}	2.81×10^{-9}	2.99×10^{-12}	None
	Karaoke -room	—	—	2.30×10^{-9}	None	1.05×10^{-9}	None	3.11×10^{-9}	None	7.04×10^{-10}	None
	Ice TS	—	—	6.70×10^{-10}	None	3.62×10^{-12}	None	4.10×10^{-11}	None	2.79×10^{-12}	None
Outdoors	Ground	—	—	8.04×10^{-10}	None	2.61×10^{-10}	None	5.53×10^{-10}	None	7.60×10^{-10}	None
	Each floor	—	—	1.00×10^{-9}	None	6.15×10^{-10}	None	1.48×10^{-9}	None	2.01×10^{-9}	None
	Semi UG	—	—	3.67×10^{-7}	5.64×10^{-9}	4.65×10^{-6}	1.23×10^{-9}	1.18×10^{-7}	2.93×10^{-9}	1.43×10^{-7}	1.59×10^{-9}
	Narrow S	—	—	5.34×10^{-9}	None	8.49×10^{-9}	3.97×10^{-10}	1.91×10^{-8}	4.95×10^{-10}	2.61×10^{-8}	2.84×10^{-9}
Warehouse	8.30×10^{-11}	None	-	-	-	-	-	-	-	3.51×10^{-9}	None

Table 7.5.9: The dominant risk factors and safety measures for the 3rd step models

Dominant risk factors		Usage stage		Installation/ Service stages	Disposal stage
Floor-standing indoor units	Factor	Leakage gas	Leakage gas	Human error	-
	Item	Diffusion/ Ventilation	High concentration	Gas burner (Welding)	-
	Safety measures	“Unit’s fan operating with a leak detector”		“Education for workers” and “Carrying a leak detector”	
Outdoors Semi-underground	Factor	Leakage gas	Presence of ignition sources	Human error	Human error
	Item	Diffusion/ Ventilation	Boiler	Refrigerant recovery Gas burner (Welding)	Refrigerant recovery Wiring for power supply
	Safety measures	“Prohibit installation near boiler” and, “Unit’s fan operating with a leak detector” or “mechanical ventilation”		“Education for workers” and “Carrying a leak detector”	
Outdoors Narrow space	Factor	Leakage gas	Presence of ignition sources	Human error	Human error
	Item	Diffusion/ Opening	Boiler	Refrigerant recovery Gas burner (Welding)	Refrigerant recovery Wiring for power supply
	Safety measures	“Opening of 0.6 m or more for one side” or “prohibit installation near boiler”		“Education for workers” and “Carrying a leak detector”	

7.6 The Risk Assessment Considering Improper Refrigerant Charge

We proposed safety measures for C-PAC systems using R32 to satisfy an allowable level in Section 7.5. In addition, we added a consideration of accidental improper refrigerant charging, because the improvement due to these safety measures in current systems (R410A) with an improper charge (R32) could not be estimated. We assumed the following conditions for improper charging.

[The probability of improper refrigerant charge]

At Installation: 0.2 (additional charge ratio) $\times 10^{-3}$ (human error) $\times 6.5$ (accumulating years)/13 (lifetime: years)

At Service: 0.1 (failure ratio) $\times 0.15$ (charge ratio during service) $\times 10^{-3}$ (human error) $\times 6.5$ (accumulating years)

The allowable risk level was 10 times higher in order to maintain safety, because the user and worker were not aware of the use of A2L refrigerant. Table 7.6.1 summarizes the total ignition probability with improper charging, considering the distribution ratio of outdoor installation (semi-underground: 0.001%, narrow space: 2.78%). Because the ignition probabilities with the improper charging satisfied the allowable levels, we supposed that a safety measure such as change in the charging port specification of the C-PAC outdoor unit was not needed.

Table 7.6.1: Risk assessment with an improper refrigerant charge

Life stages	Installation		Usage		Service		Disposal	
Allowable risk level	1.3×10^{-9}		1.3×10^{-10}		1.3×10^{-9}		1.3×10^{-9}	
Improper charge	Installation		Installation + Service		Installation + Service		Installation + Service	
Improper probability	1.0×10^{-4}		2.0×10^{-4}		2.0×10^{-4}		2.0×10^{-4}	
Ignition probability	w/o SM*	Total**	w/o SM*	Total**	w/o SM*	Total**	w/o SM*	Total**
Floor standing	1.70×10^{-8}	1.70×10^{-12}	9.39×10^{-9}	1.88×10^{-12}	9.28×10^{-9}	1.86×10^{-12}	-	-
Semi-UG/Narrow S	3.67×10^{-12}	3.67×10^{-16}	2.83×10^{-10}	5.66×10^{-14}	5.32×10^{-10}	1.06×10^{-13}	1.43×10^{-12}	2.86×10^{-16}

*without safety measures, **Total ignition probability = (w/o SM) \times (improper probability)

7.7 Summary

We carried out a risk assessment of C-PAC with A2L refrigerant in three steps.

For the typical normal models of C-PAC systems, the ignition probability using R32 satisfied the allowable risk without additional safety measures. However, for some severe cases, safety measures were needed to satisfy the allowable level. For the usage stage and work (Installation, Service, and Disposal) stages, a “floor-standing indoor unit model,” outdoor “semi-underground” and “narrow space” installation models needed safety measures to reduce the dominant risk factors. We plan to introduce safety measures in “the installation manual for C-PAC using R32.” We supposed that a change in the charging port specification of a C-PAC outdoor unit was not needed because of the low risk of improper charging. After additional studies (the flammability with humidity of other A2L refrigerants other than R32 and the degree of hazardous ignition accidents with A2L) are carried out in near future, we plan to add the latest information to our risk assessments to attain more a practical assessment.

References

- Imamura, T., 2014, Experimental Evaluation of Physical Hazard of A2L Refrigerants, The International Symposium on New Refrigerants and Environment Technology 2014, pp73-78
- Japan Tobacco Inc., 2013, Smoking Research in Japan
- Kataoka, O., 2000, The International Symposium on HCFC Alternative refrigerants and Environmental Technology 2000, pp218-223
- National Institute of Technology and Evaluation, 2013 NITE Statistics
- Takaichi, K., Taira, S., Watanabe, T., Fiscal 2013 Progress Report of Risk Assessment of Mildly Flammable Refrigerants, the Japan Society of Refrigerating and Air Conditioning Engineers, pp78-89
- Takizawa, K., 2014, Fundamental and Practical Flammability Properties, The International Symposium on New Refrigerants and Environment Technology 2014, pp79-84
- The Japan Electrical Manufacturers' Association, 2013 JEMA Statistics
- The Japan Refrigeration and Air Conditioning Industry Association Environment Committee Risk Assessment of Mildly Flammable Refrigerants WG, 2012, The 1st Report of Mini-Split Risk Assessment SWG, pp27-28
- Yajima, R., Fiscal 2013 Progress Report of Risk Assessment of Mildly Flammable Refrigerants, the Japan Society of Refrigerating and Air Conditioning Engineers, pp90-100

8. Progress of Risk Assessment for VRF System

8.1 Introduction

Table 8.1.1 shows the progress in risk assessments up to the present. The purpose of a risk assessment is to accurately evaluate the risk of variable Refrigerant Flow systems (VRF systems) using mildly flammable low-GWP refrigerants and establish safety standards based on those results to ensure sufficient safety in the market. To reduce global warming, those products have to gain market acceptance. This will require progress to be made in the development of viable safety standards that eliminate the need for excessive regulations. In the first assessment stage, basic data were collected for features such as the leak rate and ignition source in order to establish a risk assessment method. In the second assessment stage, the probability of fire accidents was estimated by extracting installation cases with substantial risks in order to propose safety measures capable of reducing risk. In the third assessment stage, the probability of fire accidents was estimated for the overall market, including installation cases that are close to actual market situations, in order to propose safety regulations compatible with commercialization. Safety standards were proposed to reduce the probability to allowable values.

In this risk assessment, R32 was used as a representative mildly flammable refrigerant.

Table 8.1.1 Progress in risk assessments for VRF system with A2L refrigerants

	The progress of risk assessments		
	1 st Step	2 nd Step	3 rd Step
	'11/4 ~ '12/7	'12/8 ~ '14/9	'14/1 ~ '15/3
Objectives	• Establishment of method for risk assessments	• Proposal of safety measures for guideline	• Harmonization of regulations and commercialization
Actions	• Investigation of probability of refrigerant leakage and human errors • Evaluation of ignition sources • Calculation method of fire accidents	• Identify worst case installation and safety measures • Proposal to international standards	• Correction of conditions for ventilation • Proposals for revision of refrigeration safety rules

8.2 Issues for VRF Systems Using Mildly Flammable Refrigerants

Table 8.2.1 lists the features of a VRF system. The most distinctive feature is the large amount of refrigerant charge in the refrigerant circuit, which can be completely discharged from a single indoor unit in the case of an indoor refrigerant leak. Because the refrigerant piping has many connections, rigorous refrigerant leak checks are conducted in a two-layer check system after the piping is installed: a tightness leak test performed under positive pressure and a vacuum leak check under negative pressure. In addition, specialists and highly skilled service providers normally perform mounting installation, repairs, and maintenance, which lower the occurrence of operational errors.

Mildly flammable A2L refrigerants feature an especially high lower flammable limit (LFL) and minimum ignition energy (MIE) compared to other flammable refrigerants. The high LFL means that a large amount of refrigerant is needed to generate a flammable space. Even ignition sources that can ignite a highly flammable propane gas cannot ignite an A2L refrigerant with a large MIE.

When calculating the probability of fire, it is

Table 8.2.1 Features of VRF systems and A2L refrigerants

Features of VRF system compared with single split	Risk
➤ Large amount of refrigerant charge that can all leak into just one room	up
➤ Numerous joints connecting refrigerant circuit or parts of valves, vessels and sensors	
➤ Strict check of refrigerant sealing and leaks	down
➤ Highly skilled personnel for installation, repair and maintenance	
➤ A variety of system configuration, mode free type, water cooled or ice storage type, etc.	Risk should be specified
➤ Wide range capacity of outdoor and indoor units	
Features of A2L refrigerants compared with A2, A3	Risk
➤ Lower size of flammable cloud because of larger LFL	down
➤ Type of ignition source is limited because of larger MIE	

necessary to determine how a flammable space would occur in the event of a refrigerant leak and which ignition sources are present that can ignite the refrigerant.

8.3 Identification of Risks

The second risk assessment investigated the likelihood of refrigerant accumulation depending on the indoor unit configuration and installation site, ignition sources depending on the business installation type, and ventilation conditions. Installation cases thought to have high risks were selected. Among the indoor units, the selected cases included instances of floor-standing units (e.g., restaurants having small rooms prone to refrigerant accumulation and open flames) and ceiling cassette air conditioners (e.g., *karaoke* shops that eliminate gaps under doors to prevent sound leakage, which severely limits natural ventilation). The ceiling spaces were also usually assumed to have limited ventilation capabilities. Risks were extracted for outdoor units in areas prone to refrigerant accumulation and for units installed on each floor, semi-underground, or in machinery rooms.

8.4 Preparations for Risk Assessment

8.4.1 Setting allowable levels

The probability of fire from an allowable risk typically differs depending on the degree of severity. However, because the assessment of the degree of danger was incomplete, we set the allowable levels under the assumption that all fire accidents are serious and fatal. There are approximately 10 million indoor units in use in the VRF system market; thus, if the allowable level for the occurrence of a serious accident is once every 100 years, the allowable level for time of use indoors would be 10^{-9} or less. The number of units was increased four times for time of use outdoors, so we multiplied 10^{-9} by 4. Apart from the time of system operation, the people who normally handle equipment are service providers, not consumers. Thus, it is likely that the degree of danger can be reduced through self-protection even if an accident occurs. Therefore, the allowable probability of an accident was increased by one order of magnitude and assumed to be 10^{-8} or less. This point incorporates the approach of Professor Mukaidono of Meiji University.

8.4.2 Probability of number of leaks occurring for different refrigerant leak velocities

The international standard (ISO 5149 Part 1 Ch A5) for the amount of refrigerant charge for VRF systems has adopted an indoor refrigerant leak velocity of 10 kg/h under the condition of no vibration from compressors. To understand the actual conditions, we recovered parts that cause refrigerant leaks in the market and determined the bore diameters by conducting a leak velocity test with nitrogen. The refrigerant leak velocity was obtained from the bore diameters and refrigerant pressure.

Fig. 8.4.1 shows the results of the 22 indoor unit parts with leaks that were recovered from the market. The bars with arrows above them indicate emergency calls to service providers based on reports from customers of white smoke coming out of the indoor units. Of the four instances, the leak velocity of the liquid was relatively high for three of them (1–10 kg/h). The leak velocity was 0.01 kg or less in only one case. This one case was assumed to have no high-speed refrigerant leak; the customer reported the incident after seeing steam produced during operation after the equipment had run out of gas. As the other cases with white smoke indicated a refrigerant leak velocity of close to 10 kg/h, we can infer that, if a high-speed leak occurs, in many cases the customer would see white smoke and realize that there is an abnormality. Using a similar method, we also measured 26 leak samples from outdoor units. Fig. 8.4.2 shows the results. Compared with the indoor units, the outdoor units had higher leak velocities; in three cases, the leak velocity exceeded 10 kg/h.

Based on the above results of the samples, finding the probability of the number of leaks at different velocities at the scale of parts per million (ppm) is difficult. Therefore, for all cases of leaks handled by service providers over a period of 1 year, we extracted the number of cases of customers reporting white smoke or an abnormal smell as well as the number of cases where service providers diagnosed leaks as originating from a broken pipe or hole in the heat exchanger or pipe. To calculate the number of high-speed leaks, we multiplied this number by 10 for indoor units and by 100 for outdoor

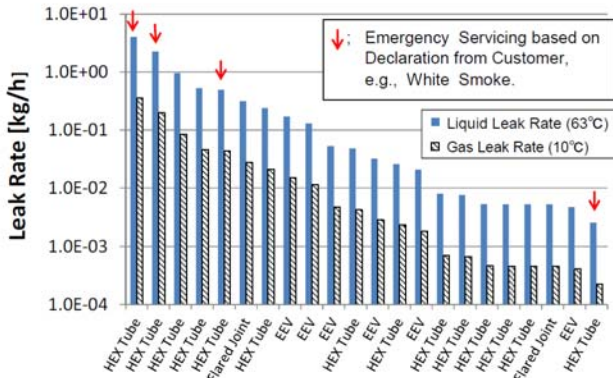


Fig. 8.4.1 Leak rate of indoor field samples

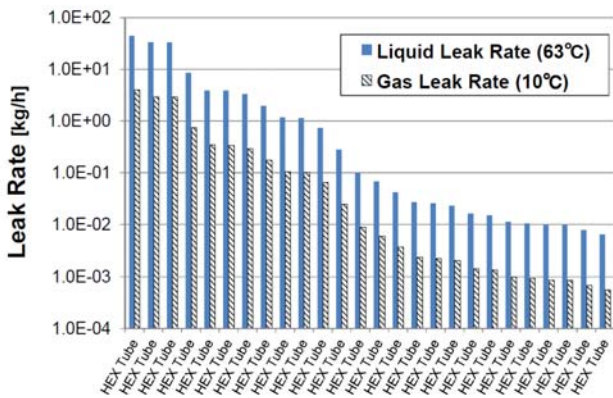


Fig. 8.4.2 Leak rate of outdoor field samples

as incorrect valve operation by the service technician. Table 8.4.2 presents data for the probability of human error from Hashimoto (1988), and Table 8.4.3 indicates data from Suzuki (2001). Operation was assumed to take place under normal, relaxed conditions. The range of data in the literature suggests that the appropriate value for the occurrence of human error during general air conditioner work is 0.001. Because technicians and service providers who work on a VRF have a relatively high level of technical expertise, they are less likely to commit operational errors. Education and training can be expected to lower the occurrence by one order of magnitude. Consequently, the probability of human error during VRF work was established to be 0.0001.

Table 8.4.2 Probability of human error I

Phase	Mode of consciousness	Physiological state	Probability
0	Unconscious, Syncope	Sleeping	1
I	Blurring	Weary, Snoozing	> 1E-1
II	Normal, Relaxed	At rest, Usual work state	1E-2 to 1E-5
III	Normal, Clear	Active state	< 1E-5
IV	Excited	In a hurry, Panic	> 1E-1

Table 8.4.1 Leak probability classified by leak rate

Number of leaks reports indicating rapid leaks, 2010, Manufacturer B

	White Smoke	Smelled Burning	Holes in Pipe	Nrp
Indoor Unit	0	1	0	1
Outdoor Unit	1	3	3	7

Probability of leak classified in leak rate

	Total	Slow Leak	Rapid Leak	Burst Leak
		~1 [kg/h]	~10 [kg/h]	~75 [kg/h]
Indoor Unit	1	0.986	0.014	0
Outdoor Unit	7600	6126	1338	137

[Method]

Leak Probability : Weighted mean value of probability for each JRAIA manufacturer
 Number of rapid leaks = Nrp × 10 (indoor) or 100 (outdoor)
 Number of burst leaks = Number of rapid leak × 0.1 (outdoor) , 0 (indoor)
 Number of slow leaks = Total - (rapid + burst)

Nrp : Number of leaks as reported by customer or service technician indicating rapid leak, white smoke, smell (customer comment), or breakage or hole in pipe (service technician comment).

units. Because there were no burst leaks for the indoor units of VRF systems, we calculated the number of burst leaks to be zero. We judged that the remaining leaks were slow leaks of 1 kg/h or less. For outdoor units, as there were samples of leaks exceeding 10 kg/h, we calculated 1/10 of the high-speed leak cases to be burst leaks. Table 8.4.1 presents the results.

8.4.3 Probability of human error

Refrigerant leaks during the work stages (i.e., installation, repair, and disposal) occur as a result of human error, such

Table 8.4.3 Probability of human error II

Caution label	Physiological	Probability	Duration
-	Panic	> 1E-1	
0	Snoozing		
I	Fatigue due to monotonous work	> 1E-2	
II	During normal work	1E-2 to 1E-4	
III	Active state	< 1E-5	15~20min.

8.4.4 Ignition source assessment

Table 8.4.4 presents ignition sources that were assumed at this time. According to the results of Takizawa (2013) from the Risk Assessment Research Committee and the Imamura research team (2013), mildly flammable refrigerants are not ignited by electrical outlets commonly found indoors, electrical light switches, sparks from the electrical lighters of smokers, or static electricity generated by the human body. Oil lighters and matches can become ignition sources and are believed to make up 5% of all smoking tools. Propane more easily ignites from these ignition sources commonly found indoors. Consequently, propane and mildly flammable refrigerants were determined to have a significant difference in fire probability.

8.4.5 Calculation method for probability of fire

A fire occurs when a refrigerant leak causes the formation of a flammable space and an ignition source that can ignite the A2L refrigerant encounters the flammable space in both space and time. Here, fire is defined as all ignition events if the flammable space of a refrigerant happens to contact an ignition source, regardless of the order of magnitude of the ignition. Table 8.4.5 present this probability calculation.

The fire trigger is the operation of the ignition source (e.g., electric spark). In the case of flammable gas coming into contact with a burning candle and igniting, the trigger is the formation of a flammable space. If the formation of a flammable space happens first in time, the trigger is the operation of the ignition source; if the cause of ignition first exists in a continuous state, the trigger is the flammable gas. The probability of fire occurring from one ignition source is the sum of these two triggers. In order to calculate the risk of each life stage, the probability of fire is calculated after the dominant trigger is determined.

8.4.6 Setting of indoor model and analysis details

An investigation was performed based on a simulation under conditions leading to the formation of indoor flammable regions when refrigerant leaks from the indoor unit. A simulation model of a small conference room in an office was assessed under various conditions and the assumption that the VRF is installed under standard conditions.

(1) Small conference room of office

A model was established where an office was assumed to be a standard VRF case. The 56 kW model (20 hp) was selected to represent the outdoor unit capacity based on the survey results for the capacity distribution of a number of units shipped for office rooms. For the indoor unit capacity, a 7.1 kW model (2.8 hp) was selected with a configuration of eight indoor units connected to each outdoor unit. Here, the air conditioning load was established to be a floor area of 170 W/m². This is shown in Fig. 8.4.3. The risk assessment was performed by targeting a small conference room (6.5 m

Table 8.4.4 Ignition sources

			Y: Ignited	N: not ignited
		Ignition Source	R32	R290 (ref.)
Spark (in flammable cloud)	Electric Parts	Appliance (cause of fire)	Y	Y
		Parts in Unit	N	Y
		Power Outlet, 100V	N	Y
		Light Switch	N	Y
	Smoking Equipment	Match	Y	Y
		Oil Lighter	Y : being evaluated	Y
		Electric Gas Lighter	N	Y
Work Tool	Metal Spark (forklift)	Y	Y	
	Electric Tool	N	Y	
	Recovery Machine	N	Y	
Body	Static Electricity	N	Y	
Open Flame (contact with flammable cloud)	Smoking Equipment	Match	Y	Y
		Oil or Gas Lighter	Y	Y
	Combustion Equipment	Heater	Y	Y
		Water Heater	Y	Y
		Boiler	Y	Y
Work Tool	Cooker	Y	Y	
	Gas Burner	Y	Y	

Table 8.4.5 Calculation of probability of fire

Trigger of Fire	PF	PT	PS
Ignition of Device	$PF_i = N/V_r \times M \times PL$ $= N/V_r \times V_r \times T_i \times PL$	$PT_i = N \times T_i$	$PS = V_r/V_f$
Generation of Flammable Space	$PF_g = N \times T_b \times V_r/V_f \times PL$	$PT_g = N \times T_b$	
Total	$PF = PF_i + PF_g$ $= N \times V_r/V_f \times (T_i + T_b) \times PL$ $= PT \times PS \times PL$	$PT = PT_i + PT_g$ $= N \times (T_i + T_b)$	$PS = V_r/V_f$

PF : Probability of Fire [time/(year × unit)]
 PL : Probability of Leak [time/(year × unit)]
 PT : Probability of Encounter in time between Ignition Source and Flammable Gas [-]
 PS : Probability of Encounter in space between Ignition Source and Flammable Gas [-]
 N : Number of Operations of Ignition Source [time/min]
 V : Volume [m³]
 T : Duration [min/time]
 M : Time Multiplied by Volume of Flammable Region [min × m³/time]

$$M = \int (V_f \times T_f) dt$$

suffix

i : Trigger is Operation of Ignition Source
 g : Trigger is Generation of Flammable Space
 r : Room
 f : Flammable Region
 b : Ignition Source

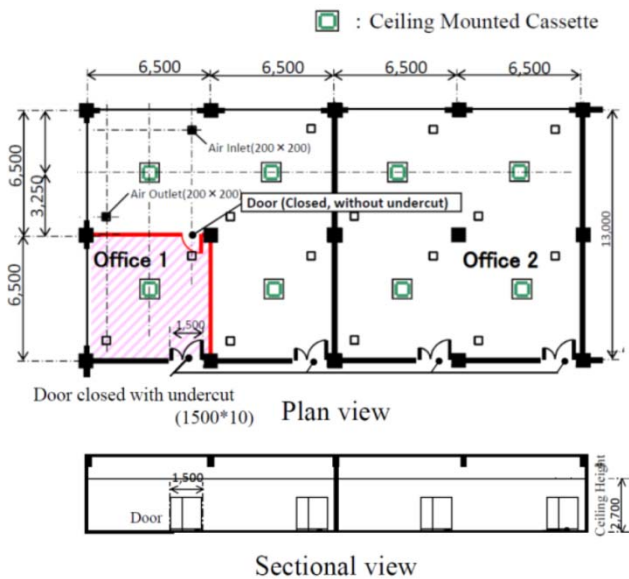


Fig. 8.4.3 Meeting room in office (Ceiling cassette type)

Because the wind velocity was established to be 2.0 m/s, as specified by the Public Buildings Association (2006), the air inlet and air outlet were given dimensions of 0.2 m × 0.2 m. For the door configuration, the width was 1500 mm, and the height of the door undercut was set to 10 mm, as recommended by the Center for Better Living (Ventilation Equipment Manual, 2003).

The difference in refrigerant density was compensated for by setting R410A as the standard for the refrigerant amount. The calculation was performed by multiplying this value by a coefficient of 0.85 for R32 and 0.95 for R1234yf. Although the refrigerant amount (Table 8.4.6) was determined under the assumption of standard installation, the case of the maximum refrigerant amount was also evaluated (Table 8.4.7).

A simulation was performed under the conditions given in Table 8.4.8 in order to confirm the impact of each condition, such as leak rate and presence of a door undercut, and the impact of the effect of ventilation and refrigerant shut-off from leak detection. The same analysis method used by Tokyo University was performed to extract values such as the diffusion coefficient of refrigerant and air. Here, the refrigerant leak velocity was set to 1 kg/h for the case of a small leak and 10 kg/h for the case of a high-speed refrigerant leak. Fig. 8.4.4 expresses the calculation model. Tokyo University and the Japan Refrigeration and Air Conditioning Industry Association (JRAIA) jointly executed the simulation. Table 8.4.8 presents the results for the space-time product of the flammable space.

No. 2 and No. 4 are examples where the effect of natural ventilation from the door gap was evaluated. The former was with a refrigerant leak velocity of $E = 10$ kg/h, while the latter had $E = 1$ kg/h. Figs. 8.4.5 and 8.4.6 show the concentration distribution and flammable region volume when a refrigerant amount of 88.1 kg was completely leaked under the No. 2 conditions. In this case, the flammable region formed into a column shape at the central part of the room with the leak point in the lower part, and the size was stable. The integrated value for the flammable space volume shown in Fig. 8.4.6 became the space-time product; in this case, it was 2.80×100 m³·min. Figs. 8.4.7 and 8.4.8 show the concentration distribution and velocity distribution when the refrigerant amount of 26.3 kg was completely leaked under the No. 4 conditions. Based on the concentration distribution for the refrigerant shown in Fig. 8.4.7, a flammable

Table 8.4.6 Typical refrigerant charge amount

		Charge amount [kg]		
		R410A	R32	R1234yf
Outdoor Unit	56kW	19.0	16.1	18.1
Indoor Unit	7.1kW * 8units	-	-	-
Connecting Pipe	Liquid φ15.9 40m	7.6	6.5	7.2
	Liquid φ9.5 72m	4.3	3.7	4.1
Total		30.9	26.3	29.4

Table 8.4.7 Maximum refrigerant charge amount

		Charge amount [kg]		
		R410A	R32	R1234yf
Outdoor Unit (Shipment)		40.6	-	-
Additional amount (Installation)		63	-	-
Total		103.6	88.1	98.4

× 6.5 m) that received air conditioning from one indoor unit. Ventilation was provided by one air inlet and one air outlet in the ceiling and one gap under the door (undercut part). The ventilation flow from the air inlet and air outlet was 169 m³/h based on the registered number of people according to Article 28 of the Building Standards Act.

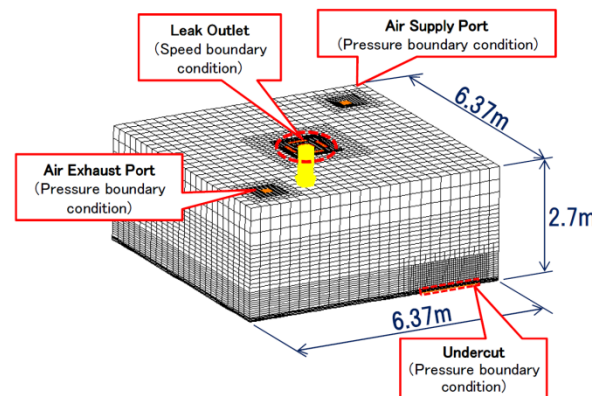


Fig. 8.4.4 CFD model (small office room)

space only formed in close proximity to the leak opening of the indoor unit. However, the velocity distribution clearly showed that the R32 concentration in space was not increased by the air flow from the air inlet and outlet in the ceiling.

Based on these results, we know that natural ventilation can be expected to control the rise in concentration. However, we also know that an air inflow inlet is necessary along with a gap that discharges leaked refrigerant in order to lower the space-time product. With regard to the size of the door undercut, there is also concern regarding reliability, such as the variance in the market. This will be clarified in the future along with leak detection, installation conditions, and specifications for forced

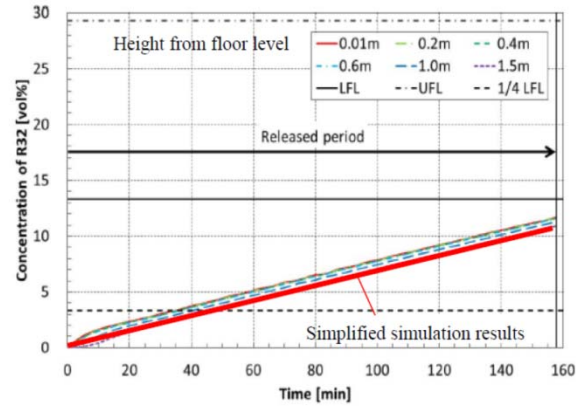


Fig. 8.4.9 Mean concentration in

Table 8.4.8 Conditions and results of CFD simulations for small office room

No.	Refrigerant	Charge Amount M [kg]	Leak Velocity [kg/h]	Ventilation Amount [m ³ /h]	Undercut	Vent	Condition	Space-Time Product of Flammable region	
								M = 26.3 ⁽²⁾	M = 88.1
1	R32	26.3	10	0	N	Open	Most severe condition. Widest flammable space	1.70*10 ⁰	3.66*10 ⁴
2		88.1	10	0	Y	Open	Natural ventilation through undercut	8.30*10 ⁻¹	2.80*10 ⁰
2'		10	0	Y	Closed	Natural ventilation through undercut, Vent closed	1.62*10 ⁰	-	
4		1	0	Y	Open	Natural ventilation through undercut	0.00*10 ⁰	-	
5		10	169	Y	Open	Mechanical ventilation, ACH=1.5 [h]	7.00*10 ⁻¹	-	
6		10	0 to 169 ⁽¹⁾	Y	Open	Vent. starts after leak detection	7.30*10 ⁻¹	-	
8		10 to 1 ⁽¹⁾	0	N	Open	Shut-off valve operates after leak detection	3.10*10 ⁻²	-	
9'		R1234yf	29.4	10	0	Y	Open	Effect of refrigerant in No.2	6.30*10 ⁻¹

*1) Operation after activation of leak detector

*2) Charge amount of R32, M = 29.4 [kg] in case of R1234yf

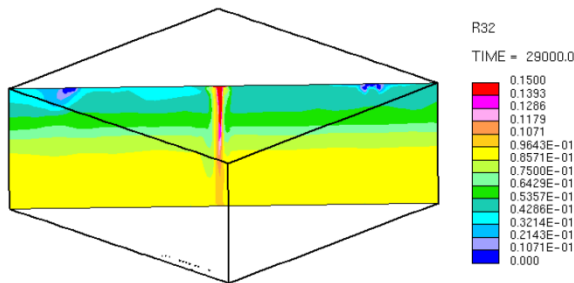


Fig. 8.4.5 Concentration distribution of model No. 2

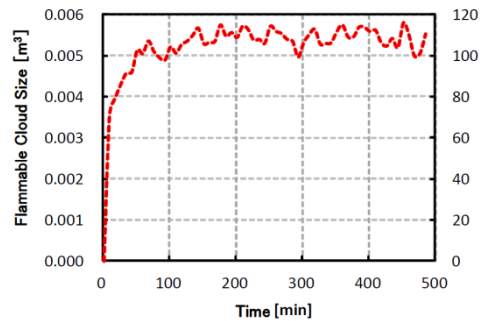


Fig. 8.4.6 Flammable volume of model No. 2

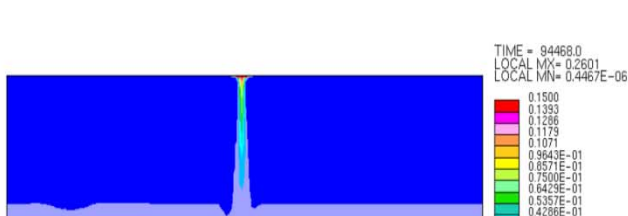


Fig. 8.4.7 Concentration distribution of No. 4

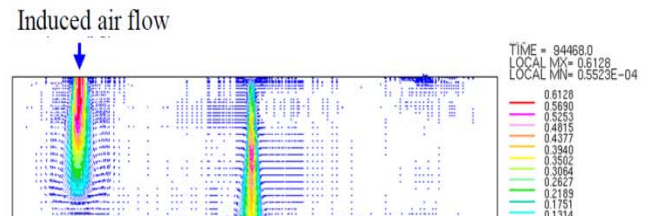


Fig. 8.4.8 Velocity distribution of No. 4

ventilation.

Model No. 6 operates mechanical ventilation equipment, and model No. 8 stops refrigerant leaks through the operation of a shutoff valve in refrigerant piping. Simulations with these models showed that these approaches may reduce the space-time product for flammable space and thus are valid safety measures.

Incidentally, we found that the results of a simple simulation based on the model concentration (2011) were consistent with the refrigerant concentration with a ceiling installation type unit (Fig 8.4.9). Thus, we decided to perform a simple simulation using models where the ventilation flow is regulated by a ceiling installation type unit. The results for cases assumed to have high risk are presented below.

(2) Small rooms of restaurants

The risk is particularly high for floor models used at a low position immediately after a leak because the flammable region forms and stays in the vicinity of the floor. The cases assumed floor models installed in individual rooms of Japanese-style restaurants. Fig. 8.4.10 shows the models. The refrigerant amounts were set to 52.8 kg for R32 and 58.5 kg for R1234yf. Table 8.4.9 presents the analysis conditions and results. For the case with no measures taken, the ventilation openings for the air inlets and outlets were established in the ceiling, and the ventilation flow was set to 112 m³/h. When a gas cooking stove is operated (calorie control amount of 3kW), a ventilation flow of 500 m³/h is necessary to maintain an indoor CO₂ concentration of 1000 ppm; however, the threshold value was set to 1/5 of this value to ensure safety. When leaks occurred in the floor models, the refrigerant remained in the vicinity of the floor. However, when there was mechanical ventilation with air inlets and outlets installed in the ceiling, the flammable space became large without dilution of the refrigerant. For cases where the measures were taken according to the JRAIA guidelines GL-13, it was necessary to construct air outlets in the vicinity of the floor. The ventilation flow was set to 164 m³/h (= 10/0.061) to ensure that the concentration would not exceed RCL 0.061 kg/m³ at a leak velocity of 10 kg/h. The results showed that changing the height (underside) of air outlets by 30–300 mm had a significant impact on the flammable space volume.

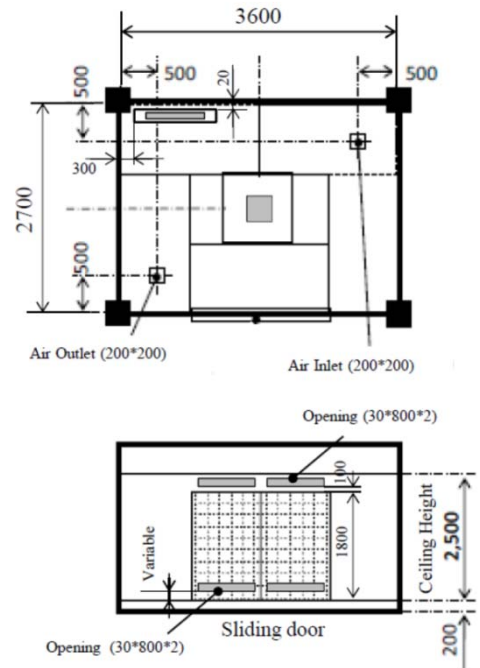


Fig. 8.4.10 Restaurant (Floor standing type)

Table. 8.4.9 Conditions and results of CFD simulations for floor-standing unit in Japanese restaurant

	Analysis Condition						Flammable Region			
	Refrigerant	Charge [kg]	Leak Rate [kg/h]	Mixing in Unit	Ventilation Amount [m ³ /h]	Ventilation Condition		Mean Volume [m ³]	Time [min]	Space-Time Product [m ³ min]
						Inlet	Outlet			
Without Measures	R32	52.8	10	No	112	Ceiling	Ceiling	1.17	910	1070
				Yes			Ceiling	1.28	900	1150
With Measures	R32	52.8	10	Yes	164	Ceiling	300mm above floor level	0.01	320	416
							200mm above floor level	0.10	317	30.7
							30mm above floor level	1.30	317	2.40

(3) Karaoke

Because of their high level of airtightness to ensure sound-proofing, *karaoke* rooms were also assumed to have high risks. We referred to actual surveys of *karaoke* boxes performed by Nomura (2011) and Kitajima (2011) on *karaoke* boxes. In order to prevent sound leakage, mechanical ventilation was employed. Fig. 8.2.11 presents the models. The maximum refrigerant amount was set to 88.1 kg, the volume of the *karaoke* box was set to 9.5 m³, and customers changed once every 3 h. However, once the refrigerant concentration was lowered after the customers changed, we

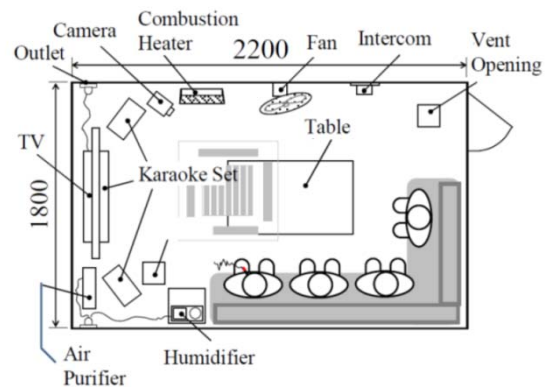


Fig. 8.4.11 Karaoke (Ceiling cassette type)

made the entire room a flammable space for a short time. We assumed candles, combustion-type heaters, gas stoves, and electrical equipment, beginning with the *karaoke* equipment. The concentration was determined according to the simplified simulation.

(4) Ceiling space

The ceiling space was also investigated because it is a small space with high airtightness containing refrigerant piping. As shown in Fig. 8.4.12, the ceiling space for the previously mentioned small conference room of an office was targeted. The ceiling space compartment of the conference room was completely separated from other spaces, and we hypothesized a worst-case scenario at the time of system operation. During equipment use, the entire area would become a flammable region after a refrigerant leak, and this was assumed to last for 10 years. We considered the ignition of an indoor unit and short-circuit accidents as the ignition source. For servicing, we set the flammable region as continuing for 4 h; this was shorter than in the case of system operation because dilution can be expected through opening for inspection. The volume was determined by assuming a ceiling space for offices and small rooms.

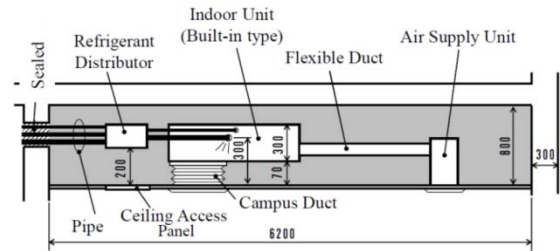


Fig. 8.4.12 Ceiling space (ceiling duct type)

(5) Beauty salon backroom

The case of a fire source from the water-heating equipment in a narrow space where no ventilation is expected was considered (target size: 3150 mm × 1850 mm). According to a survey by the Ministry of Health, Labour and Welfare, when six employees and operation of 10 h are assumed, the use of a gas stove in the backroom for sterilizing tools and taking breaks is estimated to be 470 h annually. Both ceiling installation and floor types were assumed.

(6) BBQ restaurant

The risk was also presumed to be high at BBQ restaurants using strong heat in individual rooms (target room: 3825 mm × 2050 mm). The annual operation time for a gas stove in a targeted individual room was estimated to be 2050 h from a survey on the frequency of customer visits to BBQ restaurants. Both ceiling installation and floor type models were assumed.

(7) Investigation for when ventilation stops

Cases where the ventilation does not operate in a location assumed to require ventilation were investigated. Based on the results of a survey, the failure rate of ventilation equipment was set to 0.025%. This was incorporated into the evaluation because the impact is quite significant, particularly when an individual smokes while working overtime and ventilation has stopped.

(8) Investigation on leak of floor model

As previously stated, because flammable regions are prone to form on the floor immediately after a leak occurs in a floor model, countermeasures are essential for leak detection. Indoor units have a leak detection sensor, and a simulation was performed to consider safety measures that reduce flammable regions by mixing indoor air through the operation of ventilation in the event of leak detection.

8.4.7 Setting of outdoor model

We selected an upper air outlet and three-sided heat exchange type model with a 56 kW capacity (28 kW × 2

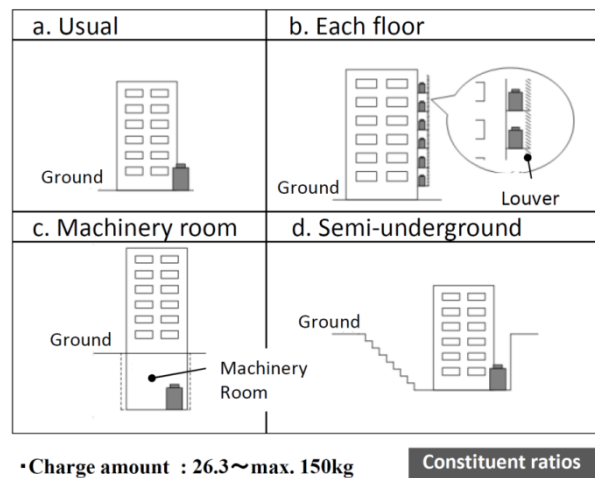


Fig. 8.4.13 Outdoor installation models

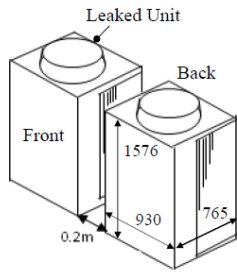


Fig. 8.4.14 Usual (Open space)

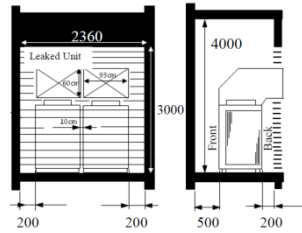


Fig. 8.4.15 Each floor

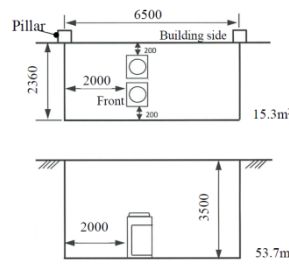


Fig. 8.4.16 Semi-underground

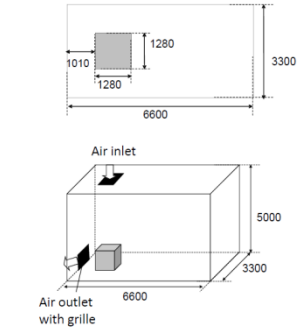


Fig. 8.4.17 Machinery room

units), which is the most common among market installations. Fig. 8.4.13 presents the installation patterns. We assumed four installation patterns: the usual installation pattern with no obstructions in the vicinity, installation on each floor, installation in a machinery room, and semi-underground installation. The refrigerant amount was set to 85% (26.3 kg) of the regulated amount of R32, and the conditions were set to a uniform leak from one heat exchanger in a connected installation.

Figs. 8.4.14–8.4.17 show each installation for the outdoor unit models. Table 8.4.10 presents the analysis results. There was no hindrance under the condition of a 10 kg/h refrigerant leak velocity, and no flammable spaces formed during any installation step. A flammable space formed when the velocity was 75 kg/h with all installation patterns.

Fig. 8.4.18 shows the analysis of the concentration distribution with an underground installation. The leak velocity was

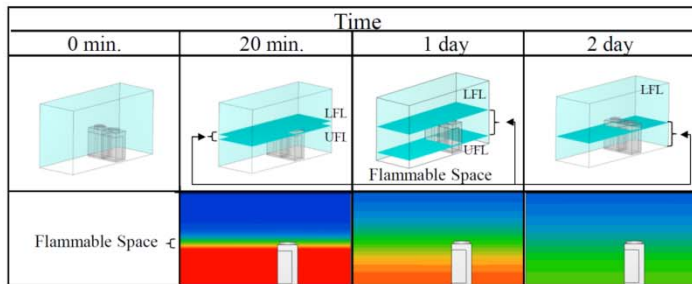


Fig. 8.4.18 Concentration distribution for semi-underground model

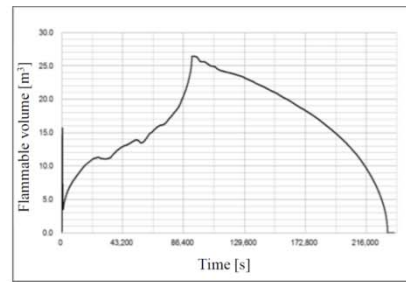


Fig. 8.4.19 Time transition for flammable areas

Table 8.4.10 CFD results of outdoor unit

	Analysis Condition						Results -- Flammable cloud --		
	Installation Case	Capacity	Leak rate	Leak amount	Air velocity	Leak time	Mean volume	Time	Space-time product
		[Hp]	[kg/h]	[kg]	[m/s]	[min]	[m³]	[min]	[m³ min]
Each case (No vent)	Typical	20	10	26.3	0	158.8	0.00E+00	0.0	0.00E+00
	Each floor						1.01E-06	253.0	4.27E-06
	Typical	20	75	26.3	0	21.0	8.31E-02	21.0	1.75E+00
	Each floor						1.88E-01	21.3	4.02E+00
	Semi-underground						1.64E+01	3852.0	6.31E+04
Semi-underground height 0.8m	5.31E+00	289.7	1.54E+03						
Semi-underground (Suction duct)	Vent. Air : 520m³/h	20	75	26.3	0	21.0	1.38E+00	23.3	3.22E+01
	Vent. Air : 260m³/h						4.03E+00	28.3	1.14E+02
	Room volume : 26.8m³						2.12E+00	22.5	4.78E+01
	Vent. Air : 260m³/h								
	Room volume : 54.5m³						1.33E+00	83.4	1.11E+02
	Vent. Air : 130m³/h								
Outdoor fan operating									
Vent. Air : 520m³/h	150	120.0	1.83E+00	122.2	2.24E+02				
Mechanical room (Suction and supply)	Air change rate : 2 times/h	20	75	26.3	0	21	5.81E+00	31.5	1.83E+02
	Air change rate : 4 times/h						5.25E-01	21.4	1.12E+01
	Air change rate : 8 times/h						6.24E-02	21.1	1.32E+00

75 kg/h. Up to 20 min after the leak was completed, the flammable region cloud rose from the floor, and the thickness of the flammable region cloud increased from dispersion after the leak completion. Although the flammable regions for installation patterns excluding underground dissipated after the leak completion within tens of seconds, underground installation caused the refrigerant to be retained, which led to the formation of a flammable region. The flammable region did not dissipate for up to 64 h.

With semi-underground installation, the amount of refrigerant charge was large compared to the volume of the space, so the space-time product tended to become large.

As a safety measure, ventilation was provided by a suction duct or outdoor unit fan when a leak was detected. Fig. 8.4.20 shows the analysis results for the flammable region distribution 20 min after the start of a refrigerant leak in a semi-underground installation where safety measures were in place. A suction duct was placed 0.5 m above floor level at a 0.5 m angle. A simulation was performed for fan operation in the vicinity of the outdoor unit.

With the suction duct, the time needed for the flammable region to dissipate at a rate of 520 m³/h

was reduced to 23 min because the residual refrigerant concentration was forcibly exhausted. Compared to the case when safety measures were not in place, the time for the flammable region to dissipate was dramatically reduced. The time needed for the flammable region to dissipate decreased as the volume of air ventilated by the outdoor unit fan increased.

The machinery room exhibited the same effect. As an example, Fig. 8.4.21 presents the disparity in the rate of circulation for the flammable region distribution 20 min after a refrigerant leak. The rate of circulation should be changed to suit the different air volumes. A circulation rate of 2 times/h required 31 min to dissipate the flammable region, and a circulation rate of 4 times/h reduced the time to 21 min.

8.5 Results of Risk Assessment and Safety Measures

The risk assessment results are presented for each life stage.

8.5.1 During transportation stage (Manufacture of product)

The transportation stage was divided into warehouse storage and transportation, and various risk assessments were performed.

In the investigation, 1000 units were assumed to be stored in a medium-sized warehouse with an area of less than 1000 m² and standard fireproof structure according to the Building Standards Act. The space-time product for the flammable space at the time of a refrigerant leak was set to 8.4×10^{-3} m³·min. Cigarette lighters owned by workers and the spark

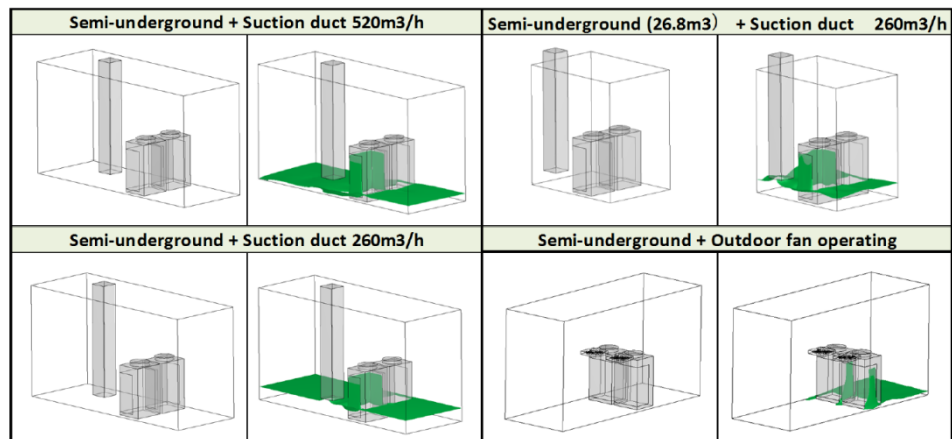


Fig. 8.4.20 CFD results of flammable area for semi-underground model (20 min. after leak start)

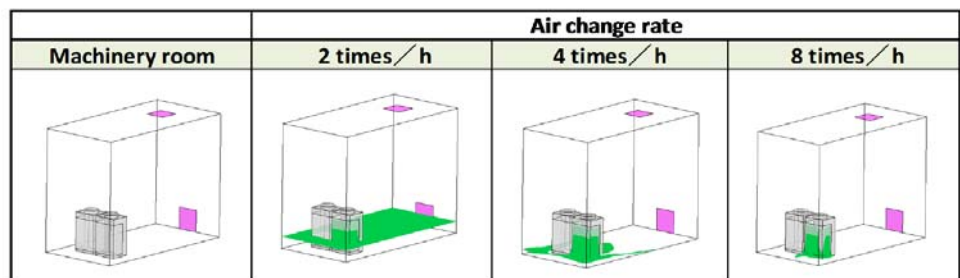


Fig. 8.4.21 CFD results of flammable area for machinery room model (20 min. after leak start)

ignition when the forklift handles freight were assumed to be ignition sources, and the frequency of the refrigerant leaks was set to be the same as during use. The storage frequency of the air conditioners was set to 1/15 based on a service life of 15 years. Fig. 8.5.1 shows the FTA that was created based on the above conditions. This resulted in an ignition probability of 7.8×10^{-17} – 1.2×10^{-16} (ignition/unit for 1 year), which was below the allowance of 10^{-9} .

Ignition sources are not believed to exist inside freight rooms, so there was no ignition combustion even when the refrigerant leaked. Because the leaked refrigerant simply diffused from the freight rooms at the time of loading and unloading, there were no flammable regions. Consequently, we determined that there was no risk during the transportation stage.

8.5.2 During installation

An indoor unit for ceiling installation was installed in an office with a floor space of 40.6 m², and the outdoor unit was assumed to be installed semi-underground. The refrigerant amount was 26.3 kg. The brazing of piping joints was assumed to be the primary ignition source. Usually, connection pipes are brazed when the pipe is not connected to the outdoor unit. Brazing operation was assumed in 10% of the cases where the outdoor unit was connected, and the ignition of refrigerant leaks from piping during brazing operation was assumed to be from gas burners through a valve malfunction or human error.

The fire probability from the use of a gas burner was determined from the mean brazing time and piping connection operation time.

We determined the probability of fire occurring indoors and in ceiling spaces (value of 1 year per 1 power supply unit) from an analysis of electric shock/secondary accidents (Chugoku Electricity Management Engineer Association, fiscal year 2009). The power supply unit was assumed to be approximately equal to one building case. The spatial volume and other parameters were determined by using the survey analysis results for electric shock/secondary accidents based on office building stock data (current to December 2009) of the Japan Real Estate Institute (incorporated foundation). These were then calculated and used for the probabilities of ignition sources related to electrical and heating equipment. We also considered boilers as possible ignition sources for the trial operation of outdoor units.

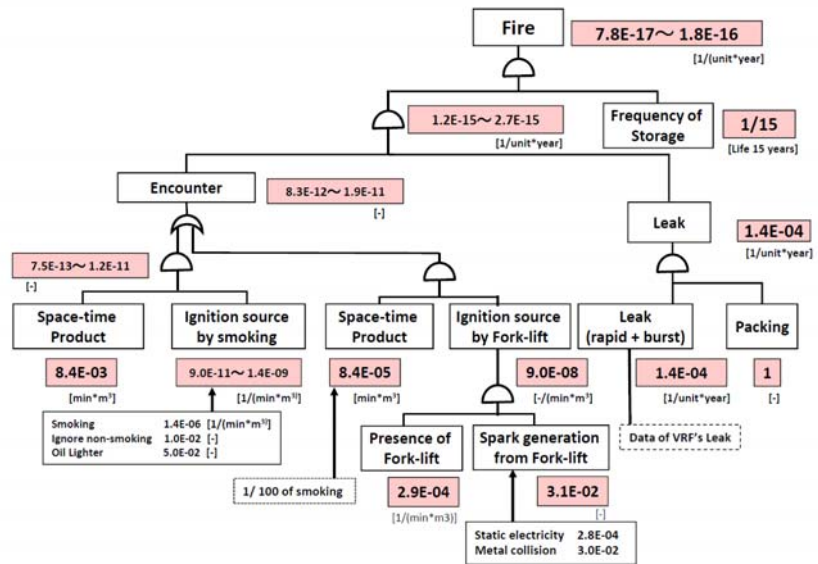


Fig. 8.5.1 FTA of storage in warehouse

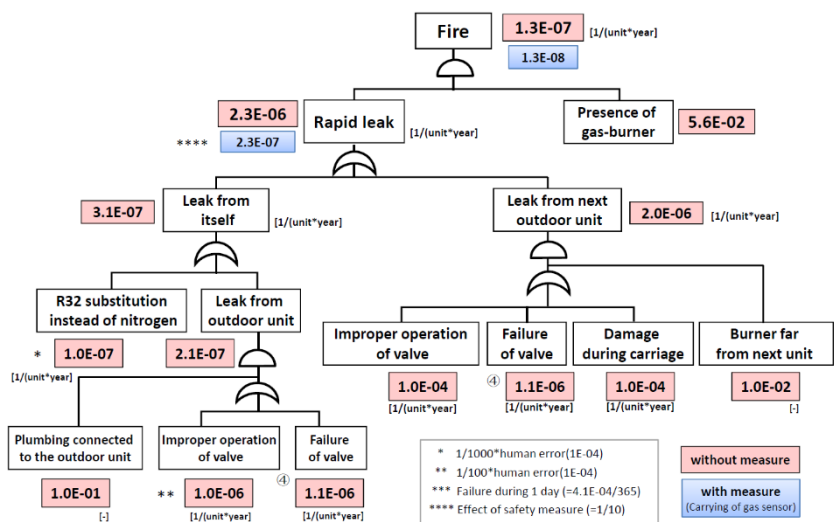


Fig. 8.5.2 FTA of semi-underground installation

For the main causes of refrigerant leaks, we considered 1) valve malfunction, 2) faulty valve operation (forgetting to close) 3) a mistaken charge of R32 refrigerant to replace N2, 4) the reuse of existing pipes with a risk of leaking, 5) piping connected to outdoor unit prior to piping work (10% assumption), and 6) temporary storage near the brazing work of an unconnected outdoor unit (1% assumption).

An FTA was created to reflect the above, and the accident probability was determined for common outdoor unit cases: aboveground installation (94%) and ceiling installation of indoor units (99%). The resulting risk was 1.9×10^{-9} , which was within the allowable range. Overall, the results slightly exceeded the target value; the primary factor was the brazing work time to connect piping. The other values were within the target ranges.

We determined that refrigerant leak detection devices should be carried during brazing operation as a countermeasure. This lowered the overall ignition probability by one order of magnitude (1.1×10^{-8} to 1.9×10^{-9}) and thus below the target value (1.0×10^{-8}).

Table 8.5.1 Fire accident probability of installation

		Indoor unit : Ceiling	
		Outdoor unit : Semi-underground	
Ignition source	Location	Ignition source	Probability of fire accident
Smoking tools	Outdoor unit	Oil lighter, match	1.9E-10~9.3E-10
Other than smoking tools	Connecting pipe	Brazing burner	1.30E-07
	Connecting pipe in test run	Electrical or Heating appliances	2.20E-14
	Indoor unit in test run	Electrical or Heating appliances	2.40E-18
	Outdoor unit in test run	Electrical or Heating appliances	1.60E-08
	Outdoor unit in elevator	Electrical parts	2.8E-22~1.2E-21
Total	Σabobe * Frequency of installation		1.10E-08

8.5.3 During system operation (Indoors)

An overall FTA was constructed in addition to the cases cited as standard cases and severe risks. As presented in a previous report, we calculated the ignition probability in a simplified manner for 28 building uses that differed in terms of the presence of ventilation, type of ignition source, and room size. We then evaluated the results for *karaoke* rooms, restaurant guest rooms, and ceiling spaces. This time, we also investigated the cases of salon backrooms, BBQ restaurants, and ventilation stoppage at night, as presented in section 8.4.6.

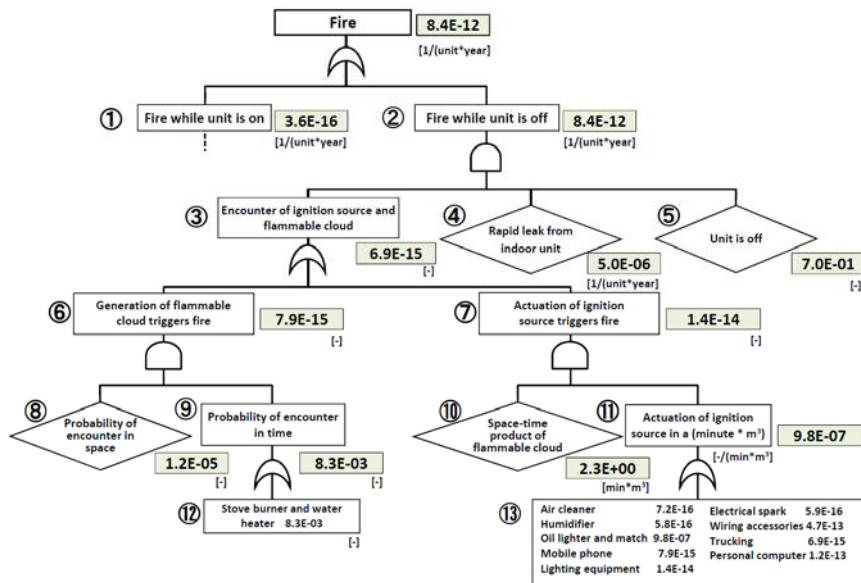


Fig. 8.5.3 FTA of indoor operation (office, continuous ventilation)

Fig. 8.5.3 shows the FTA for ventilation in office 1 and a small conference room, rapid leaks, and cases where no measures were taken. These were investigated as examples of standard cases. The tree was first roughly divided into two phenomena: during operation and during stopped operation. However, because the various branches of the substructure are similar, here we use operation (1) as an example. As discussed in Section 8.4.2, the probability during operation (5) is the product of the uppermost part having a probability of fire (3) and the probability of failure for a rapid refrigerant leak in an indoor unit (4) and becomes 0.3. Because the space-time product for a flammable space and ignition source differ with regard to the probability of the ignition source in the two cases of the flammable space as the trigger (3) and the movement of the ignition source as the trigger (6), the probability is either the result of calculating the probabilities

individually or the product. The probability of occurrence is derived from the product and (8) (10) the probability related to the generation of a flammable region for both (6) (7) and (9) (10) with regard to the probability of an ignition source. The numerical values within the FTA were taken from the results given in Section 8.4.6 on the space-time product for a flammable space and the results given in Section 8.4.4.

As a severe case, the probability of ignition was investigated for when ventilation was stopped at night. Fig. 8.5.4 shows the FTA. Oil light-

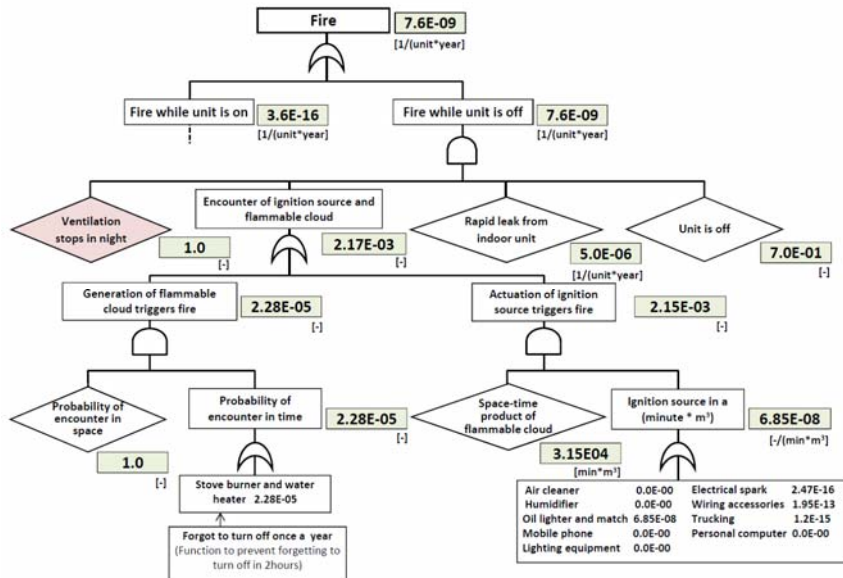


Fig. 8.5.4 FTA of indoor operation (office, ventilation stops at night)

Table 8.5.2 Fire accident probability for each indoor model case

Model case		Room size	Type	Ventilation (without measures/with measures)	Ref. charge kg	Results		
						Constituent ratio	without measure	with measure
Typical case	Office	109.6	Ceiling	Mechanical vent./-	88.1	3.8E-01	3.5E-12	-
Severe risk case	Office, ventilation stops in night	109.6	Ceiling	Vent. stops at night/Mechanical vent.	88.1	3.8E-01	7.6E-09	3.5E-12
	Restaurant	24.3	Floor standing	No vent./Mechanical vent.	52.8	2.0E-02	3.8E-07	2.6E-10
	Karaoke	9.5	Ceiling	No vent./Mechanical vent.	88.1	2.1E-03	1.8E-07	0.0E+00
	Hair salon	14.0	Ceiling	No vent./Mechanical vent.	88.1	1.6E-03	1.3E-09	6.8E-12
	BBQ restaurant	19.6	Ceiling	No vent./Mechanical vent.	88.1	7.8E-04	2.8E-09	1.5E-11
	Ceiling space	30.8	Ceiling concealed	No vent./Periodic inspection	20.0	1.0E+00	3.0E-10	3.0E-11
	Total						0.0E+00	3.0E-11

ers and matches were set as the ignition sources—for example, when employees working overtime use them to smoke at night while the ventilation has stopped. Of the room inhabitants, 25% (8.5 people) were assumed to work overtime, and 23.9% were assumed to be smokers. Then, 1/10 of the room inhabitants (separated for smoking) were assumed to smoke within the office. The smoking frequency was set to 1.6 cigarettes/h. The usage rate of oil lighters and matches was assumed to be 5% of 6.85×10^{-8} , which became the 11) existence probability per hour and volume. Based on the results, the probability of an ignition accident occurring when ventilation is stopped at night was found to be 7.6×10^{-9} . Thus, the risk was unallowable because it was $> 1.0 \times 10^{-9}$.

The probability for the occurrence of ignition was investigated using the above FTA for all standard and severe cases presented in Section 8.4.6. The overall total for the product of the component ratio and probability of ignition occurrence for each case became the probability for the occurrence of an ignition accident in the indoor unit. Table 8.5.2 presents the collected component ratios and probabilities of ignition occurrence for each assumed case.

The probability of ignition did not reach or go below the target value of 1.0×10^{-9} for the worst-case scenario assuming inoperable forced ventilation in severe cases. The target values were satisfied in most cases when forced ventilation was applied based on the Building Standards Law, but further measures needed to be taken for restaurants (floor-standing). When all measures were taken, the probability of ignition became 3.7×10^{-11} , which was below the target level.

8.5.4 Investigation of floor-standing safety measures

The safety measures for floor-standing units that are prone to flammable regions above the floor were investigated.

When the retention of refrigerant leakage was detected near the floor surface, the indoor fan stirred and diluted the refrigerant by drawing the leaked refrigerant upwardly by forced convection. This stopped the formation of a flammable

region. CFD analysis was performed to investigate the extent of dissipation obtained with this method. The leaked refrigerant was assumed to be drawn upward by operation of a fan blowing vertically from the upper part and from the bottom part built in an indoor Low Boy floor-standing unit having a product height of 600 mm.

Fig. 8.5.5 shows the analysis model. Fig. 8.5.6 shows the analytical results when the fan operated at a wind velocity of 2 m/s and air flow of 7 m³/min inside a 4 m × 4 m × 2.5 m room. The upward drawing to the ceiling was clearly visualized. Even when all of the refrigerant (9.18) was leaked (calculated from the room volume (40 m³) × LFL × 0.75), sufficient dilution was realized without reaching a refrigerant concentration of LFL × 0.75, including in the vicinity of the floor. Circulation based on operating a fan with these wind velocity and air flow conditions when a refrigerant leak is detected may be a viable safety measure for floor-standing units. If the amount of refrigerant is more than LFL × 0.75 × room volume, safety measures other than the stirring with indoor fan, such as the mechanical ventilation, shut-off valves or safety alarms are necessary.

Fig. 8.5.7 shows the analytical results for a wind velocity of 1 m/s and air flow of 7 m³/min. We found that the height became low and that the air was drawn upward without reaching the ceiling. Although sufficient dilution occurred under these conditions, when the conditions were further changed, air was drawn upward without reaching an adequate height,

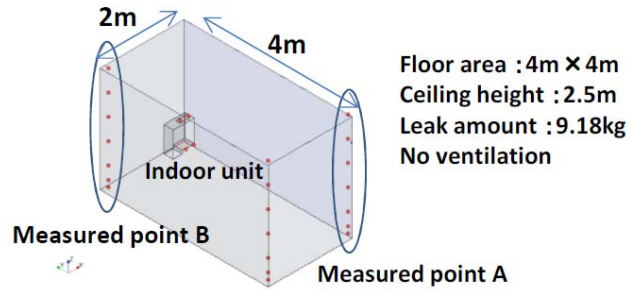
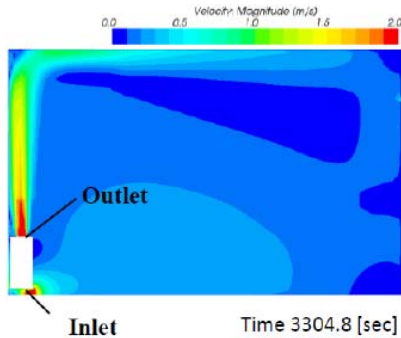


Fig. 8.5.5 CFD model for floor-standing unit

Velocity distribution in vertical section



Concentration distribution at end of leak

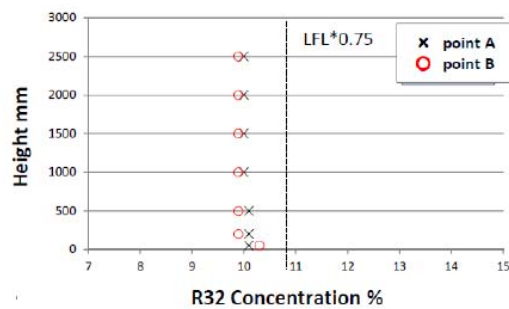
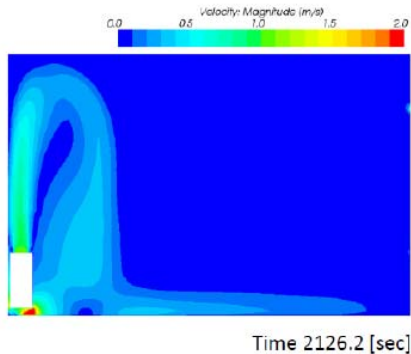


Fig. 8.5.6 Dilution effects with fan's operating (V = 2 m/s, air volume = 7 m³/min, leak rate = 10.0 kg/h)

Velocity distribution in vertical section



Concentration distribution at end of leak

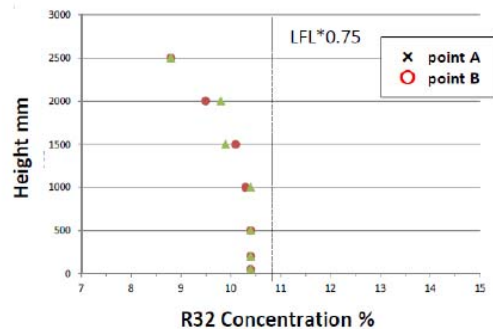


Fig. 8.5.7 Dilution effects with fan operating (V = 1 m/s, air volume = 7 m³/min, leak rate = 15.54 kg/h)

and this safety measure was insufficient.

We are currently investigating the operating conditions for the fan and allowable range of refrigerant charge to develop an effective safety measure.

8.5.5 During system operation (Outdoors)

For outdoor unit equipment, we established four installation patterns: usual, on each floor, in the machinery room, and semi-underground. We selected three ignition sources: smoking (match, lighter), electrical sparks of the outdoor unit, and a boiler.

We calculated the fire probability from the space-time product based on the concentration analysis results and number of times that the ignition source was operated. Those numbers were calculated based on the following. With regard to smoking, a 10% probability was taken for equipment other than for servicing (50% for semi-underground and machinery room). A 1 day/10 years probability was selected for the annual servicing of other equipment. A 10% probability was selected that service personnel smoke in the workplace for 1 day, and a 10% probability was selected that the serviceman would ignore warning labels. Japanese men have a smoking rate of 33.6% and smoke a daily average of 16 cigarettes (JT statistics). A 5% probability was selected for a match or lighter becoming the ignition source, and the time to light one cigarette for smoking was set to 5 s. The smoke and ignition from the electrical sparks of an outdoor unit cause 5.6 fire accidents every year (NITE statistics). For the boiler, the following assumptions were made: a market penetration rate of 0.1%, boiler operation ratio of 21.9% (annual operation time: 8 h × 20 days/month × 12 months), and the refrigerant has a flammable region concentration that always ignites when drawn into the burner part.

An FTA was created based on the above preconditions, and the fire probability for each installation pattern was calculated. The results are given in Table 8.5.3. Fig. 8.5.8 describes the FTA structure for a semi-underground installation. The fire probability was found to be less than the criterion of 4.0×10^{-9} for usual installation and installation on each floor. Consequently, safety measures were unnecessary. However, the refrigerant diffusion velocity for leaks from a semi-underground installation was extremely slow, and the ignition probability was 1.1×10^{-7} , which was above the allowance level.

However, because the analytical results proved that installation may be allowed depending on the semi-underground height and refrigerant amount, we decided to create criteria to determine the risk (advisability standards for safety measures) that are easy to understand. We set the LFL ratio to <1 and the standard semi-underground height to 3.5 m, and we developed criteria based on the following preconditions. Here, LFL ratio is defined as the following equation. The unit of LFL is $[\text{kg}/\text{m}^3]$.

$$LFL \text{ ratio} = \frac{\text{charge amount}}{LFL \times \text{room volume}}$$

Preconditions

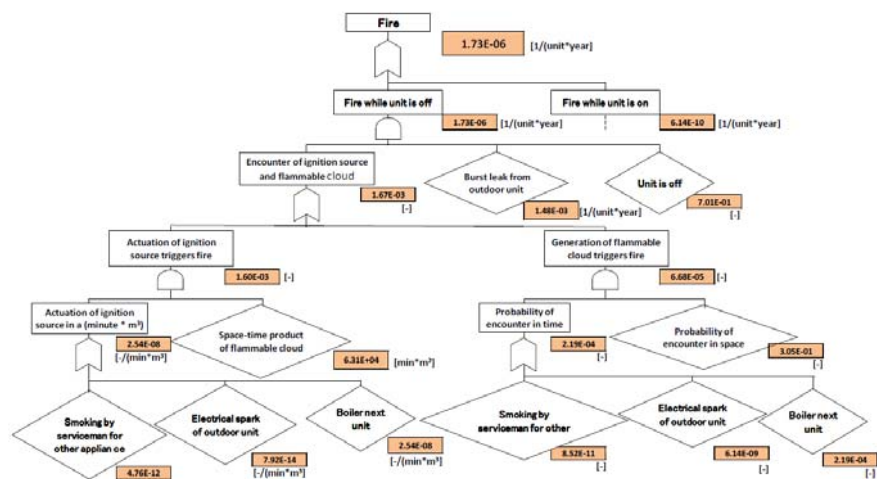


Fig. 8.5.8 FTA of outdoor operation at semi-underground (without measures)

Table 8.5.3 Fire probability of outdoor unit

	Smoking	Electric spark	Boiler
Usual	9.24E-17	5.25E-16	2.09E-11
Each floor	3.00E-14	8.47E-14	3.37E-09
Semi-underground	3.12E-11	7.12E-12	1.73E-07
Machinery room	5.54E-15	3.12E-14	1.24E-09

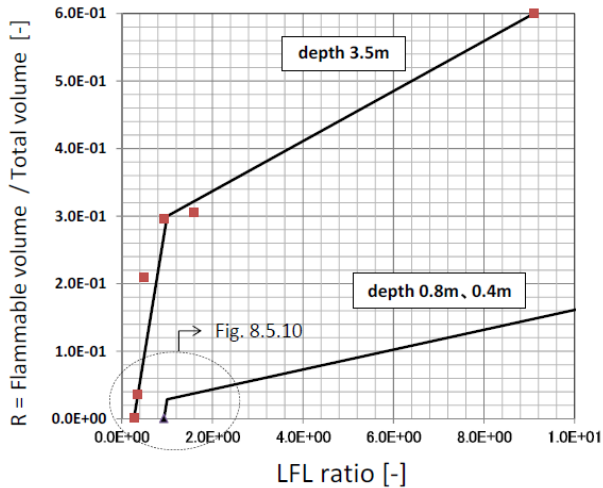


Fig. 8.5.9 Flammable volume for semi-underground

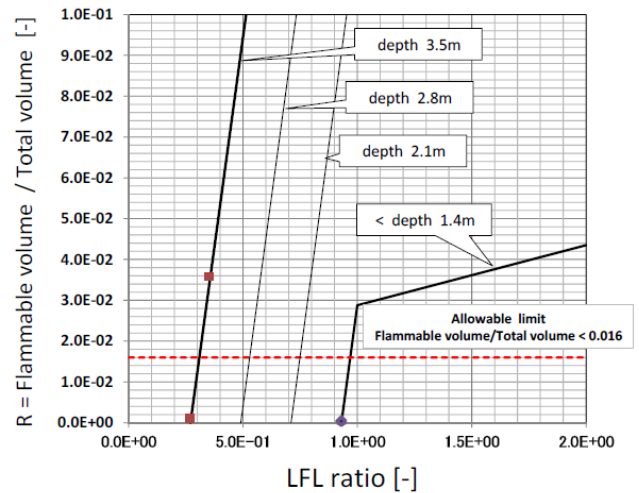


Fig. 8.5.10 Enlarged view of Fig. 8.5.9

- (1) There is generally a proportional relationship between the flammable region and spatial volume [m^3/m^3] when the LFL ratio is < 1 .
- (2) When R (=the flammable region/the volume of semi-underground) ≤ 0.016 , the ignition probability is below 4.0×10^{-9} .
- (3) In the case that the height of semi-underground is 3.5 [m], the range of 1.4 [m] downward from the semi-underground surface does not occur flammable region (Figure 8.5.11). Incidentally, the dominant ignition source was found to be a boiler, and a correction factor was determined so that the height of the burner from the floor surface would be 0.15–0.8 m. Because only the flammable region generation trigger was determined and the on trigger was not included in the ignition source, the probability was multiplied by a safety factor of 1.2.

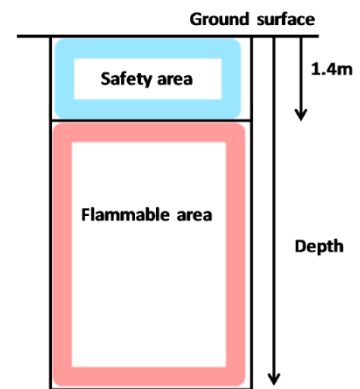


Fig. 8.5.11 Occurrence of flammable area with semi- underground installation

Criterion 1 $R = (0.411 \times \text{LFL ratio} + R_0) \times \text{correction factor} \times \text{safety rating} \leq 0.016$

Here, R_0 is equal to the $(\text{semi-underground height} - 1.4) / (3.5 - 1.4) \times (0.382 - 0.109) - 0.382$.

The slope of the line is 0.411 and the y-intercept is R_0 in Fig.8.5.10.

To simplify its use, this criterion errs on the side of safety.

Criterion 2 $\text{LFL ratio} \leq -0.3 \times \text{semi-underground height} + 1.3$

Table 8.5.4 Effect of refrigerant charge on flammable volume

Semi-underground (without measure, unit is off)								LFL = 0.307[kg/m ³]	
Ref. charge	Floor area	Height	Space volume	M/V	M/V/LFL	Mean flammable volume	V_f / V		
M [kg]	[m ²]	[m]	V [m ³]	[-]	[-]	V_f [m ³]	[-]		
26.3	15.3	3.5	53.7	0.49	1.60	1.64E+01	3.05E-01		
150	15.3	3.5	53.7	2.79	9.10	3.22E+01	6.00E-01		
26.3	26.3	3.5	91.9	0.29	0.93	2.72E+01	2.96E-01		
26.3	49.0	3.5	171.4	0.15	0.50	3.59E+01	2.09E-01		
26.3	70.4	3.5	246.4	0.11	0.35	8.82E+00	3.58E-02		
26.3	91.8	3.5	321.2	0.08	0.27	3.36E-01	1.05E-03		

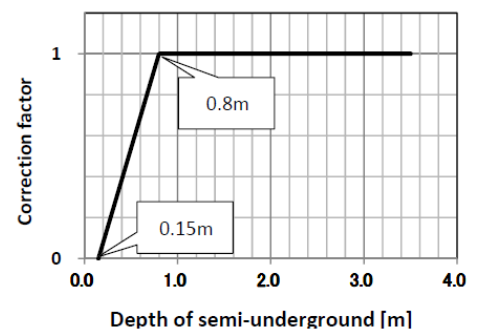


Fig. 8.5.12 Correction factor

8.5.6 Safety Measures for Outdoor Unit

The ignition probabilities for the usual installation and installation on each floor were under the allowable value of 4.0×10^{-9} . Thus, safety measures were unnecessary. Here, we describe semi-underground and machinery room installations.

Even when the conditions at semi-underground does not satisfied these criterions above mentioned, installation is possible with ventilation. When a ventilation duct is installed as shown in Figure 8.5.13, space A is the generated flammable region, and no flammable region is generated in the area above the surface of the intake ventilation duct. Once the relationship, between the air change rate and the value of mean volume of the flammable region divided by a volume of space A (Fig 8.5.13, Va), was analyzed, a correlation was developed for methods (1) and (2) based on the primary characteristics presented in in Fig. 8.5.12. Equation (8.1) is the same as assumption (2) in a previous section. Equation (8.2) was determined from the line of LFL ratio 1.6 in Figure 8.5.12. Equation (8.3) is obtained from the formula (8.1) and (8.2).

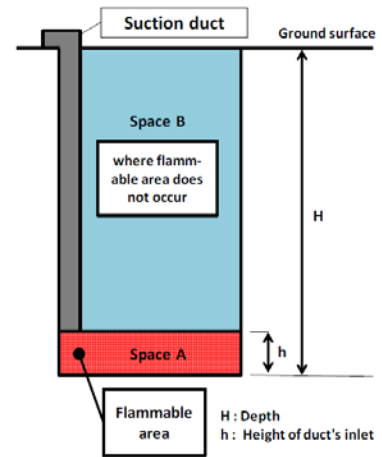


Fig. 8.5.13 Flammable area with ventilation

$$h/H \times \text{mean flammable volume} / V_a \leq 0.016 \quad (8.1)$$

$$\text{Mean flammable volume} / V_a = 1 - \text{air change rate} / 12.5 \quad (8.2)$$

$$\text{Minimum air change rate} \geq 12.5 - 0.4 \times H \quad (8.3)$$

Here, $h = 0.5 \text{ m}$ was assumed.

For the machinery room, standard ventilation equipment was installed. An air inlet was installed in the ceiling, and a forced exhaust air outlet was installed near the floor. The risk assessment was performed with regard to the spatial volume, floor space, and air change rate. The failure rate for ventilation equipment is 0.025%/year. However, this is a risk that cannot be ignored; thus, it was decided to install two sets of ventilation equipment. Table 8.5.5 gives the resulting installation conditions that satisfied the ignition probability of 4.0×10^{-9} .

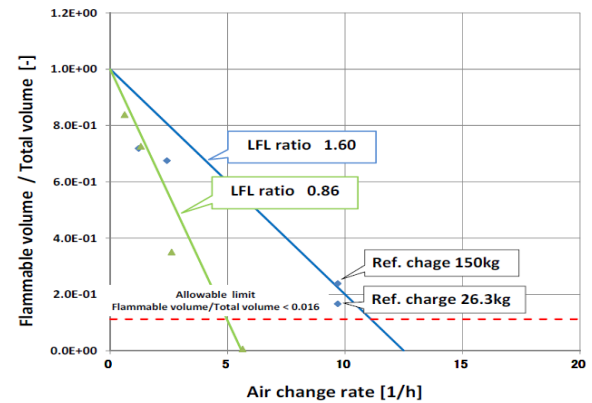


Fig. 8.5.14 Effect of air change rate on flammable volume

8.5.7 During repair

The risks during the repair of ceiling space were investigated for outdoor units, indoor units, and piping that are installed onsite. Here, we mainly describe the results for outdoor semi-underground installations, which were assumed to have high risks because of the time needed for diffusion when all of the refrigeration leaks out at once.

Ignition sources were assumed to be 1) brazing burners, 2) smoking by service personnel, 3) and others (electrical sparks, combustion equipment like boilers, live electrical work). The refrigerant leaks were considered to come from i) piping that comes undone with a burner (insufficient refrigerant time, forgotten steps) and ii) excluding service work (i.e., the cause is not related to service work such as cracks in the piping).

The following was established: a service time of 5 h (refrigerant collection: 1 h + changing parts: 0.5 h + refrigerant charge: 0.5 h + trial operation: 0.5 h), brazing time of 8 min (2 min \times 4: twice for brazing to remove parts and twice to attach parts), and burner work space of 1.3 m (height: 2 m \times width: 1 m \times depth: 0.5 m).

Fig. 8.5.15 shows the FTA (non-measure case). The calculated ignition accident probability was 3.6×10^{-7} , which exceeded the allowable value (1.0×10^{-8}). To reduce the risks from the brazing burner, which was the dominant ignition source, measures were needed with regard to the handling of the burner during work. The following measures were

Table 8.5.5 Safety measures for machinery room

Size of machinery room	Safety measures
Volume $V \geq 95\text{m}^3$ and, Floor area $A \geq 19\text{m}^2$	2 series of apparatus with ACR ≥ 2 [-/h]
$V \geq 55\text{m}^3$ and, $A \geq 11\text{m}^2$	2 series of apparatus with ACR ≥ 8 [-/h]
Other than above	Not allowed

proposed to lower the ignition probability.

Measure (1) Provide educational training for service personnel (e.g., extinguishing the burner immediately when a refrigerant leak is noticed during burner work).

Measure (2) Require service personnel to carry refrigerant leak detection devices and check for refrigerant leaks before and during work.

The ignition probability was calculated when both safety measures given above were used for outdoor use (ventilation by intake duct). The resulting ignition probability was 2.1×10^{-9} , which was less than the allowable value (1.0×10^{-8}).

Even when outdoor semi-underground installations were excluded, the constituent ratio was not large for the installation type (outdoor/ above ground installation, outdoor each floor installation, indoor ceiling installation). However, the risk assessment was performed on installation types with high risks (machinery room installation for outdoor units, indoor floor-standing installation, and ceiling space installation for piping). Table 8.5.6 presents the ignition accident probability for each. The indoor ceiling installation, outdoor/aboveground installation, outdoor installation on each floor, and ceiling space installation for piping had risks within the allowable value (1.0×10^{-8}), but the indoor floor-standing installation and machinery room installation for outdoor units exceeded the allowable value. Similar to outdoor semi-underground installation, when natural ventilation was ensured (ISO5149 Part 3¹²) and the lower edge of the door was set 30 mm from the floor surface for indoor floor-standing installations, and ventilation devices were installed for outdoor use of machinery room installations, the risks were less than the allowable value (1.0×10^{-8}) with the above two measures of providing educational training to service personnel and having them carry refrigerant leak detection devices.

8.5.8 During disposal

We examined the risks during work to dismantle the units and pipes at an installation site. The probability for a refrigerant leak to occur was calculated by considering causes such as forgetting to open valves during refrigerant collection/malfunctions, forgetting to close valves during unit dismantling/malfunctions, incomplete piping connections, piping cracks/substandard conditions, and damage from external pressure. The probability for fire was calculated by assuming ignition sources such as smoking, electrical short-circuits accompanying wiring work, and burners. These were multiplied to determine the probability of fire accidents. For fire ignition scenarios with burners, we considered situations where refrigerant leaking from units for replacement were ignited by burners being used in the piping work of new units. In this

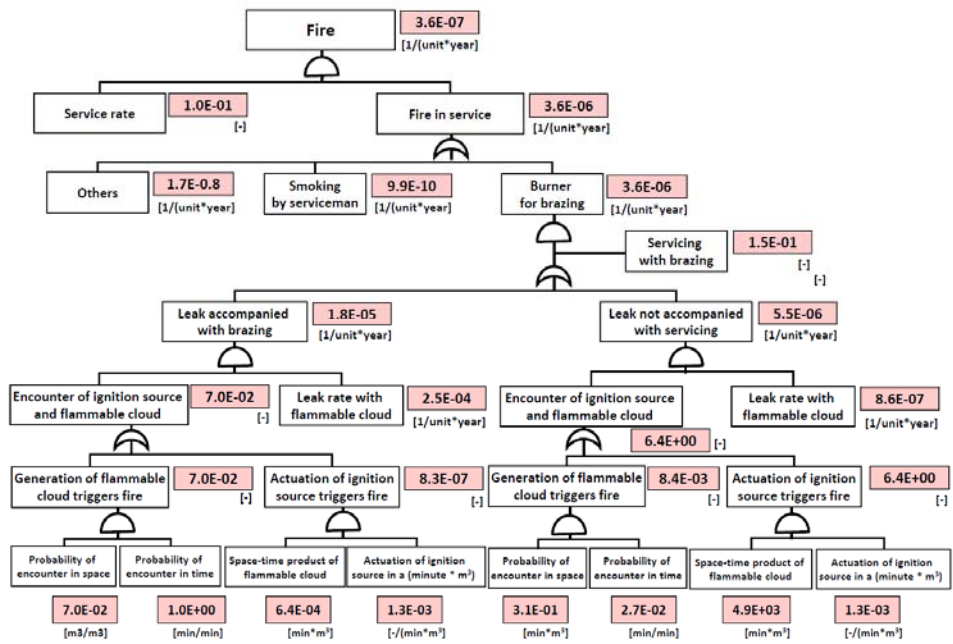


Fig. 8.5.15 FTA of servicing at semi-underground installation (without measures)

Table 8.5.6 Fire accident probability during servicing

Model case	Fire accident probability	
	without measure	with measure
Outdoor , Usual	1.4E-09	1.4E-10
Outdoor , Each floor	3.1E-09	3.4E-10
Outdoor , Semi-underground	3.6E-07	2.1E-09
Outdoor , Machinery room	8.6E-07	5.4E-09
Indoor , Ceiling	8.7E-11	8.8E-12
Indoor , Floor standing	1.2E-08	3.9E-11
Indoor , Ceiling space	3.0E-09	3.0E-10

scenario, the refrigerant leak from removed old units was assumed to happen while the burner was being used continuously on the working pipes of the new unit.

The ignition probabilities for outdoor units installed semi-underground with and without replacement measures were 7.76×10^{-7} and 3.04×10^{-9} , respectively. The ignition probabilities for outdoor units installed in machinery rooms with and without replacement measures were 8.07×10^{-7} and 5.57×10^{-9} , respectively. For both cases, the risk with measures exceeded the allowable value (10^{-8}). Accordingly, the following countermeasures were assumed to lower the ignition probability.

Measure (1) <Training for naked flame/combustion appliance> Provide risk education and warning notices with regard to smoking and using combustion equipment. Train workers to immediately extinguish the fire of burners in the event of a refrigerant leak. This lowers the risk to 1/10.

Measure (2) <Carrying refrigerant leak detection devices> Require workers to carry a refrigerant leak detection device when working in narrow places (e.g., semi-underground, machinery rooms). This lowers the risk to 1.09×10^{-1} . (The risk became 1/100 when a refrigerant leak sensor was carried, and the probability of forgetting to carry a detection device was 1/10.)

Replacement and non-replacement produced fire probabilities of 8.61×10^{-9} and 1.85×10^{-10} , respectively, for underground installations and 9.16×10^{-9} and 4.31×10^{-10} , respectively, for machinery room installations when measures (1) and (2) were both executed. The risks fell within the allowable risk range (under 10^{-8}). Even for the other installation cases, Measure (1) should be performed. For cases of replacement during operation, measure (1) causes the probability of fire to fall within the allowable risk range in all installation cases. The ratio with measures was assumed to be 50% overall, and the ratio of new unit equipment being able to operate during replacement was set to 10%. The ratios of the replacement and simultaneous processes were weighted, and the accident probability was determined for each installation.

A constituent ratio was assumed for each model (ceiling installation/wall mounted: 99%, floor-standing unit: 1%; constituent probability of indoor unit and outdoor installation: 94.39%, each floor: 5%, semi-underground: 0.01%, machinery room: 0.6%, and ceiling space installation: 99%), and the ignition probability was calculated for the constituent ratio of the units. The ignition probability during disposal was determined to be 6.28×10^{-10} without measures and 5.36×10^{-11} with measures.

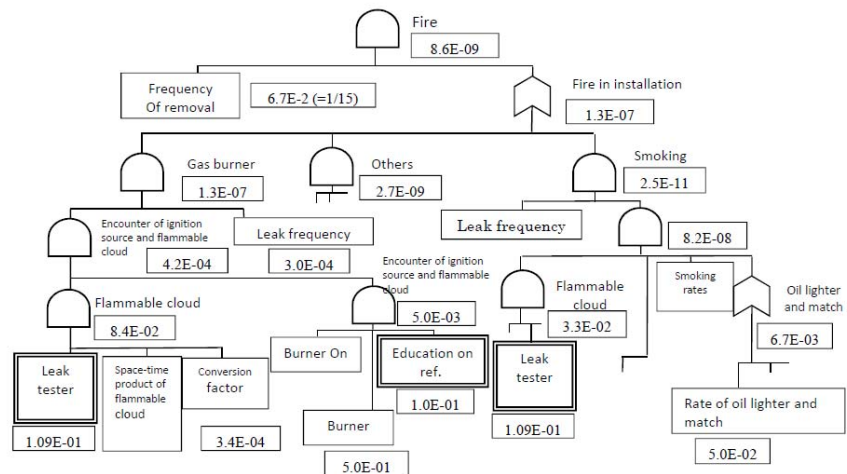


Fig. 8.5.16 FTA of removal for semi-underground (with measures)

Fig. 8.5.16 shows the FTA (case with measures) for the fire probability during removal work underground as an example. The probability for the generation of flammable space was calculated based on flow analysis of the refrigerant leaks in the case of each installation.

8.6 Summary of Risk Assessment

8.6.1 Probability of fire during indoor operation

Table 8.6.1 summarizes the results. The probabilities are given for the case without measures or mechanical ventilation and the case with mechanical ventilation as specified by the Building Standards Act.

For the case with no mechanical ventilation or when ventilation is stopped at night, the probability of a fire accident exceeded the allowable values. When the amount of ventilation was as specified under the Building Standards Act (largely the same as the ventilation stated in ISO5149 Part3), the probability was under the allowable value with the exception of restaurants (floor-standing). When the location of the exhaust vent opening for mechanical ventilation was near the floor, the probability was under the allowable values.

In order to understand how accidents are generated in the market, the bottommost column of the table presents the total of the products from multiplying the constituent ratio P by the fire accident probability A for each installation case. Because not all installation cases are included, the total for the constituent ratio remained at 40%. However, because the installation cases with the largest risks were extracted, the difference with a distribution ratio of 100% should be less than an order of magnitude.

8.6.2 Probability of fire during outdoor use

Table 8.6.2 presents the results. The probability of fire exceeded the allowable level because the refrigerant accumulated in the semi-underground and machinery room installations without mechanical ventilation.

8.6.3 Probability of fire during work

Table 8.6.3 presents the results. The probability of fire exceeded the allowable value during the repair of floor-standing indoor units and each work operation for the semi-underground and machinery room installations. The probability of an accident in the market was under the allowable values.

8.6.4 Probability of fire in market

Table 8.6.4 summarizes the fire probability in the market. The allowable

Table 8.6.1 Probability of fire accident during indoor operation

In each installation cases				[time/(unit*year)]			Not allowable	Allowable	
Installation case				Fire accident probability A					
Site	Type	Constituent ratio P	Allowable probability	Without measures		With measures			
				No vent	Vented				
Indoor	Karaoke	Ceiling	2.1E-03	1.0E-09	1.8E-07	4.4E-11	0.0E+00		
	Restaurant	Floor	2.0E-02		3.8E-07	5.4E-09 ^{*1)}	2.6E-10 ^{*2)}		
	Hair salon	Ceiling	1.6E-03		1.3E-09	1.2E-10	6.8E-12		
	BBQ restaurant	Ceiling	7.8E-04		2.8E-09	4.4E-10	1.5E-11		
	Ceiling space	Ceiling concealed	1.0E-00		3.0E-10	-	3.0E-11		
Ventilation turned off at night									
Installation case				Fire accident probability A					
Site	Type	Constituent ratio P	Allowable probability	Without measures		With measures			
				No vent	Vented				
Indoor	Office	Ceiling	3.8E-01	1.0E-09	7.6E-09 ^{*1)}	3.5E-12	3.5E-12		
Total in market									
Total = Σ(P * A)				4.0E-01	1.0E-09	1.1E-08	1.1E-10	3.7E-11	

^{*1)} Supply and exhaust on the ceiling surface cannot dilute refrigerant gas leaked from floor unit.
^{*2)} Measures are mechanical ventilation with a vent opening near the floor, or, agitation by the indoor fan.
^{*3)} Ventilation turned off 18:00 to 09:00. Ignition sources are smoking by overtime people and water heater driving after people left from office.

Table 8.6.2 Probability of fire accident during outdoor operation

In each installation cases				[time/(unit*year)]			Not allowable	Allowable	
Installation case				Fire accident probability A					
Site	Type	Constituent ratio P	Allowable probability	Without measures		With measures			
				No vent	Vented				
Outdoor	Usual	9.4E-01	4.0E-09	1.9E-11	-	-			
	Each floor	5.0E-02		3.0E-09	-	-			
	Semi-underground	1.0E-04		1.1E-07	-	2.5E-13 ^{*1)}			
	Machinery room	6.0E-03		6.1E-08	-	3.2E-09 ^{*2)}			
Total in market									
Total = Σ(P * A)				1.0E+00	4.0E-09	5.4E-10	-	1.9E-11	

^{*1)} Mechanical ventilation with suction duct
^{*2)} Mechanical ventilation, 2times/h*2system

Table 8.6.3 Probability of fire accident during each work stage

In each installation cases				[time/(unit*year)]						Not allowable	Allowable	
Installation case				Fire accident probability A								
Site	Type	Constituent ratio P	Allowable probability	Installation		Repairing		Disposal				
				Without meas.	With meas.	Without meas.	With meas.	Without meas.	With meas.			
Indoor	Office	Ceiling	3.8E-01	1.0E-08	1.9E-09	-	8.7E-11	8.8E-12	2.9E-14	2.9E-15		
	Restaurant	Floor	2.0E-02		1.9E-09	-	1.2E-08	3.9E-11	3.4E-12	3.4E-13		
	Karaoke	Ceiling	2.1E-03		-	-	-	-	-	-	-	
Outdoor	Usual	-	9.4E-01	1.0E-08	1.9E-09	-	1.4E-09	1.4E-10	2.4E-10	3.2E-11		
	Each floor	-	5.0E-02		1.9E-09	-	3.1E-09	3.1E-09	1.0E-09	1.4E-10		
	Semi-underground	-	1.0E-04		1.1E-08	1.9E-09	3.6E-07	2.1E-09	3.3E-08	4.8E-10		
	Machinery room	-	6.0E-03		1.1E-08	2.1E-09	8.6E-07	5.4E-09	2.2E-08	3.3E-10		
Total in market												
				Without meas.		With meas.		Without meas.		With meas.		
Indoor total = Σ(P * A)				4.0E-01		1.0E-08		1.0E-09		4.1E-12		
Outdoor total = Σ(P * A)				1.0E+00		1.0E-08		9.0E-09		3.7E-10		

level was only exceeded during indoor use with no mechanical ventilation. As stated above, the probability of fire was increased when ventilation was stopped at night. The risk was below the allowable value during outdoor use and work operation.

When the ventilation conformed to the Building Standards Act and safety measures were enacted, the probability for fire was below the allowable limits for all cases. Based on these results, ventilation and safety measures should be required. Table 8.6.5 presents the safety measures that were derived from the risk assessment results.

8.7 Summary of Important Safety Matters

8.7.1 Regulations according to High Pressure Gas Safety Law

Table 8.7.1 summarizes the regulations according to Japan’s High Pressure Gas Safety Law. Mildly flammable refrigerants such as R32, R1234yf, R1234ze(E) are separated from as other inert fluorocarbons in the Refrigeration Safety Regulations and are subject to even stricter limitations than inert fluorocarbons such as 410A. VRF belongs to a legal refrigeration range of 3–20 tons and falls into the “not subject to” or “other production” categories when R410A is used. The only requirements are for sufficient pressure and an airtightness test at the time of local installation. With mildly flammable refrigerants such as R32, using more than 5 tons changes it to “second class production.” When there are construction activities or changes, the client is obliged to notify the governor of the prefecture 20 days in advance. For commercial-use air conditioners, regulations for the advance notice of VRF have become a large hindrance to the spread of mildly flammable refrigerants. Therefore, it is necessary to clarify important safety points as an alternative to advance notification.

8.7.2 Safety countermeasures as function of indoor unit

For the indoor safety of VRF, when the rate of refrigerant charge (= refrigerant amount/volume of the room) is greater than values in the international safety standard ISO5149 Part1, devices for leak detection, ventilation, warning alarms, and refrigerant shut-off need to be installed. These safety measures are implemented at the time of installation, but uncertainty remains over their proper implementation. To ensure that these safety measures are properly performed, they are

Table 8.6.4 Estimated probability of fire accidents in market

		[time/(unit•year)]		Not allowable	Allowable	
Life stage	Covered Constituent ratio P	Allowable probability	Total = Σ(P * A)			
			Without meas.		With meas. (2)	
			No vent.	Vented (1)		
Operation	Indoor	4.0E-01	1.0E-09	1.1E-08 *3)	1.1E-10	3.7E-11
	Outdoor	1.0E-00	4.0E-09	5.4E-10	—	1.9E-11
Working	Indoor	4.0E-01	1.0E-08	1.0E-09	—	4.1E-12
	Outdoor	1.0E-00	1.0E-08	9.0E-09	—	3.7E-10

*1) Flammable space –time product with ventilation rates by building code is adopted. Failure rate is 0.025%.
 *2) Continuous ventilation is assumed in case with safety measures.
 *3) Ventilation is turned off 18:00 to 09:00.

Table 8.6.5 Safety measures derived from risk assessment

Installation case		Using	Repairing
Floor	Restaurant	Mechanical Ventilation	Carrying leak detector + Education
Ceiling	Karaoke	Mechanical Ventilation	—

Installation case	Installation	Using	Repairing	Disposal (Removal)
Semi underground	Carrying leak detector	Mechanical Ventilation	Ventilation + Carrying leak detector + Education	Carrying leak detector + Education
Machinery room		Existing Mechanical Ventilation		

Table 8.7.1 Japanese regulations of High pressure Act

Refrigerants		Classification by legal refrigeration ton			
		3 ton	5 ton	20 ton	50 ton
Inert Fluorocarbon	R410A R134a	Exempt	Others	II	I
Other than inert Fluoro-carbon	R32 R1234yf R1234ze(E)	Exempt	Others (Pressure & Seal tests)	II (Notification)	I (Permit)
Others	R290 + He + CO ₂	Exempt	II	I	

Capacity range of VRF

prepared as a function of the indoor unit. Specifically, the detection, ventilation, and refrigerant shut-off devices are interlocked with the main body of the indoor unit, and the detection and refrigerant shut-off devices are integrated in the structure of the main body. Important Safety Matters A–E are given below.

- Important Matter A: The required refrigerant concentration (refrigerant charge in kilograms/volume of room) should be less than LFL/4.
- Important Matter B: Detection equipment is established indoors, and mechanical ventilation equipment is provided.
- Important Matter C: Detection equipment is established indoors, and a means to shut off when a refrigerant leak detected is provided.
- Important Matter D: Detection equipment is established indoors, and a means to generate a warning when a refrigerant leak is detected is provided.
- Important Matter E: The refrigerant charge for a single refrigerant system is less than X kg (X is to be determined).

In ISO5149, for mildly flammable refrigerants, the maximum amount is $195 \text{ m}^3 \times \text{LFL kg/m}^3$. For example, the upper limit for R32 is 60 kg, but research is ongoing to confirm that this value ensures safety within a room. With regard to warnings, they may need to be combined with other important matters depending on the refrigerant amount.

Floor-standing units were determined to require leak detection devices and an indoor fan to mix the refrigerant when a leak is detected.

8.7.3 Ideal regulations for safety and commercialization

Fig. 8.7.1 compares the fire probabilities of a VRF and room air conditioners using R32 and room air conditioners using R290 (propane). It also shows the allowable fire probability that can be obtained (i.e., once in 100 years). For R290 mini-split air conditioners, we used the fire probability obtained from a risk assessment that JRAIA (Yao et al.) performed in 2000. The refrigerant amount was 500 g, the room volume was 16.8 m^3 (floor area: $7 \text{ m}^2 \times$ ceiling height: 2.4 m), and the leak probability was 2.0×10^{-4} [frequency/units · years]. The number of ignition source for R290 is 2.9 times of operation times of smoking tools with consideration of other ignition sources. The result of room air conditioners using R32 is quoted from section 6. For R32 VRF, we showed that stopping ventilation at night in an office had the most dominant effect on the fire probability.

The fire probability of room air conditioners using R32 was lower than the allowable fire probability. In order to meet the allowable value, the mini-split air conditioner using R290 required safety measures that lowered the risk by a power of -6, while the VRF using R32 required safety measures lowering the risk by a power of -1.

How to ensure safety for the VRF using R32 is not necessarily limited to regulations, also within the option means also including such public regulations and industry voluntary standards.

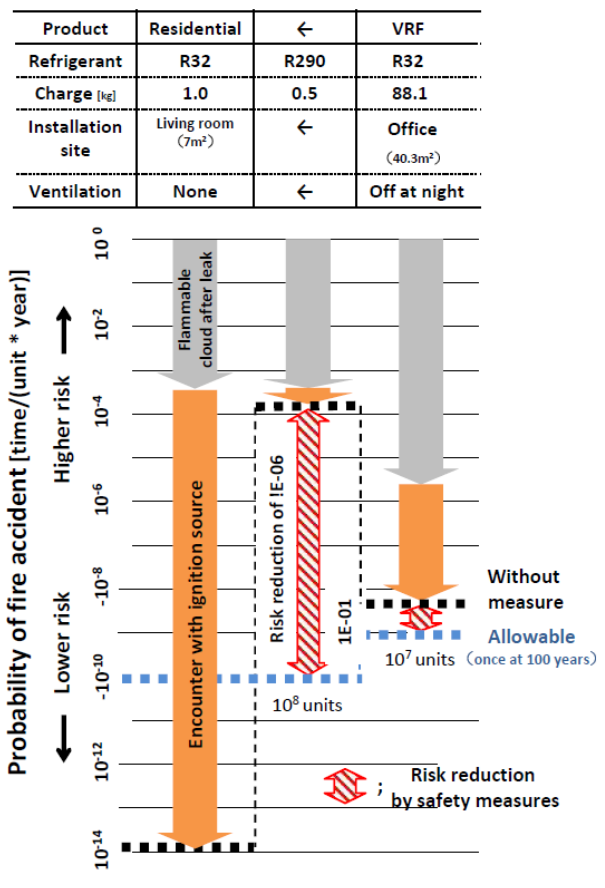


Fig. 8.7.1 Fire accident probability of R290 (RAC) and R32 (VRF)

By providing safety measures and protective devices, the risk was lowered to between 10^{-1} and 10^{-3} (METI Risk Assessment Book P19). Depending on the development of safety measures for functions of the indoor unit that have not yet been clarified, it should be reasonable to expect results that lower the risk by more than order of magnitude.

Future technological developments may realize the incorporation of safety measures as functions of the air conditioner, but this will require advances by the manufacturers.

8.8 Summary and Future Tasks

We performed a risk assessment on a VRF using the mildly flammable refrigerant R32, which has a low impact on global warming, and proposed safety measures to lower the fire probability to less than one time in 100 years for indoor/outdoor use, installation, repair, and disposal in even the most severe cases. Furthermore, we estimated the overall probability of a fire accident during use in the market and clarified that the fire probability can be lowered to less than one time in 100 years through the use of safety measures as functions of the air conditioner.

In the future, we will compile these safety measures as a technological standard. We believe that the industry should establish safety measures which are part of the air conditioner in place of laws and regulations, such as advance notice before installation.

References

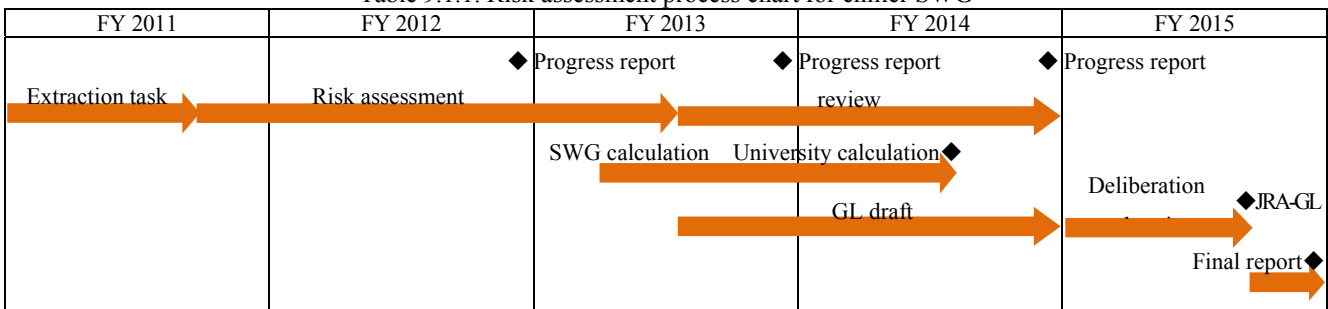
- Public Buildings Association, 2006, Design Criteria for Building Facility Compiled by MLIT Imamura, JSRAE, Progress Report, 44, 2013
- Kitajima, 2011 Actual Survey on the Air Environment at Various Numbers of People in *Karaoke* Rooms, Shibaura Institute of Technology,
- Building Standards Act, Article 28
- Building Standards Act, Order for Enforcement, Article 20, 2
- 2011 Simplified Simulation Model, 2011, Progress Report by VRF SWG
- Suzuki et al., Quality Control, JUSE Press, No. 9, 2001/9
- Takizawa, JSRAE, Progress Report, P54, 2013
- Guideline of design construction for ensuring safety against refrigerant leakage from multi-split system air conditioners, JRA GL-13
- Nomura, 2011, Actual Survey of the Air Environment of 20 *Karaoke* Box Stores in Tokyo, Shibaura Institute of Technology
- Hashimoto, 1988, Japan Ergonomics, Japan Industrial Safety & Health Association
- Better Living, Ventilation Equipment Manual, P17, 2003
- Mukaidono, Concept of Safety, Trends in Academic, Sep. 2009, P14
- Yao et al., 2000, Risk Assessment of Room Air Conditioner using R290, International Symposium on Environment and Alternative Refrigerants 2000, Kobe
- http://www.jraia.or.jp/product/com_aircon/pac_gl13.html
- ISO5149: Refrigerating systems and heat pumps – Safety and environmental requirements (2014)
- Part 1) Definitions, classification and selection criteria
- Part 2) Design, construction, testing, marking and documentation
- Part 3) Installation site
- Part 4) Operation, maintenance, repair and recovery

9. Progress in Chiller Risk Assessment

9.1 Introduction

The heat source systems supplying hot or cold water to central air-conditioning systems use R410A or R134a hydrofluorocarbon refrigerants. Both refrigerants have a global warming potential (GWP) exceeding 1000, thus could contribute to climate change. Therefore, it is necessary to ultimately replace them with low-GWP alternatives. R1234yf, R1234ze(E), R32, and mixtures thereof have been evaluated in drop-in, retrofit, and performance tests. All of these low-GWP refrigerants are mildly flammable. Risk assessments (RAs) (Table 9.1.1) for fires and burns in chiller systems using these mildly flammable refrigerants have been undertaken since fiscal 2011. The scope of this study included air-cooled heat pumps installed outdoors and water-cooled chillers installed in machine rooms and using as a central air-conditioning heat source with a cooling capacity ranging from 7.5 to 175,000 kW. Mobile chilling equipment that cannot be permanently installed was excluded. This year, the Chiller Sub-Working Group (Chiller SWG) executed (a) a risk quantification based on the results of a refrigerant leak analysis conducted jointly by The University of Tokyo and the Chiller SWG, reviewing the probability of ignition and the associated risk, (b) RAs based on the requirements for chiller design and the conditions of the facilities that incorporate the measures and the actions, (c) the drafting of JRAIA guidelines (GLs) for the generalizing of technical requirements. The progress made towards this end is summarized in this report.

Table 9.1.1: Risk assessment process chart for chiller SWG



9.2 Prerequisites for Performing Risk Assessments

Chillers using mildly flammable refrigerants have the same structures and potential applications, such as supplying cold or hot water to an air-conditioning system or industrial process, as those of conventional equipment. Therefore, the RAs and safety design^{1), 2)} applied to the assessment of non-flammable refrigerant leakage are regarded as being applicable to this study. In addition, because refrigerant leakage occurs because of a series of failures and human errors, the fault tree analysis (FTA) method is a commonly adopted technique for estimating the probability of occurrence. Furthermore, leakage accidents involving highly pressurized gaseous refrigerants must be reported, and statistical data³⁾ on leakage from equipment of the same structure is available. Consequently, the Chiller SWG performed RAs using actual data.

These mildly flammable gases, compared with well-known flammable gases, have a higher LFL and larger ignition energy. More specifically, they are less flammable, such that a larger amount of gas is required to form a flammable space. Therefore, the volume and the duration of the flammable space were quantitatively evaluated using CFD methods for a range of installed conditions. Meanwhile, data on the refrigerant characteristics, ignition sources, and common structures of

the equipment were taken from those used by the WG for mini-split air conditioners (Split SWG) and that for multi-packaged air-conditioning systems (Multi SWG), because their RAs have already started.

9.2.1 Features and tasks of the chiller

The chiller is a heat source system that uses cold or hot water as the heat transfer medium and which uses refrigerant only in the unit installed in the machine room. This means that the amount of refrigerant per heat calorie is smaller than a multi-packaged air-conditioning unit system, but large-capacity chillers have most of their large amount of refrigerant in the machine room. Next, we focus on shipment and installation. A small- or medium-capacity chiller already filled with refrigerant is shipped after the completion of gastight and vacuum tests. A large-capacity chiller (such as a centrifugal water chilling unit) is normally shipped and installed exactly as dispatched from the factory, because the refrigerant is filled after installation in a machine room. For those units which are disassembled at the time of shipment and reassembled using flanges and joints which do not require brazing or welding, that installation is simpler than that of a multi-packaged air-conditioning unit system which requires brazing. In addition, units that are filled with refrigerant after the completion of the gastight and vacuum tests are installed, inspected, and repaired by trained professional engineers.

9.2.2 Risk assessment procedure

RAs are executed according to the following procedure, following the basic risk assessment flow, as shown in Figure 5.2.1.

- (1) The basic specifications of the chiller of an RA are defined according to the application, cooling capacity, structure, and installation location.
- (2) Risks in every life stage (LS) of the chiller are separated into six stages, from the logistics stage to the disposal stage, and then analyzed.
- (3) The relationship between probable ignition sources and the cases of refrigerant leakage was clarified using the FTA method, and then the probability of the occurrence of burns and accidental fires was calculated by considering the ignition source density, leak probability, and the flammable space volume integrated with respect to the time of the leak. Because each accident or case is an independent event, the combined probability of each case indicates the annual probability of the occurrence of accidents per unit.
- (4) Safety requirements for the chiller and the facility are established to reduce high-risk hazards, and then GLs for their technical requirements are drawn up.

9.2.3 Basic model of chiller for RAs

The chiller specifications shown in Table 9.2.1 were selected for RAs. These are those of standard models with the greatest shipped capacity, with the average dimensions provided by each company.

Table 9.2.1: Basic specifications of chiller for RAs

Cooling type of condenser	Water cooling	Air cooling
Cooling capacity (kW)	Approx.180	Approx. 90
Refrigerant charge (kg)	23.4	11.7 (single refrigeration circuit)
Outer dimensions (m)	1.28 W × 1.28 D × 1.28 H	1.00 W × 3.00 D × 2.30 H
Installation location	Machine room	Outdoors

9.2.4 Definition of life stages

Six life stages (LSs) were considered, including the “overhaul of chiller” term, which was added to the LSs already referenced in the RA^{1), 2)}: “logistics,” “installation,” “usage,” “repair,” and “disposal.” “Installation” and “usage” were evaluated for a water-cooled chiller and an air-cooled heat pump, respectively. Since operators are exposed to risks in every

LS except “logistics” and “disposal,” only four LSs were considered when summarizing the probability of occurrence. The ratio of the number of water-cooled chillers to air-cooled heat pumps was determined to be 3:7 when using domestic shipment data. The type of the target and LS ratio for each LS are shown in Table 9.2.2.

Table 9.2.2: Sales of chillers in each life stage

LS	Target	Ratio		Number of sales	LS ratio
		Air-cooled heat pump	Water-cooled chiller		
Logistics	Supplier	Total		9687	0.0517
Installation	Operator	7	3	9687	0.0517
Usage	Operator	7	3	134,000	0.7145
Repair	Operator	Total		22,637	0.1207
Overhaul	Operator	Total		1838	0.0098
Disposal	Supplier	Total		9687	0.0517

9.2.5 Basic configuration of FTA

For each leakage velocity (burst leak, rapid leak, and slow leak), an ignition probability calculation was performed using the basic FTA (Figure 9.2.1) in which the area of the flammable space formed and the probable existence of an ignition source were multiplied by the LS ratio for each of the six LSs and then summed. The probable ignition sources for each LS were evaluated using the FTA for the probability of the existence of an ignition source at every LS (Figure 9.2.2). The probability of the occurrence of accidental fires and burns was calculated by combining the values of the basic FTA for each leakage velocity.

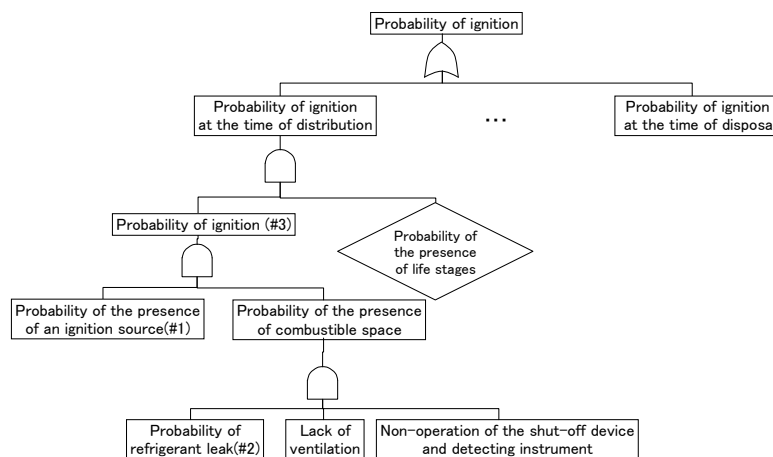


Figure 9.2.1: Basic FTA for each type of leakage

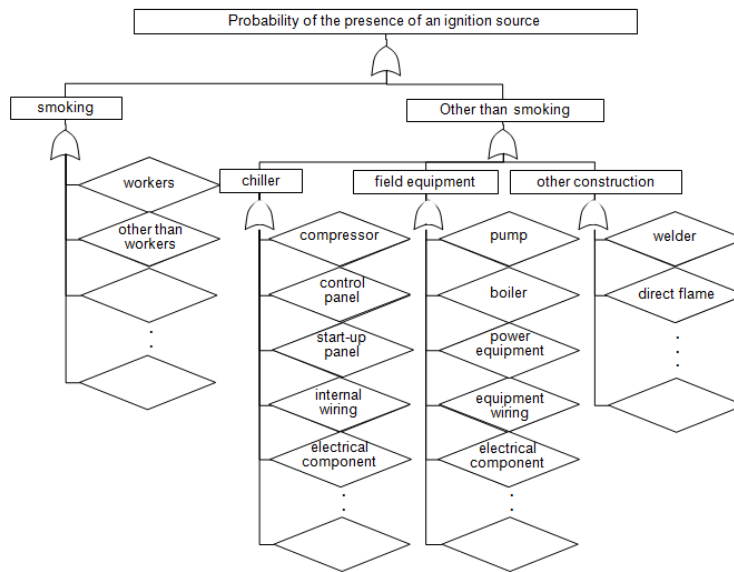


Figure 9.2.2: Basic FTA for evaluating probable ignition sources in each life stage

9.2.6 Risk assessment map and risk assessment list

Each case should assume the severity of harm and suggest the measures and actions to be implemented; hence, the results of such assumptions and suggestions were recorded using the risk assessment list (R-List, Table 9.2.3). The R-List specifies the category of the risk region on a risk assessment map (R-Map, Table 9.2.4) for every case. If the risk level is in region A or B, measures and actions are suggested to shift the risk level to the C region. The acceptable probability and the severity of harm on the R-map were defined as below.

(1) Probability of hazard

Annual sales of water-cooled chillers and air-cooled heat pumps in Japan are around 134,000 units, according to JRAIA shipment statistics. This represents one-hundredth of the sales of multi-packaged air-conditioning unit systems. The probability of the occurrence of harm to a user is described in the risk assessment handbook published by the Ministry of Economy, Trade and Industry⁴(HB). For units in industrial and commercial applications, the acceptable probability of the occurrence of harm categorized as “catastrophic” is 1.0×10^{-6} cases/(unit·year). Given the current stock of chillers, this probability corresponds to a probability of occurrence of once every ten years, which is 7.9×10^{-7} cases/(unit·year). Considering the difficulty in estimating the severity of the harm caused by the ignition of mildly flammable gases, it is vital to control the probability of occurrence at this level.

(2)Severity of harm

The severity of harm is based on the definition of fire in the HB.

Table 9.2.3: Risk assessment list

Timing of severity occurrence	Equipment/Case/Cause		Details of severity condition				
	Life stage/ Service status	Subject	Equipment	Ignition source	Mis-operation (mis-work)	Severity condition	Accident category
Usage/ offline	Facility	Electrical equipment/ component	Short circuit due to defective wiring	Damage to compressor casing	Refrigerant leak due to equipment damage resulting in ignition by an ignition source	Property damage	Damage to equipment
						Injury	Burns

<Before countermeasures>

Risk assessment		Anti-explosion assessment			Risk level
Severity of harm	Probability of occurrence	Ventilation grade	Ventilation level/efficacy	Assessment	
II	0	Grade 2	High/Low	Zone 2	C
I	0	Grade 2	High/Low	Zone 2	C

<After countermeasures>

Risk assessment		Anti-explosion assessment			Risk level
Severity of harm	Probability of occurrence	Ventilation grade	Ventilation level/efficacy	Assessment	
0	0	Grade 2	High/Low	Zone 2	C
0	0	Grade 2	High/Low	Zone 2	C

Table 9.2.4: Risk Assessment Map

Reference data from HB		Chiller market (for risk assessment)		Risk region								
Probability of hazard cases/(unit-yr)		Frequency of hazard cases/(unit-yr)	Probability of hazard cases/(unit-yr)									
5	Frequent Consumer goods: 10^{-3} Industrial products: 10^{-1}	1 out of 10 units once every year	1.0×10^{-1}	13	24	27	29	30	<table border="1"> <tr> <td style="background-color: #cccccc;">A region: 25~30 Intolerable</td> </tr> <tr> <td style="background-color: #cccccc;">B region: 14~24 Acceptable (If the risk is as low as reasonably practicable)</td> </tr> <tr> <td style="background-color: #cccccc;">C region: 1~13 Acceptable</td> </tr> </table>	A region: 25~30 Intolerable	B region: 14~24 Acceptable (If the risk is as low as reasonably practicable)	C region: 1~13 Acceptable
A region: 25~30 Intolerable												
B region: 14~24 Acceptable (If the risk is as low as reasonably practicable)												
C region: 1~13 Acceptable												
4	Probable Consumer goods: 10^{-4} Industrial products: 10^{-2}	1 out of 100 units once every year	1.0×10^{-2}	12	20	23	26	28				
3	Occasional Consumer goods: 10^{-5} Industrial products: 10^{-3}	134 times once every year	1.1×10^{-3}	10	16	19	22	25				
2	Remote Consumer goods: 10^{-6} Industrial products: 10^{-4}	14 times once every year	1.1×10^{-4}	6	9	15	18	21				
1	Improbable Consumer goods: 10^{-7} Industrial products: 10^{-5}	1 to 2 times once every year	7.9×10^{-6}	3	4	8	14	17				
0	Incredible Consumer goods: 10^{-8} Industrial products: 10^{-6}	1 to 2 times once every 10 years	7.9×10^{-7}	1	2	5	7	11				
R-map (ISO/IEC Guide 51) (JIS Z 8051)				0	I	II	III	IV				
				None (No injury)	Negligible (Smoke generation of product Start)	Marginal: (Fire and ignition of product Mild impairment)	Critical: (fire Serious injury)	Catastrophic: (Death, Permanent fault, Fire(Fire of buildings))				
Severity of harm→												

9.3 Flammable space analysis model for refrigerant leak

When refrigerant leaks, the time-dependent volume of the flammable space can be calculated by using a CFD method. This analysis was performed in collaboration between the University of Tokyo and the Chiller SWG, as shown in Section 9.7.

9.3.1 Analysis model

(1) Equipment installed in machine room

A machine room in which a water-cooled chiller is installed should be provided with a specified amount of ventilation, and

combustion equipment should be installed in accordance with the technical standards^{5), 6), 7)} for each model. The required floor area for a machine room for a specific chiller volume was found using the research lists for completed facilities produced by the Journal of Heating and Air-Conditioning Sanitary Engineering (2007–2010) (Figure 9.3.1). The height of the machine room is 5 m and its volume is 109 m³ (21.8 m² × H5 m) which is close to the minimum volume of 75 m³ (15 m² × H5 m). The shape of the machine room floor was rectangular (1:2). The chiller was assumed to be installed on half of the floor, while the auxiliaries were installed on the other half. The required maintenance space is at least 1.2 m in front of the control panel and at least 1.0 m on the other sides (Figure 9.3.2). The air supply and exhaust louver area were determined by referring to the “Mechanical Equipment Construction Edition” of the Kagoshima prefectural building standards. To discharge the refrigerant, which is heavier than air, an air supply port was installed on the ceiling immediately above the body of the equipment and an exhaust port was located on the wall behind the equipment. It was assumed that a refrigerant leakage point is located 0.15 m (including legs) from the floor, which is the lowest part of the equipment. The shape of the leakage point was assumed to be a cylindrical nozzle 0.10 m in length, resembling a pipe. In addition, the machine room was 15 m underground and it was assumed that refrigerant was exhausted through a chimney extended from an exhaust port to the ground.

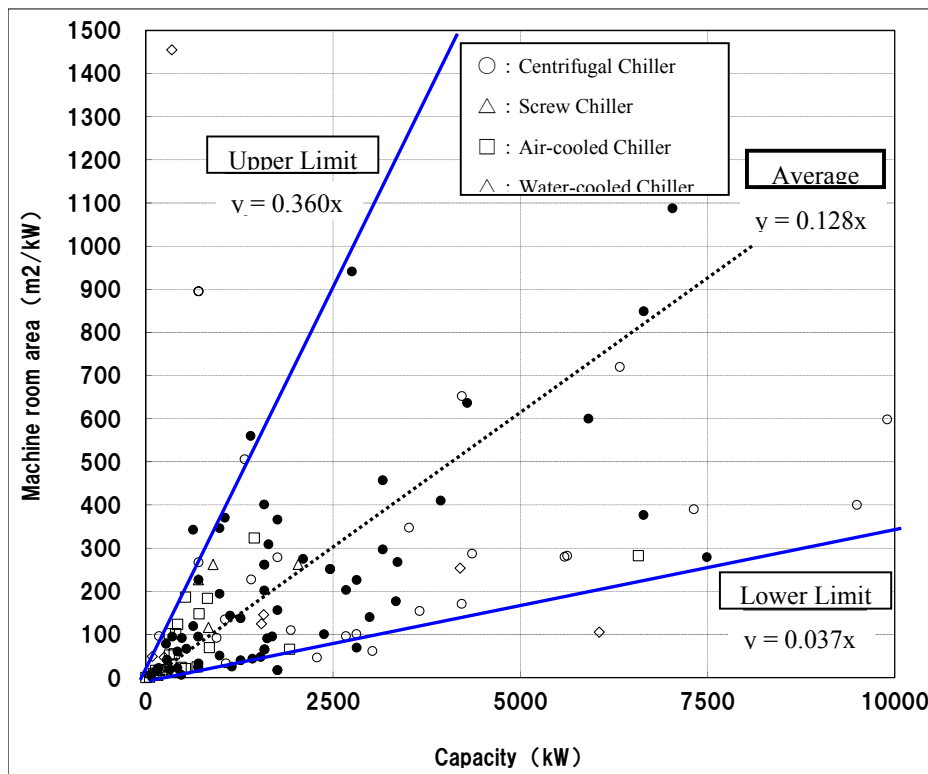


Figure 9.3.1 Relationship between machine room area and chiller capacity

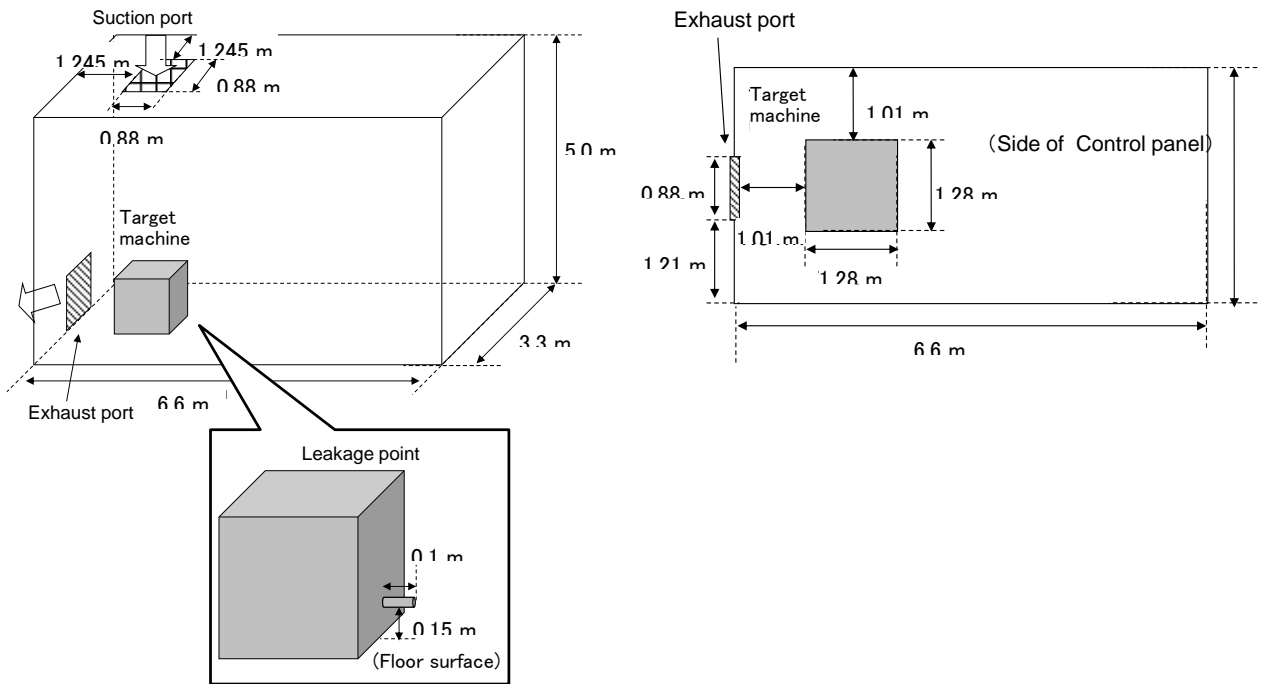


Figure 9.3.2 Outline of machine room

(2) Equipment installed outdoors

In general, an air-cooled heat pump installed outdoors (such as on a roof) without any surrounding walls, thus has no chance of forming a flammable space due to the free-flowing air. However, in a situation where the equipment is surrounded by soundproof walls, a flammable space can be formed. Based on the soundproofing installation procedure described by the manufacturer, an analysis model with four walls, two plain and two with an aperture ratio of 25%, is assumed (Figure 9.3.3). The refrigerant leaks from the air-heat exchanger or from the inside of the decorative panel of the unit.

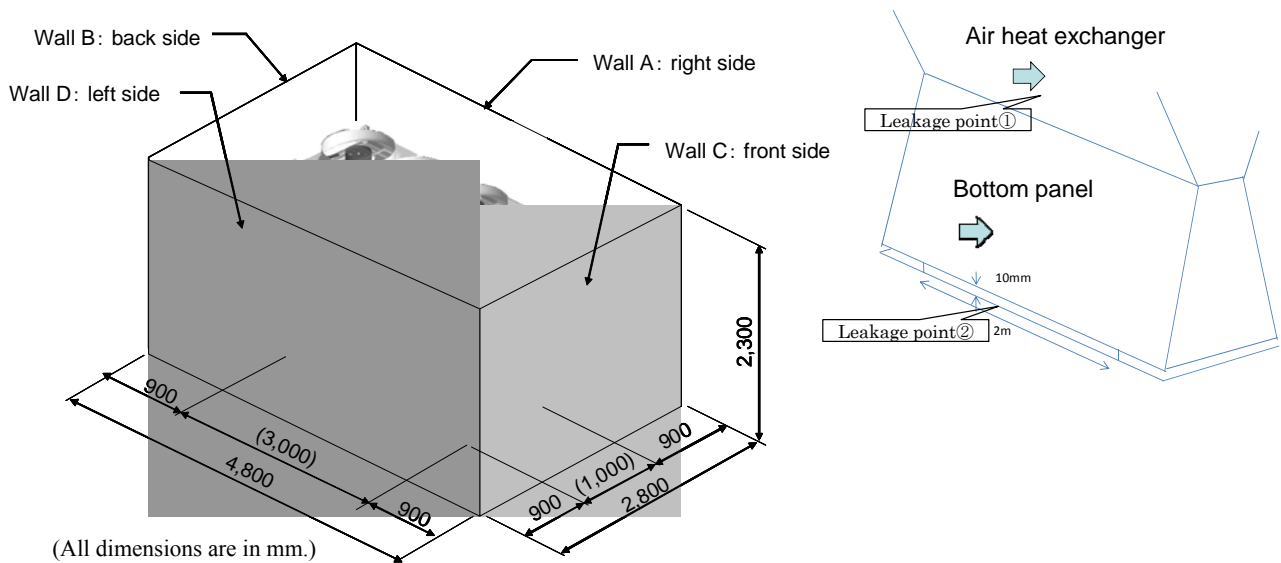


Figure 9.3.3 Air-cooled chiller analysis model

9.3.2 Definition of flammable region and amount of leaked refrigerant

The representative physical properties of the refrigerants are listed in Table 9.3.1. Since R1234ze(E) is inflammable in dry air, a lower flammability limit (LFL) and an upper flammability limit (UFL), equivalent to a humidity level of 90% at 23°C, were applied. The leakage rate was calculated in accordance with JRA GL-13⁸⁾ (Table 9.3.2) with R32 as the baseline. Each of the leaked refrigerants was assumed to have been discharged into the air at 20°C saturation pressure (gauge).

Table 9.3.1 Flammability of refrigerants⁹⁾

		Limit of flammability		Maximum burning velocity cm/s	Diffusion coefficient cm ² /s
		LFL vol%	UFL vol%		
R32		13.5	27.5	6.7	0.135
R1234yf	Dry air	6.7	11.7	1.5	0.075
	Wet air	5.15 ^{※1}	13.6 ^{※1}	5.9 ^{※2}	
R1234ze(E)	Dry air	not flammable	not flammable	not flammable	0.074
	Wet air	5.9 ^{※1}	12.6 ^{※1}	5.2 ^{※2}	

※1 Absolute humidity 0.016kg/kgDA (Equivalent of 23°C 90%RH)

※2 Absolute humidity 0.03kg/kgDA (Equivalent of 35°C 83%RH)

Table 9.3.2 Flow rate of leak

Leak		Slow leak	Rapid leak	Burst leak
Refrigerant	R32	1 kg/h ^{※1} or less	10 kg/h	75 ^{※1} or 200 kg/h
	R1234yf	0.9 kg/h ^{※1} or less	8.9 kg/h	67 ^{※1} or 178 kg/h
	R1234ze(E)	0.7 kg/h ^{※1} or less	7.3 kg/h	54 ^{※1} or 145 kg/h
Location		Pinhole, Welded part, Braze part, Cauterized part	Cracking flare, Flare-welded part, Flare fitting joint, Cauterized part	Slip-out from flare fitting joint, Pipe fitting

※1 Analysis condition

9.3.3 Analysis condition

(1) Equipment installed in machine room

Analysis of the standard chiller model installed in a machine room was performed using a combination of the types of refrigerant, leakage amounts, and air change rates. Referring to ISO5149-Part 3, the air change rates were set to four air changes/h, two air changes/h, and no air changes/h. To calculate the period from the start of a refrigerant leak until it is fully ventilated, an unsteady state analysis was performed (case 1). Next, the period of ventilation shut-down was assumed, such as during a blackout. An unsteady-state analysis was performed to calculate the time-dependent volume of the flammable space from the time the refrigerant leakage fills the machine room until after ventilation (case 2).

(2) Equipment installed outdoors

Cases of leakage from an air-heat exchanger or from inside the decorative panel of the unit were calculated using the assumed leakage points. The time-dependent volume of the flammable space from the start of a refrigerant leak until the flammable space disappears was calculated by applying an unsteady-state analysis.

9.3.4 Analysis results

(1) Equipment installed in a machine room (case 1)

For a rapid leak, a large flammable space is formed and the time-dependent volume becomes large when there is no ventilation. However, for a burst leak, since the diffusion of gas in the space occurs more quickly than in the case of a rapid leak, the large space of the refrigerant concentration under LFL exists in the machine room and the time-dependent

volume becomes small. For ventilation with an air change rate of two air changes/h and four air-changes/h, both flammable spaces are reduced drastically and therefore the time-dependent volumes actually become small (Table 9.3.3). The analysis results for a rapid leak of R1234ze(E) without ventilation are such that the time-dependent volume and surface for the same maximum level of LFL are as shown in Figure 9.3.4. Furthermore, the analysis results for a rapid leak of R1234ze(E) with ventilation at four air-changes/h are such that the time-dependent volume and surface of the same maximum level of LFL are as shown in Figure 9.3.5. These results show that ventilation of the machine room provides an effective means of minimizing the flammable space.

Table 9.3.3 Results of unsteady-state analysis (machine room)

Machine room volume [m ³]	Refrigerant	Leak	Air change rate [air-changes/h]	Time-dependent volume [m ³ min]		
			0	2	4	
109	R32	Burst leak	Leakage rate [kg/h]			
		Rapid leak	75	0.011	0.008	0.006
	R1234ze(E)	burst leak	10	2481	0.0004	0.0007
		Rapid leak	54	0.027	0.017	0.015
			7.3	3129	0.001	0.0009

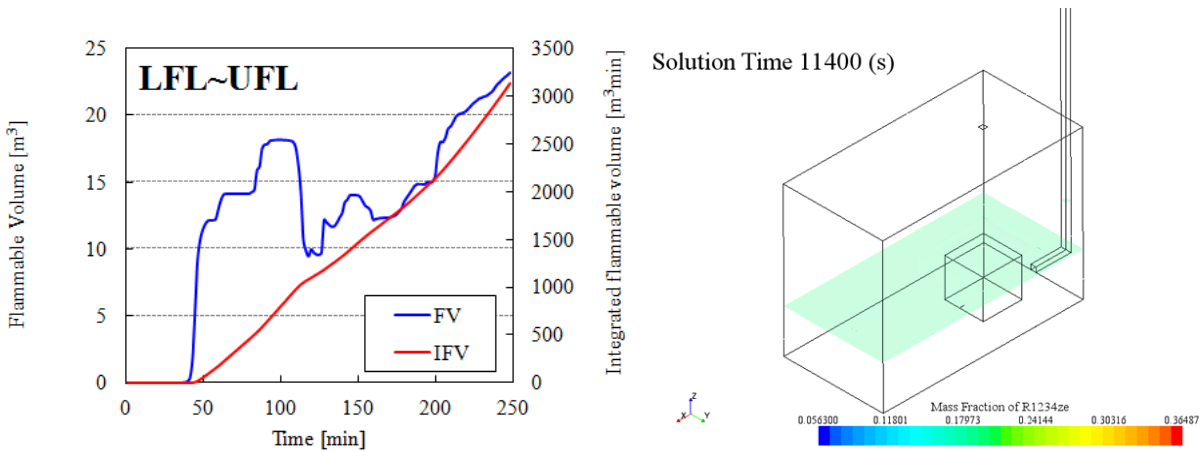


Figure 9.3.4 Refrigerant concentration, time-dependent volume (R1234ze(E)_wet, zero air-changes/h, rapid leak)

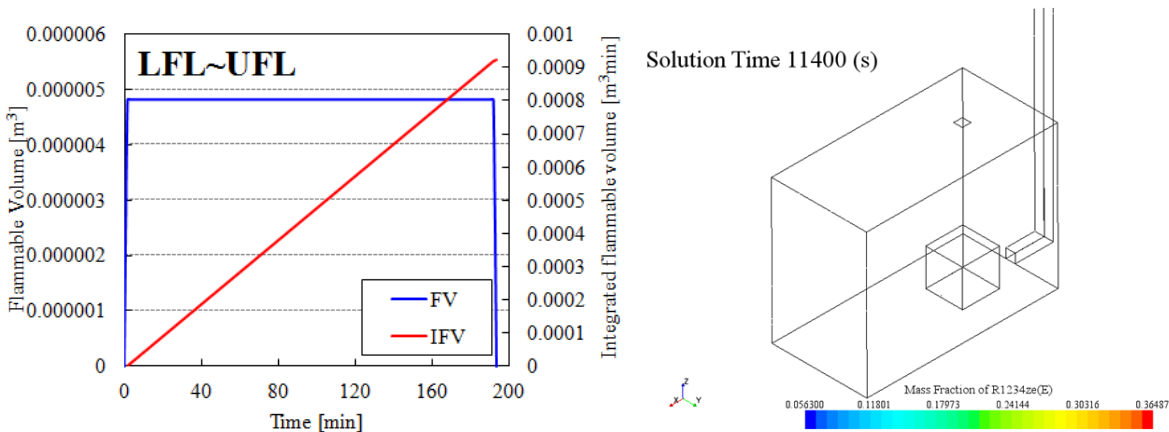


Figure 9.3.5 Refrigerant concentration, time-dependent volume (R1234ze(E)_wet, four air-changes/h, rapid leak)

(2) Ventilation of a refrigerant-filled machine room (case 2)

The change in volume of the flammable space after the start-up of the ventilation for a refrigerant-filled machine room is shown in Figure 9.3.6. The flammable space disappeared after 6 min for an average room volume of 109 m³ and after 20 min for a minimum volume of 75 m³ (using a ventilation rate of four air-changes/h.). This result is specified in the guidelines to restrict entry to the machine room and startup conditions at the restart of refrigeration equipment after a long-term stoppage.

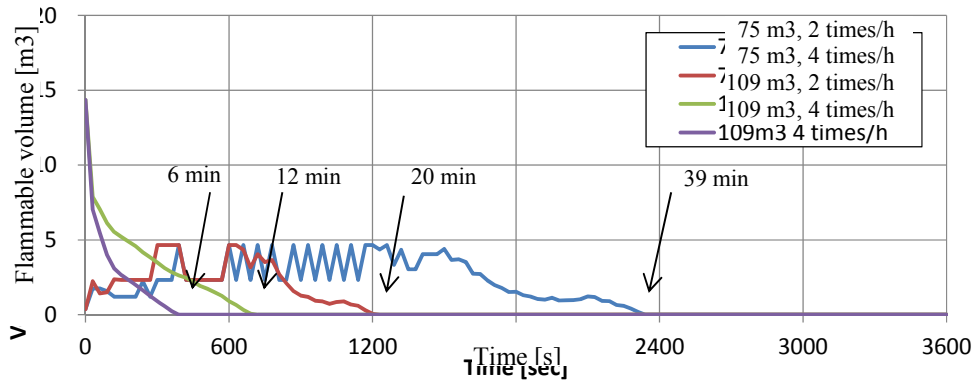
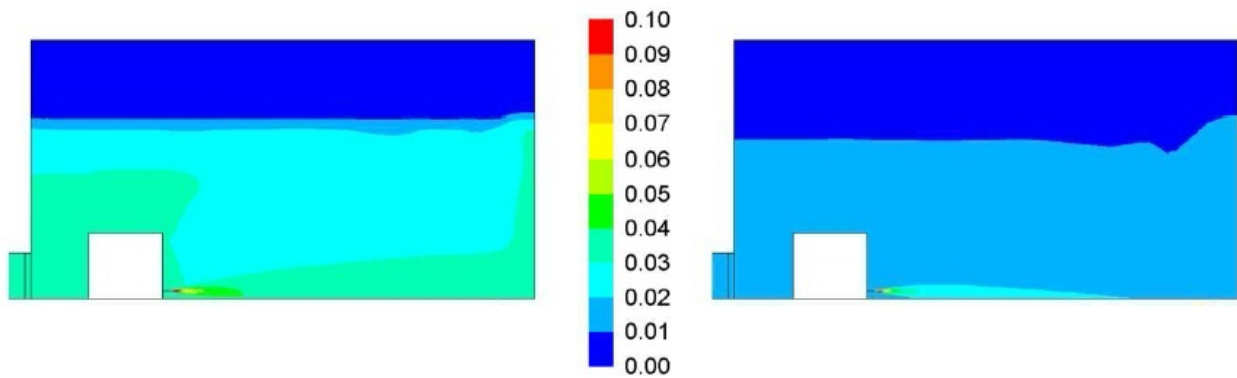


Figure 9.3.6 Flammable volume after ventilation

(3) Influence of refrigerant quantity

The condition of analysis for the standard chiller in the standard machine room model was the evaluation of relatively small volume ventilation for a given quantity of refrigerant leakage. For larger chillers, the refrigerant continues to leak for longer due to there being a larger amount of refrigerant. Referring to domestic laws, a bigger chiller with a capacity of 300 kW and a machine room with a volume of 192 m³ were selected. The room volume was derived from Figure 9.3.1 and the chilling capacity is the lowest among the chillers which fall under the jurisdiction of domestic law. The volume of the machine room was 192 m³, as derived from Figure 9.3.1. A steady-state analysis was carried out with the condition of continuing a burst leak. At a ventilation rate of four air changes/h, the concentration of refrigerant was less than 2% and a flammable space does not form. At a ventilation rate of two air changes/h, the concentration of the refrigerant was more than 4%, but the flammable space was very small and confined to the immediate vicinity of the nozzle. The result of the analysis of a burst leak of R1234ze(E) and the concentration distributions at the two ventilation rates are shown in Figure 9.3.7. It is thought that a flammable space does not form regardless of the amount of leaked refrigerant in a room with mechanical ventilation in which a chiller with a capacity of more than approximately 300 kW is installed.



(a) Two air-changes/h

(b) Four air changes/h

Figure 9.3.7 Concentration distribution resulting from continuous refrigerant leakage (R1234ze (E), burst leak, 192 m³)

(4) Equipment installed outdoors

The results of the analysis of equipment installed outdoors are listed in Table 9.3.4. As an example, Figure 9.3.8 shows the LFL for a rapid leak and a burst leak resulting from leakage from a decorative panel, and the LFL of the leakage of R32 from inside the decorative panel. For leakage from the air-heat exchanger, the flammable space is small enough to be negligible. For leakage from the inside of the decorative panel, a flammable space is formed as a result of refrigerant gas being stagnant in the lower part of the unit, such that ignition sources must be evaluated.

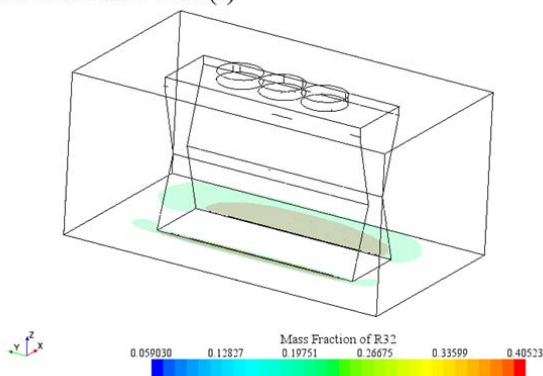
Table 9.3.4 Results of unsteady-state analysis (air-cooled chiller)

Capacity [Hp]	Leakage point	Refrigerant	Leak	Leakage rate [kg/h]	Time-dependent volume [m ³ min]
					Wind velocity 0 [m/s]
30	Air heat exchanger	R32	Rapid leak	10	0.0002
		R1234ze(E)	Rapid leak	7.3	0.0003
	Bottom panel	R32	Rapid leak	10	3.732
			Burst leak	75	4.242
		R1234ze(E)	Rapid leak	7.3	3.989
			Burst leak	54	5.685

(a) Rapid leak

(b) Burst leak

Solution Time 4200 (s)



Solution Time 550 (s)

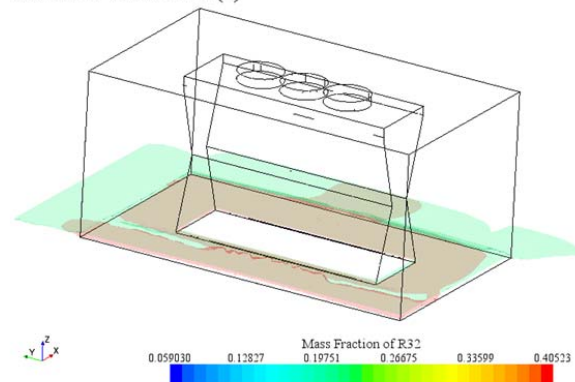


Figure 9.3.8 Contour figure of R32 leak from bottom panel (wind velocity 0 m/s)

9.4 Ignition probability

9.4.1 Ignition sources in a machine room

This section describes the ignition sources in a machine room in which a water-cooled chiller is installed. Access to the machine room is limited to professional engineers such as operators, service personnel, and construction subcontractors, with entry being prohibited to unauthorized persons. In addition, open flame or smoking is not permitted and there are only a limited number of ignition sources in the machine room. The machine room is equipped with a power board to start the chiller, and features large-capacity breakers and solenoid switches. In addition, the chiller itself features accessories such as a control panel with built-in control equipment and various electrical components. Furthermore, a cold-water pump and a cooling water circulation pump are provided along with an auxiliary power board with built-in breakers and solenoid switches. The air drawn into a burning appliance is introduced directly to the machine room with a blower, and ventilation air is evacuated outdoors through an independent air duct. The machine room is equipped with forced ventilation equipment and the Building Standards Act designates the ventilation volume that is required by burning appliances and required to remove the heat from the apparatus. ISO5149-part3⁶⁾ mandates that a ventilation volume equivalent to an air change rate of four times the volume of the machine room per hour. Figure 9.4.1 shows an image of the machine room, and Tables 9.4.1 and 9.4.2 list the ignition sources present in a machine room. Each evaluation of whether the listed ignition sources are ignited was executed based on the burning characteristics of the refrigerant and the study results by the research committee to assess the risks associated with mildly flammable refrigerants.

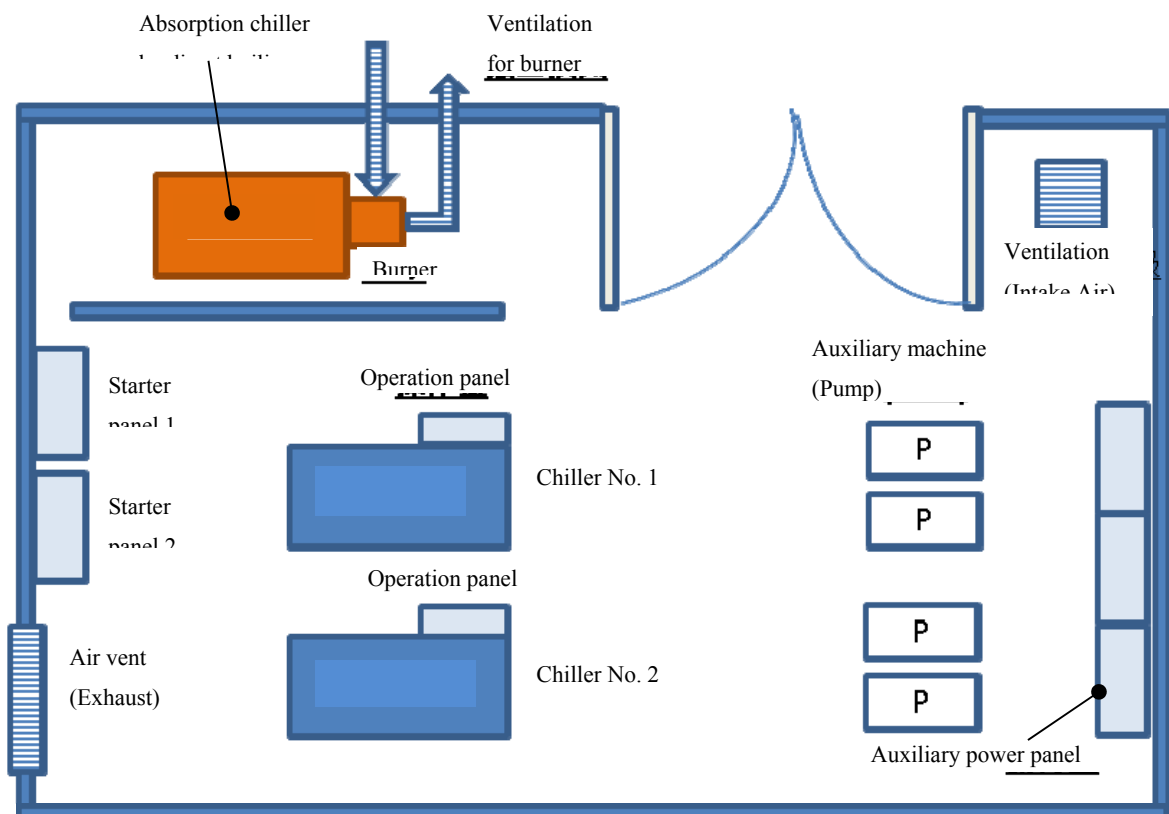


Figure 9.4.1 Image of machine room

Table 9.4.1 Ignition source apparatus in a machine room (sources of sparks)

Category	Spark		
	Ignition Source	Evaluation ○: Ignition ×: Non-ignition	Remarks
Electrical parts	Home appliances and a small-size electrical products	×	5 kVA or below
	Electrical parts inside equipment	○	Solenoid switch with capacity of 5 kVA or above
	AC power source	×	Equivalent to quenching distance
	Lighting switch	×	Equivalent to quenching distance
Work tools	Metal spark (fork of a forklift)	○	-
	Electrical power tool	×	Small capacity
	Refrigerant recovery apparatus	×	Small capacity
Human body	Static electricity built up on human body	×	Minimum ignition energy or less

Table 9.4.2 Ignition apparatus in machine room (using open flames)

Category	Open flame		
	Ignition Source	Evaluation ○: Ignition ×: Non-ignition	Remarks
Smoking supplies	Match	○	Ignition = open fire
	Oil lighter	○	Open fire once ignited
	Piezoelectric ignition lighter	×	Lighter not ignited
Burning appliance	Electric radiant heater	○	Prohibited
	Electric fan heater	×	Prohibited
	Gas water heater	○	Prohibited
	Gas boiler (burner)	×	No timing of ignition
	Ventilation duct, boiler surface	×	140°C or below
	Gas cooking appliance	○	Prohibited
Work tool	Burner for brazing	×	High gas velocity

9.4.2 Ignition sources

Ignition sources in a machine room include a boiler with a combustor, a hot and chilled water generator, a drive motor (e.g., a pump), a ventilation instrument fan, a heating apparatus such as an electric stove, a reflective kerosene stove, a kerosene fan heater, a lighting apparatus, an exhaust duct of a combustor, a gas or electric oven, static electricity, very large electrical apparatus, power tools, and a brazing burner. Open flames, metal sparks, and very large electrical apparatus can all be ignition sources, as indicated by a comparison of the results of an ignition test of low-flammability refrigerant^{(10), (11), (12)} and the surface temperature of the apparatus. A boiler and the exhaust of a direct-type hot- and chilled-water generator lead to the exterior of a building through a duct. The air in a machine room is used for the intake, and the flame of a burner can be an ignition source in the event of the leakage of refrigerant (Figure 9.4.2). Therefore, the timing sequence from ignition to stop must be confirmed. After starting a separate fan, the pilot burner is ignited by an ignition device, followed by the main burner. During normal operation, the pilot burner is stopped and only the main burner is used. Upon the suspension of the test, the main burner is halted and only the fan is operated, post purge, for a defined time. During operation, a fan operates all the time. Even if refrigerant gas flows into the apparatus and is ignited, the flame in the combustor does not blow back

into the machine room. Consequently, there is no possibility of fire being caused by leaking refrigerant gas. Because an apparatus such as a stove or an oven is prohibited from being taken into the machine room, it is excluded from the list of ignition sources.

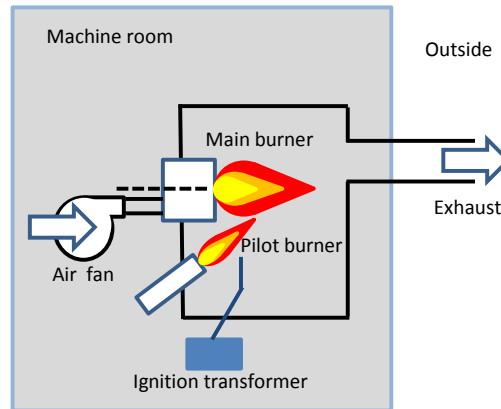


Figure 9.4.2 Image of burner in absorption chiller

9.4.3 Ignition by smoking

Smoking gives rise to the possibility of the open flame of a match or lighter igniting leaked refrigerant gas. Therefore, the smoking behavior of personnel (including operators) was investigated, and the probability of ignition due to smoking at each LS was calculated. Although lighters were verified as being unlikely to ignite the gas in an ignition test, the number of smoking times was determined as the number of times ignition occurred.

- (1) 53% of the personnel smoked and 28% had smoked in the machine room. During the past year, 7% of all the personnel sampled had smoked on-site.
- (2) A lighter is used as the ignition source by 99.6% of smokers, while 0.4% used a match.
- (3) An electric lighter was used by 95% of the lighter users, while 5% used an oil lighter.
- (4) The number of cigarettes smoked per person per day was 19.1.¹³⁾
- (5) Personnel worked 8 h/day with an activity time of 18 h.
- (6) Two people work at the site for four days in a week.
- (7) The duration of an open flame per smoking event is 2 s.
- (8) The period in a day in which ignition sources are present is 8 h, corresponding to the working day of the personnel.

From the above survey, the probability of the existence of an ignition source because of smoking is estimated to be $(0.07 \times 19.1 \times 2/3600 \times 8/18 \times 4/365 \times 2)/8 = 9.04 \times 10^{-7}$.

9.4.4 Ignition by electrical components

Among the electrical components in the machine room (e.g., electric drive motors, electromagnetic switches, circuit breakers, printed-wiring boards, and transformers), only an electromagnetic switch can possibly give rise to an ignition source in the form of an arc.

As the electrical rating increases, the energy of the arc and the probability of it constituting an ignition source increase. However, those electrical components with an electrical rating of no more than is 5 kVA are not assumed to constitute an ignition source, as noted by Dr. Takizawa, Advanced Industrial Science and Technology and DOE/CE/23810-9 (ADL

Author.D. Little)²⁾.

The rating of each type of chiller has been summarized, and for a power system chiller of no more than 20 horsepower (for which the legal refrigeration capacity is 13 tons), the rating is generally no more than 5 kVA.⁵⁾ There is no electrical component with a capacity of more than 5 kVA in the control system of a product with more than 20 horsepower. The ignition sources were narrowed down to electromagnetic switches, thus the probability of the existence of an ignition source was estimated from the frequency of the occurrence of electromagnetic switches. Assuming that the contact time at the point is 1 s, the maximum number of startup/shutdown cycles is 6 times/h (screw chiller) or 2 times/h (centrifugal chiller). The maximum number of startup/shutdown cycles of a chiller was estimated to be $6 \times 0.952 + 2 \times 0.048 = 5.8$ times/h, considering that the ratio of screw chillers to centrifugal chillers is 0.952:0.048. The probability of an ignition source is estimated to be $(1/3600 \times 5.8 \times 12)/12 = 1.61 \times 10^{-3}$ for every 12 h of operation.

9.5 Probability of the occurrence of refrigerant leakage

An analysis of the seventy-four refrigerant leakage accidents reported to the High Pressure Gas Safety Institute of Japan (KHK) indicated that the leakages were from the small-bore piping or seals. The leakages are similar to those from multi-packaged air-conditioning unit systems. Therefore, we categorized them as “burst leakage,” “rapid leakage,” and “slow leakage” as described in JRA-GL13⁸⁾. All of the leakages categorized as burst leakage were due to the breakage of small-bore pipes as a result of vibration or slight cracks in the pipes produced during maintenance work. The rapid leakages originated from capillary piping and sensors or from slight cracks during maintenance work. And both burst and rapid cases were gas leaks. A slow leakage resulted from the deterioration of the sealing materials, cracking, or the insufficient tightening of joints. These notifications were compared with the maintenance data from each company participating in the SWG. The probability of the occurrence of a refrigerant leakage in each leakage category was calculated for the water-cooled chillers, air-cooled heat pumps, and centrifugal water chilling units from the proportional rate to the number of chillers available which was estimated from past shipment data of each company from 2004 to 2011 (Table 9.5.1). Because the obtained maintenance data almost matched those in the accident notifications reported to KHK, the data were considered trustworthy. Burst and rapid leakages from centrifugal water chilling units have not occurred.

Table 9.5.1 Frequency of leakages in 2004-2011

2004-2011	Probability of the occurrence of refrigerant leakage [1/(unit*year)]			
	Water-cooled chiller	Air-cooled heat pump	Centrifugal water chilling unit	Total
Burst leak	5.83×10^{-6}	1.35×10^{-5}	0	1.07×10^{-5}
Rapid leak	1.07×10^{-4}	1.87×10^{-4}	0	1.56×10^{-4}
Slow leak	1.64×10^{-3}	2.21×10^{-3}	7.09×10^{-3}	2.27×10^{-3}

9.6 Risk assessment

9.6.1 List of risk assessment conditions

For the current calculation of the risk of burning and accidental fires, the time-dependent volume of the flammable space for a burst and rapid leak was calculated along with the probability of the presence of each ignition resource during that time. The calculation conditions are defined below, and it is assumed that each of the six LSs has different sources.

(1) Four items of equipment are installed, assumed to be a heat-source system, and the start-up/shutdown cycles of

adjacent equipment are considered.

- (2) The ventilation of the equipment is to be two air-changes/h \times 2 lines, four air-changes/h with the failure rate of the duct fan estimated to be $2.5 \times 10^{-4}/(\text{unit}\cdot\text{year})$.
- (3) The probability of no ventilation of the equipment is 1%, and the LS of the installation and disposal is 50%.
- (4) For LS, the logistics and disposal without a user's direct contact are excluded from the probability of accidents while the values are specified.
- (5) The probability of the existence of a flammable space when there is no ventilation is defined as being the same as the probability of refrigerant leakage.
- (6) For a small leak when the machine room has ventilation, the probability of existence is 0 because the existence of a flammable space is not considered.
- (7) The probability of the existence of a flammable space is given as the time-dependent volume of the flammable space $[\text{m}^3\text{min}]/(\text{target space } [\text{m}^3] \times 8760 \text{ h} \times 60 \text{ min})$. The target space of an air-cooled heat pump is defined as the area surrounded by soundproof walls.
- (8) Ignition sources are assumed to exist throughout the entire flammable space, including the floor surface. For example, the case of a lighter flame at the ground level is not excluded.
- (9) The time-dependent volume of R1234ze(E) was applied for a water-cooled chiller, and R32 was applied for an air-cooled heat pump.

9.6.2 Probability of accidental fire

The results of a leakage analysis show that, for a rapid leak from a chiller installed in the machine room, a large flammable space exists and the time-dependent volume becomes large and in other cases even when there is no flammable space, there is a risk of the time-dependent volume developing into a whole room if the position of the leakage port, the leakage direction, or the leakage mass velocity changes because of there being large volumes with a concentration a little less than that of LFL. The probability of an accidental fire is that of an accidental fire at one device in one year. So, it is calculated as the sum multiplied by the probability of the existence of an ignition source, the probability of existence of a flammable space, and the number of refrigerant leakages in each LS. The probabilities of there being an accidental fire for each leakage type in each LS are listed in Table 9.6.1. The probabilities of there being an accidental fire were evaluated both without the ventilation and with the ventilation. The probabilities of there being an accidental fire for each LS in the case of chillers both with and without countermeasures against risks are listed in Table 9.6.2. A previously measured value describes the risk with no ventilation and shows the probability of an accidental fire by ignition source existence, whenever low-flammability gas leaks, and the concentration of the refrigerant is within the flammable range. During LS under the user's management, the probability of burst leaks, rapid leaks and slow leaks are summed to give 1.32×10^{-4} accident/(unit·year), a larger value than the actual one. For example, if the machine room is narrow and without ventilation at 1%, the probability is 1.32×10^{-6} accident/(unit·year), which is not acceptable to the user. The probability of there being an accidental fire in case of a chiller with countermeasures is calculated from the probability of an accident in a flammable space of a standard chiller model with ventilation and a machine room. In addition, the installation condition of an air-cooled heat pump in this analysis is assumed to have soundproof walls, which is more severe than the actual conditions. The probability during LS under user's management is 3.90×10^{-12} accident/(unit·year), which is evaluated as being "improbable".

Table 9.6.1 Probability of accidental fire for each leakage type

LS	Without ventilation [1/(unit*year)]			With ventilation [1/(unit*year)]		
	Burst leak	Rapid leak	Slow leak	Burst leak	Rapid leak	Slow leak
Logistics	1.73×10^{-8}	2.77×10^{-7}	3.99×10^{-6}	4.55×10^{-18}	1.51×10^{-13}	0
Installation [carry-in]	1.96×10^{-8}	3.13×10^{-7}	4.33×10^{-6}	1.53×10^{-15}	2.40×10^{-12}	0
Installation [trial]						
Usage [machine room]	2.51×10^{-7}	4.01×10^{-6}	5.76×10^{-5}	6.99×10^{-15}	4.90×10^{-13}	0
Usage [outdoor]						
Repair	2.64×10^{-7}	4.22×10^{-6}	6.07×10^{-5}	2.07×10^{-14}	9.83×10^{-13}	0
Overhaul						
Disposal	6.98×10^{-8}	1.12×10^{-6}	1.61×10^{-5}	5.48×10^{-15}	9.23×10^{-12}	0

Table 9.6.2 Probability of accidental fire

	LS	LS ratio	Without ventilation [1/(unit*year)]		With ventilation [1/(unit*year)]	
			LS	LS under user's management	LS	LS under user's management
Suppliers	Logistics	0.0517	4.28×10^{-6}	-	1.51×10^{-13}	-
Operator	Installation [carry-in]	0.0517	4.67×10^{-6}	1.32×10^{-4}	2.40×10^{-12}	3.90×10^{-12}
	Installation [trial]	(0.0023)				
	Usage [machine room]	0.2144	6.19×10^{-5}			
	Usage [outdoor]	0.5002	6.52×10^{-5}		4.97×10^{-13}	
	Repair	0.1207			1.00×10^{-12}	
Overhaul	0.0098					
Suppliers	Disposal	0.0517	1.72×10^{-5}	-	9.23×10^{-12}	-

9.6.3 Technical requirements for safety

This section describes the requirements, comparing them with KHKS0302-3⁵⁾, ISO5149-3¹⁴⁾ (2014), and Japanese domestic legal standards and requirements for the reference of this RA.

1) Ventilation of machine room

Mechanical ventilation should be required at all times. The baseline air change rate for a machine room should be between two and four air-changes/h, depending on the size of the machine room. The ventilation system should consist of two lines. The exhaust port should be installed close to the floor where the refrigerant tends to settle, such that it can be discharged directly through a duct. Ventilation equipment should be operable from outside the machine room.

2) Refrigerant detector and refrigerant leakage alarm

One or more instruments that detect refrigerants and which have a sensor at an undisturbed position should be installed. The sensor should be positioned where the refrigerant will tend to collect. The refrigerant detector and refrigerant leakage alarm should be run off an independent power supply such as uninterruptable power supply (UPS). The instrument is to be linked to an alarm (e.g., both audible and visible) that is noticeable from outside a machine room.

3) Prohibition of open flame

Any apparatus with an open flame (e.g. heating apparatus, water heater, or stove) should be prohibited in a machine room.

4) Smoking and other uses of fire should be strictly prohibited.

5) Inspection

The machine ventilation, refrigerant detector, refrigerant leak alarm, and the UPS should have periodic inspections during installation and the air change rate should be as recommended by the manufacturer; all inspection records should be stored.

6) Instrument protection

The normal operation of the refrigerant detector and the mechanical ventilation of the machine room should be configured to be interlocked with the start-up of the chiller.

9.7 Simulation of Leakage from Chillers

This section presents the details of a simulation of a leakage from a chiller and the evaluation thereof, as conducted by the University of Tokyo.

9.7.1 Calculation method

Tables 9.7.1 and 9.7.2 list the leakage scenarios and the input conditions considered in this study. The commercial CFD program STAR-CCM+ was used. A realizable $k-\epsilon$ turbulence model was adopted. An unsteady compressible fluid and multicomponent ideal gas were adopted. Both the air and the refrigerant were assumed to be ideal gases, and the density was calculated using the equation of state of an ideal gas. R1234ze(E) is non-flammable in dry air, such that the upper and lower flammability limits (UFL and LFL) and the burning velocity (BV) of R1234ze(E) at a temperature and relative humidity of 23°C and 90%, respectively, were adopted. The leak point was defined as a constant mass flow rate boundary, and the mass flow rate was changed to zero after the leakage finished. Apertures were treated as a constant pressure boundary corresponding to the atmospheric pressure.

Figure 9.7.1 shows the geometries analyzed. The details of these geometries are described below.

(a) Leakage from a water-cooled chiller

A water-cooled chiller with dimensions of 1.28 m × 1.28 m × 1.28 m was assumed to be installed in a basement machine room. Two machine room volumes were considered, specifically, 6.6 m × 3.3 m × 5.0 m (109 m³) and 5.6 m × 2.7 m × 5.0 m (75 m³). The chiller was located 1.01 m from the wall and was assumed to have a nozzle-shaped leakage port, the length of which was 100 mm and located 150 mm from the floor on the chiller body. Refrigerant leaked from this port horizontally. Here, both a rapid leakage and burst leakage were considered. The leakage at the port outlet had a sonic velocity, because the scenarios assumed the cracking of the tube in which the refrigerant flows and refrigerant leaking into the machine room. The inner diameter of the leakage port was adjusted as the leakage velocity was equal to the sonic speed. The inlet of the exhaust duct from which the duct extended 15 m upwards was located on the bottom of the wall behind the chiller. The air inlet from which air was supplied when air ventilation was operated was located in the ceiling above the chiller. When the air ventilation was stopped, the air inlet was treated as an aperture. The aperture ratios and the air velocities at the air inlet and exhaust duct inlet were 0.7 and 2.0 m/s, and 0.3 and 4.0 m/s, respectively. These areas were adjusted as the ventilation conditions listed in table 9.7.1 were satisfied. Approximately 500,000 non-equidistant mesh points were used to discretize the governing equations.

Table 9.7.1 Leakage scenarios (Reference “ISO 5149-3, 2014”)

Case no.	Refrigerant	Charged amount	Room volume	Leakage velocity	Ventilation (Airflow)	Air vent			
water-cooled chiller									
1	R32	23.4 kg	109 m ³	10 kg/h	0 m ³ /h	present			
2				(rapid leakage)	218 m ³ /h	present			
3					436 m ³ /h	present			
4				75 kg/h	0 m ³ /h	present			
5				(burst leakage)	218 m ³ /h	present			
6					436 m ³ /h	present			
7				75 m ³	10 kg/h	0 m ³ /h	present		
8			(rapid leakage)		150 m ³ /h	present			
9					300 m ³ /h	present			
10			75 kg/h		0 m ³ /h	present			
11			(burst leakage)		150 m ³ /h	present			
12					300 m ³ /h	present			
13	R1234ze(E)	23.4 kg	109 m ³	7 kg/h	0 m ³ /h	present			
14				(rapid leakage)	218 m ³ /h	present			
15					436 m ³ /h	present			
16				54 kg/h	0 m ³ /h	present			
17				(burst leakage)	218 m ³ /h	present			
18					436 m ³ /h	present			
19				75 m ³	7 kg/h	0 m ³ /h	present		
20			(rapid leakage)		150 m ³ /h	present			
21					300 m ³ /h	present			
22			54 kg/h		0 m ³ /h	present			
23			(burst leakage)		150 m ³ /h	present			
24					300 m ³ /h	present			
air-cooled chiller									
25	R32	11.7 kg	31 m ³	10 kg/h	(0 m/s)	(outdoor)			
26				(rapid leakage)	(0.5 m/s)	(outdoor)			
27				75 kg/h	(0 m/s)	(outdoor)			
28				(burst leakage)	(0.5 m/s)	(outdoor)			
29				10 kg/h	(0 m/s)	(outdoor)			
30				(rapid leakage from bottom apertures)	(0.5 m/s)	(outdoor)			
31				75 kg/h	(0 m/s)	(outdoor)			
32				(burst leakage from bottom apertures)	(0.5 m/s)	(outdoor)			
33				R1234ze(E)	11.7 kg	31 m ³	7 kg/h	(0 m/s)	(outdoor)
34							(rapid leakage)	(0.5 m/s)	(outdoor)
35							54 kg/h	(0 m/s)	(outdoor)
36							(burst leakage)	(0.5 m/s)	(outdoor)
37	7 kg/h	(0 m/s)	(outdoor)						
38	(rapid leakage from bottom apertures)	(0.5 m/s)	(outdoor)						
39	54 kg/h	(0 m/s)	(outdoor)						
40	(burst leakage from bottom apertures)	(0.5 m/s)	(outdoor)						

Table 9.7.2 Input conditions (Reference “Takizawa, K. *et al.* 2011, NIST 2013”)

Refrigerant		R32	R1234ze(E)
Temperature	°C	20	20
Pressure		atmospheric pressure	atmospheric pressure
Absolute humidity	kg/kg DA (dry)		0.016
Mass charged in water-cooled chiller	kg	23.4	23.4
Mass charged in air-cooled chiller	kg	11.7	11.7
Lower flammability limit (LFL)	vol.%	13.5	5.9
Upper flammability limit (UFL)	vol.%	27.5	12.6
Burning velocity (BV)	m/s	0.067	0.052
Molecular weight	kg/kmol	52.024	114.04
Specific heat at constant pressure	J/kg.K	842.01	881.88
Thermal conductivity	W/m.K	1.2187×10^{-2}	1.2683×10^{-2}
Viscosity	Pa.s	1.2398×10^{-5}	1.2151×10^{-5}
Diffusivity in air	m^2/s	1.35×10^{-5}	7.4×10^{-6}

(b) Leakage from an air-cooled chiller

Refrigerant was modeled as leaking from an air-cooled chiller with dimensions of 3.0 m × 1.0 m × 2.3 m, placed outdoors. The chiller was surrounded by four walls, two of which are sound insulating walls with an aperture ratio of 25%, while the other two are normal walls. There was no ceiling. The chiller body was located at the center of the space. Here, two leakage types were assumed, namely, leakage from a crack in the heat exchanger tube, and leakage from the bottom apertures caused by an inner burst. For direct leakage, a nozzle-shaped leakage port was assumed to be located 150 mm above the body center. The inner diameter of the leakage port was to give a leakage velocity that was equal to the sonic speed. For leakage from the bottom apertures, two apertures with a size of 2.0 m × 0.01 m were located at the bottom between the floor and chiller panels where refrigerant flowed slowly onto the ground. Wind with a velocity of 0.5 m/s was assumed to blow along the sound insulating wall. Approximately 700,000 non-equidistant mesh points were used.

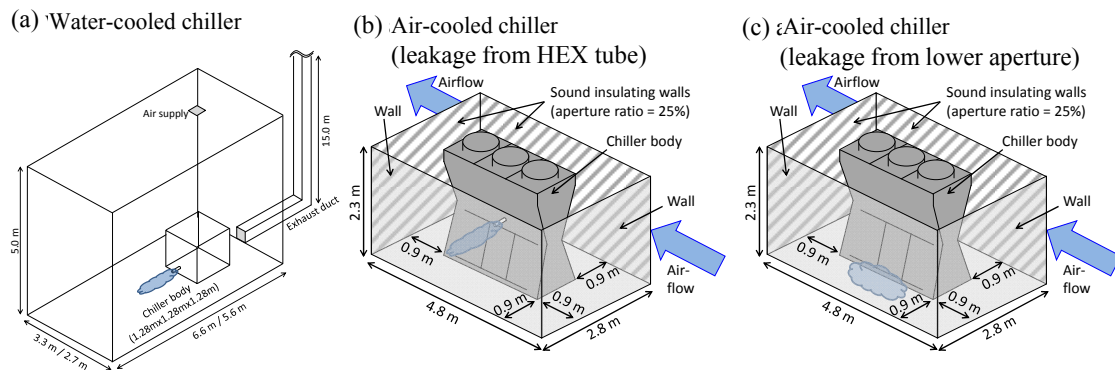


Fig. 9.7.1 Analytical geometries

9.7.2 Results and discussion

To evaluate the results, the term $\int V dt$ was used, which means the time-integrated flammable volume. Here, two kinds of flammable volumes were considered. The term V_{FL} represents the volume whose gas concentration is between LFL and UFL, while the term V_{BVFL} represents V_{FL} with an air velocity that is lower than the burning velocity. In addition, the residence time of V_{FL} was also confirmed. Table 9.7.3 lists the predicted V_{FL} residence times and time-integrated flammable volumes $\int V_{FL} dt$, $\int V_{BVFL} dt$. Figures 9.7.2 and 9.7.3 show the eight flammable volumes V_{FL} , V_{BVFL} , and time-integrated flammable volumes $\int V_{FL} dt$, $\int V_{BVFL} dt$ with the change in time, and LFL and UFL isosurfaces just before the leakage finishes, respectively.

(a) Leakage from a water-cooled chiller

The results listed in Table 9.7.3 for case nos. 1–24 represent the leakage from a water-cooled chiller, while Figures 9.7.2 (a)–(d) and 9.7.3 (a)–(d) show the result for representative cases 4, 7, 16, and 19. For case nos. 1, 13, and 19, calculations were stopped before the flammable volumes vanished because of their very long residence time. Therefore, the actual presence time and time-integrated flammable volumes must be larger than the values listed in Table 9.7.3. These results show that V_{FL} increased considerably and did not disappear even after the leakage finished when rapid leakage occurred in a room with a volume of 109 m³ without air ventilation (see case nos. 1 and 13). However, when the burst leakage occurred or when the room volume was 75 m³, there was the possibility of the V_{FL} not developing without air ventilation (see case nos. 4, 7 and 16). When the room volume is large, a high concentration region develops in the lower part of the room and the refrigerant does not diffuse into the upper part because the leakage port is located near the floor. On the other hand, when the leakage mass flow rate is larger or when the room volume is smaller, refrigerant spreads into the wider or higher parts of the room, which leads to a larger volume with a concentration lower than LFL, causing V_{FL} to be restricted. However, it should be noted that the risk of combustion in these cases is not small. This is because the results for these cases indicate that there are large volumes with a concentration that is a little less than LFL, and there is a risk that V_{FL} will develop into the entire room if the position of the leakage port, leakage direction, or the leakage mass velocity changes.

For the air ventilation, V_{FL} was small enough with an air ventilation volume per hour that is twice the machine room volume. It is thought that an adequate air ventilation volume is important for safety, and that the operation of the blast fan is also effective.

(b) Leakage from an air-cooled chiller

The calculation results listed in Table 9.7.3 for case nos. 25–40 represent the leakage from an air-cooled chiller, while figures 9.7.2 (e)–(h) and 9.7.3 (e)–(h) show the result for representative case nos. 30, 32, 38, and 40. From these results, for the leakage from a crack on the heat exchanger tube (see case nos. 25–28 and 33–36), the refrigerant spread out and the V_{FL} existed only at the periphery of the leakage port, which led to there being very small time-integrated flammable volumes, because the location was an outdoor space. For leakages from bottom apertures caused by an inner burst, the leakage occurred near the ground. For this reason, the refrigerant was not accelerated by gravity and does not spread into an upper space; therefore a V_{FL} layer with a thickness of approximately 0.01 m is generated on the ground. Especially in the case of a burst leakage, V_{FL} developed over the entire ground area (see case nos. 31, 32, 39 and 40). However, it vanished immediately after the leakage finished because of outdoor space. The effect of the airflow was negligible.

Table 9.7.3 Predicted V_{FL} residence times and time-integrated flammable volumes

Case no.	V_{FL} residence time, min	$\int V_{FL} dt$ m ³ min	$\int V_{BVFL} dt$ m ³ min	Case no.	V_{FL} residence time, min	$\int V_{FL} dt$ m ³ min	$\int V_{BVFL} dt$ m ³ min
water-cooled chiller				air-cooled chiller			
1*	up to 200	up to 2481	—	21	193.3	0.0009	0
2	141.7	0.0008	0	22	26.7	0.784	0
3	141.7	0.0007	0	23	26.7	0.046	0
4	20	0.011	0	24	26.7	0.025	0
5	20	0.008	0	25	70.8	0.0002	0
6	20	0.006	0	26	70.8	0.0002	0
7	141.7	0.112	0	27	9.67	0.0007	0
8	141.7	0.0008	0	28	10	0.0007	0
9	141.7	0.0007	0	29	71.7	3.989	2.054
10	20	0.037	0	30	71.7	4.038	2.313
11	20	0.016	0	31	10.8	5.685	0.646
12	20	0.012	0	32	10.4	5.544	0.662
13*	up to 248	up to 3129	—	33	96.7	0.0003	0
14	210	0.001	0	34	96.5	0.0003	0
15	193.3	0.0009	0	35	14.2	0.001	0
16	26.7	0.027	0	36	13.3	0.001	0
17	26.7	0.017	0	37	96.7	3.989	2.054
18	26.7	0.015	0	38	97.5	4.038	2.313
19*	up to 200	up to 3636	up to 1464	39	14.2	5.685	0.646
20	193.3	0.0009	0	40	14.2	5.544	0.662

* Calculations were stopped before the flammable volumes vanished because of their very long residence times.

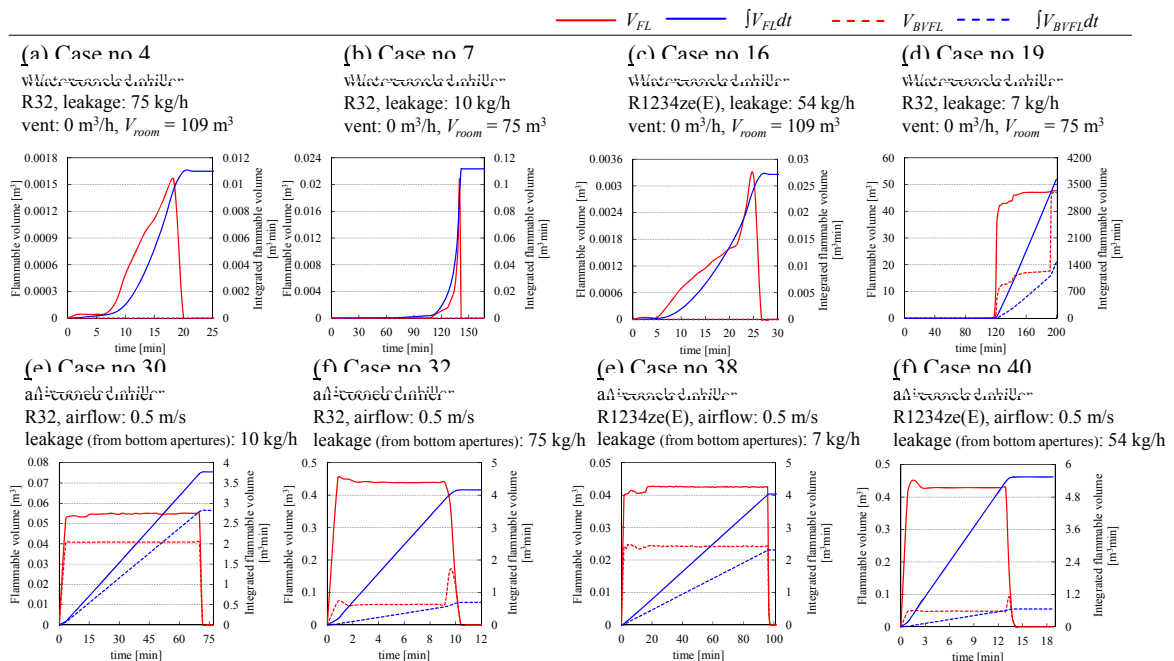


Fig. 9.7.2 Flammable volumes V_{FL} , V_{BVFL} , and time-integrated flammable volumes $\int V_{FL} dt$, $\int V_{BVFL} dt$ with change in time

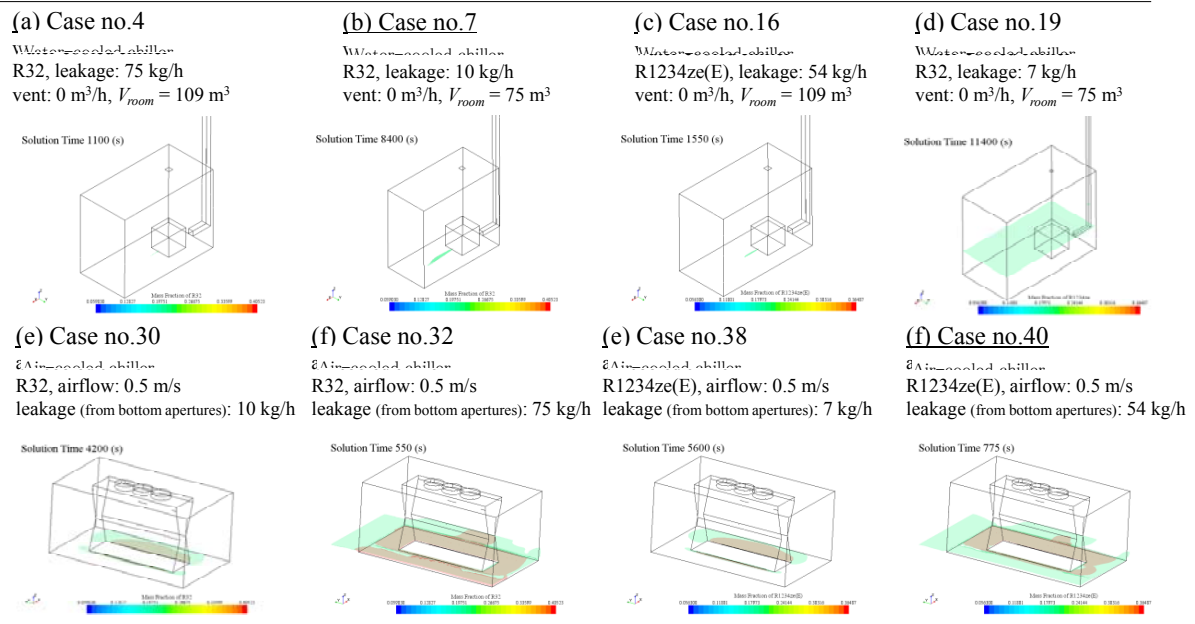


Fig. 9.7.3 LFL and UFL isosurfaces immediately before leakage ends

9.8 Conclusions

As a result of the risk assessments performed by the Chiller SWG, it was confirmed that the frequency of accidental fires and burns was low enough considering the probability of the occurrence of refrigerant leakage and the probable existence of ignition sources for water-cooled chillers and heat pumps using low-flammable refrigerant. In addition, it was confirmed that the probability of the occurrence of an accident became smaller than once every hundred years in the machine room with appropriate machine ventilation, between two and four air-changes/h by two lines. The general outlines of safety requirements determined through RAs are (1) Guarantee of the mechanical ventilation with required air flow rate in a machine room, (2) Monitoring of refrigerant leakage by at least one refrigerant detector, (3) Interlock of chiller with the refrigerant detector and the mechanical ventilation, (4) Guarantee of the refrigerant detector and the alarm device of refrigerant leakage which run on an independent power supply such as uninterruptable power supply (UPS). Furthermore, a draft of the GLs for the chilling equipment based on those technical requirements has been made up. In the next fiscal year, the SWG will work towards the development of GLs and an general overview of RAs.

The simulation conducted in this study yielded the following findings.

- 1) For leakage from a water-cooled chiller, air ventilation is effective to restrict V_{FL} . When air ventilation is not provided, there is the possibility of V_{FL} developing.
- 2) In the case of a leakage from an air-cooled chiller situated outdoors, even if the leakage from a crack in a heat exchanger tube occurs, the refrigerant spreads out and the time-integrated flammable volumes are small. Regarding the leakage from the bottom apertures caused by an inner burst, V_{FL} spreads onto the ground, but vanishes immediately after the leakage ends.

References

Report on the Result of Risk Assessment Consideration of Room Air-Conditioner with R290 Refrigerant: The Japan Refrigeration and Air Conditioning Industry Association Environment Committee Refrigerant Global Warming Response Commission: Summary Of the Non-FC Refrigerant Consideration Session Meeting (1999)

Risk Assessment of HFC-32 and HFC-32/134a(30/70wt%), Split System Residential Heat Pump, Arthur D Little Inc., United state (1998)

H. Kobayashi, Statistics and Analysis of Accidents of High Pressure Gas, The High Pressure Gas Safety Institute of Japan, pp. 149-159 (2014/02)

Ministry of Economy, Trade, and Industry: Risk Assessment Handbook Practice Edition (2011)

KHKS0302-3, Standards of Refrigeration and Air-Conditioning Equipment Facilities [Facilities with Flammable Gases (including low-flammable Gases)] (2011)

JISC60079-10(2008), Electric Machinery and Instruments Used in Explosive Atmospheres-Chapter 10: Classification of Hazardous Areas

IEC60335-2-40, Household and similar electrical appliances –Safety – (2005)

Part 2-40) Particular requirements for electrical heat pumps, air conditioners and dehumidifiers.

JRA GL-13, Guideline for Ensuring Safety in the Event of a Refrigerant Leak From a Multi-Unit Air Conditioning System, JRA (2011)

Assessment of flammability of R-1234yf and R-1234ze(E), The 49th Combustion Symposium (2011/12)

T. Imamura, Evaluation of Fire Hazards of A2L Class Refrigerants, The International Symposium on New Refrigerants and Environmental Technology 2012, pp.65-68, Kobe (2012.11)

T. Saburi, Combustion Characteristics of Flammable Refrigerant Gases, International Symposium on New Refrigerants and Environmental Technology 2012, pp. 69-72, Kobe (2012.11)

K. Takizawa, Flammability Property of 2L Refrigerants, International Symposium on New Refrigerants and Environmental Technology 2012, pp. 73-79, Kobe (2012.11)

JT Website, http://www.jti.co.jp/investors/press_releases/2012/0730_01_appendix_02.html (2013)

ISO5149, Refrigerating systems and heat pumps—Safety and environmental requirements (2014)

Part1) Definitions, classification and selection criteria

Part2) Design, construction, testing, marking and documentation

Part3) Installation site

Part4) Operation, maintenance, repair and recovery

Japan Fluorocarbon Manufacturers Association (JFMA) ed., 2012, List of CFCs, HCFCs and fluorocarbons' environmental and safety data, JFMA, <http://www.jfma.org/atabase/table.html> (in Japanese)

National Institute of Standards and Technology (NIST), 2013, *Standard Reference Database 23, Version 9.1.*

10. Thermophysical Properties and Cycle Performance of Newly Developed Low-GWP Refrigerants

10.1 Introduction

The research group is working on the following subjects under the NED project entitled, “Development of low-GWP refrigerants suitable for vapor compression heat pump systems.”

- (1) Focusing on the newly developed low-GWP refrigerants such as HFO-1234ze(Z), for which data are not yet available in the public domain, in order to clarify their chemical characteristics including their safety, thermodynamic, and transport properties; heat transfer characteristics; and performance in a basic heat pump cycle.
- (2) Exploring and selecting low-GWP refrigerant mixtures, which are composed of HFO refrigerants HFO-1234ze(Z), HFC refrigerants, and/or natural refrigerants, for their potential use in commercial air conditioning systems.
- (3) Clarifying the thermodynamic and transport properties, heat transfer characteristics, and performance of the basic heat pump cycle of the low-GWP refrigerant mixture selected.
- (4) Building a fundamental technology to enable the practical use of the low-GWP refrigerant mixture.

In this report, measurements of the thermodynamic and transport properties, a proposal for the equation of state, and the cycle performance test of HFC-32/HFO-1234yf mixtures are presented.

10.2 Measurements of Thermodynamic Properties and Proposal for Equation of State for Low-GWP Refrigerants

10.2.1 Measurements of the thermodynamic properties of R 1243zf

Measurements of thermodynamic properties were performed for the new refrigerant R 1243zf (3,3,3-trifluoropropene: $\text{CF}_3\text{CH}=\text{CH}_2$), which is an HFO (hydro-fluoro-olefin) with a double bond and is the same as that of R 1234yf, R 1234ze(E), and R 1234ze(Z). The new refrigerant is expected to be used as an alternative refrigerant in air conditioners. However, in comparison with R 1234ze(Z), which was the target of our project last year, R 1243zf has a lower normal boiling point (about 247 K), and is slightly more flammable.

In this study, pressure-density-temperature ($P\rho T$) properties, vapor pressures, and saturated liquid and vapor densities were measured for the new refrigerant, R 1243zf, using two types of isochoric methods. One apparatus was used for measuring saturated densities, critical temperature, and the critical density by direct observation of the meniscus disappearance; and the other apparatus was used for measuring the $P\rho T$ properties, vapor pressures, and critical pressure. Both experiments were related to each other. For the experiments, we used a high purity sample provided from Mexichem Co., with a purity of more than 99.5 %, which was thus used without further purification.

Fourteen saturated densities of R 1243zf were obtained in a range of densities from $182.7 \text{ kg}\cdot\text{m}^{-3}$ to $723.7 \text{ kg}\cdot\text{m}^{-3}$, and in a range of temperatures from 360.7 K to critical temperature. The uncertainty of the temperature measurements was estimated to be within $\pm 10 \text{ mK}$; and the uncertainty of the density measurements was estimated to be from 0.05 to 0.2% in relation to the introduction of the expansion process, which was used to change the experimental density. The experimental data of saturated densities obtained are shown in Fig. 10.2.1. In addition, the enlarged diagram of Fig. 10.2.1 near the critical point is shown in Fig. 10.2.2. Measurements of the saturated densities for R 1243zf were made by the sample filling up of 4 times. These data are in good agreement with each other. From this result, the

reproducibility and repeatability of this experiment are confirmed. The cross symbols in Fig. 10.2.1 indicate the reported values measured by an Italian group, and their results are in good agreement with the present data, except near the critical point. However, there is no available experimental data by other researchers for the critical region.

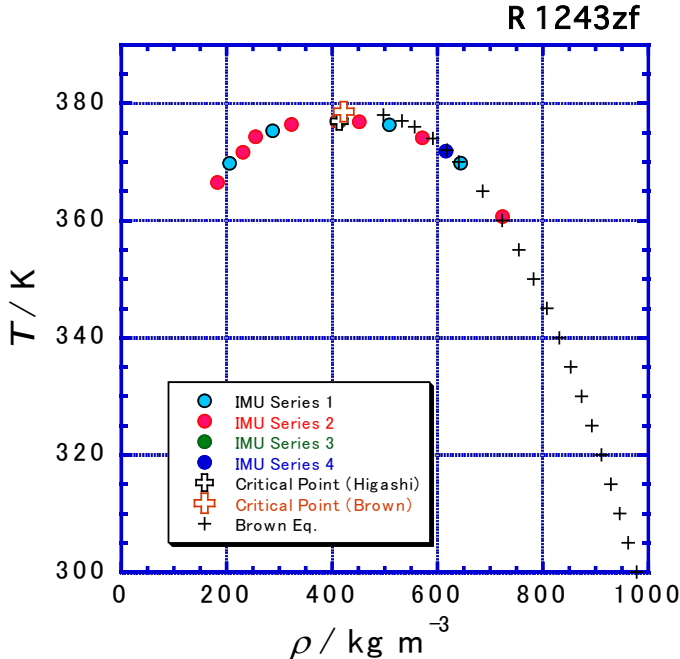


Fig. 10.2.1 Saturated densities for R 1243zf (vapor-liquid coexistence curve).

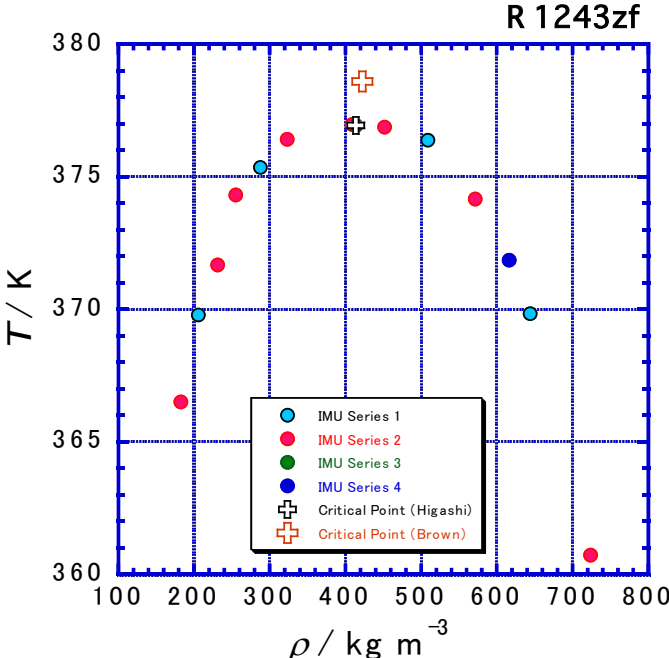


Fig. 10.2.2 Saturated densities for R 1243zf near the critical point.

By carefully observing the disappearance of the meniscus, the critical temperature and critical density were determined on the basis of the intensity of critical opalescence, as well as on the level at which the meniscus disappeared.

The critical parameters determined in this study are

$$T_c = 376.93 \pm 0.02 \text{ K} \quad \text{and} \quad \rho_c = 414 \pm 3 \text{ kg}\cdot\text{m}^{-3} \quad (10.1.1)$$

The experimental results for vapor pressure measurements are shown in Fig. 10.2.3, and those for $P\rho T$ properties are shown in Fig. 10.2.4. Nineteen data were obtained for the vapor pressures of R 1243zf at temperatures between 310 K and 375 K, and at pressures between 815 kPa and 3390 kPa. In addition, 133 $P\rho T$ property data were obtained at pressures between 815 kPa and 6902 kPa, at densities between $50 \text{ kg}\cdot\text{m}^{-3}$ and $900 \text{ kg}\cdot\text{m}^{-3}$, and at temperatures between 310 K and 430 K.

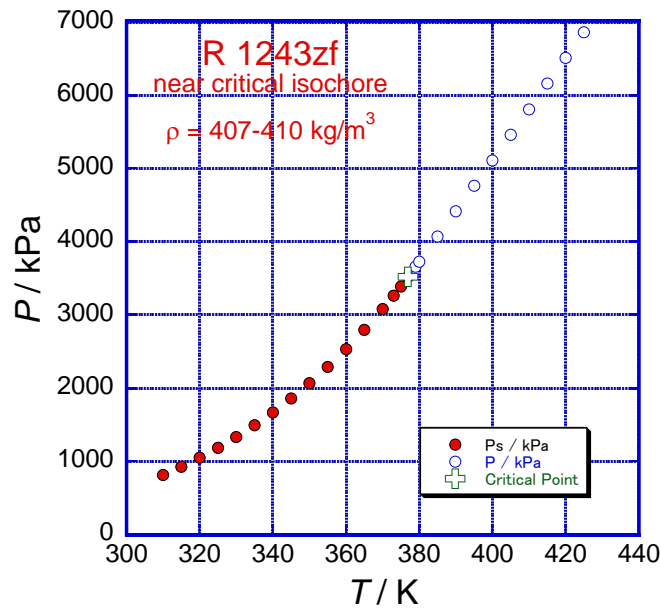


Fig. 10.2.3 Vapor pressures for R 1243zf

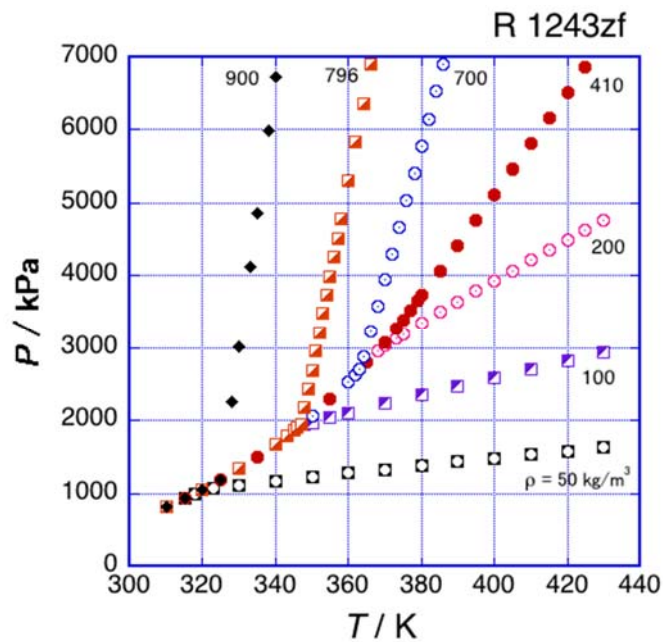


Fig. 10.2.4 $P\rho T$ properties for R 1243zf along seven isochores

The experimental uncertainties of temperature, pressure, and density were estimated within ± 10 mK, ± 2 kPa, and $\pm 0.15\%$, respectively. When the sample was filled to the critical density, the isochores were the same as for the vapor pressure curve. In addition, when the pressure was measured at the critical temperature along the critical isochores, the critical pressure could be determined directly. However, it was very difficult to fill the sample at the critical density. In this study, the vapor pressure correlation was thus firstly formulated based upon the present data and the critical pressure for R 1243zf was then determined as an extrapolation of the vapor pressure curve to the critical temperature. The critical pressure for R 1243zf and vapor pressure correlation determined in this study are summarized as

$$P_c = 3517 \pm 3 \text{ kPa.} \quad (10.2.2)$$

$$\ln\left(\frac{P_s}{P_c}\right) = \frac{T_c}{T} (N_1\theta + N_2\theta^{1.5} + N_3\theta^{3.8} + N_4\theta^5) \quad (10.2.3)$$

where $\theta = 1 - T/T_c$ and $T_c = 376.93$ K. The fitting parameters in Eq. (10.2.3) are $N_1 = -7.26583$, $N_2 = 1.34642$, $N_3 = -11.7799$, and $N_4 = 19.1288$. Eq. (10.2.3) is able to reproduce the present vapor-pressure data within 0.01% as the absolute average deviation.

10.2.2 Equation of state for R1243zf

A fundamental equation of state, which is explicit in the Helmholtz energy, was formulated for R1243zf. In this respect, the critical parameters, and the saturated liquid and vapor densities obtained in this work were used in the formulation. The equation of state has the form

$$\frac{a(T, \rho)}{RT} = \alpha(\tau, \delta) = \alpha^0(\tau, \delta) + \alpha^r(\tau, \delta) \quad (10.2.4)$$

where τ and δ are the reduced temperature and density, respectively, and are defined as $\tau = \frac{T_c}{T}$ and $\delta = \rho/\rho_c$; and α^0 and α^r are an ideal-gas part and a residual part of the Helmholtz energy, respectively. According to the ideal gas law, the ideal-gas part can be calculated analytically from an equation for the ideal-gas isobaric heat capacity, c_p^0 , using the equation

$$\alpha^0(\tau, \delta) = \frac{h_0^0 \tau}{RT_c} - \frac{s_0^0}{R} - 1 + \ln \frac{\delta \tau_0}{\delta_0 \tau} - \frac{\tau}{R} \int_{\tau_0}^{\tau} \frac{c_p^0}{\tau^2} d\tau + \frac{1}{R} \int_{\tau_0}^{\tau} \frac{c_p^0}{\tau} d\tau \quad (10.2.5).$$

Furthermore, the Joback method gives the following c_p^0 equation for R1243zf:

$$c_p^0 = N_0^0 + N_1^0 T + N_2^0 T^2 + N_3^0 T^3 \quad (10.2.6)$$

where $c_p^0 = (\text{J mol K}^{-1})$, $T = (\text{K})$, $N_0^0 = -9.030$, $N_1^0 = 0.4300$, $N_2^0 = -3.833 \times 10^{-4}$, and $N_3^0 = 1.306 \times 10^{-7}$.

The residual part is empirically determined by nonlinear least-squares fitting to the experimental data. The following functional form was given to the fitting:

$$\alpha^r(\tau, \delta) = \sum_{i=1}^{n_1} \tau^{t_i} \delta^{d_i} + \sum_{i=n_1+1}^{n_2} \tau^{t_i} \delta^{d_i} \exp(-\delta^{e_i}) \quad (10.2.7)$$

The number of terms, coefficients, and exponents were optimized so that selected experimental data could be represented within their uncertainties. In addition to the experimental data, various thermodynamic constraints were taken into account in the fitting. The equation of state formulated in this work is valid at temperatures from 250 K to 380 K, and for pressures up to 35 MPa.

Figure 10.2.5 shows deviations for vapor pressure in the experimental data from the equation of state. The vapor-pressure data obtained in this work are represented almost within $\pm 0.1\%$; and the absolute average deviation (AAD) is 0.03%. The data by Brown *et al.* (2013) agree with the equation of state within $\pm 0.3\%$, although the data were not used in the fitting. The AAD in the data by Brown *et al.* (2013) is 0.15%, which is comparable to the experimental uncertainty.

Figure 10.2.6 shows the saturation boundary calculated from the equation of state, as well as the experimental data of the saturated liquid and vapor densities. It can be seen that the equation of state agrees well with the experimental data. Deviations in experimental liquid densities by Di Nicola (2013) are shown in Fig.10.2.7. In addition, all of the data are represented within $\pm 0.1\%$; and the AAD in the data is 0.04%. It is also confirmed that the experimental vapor densities correspond to the equation of state within a deviation of 0.59%.

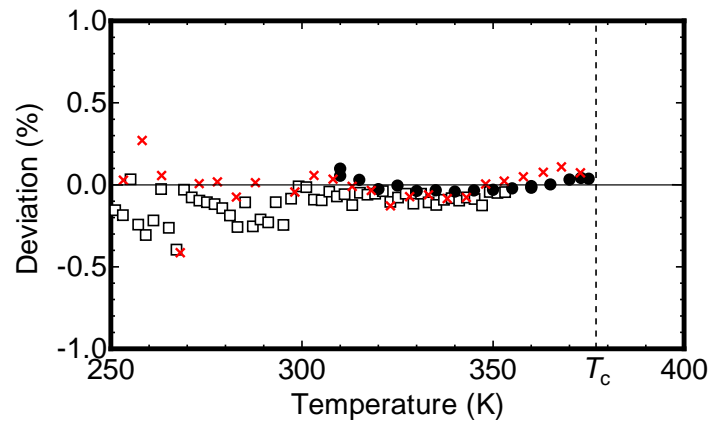


Fig. 10.2.5 Deviations in experimental data for vapor pressure from the equation of state.

(●) This study, (□×) Brown *et al.* (2013)

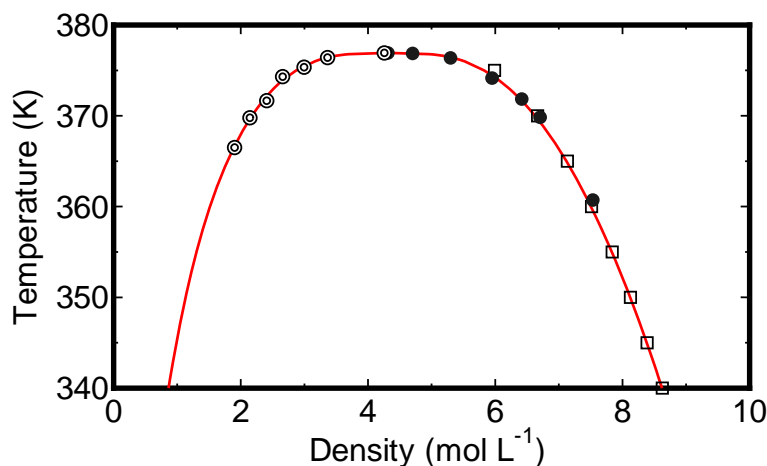


Fig. 10.2.6 Saturation boundary calculated from the equation of state and experimental data of the saturated liquid and vapor densities.

— Equation of state, (●○) This study, (□) Di Nicola *et al.* (2013)

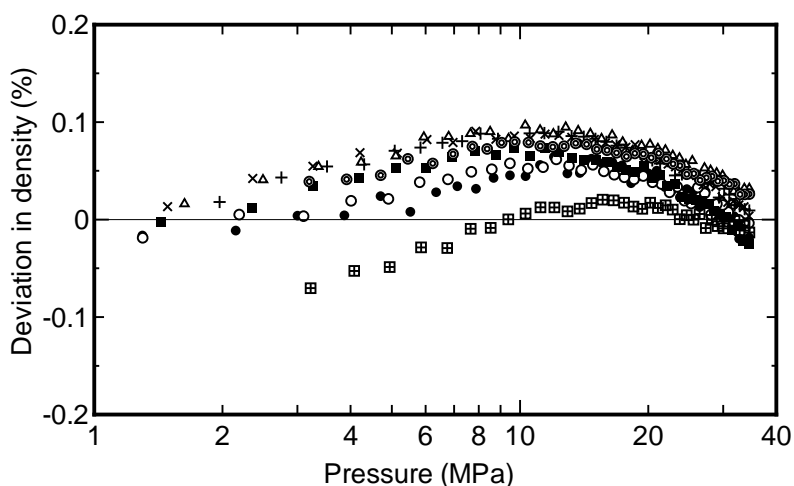


Fig. 10.2.7 Deviations in liquid densities by Di Nicola *et al.* (2013) from the equation of state.

(●) 283.15 K, (○) 293.15 K, (■) 303.15 K, (×) 313.15 K, (+) 323.15 K, (△) 333.15 K, (⊙) 343.15 K, (⊞) 353.15 K

Please note that a FLD file is available for REFPROP based on the equation of state, and this provides a simple way of calculating the thermodynamic properties of R1243zf.

10.2.3 Measurements of surface tension for low-GWP refrigerants

10.2.3.1 Measurement method

Figure 10.2.8 shows the experimental apparatus used for measuring surface tension. The surface tension was measured as the capillary elevation within a small diameter tube immersed in a liquid. Two capillaries with inner radii of $r_1 = 0.4222 \pm 0.0009$ mm, and $r_2 = 0.7526 \pm 0.0009$ mm were set vertically by a supporting brace in a pressure vessel (A), which comprised a Pyrex glass tube with an inner diameter of 17 mm and an outer diameter of 25 mm. The capillary radii were precisely measured with mercury slugs. In the preparatory procedure, the capillaries and the pressure vessel

were carefully cleansed using an alkaline aqueous solution and an ultrasound bath. The liquid of the test refrigerant was filled roughly to a half volume of the pressure vessel at room temperature. The pressure vessel was then placed in a thermostatic bath (B), and the temperature in the thermostatic bath was kept constant within a fluctuation of ± 2 mK using a main heater (J) and a PID (F) controlled sub heater (K). The temperature was measured using a 100Ω platinum resistance thermometer (C) (ASL model F500), which was calibrated against ITS-90. The uncertainty of the temperature measurement was estimated to be within ± 5 mK. At a steady state, the difference in the capillary rise between the two capillary tubes was measured using a digital travelling microscope (M) with a tolerance of 0.01 mm. Figure 10.2.9 illustrates the differential capillary-rise height. The height difference between the bottom of the meniscus in each capillary tube, Δh_m , was measured using a travelling microscope and a CCD camera. The differential height was read twice by six people to eliminate individual variations in reading. Two standard deviations of the readings, which were made 12 times, was 0.046 mm. This deviation was taken into account as the reading error in measuring the differential height. The contact angle, θ , was approximated as zero. To obtain the actual differential capillary-rise height Δh_c , the measured differential height, Δh_m , at the bottom of the meniscus in each capillary tube was corrected using the methodology of Rayleigh (1916):

$$\Delta h_c = (h_{m1} - h_{m2}) + \frac{(r_1 - r_2)}{3} - 0.1288 \left(\frac{r_1^2}{h_{m1}} - \frac{r_2^2}{h_{m2}} \right) + 0.1312 \left(\frac{r_1^3}{h_{m1}^2} - \frac{r_2^3}{h_{m2}^2} \right) + \dots \approx \Delta h_m + \frac{(r_1 - r_2)}{3} \quad (10.2.8)$$

The capillary constant, a^2 , was determined only from the capillary radii and the differential capillary-rise height:

$$a^2 = \frac{g \Delta h_c}{g_n (1/r_1 - 1/r_2) \cos \theta} \approx \frac{g \Delta h_c}{g_n (1/r_1 - 1/r_2)} \quad (10.2.9)$$

where g and g_n are the local gravitational acceleration of 9.8001 m s^{-2} at Iwaki, Japan, and the normal gravitational

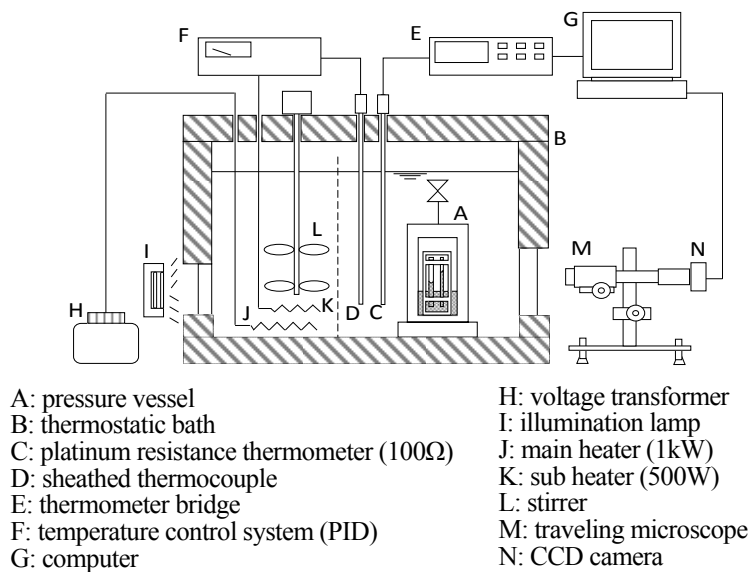


Fig. 10.2.8 Experimental apparatus.

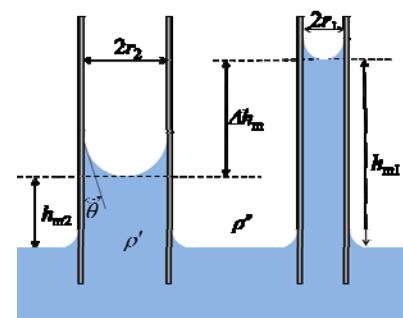


Fig. 10.2.9 Principle of differential capillary rise method.

acceleration of 9.80665 m s^{-2} , respectively. The $\cos\theta$ value is assumed to be equal to 1:

$$a^2 = \frac{2\sigma}{g_n(\rho' - \rho'')} \quad \therefore \quad \sigma = \frac{g\Delta h_c(\rho' - \rho'')}{2(1/r_1 - 1/r_2)\cos\theta} \approx \frac{g\Delta h_c(\rho' - \rho'')}{2(1/r_1 - 1/r_2)} = \left[\frac{gr_1r_2}{2(r_2 - r_1)}\Delta h_m - \frac{gr_1r_2}{6} \right] (\rho' - \rho'') \quad (10.2.10)$$

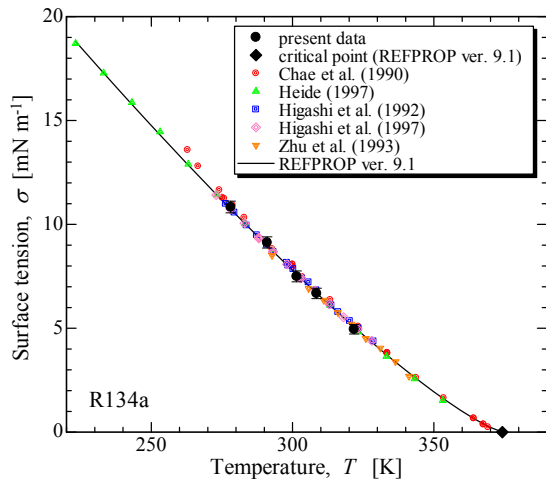
The orthobaric densities, ρ' and ρ'' , are calculated from the measured temperature using REFPROP 9.1 (Lemmon *et al.*, 2013) for R134a, R245fa, and R1233zd (E). For refrigerants R1243zf and R1234ze(Z), fluid files optimized by Akasaka *et al.* (2015, 2014) from the measurement data provided by Higashi *et al.* (2015, 2014) were used to calculate ρ' and ρ'' associated with REFPROP 9.1.

Table 10.2.1 lists the measurement uncertainties related to the equipment mentioned above. The propagated uncertainty in surface tension was estimated to be typically within $\pm 0.2 \text{ mN m}^{-1}$, and the tested R1234ze(Z) and R1233zd(E) were supplied from Central Glass Co., Ltd., Japan. The products were preliminarily well distilled, and the impurities were checked using a TCD gas chromatograph. These impurities were less than 0.1% by mole, which were considered to be within the uncertainty of the gas chromatograph. The sample of R1243zf used in this study was supplied from Mexichem, Ltd., UK, and its purity was more than 99.5 % according to the manufacturer; the sample was therefore used without further purification.

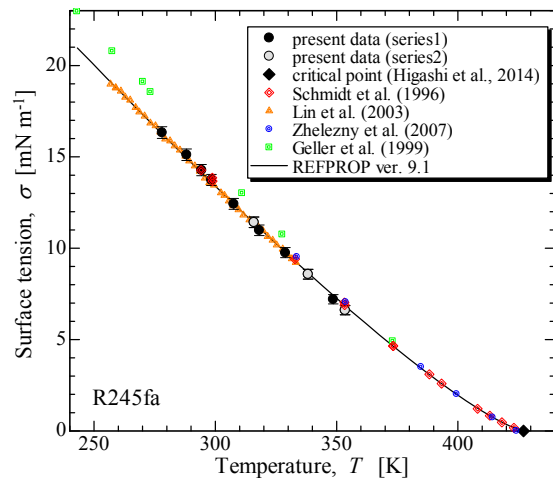
The reproducibility and repeatability of the above-mentioned measurement methods were confirmed with R134a and R245fa. Figures 10.2.10 (a) and (b) compare the surface tension between the present data and other data presented in literature for R134a and R245fa, respectively. The present surface tension data agree well with the calculated surface tension by REFPROP 9.1, and the selected data used for R134a and R245fa. As shown in Fig. 10.2.10 (b), the calculated values of data series 1 and 2, which were measured on different days, were very similar. The standard deviation of these 16 data from the calculated surface tension by REFPROP 9.1 was 0.13 mN m^{-1} , which is within the uncertainty of 0.2 mN m^{-1} . It was thus confirmed that the measurement method used was sufficiently reproducible and repeatable.

Table 10.2.1 Measurement uncertainties

Measured parameter	Equipment	Uncertainty
Temperature (ITS-90)	Platinum resistance thermometer and thermometer bridge, ASL F500	5 mK
Differential capillary-rise height, Δh_m	Digital traveling microscope, Nippon optical works Co., Ltd., NRM-D-2XZ	0.046 mm (tolerance; 0.01 mm)
Inner radii of the capillaries, r_1 and r_2	-	0.0009 mm
Orthobaric densities, ρ' and ρ''	-	0.04% of the calculated values with the representative temperature



(a) Comparison between R134a surface tension data

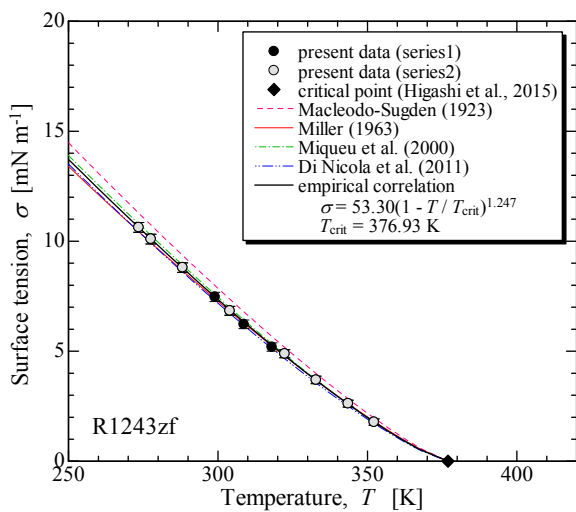


(b) Comparison between R245fa surface tension data

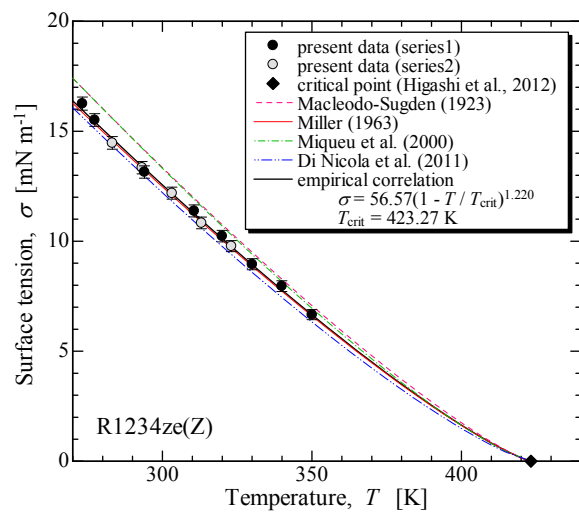
Fig. 10.2.10 Validity of measurement methods used.

10.2.3.2 Measurement results

Figures 10.2.11 (a), (b), and (c) plot the measured surface tension as a function of temperature for R1243zf, R1234ze(Z), and R1233zd(E), respectively. The circle symbols indicate the present data and the small vertical bars overlapping the symbols indicate the measurement uncertainty relating to surface tension. The diamond symbols represent the critical temperatures, T_{crit} , which were measured by Higashi *et al.* (2015) for R1243zf, by Higashi *et al.* (2014) for R1234ze(Z), and by Hulse *et al.* (2012) for R1233zd(E). The triangle symbols in Figure 10.2.11 (c) represent data for the surface tension of R1233zd(E) measured by Hulse *et al.* (2012). As seen in Figure 10.2.11 (c), the present data exhibit an approximately 1.5 mN m^{-1} greater value than their data at a given temperature. Figure 10.2.11 also compares the experimental data to the estimation methods, which are plotted with thin lines. It is evident that the Macleodo-Sugden method (Macleodo, 1923) estimates greater values, particularly for R1233zd(E), and for the three other methods the deviations are within the measurement uncertainty for R1243zf. Although the method of Miquieu *et*

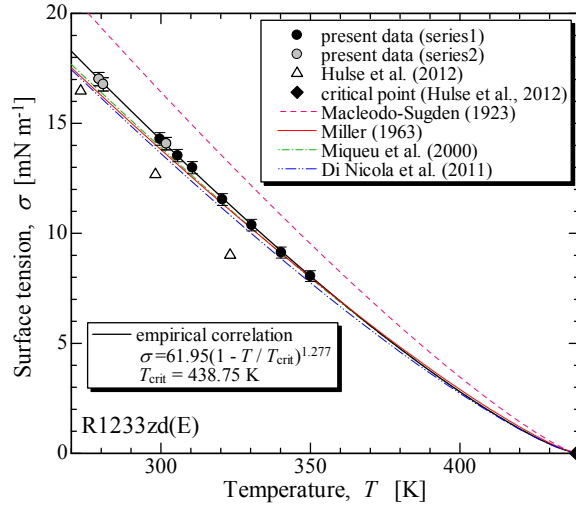


(a) R1243zf



(b) R1234ze(Z)

Fig. 10.2.11 Temperature dependence in surface tension



(c) R1233zd(E)

Fig. 10.2.11 Temperature dependence in surface tension (*continued*)

al. (2000) estimates a 0.7 mN m^{-1} greater value for R1234ze(Z), the other two methods of Miller (1963) and Di Nicola *et al.* (2011) agree to an extent that is almost within the uncertainty. However, these three methods estimate a smaller surface tension, which is between -0.25 mN m^{-1} and -0.51 mN m^{-1} .

For a more accurate estimation of the surface tension, an empirical correlation is proposed here. The solid lines in Fig. 10.2.11 (a) and (b) denote the empirical correlation, which is proposed with the following function form of the van der Waals equation, $\sigma = \sigma_0 (1 - T/T_{\text{crit}})^n$, where σ , T , and T_{crit} are the surface tension in N m^{-1} , the temperature in K, and the critical temperature in K, respectively. The coefficient, σ_0 , and the exponent, n , are optimized to fit the measured surface tension using the least square mean method. From the principle of the corresponding state, the exponent, n , was derived as 1.22 by Guggenheim (1945), and further verified by Brock and Bird (1955). This exponent ranges from 1.2 to 1.3 for most non-polar fluids (Reid *et al.*, 1987). According to the scaling law (Widom, 1974), this exponent is given as $n = 2\nu$ in three dimensions, and the critical exponent, ν , is suggested as 0.64 in his paper; however, the number 0.63 is mostly authorized nowadays (Moldover, 1985). The correlations empirically obtained from the measurement data are summarized as

$$\sigma = 59.90(1 - T/427.01)^{1.237} [\text{mN m}^{-1}] \quad \text{for R245fa} \quad (10.2.11)$$

$$\sigma = 53.30(1 - T/376.93)^{1.247} [\text{mN m}^{-1}] \quad \text{for R1243zf} \quad (10.2.12)$$

$$\sigma = 56.57(1 - T/423.27)^{1.220} [\text{mN m}^{-1}] \quad \text{for R1234ze(Z)} \quad (10.2.13)$$

$$\sigma = 61.95(1 - T/438.75)^{1.277} [\text{mN m}^{-1}] \quad \text{for R1233zd(E)} \quad (10.2.14)$$

The exponents in the empirical correlations are close to those of the suggested numbers in previous studies. As shown with the thick lines in Fig. 10.2.11, these empirical correlations agree with the measured surface tension, and represent

them within 0.13 mN m⁻¹ at temperatures between 270 K and 360 K.

10.3 Measurement and Estimation of Thermophysical Properties

10.3.1 Thermal conductivity measurement of R1234ze(Z)

A well-known transient hot-wire technique was used to measure the thermal conductivity of R1234ze(Z). Thermal conductivity of the test fluid was obtained by measuring the transient temperature variation in a platinum wire after stepwise heating. In this section, we report the measured results of thermal conductivity, including the basic theory of the transient hot-wire method, and the experimental apparatus used.

10.3.1.1 Basic theory of the transient hot-wire method

In the case of an ideal model, where an infinity-long vertical line heat source is immersed in an infinite isotropic fluid, the transient temperature variation of the line heat source after stepwise heating is expressed as

$$\Delta T = T - T_0 = \frac{q}{4\pi\lambda} \left[\ln\left(\frac{4\kappa t}{a^2}\right) - \gamma + \frac{a^2}{2\kappa t} - \frac{\beta - 1}{\beta} \cdot \frac{a^2}{2\kappa t} \left\{ \ln\left(\frac{4\kappa t}{a^2}\right) - \gamma \right\} + \dots \right] \quad (10.3.1)$$

where ΔT is the temperature change of the line heat source, q is the amount of heat per unit length, λ is the thermal conductivity of fluid, κ is the thermal diffusivity, t is time, a is the radius of the hot-wire, γ ($= 0.5772157\dots$) is Euler's constant, and β ($= (c_p)_m/(c_p)_h$) is the heat capacity ratio per unit volume between the fluid and the hot-wire. Uniform heating, constant properties, and stationary fluid are assumed in the derivation of Eq. (10.3.1), and for a small value of $a^2/4\kappa$, Eq. (10.3.1) becomes

$$\Delta T = \frac{q}{4\pi\lambda} \left[\ln\left(\frac{4\kappa t}{a^2}\right) - \gamma \right] \quad (10.3.2)$$

Differentiation of Eq. (10.3.2) with $\ln t$ gives

$$\lambda = \frac{q/4\pi}{d\Delta T/d \ln t} \quad (10.3.3)$$

Eq. (10.3.3) is a basic equation that is used to calculate thermal conductivity from the experimental data of q , T , and t . In order to realize the ideal model that satisfies the assumed conditions, it is necessary to use a long wire with a very small diameter in a cell. The size of the wire should be such that the wall of the cell does not affect the rise in the temperature of the fluid.

10.3.1.2 Experimental setup

The apparatus used for the measurements is shown in Fig. 10.3.1. Two platinum fine wires with different lengths to compensate for the end effects were immersed in the test liquid. The diameters of the platinum wires were 15 μm , and

the lengths were 120 mm and 60 mm, respectively. The test liquid was filled into the pressure vessel up to a level where the vapor-liquid interface could be observed from a view port. The diameter and height of the inner space of the pressure vessel were 40 mm and 240 mm, respectively. The pressure vessel shown in Fig. 10.3.2 was then set in a constant temperature bath, and the saturation state was maintained in each temperature condition by observing the interface.

In order to measure the transient temperature rise of the platinum wire, a Wheatstone bridge circuit was used, as shown in Fig. 10.3.3. Each arm of the

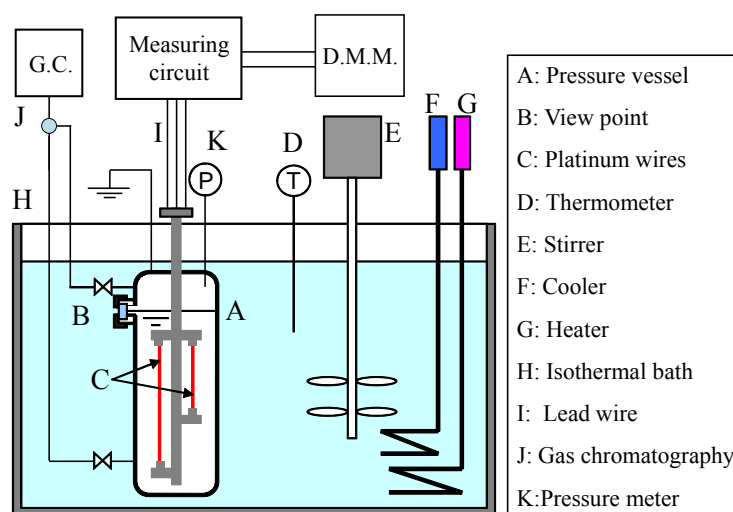


Fig. 10.3.1 Experimental apparatus

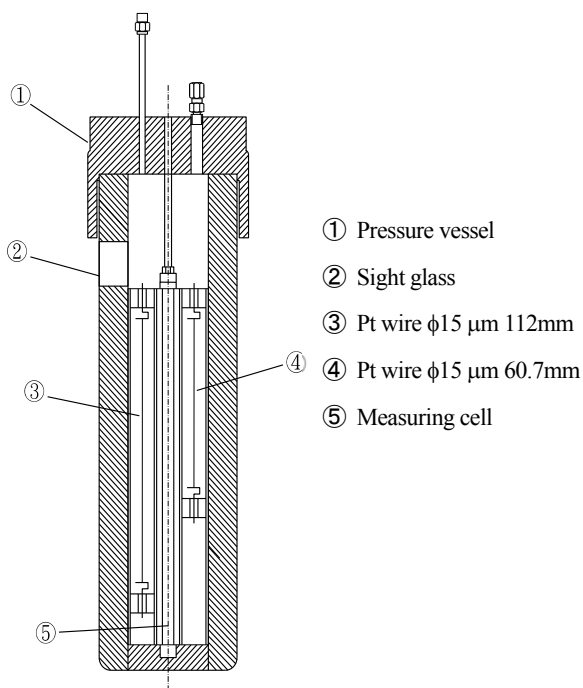


Fig. 10.3.2 Pressure vessel

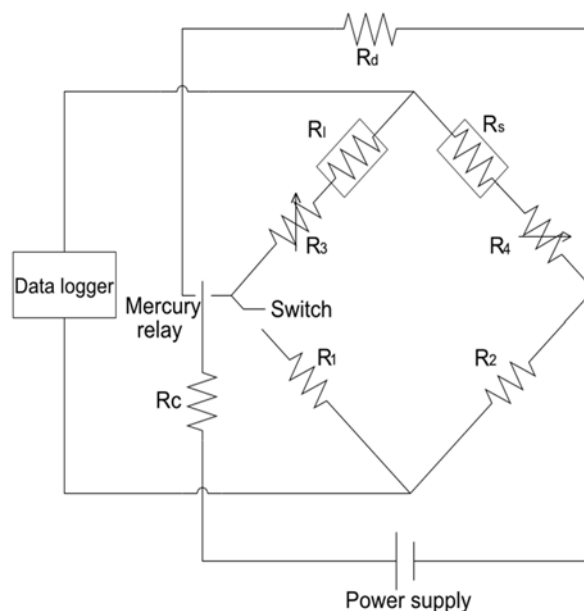


Fig. 10.3.3 Wheatstone bridge circuit used for measurements

bridge is designed to have a resistance of 100Ω . In addition, R_1 and R_2 have a constant value of 100Ω , and R_3 and R_4 are the composites of each platinum wire. Prior to the measurements, the bridge was balanced as close to null as is practical by adjusting the variable resistances R_3 and R_4 , so that each arm has a resistance of 100Ω . The circuit around the bridge in the figure is a dummy circuit. Before supplying the power to the bridge, a mercury relay was closed to the dummy circuit and electricity was passed through the dummy circuit to maintain a constant power supply voltage. After the switch in the bridge circuit was closed, a constant voltage of 8 V was supplied to the bridge by changing the mercury relay, and the voltage that developed across the bridge as a function of time was read and recorded by a digital multi-meter.

10.3.1.3 Measured results

Thermal conductivity measurements of R1234ze(Z) were conducted for the saturated liquid and the superheated vapor conditions, at temperatures between 280 K and 350 K. Figs. 10.3.4 and 10.3.5 show the measured thermal conductivity at saturated liquid and superheated vapor, respectively. The symbol and solid lines in each figure indicate the measurement and calculation obtained by the Extended Corresponding State (ECS) model.

The thermal conductivity of a fluid is represented as the sum of internal and translational modes of energy transfer:

$$\lambda(T, \rho) = \lambda^{\text{int}}(T) + \lambda^{\text{trans}}(T, \rho) \quad (10.3.4)$$

where $\lambda^{\text{int}}(T)$ is written as

$$\lambda^{\text{int}}(T) = \frac{f_{\text{int}} \eta^*}{M} \left(C_p^* - \frac{5}{2} R \right) \quad (10.3.5)$$

$$f_{\text{int}} = a_0 + a_1 T \quad (10.3.6)$$

C_p^* J/(mol·K) and R denote isobaric specific heat and the gas constant ($= 8.314472$ J/(mol·K)), respectively; η^* indicates the dilute-gas viscosity; and $\lambda^{\text{trans}}(T, \rho)$ is expressed as a function of dilute-gas thermal conductivity $\lambda^*(T)$, a residual contribution $\lambda^r(T, \rho)$, and a critical enhancement $\lambda^{\text{crit}}(T, \rho)$:

$$\lambda^{\text{trans}}(T, \rho) = \lambda^*(T) + \lambda^r(T, \rho) + \lambda^{\text{crit}}(T, \rho) \quad (10.3.7)$$

$\lambda^r(T, \rho)$ is written using the residual contribution of the reference fluid (R134a) $\lambda^r_0(T_0, \rho_0)$ as below:

$$\lambda^r(T, \rho) = \lambda^r_0(T_0, \rho_0) F_\lambda(T, \rho) \quad (10.3.8)$$

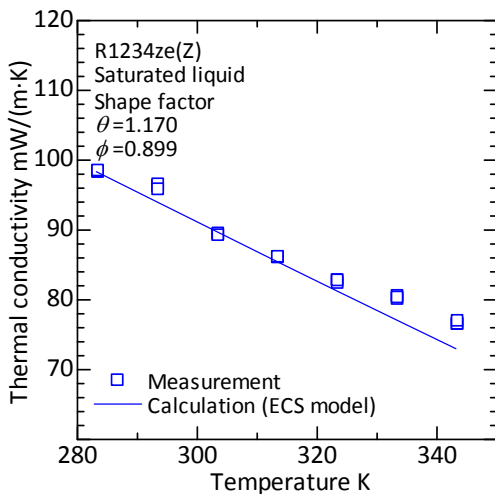


Fig. 10.3.4 Measurement and calculation results (saturated liquid)

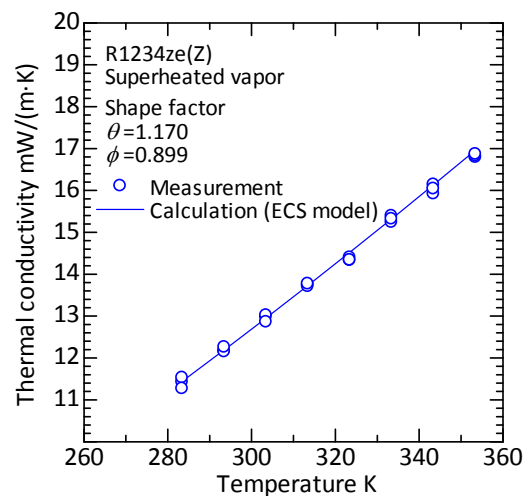


Fig. 10.3.5 Measurement and calculation results (superheated vapor)

$$F_{\lambda}(T, \rho) = f^{1/2} h^{-2/3} \left(\frac{M_0}{M} \right)^{1/2} \quad (10.3.9)$$

Here, function, f , and h in Eq. (10.3.9) are defined as below:

$$f = \frac{T_C}{T_{C,0}} \theta, \quad h = \frac{\rho_{C,0}}{\rho_C} \varphi \quad (10.3.10 \text{ a, b})$$

The parameters θ and φ are known as the shape factors, which are generally functions of temperature and density. In the case of R1234ze(Z), the parameters could be regarded as having a constant value, thereby resulting in the fitting of the experimental data. Their values are obtained as Eq. (10.3.11):

$$\theta = 1.170, \quad \varphi = 0.899 \quad (10.3.11 \text{ a, b})$$

As shown in Figs. 10.3.4 and 10.3.5, it can be seen that there is a good agreement between the measurements and the calculations. However, more data over a wide temperature and pressure range are required to apply the calculation model for a wide pressure and temperature range.

10.3.2 Viscosity measurement of R1234ze(Z)

Viscosity of R1234ze(Z) was measured using the tandem capillary tubes method. In the single capillary tube method, which is based on the well-known Hagen-Poiseuille theory, viscosity is obtained from measuring the pressure drop of the laminar flow inside a capillary tube. In the tandem capillary tubes method, the test fluid flows under a laminar flow condition, and two capillary tubes of different lengths, but with the same diameter, are connected in series in order to eliminate the pressure drop at both the inlet and outlet of the tube. This method enables measurements to be made with a better accuracy than using the single capillary tube method. In this section, the measured results of viscosity of R1234ze(Z) are presented, together with the experimental apparatus used and the basic theory of the tandem capillary tubes method.

10.3.2.1 Basic theory of the tandem capillary tubes method

The relationship between viscosity, η , and the pressure drop, ΔP , of the laminar flow inside a capillary tube (as shown in Fig. 10.3.6) is expressed below as

$$\eta = \frac{\pi a^4 \Delta P}{8Lq} \quad (10.3.12)$$

where a , ΔP , L , and q are the radius of the capillary tube, the pressure drop between the inlet and outlet of the tube, the tube length, and the volume flow rate, respectively. As shown in Fig. 10.3.6, the measured pressure drop is higher than ΔP in Eq. (10.3.12) due to end-face effect of the tube. Eq. (10.3.13) is suggested for correction of the end face effect and kinetic energy:

$$\eta = \frac{\pi a^4 \Delta P}{8(L+na)q} - \frac{m\rho q}{8\pi(L+na)} \quad (10.3.13)$$

where n and m are respectively the end face and kinetic energy correction coefficients, obtained empirically depending on the experimental apparatus; and ρ is fluid density. The schematic of the pressure distribution in the tandem capillary tubes is shown in Figure 10.3.7. The measured pressure drop of the two sections (P_2-P_1 and P_3-P_2 in Fig.10.3.7) includes that of the pressure drop of the fully developed laminar flow, and that of the inlet and outlet end faces of the tubes. The frictional pressure drop of the laminar flow was obtained by superposition of the two measured pressure drops, as below

$$\eta_{LS} = \frac{\pi a^4 (\Delta P_1 - \Delta P_2)}{8(L_1 - L_2)q} \quad (10.3.14)$$

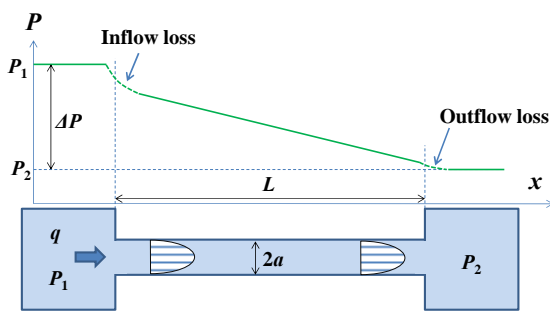


Fig. 10.3.6 Schematic of pressure distribution in a single capillary tube

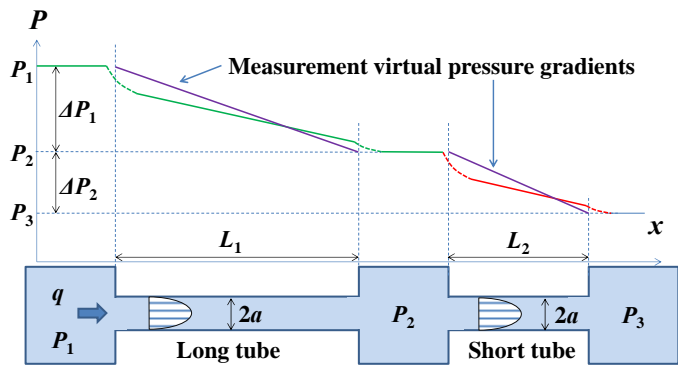


Fig. 10.3.7 Schematic of pressure distribution in tandem capillary tubes

10.3.2.2 Experimental apparatus

Figure 10.3.8 shows the schematic of the experimental apparatus. The test fluid (R1234ze(Z)) was enclosed in a pressure vessel, as shown in Fig. 10.3.9, and it then flowed in two capillary tubes of different lengths that were placed in series. Two capillary tubes had inner diameters of 0.1 mm, and their lengths are 100 mm and 50 mm, respectively.

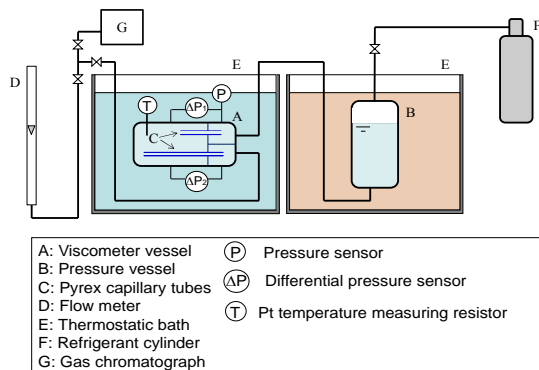


Fig. 10.3.8 Experimental apparatus

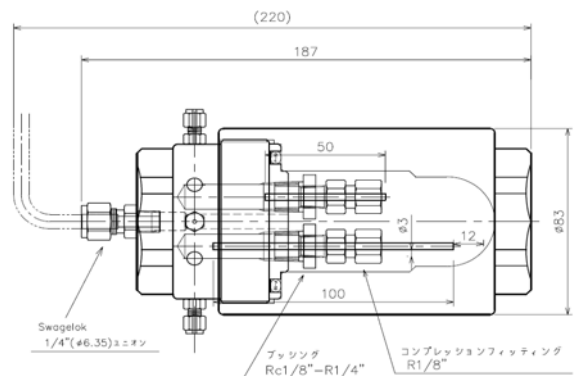


Fig. 10.3.9 Pressure vessel

The pressure drop of each tube was measured using differential pressure sensors, and the viscosity was obtained using Eq. (10.3.14).

10.3.2.3 Measurement results

The viscosity of R1234ze(Z) was measured under subcooled liquid and superheated vapor conditions at temperatures of 280 - 350 K. The data measured under the subcooled and superheated conditions are plotted in Figs. 10.3.10 and 10.3.11, respectively, where the lines in each figure indicate the prediction based on the ECS model. The viscosity, η , is represented as a sum of the dilute-gas contribution, η^* , and the residual contribution, $\Delta\eta$, as in Eq. (10.3.15):

$$\begin{aligned}\eta(T, \rho) &= \eta^*(T) + \Delta\eta(T, \rho) \\ &= \eta^*(T) + \Delta\eta_0(T_0, \rho_0) F_\eta(T, \rho)\end{aligned}\quad (10.3.15)$$

where η^* can be obtained as

$$\eta^*(T) = \frac{5}{16} \sqrt{\frac{M k_B T}{\pi N_A}} \frac{1}{\sigma^2 \Omega^{(2,2)}(T^*)} \quad (10.3.16)$$

where M , k_B , N_A , σ , and $\Omega^{(2,2)}$ are respectively the molecular mass [kg/mol], the Boltzmann constant [J/K], the Avogadro constant [1/mol], the hard-sphere diameter [m], and the collision integral, which is a function of the dimensionless temperature, T^* . The subscript, 0, in Eq. (10.3.15) indicates the value of the reference fluid. The temperature of the interest fluid, T , and the density, ρ , are corresponded with the reference fluid temperature, T_0 , and the density, ρ_0 , respectively, using Eq. (10.3.17):

$$T_0 = \frac{T}{f}, \quad \rho_0 = \rho h \quad (10.3.17 \text{ a, b})$$

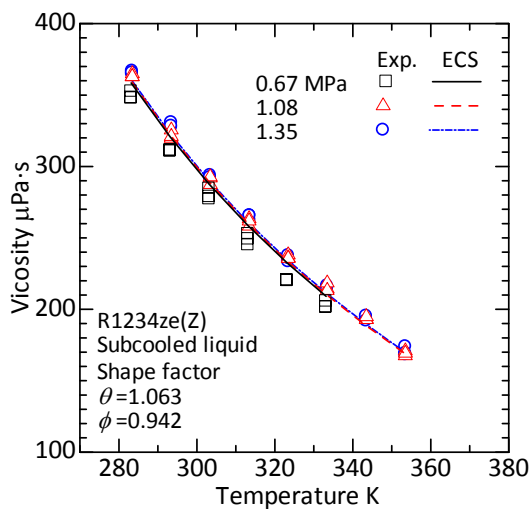


Fig. 10.3.10 Measurement and calculation results (subcooled liquid)

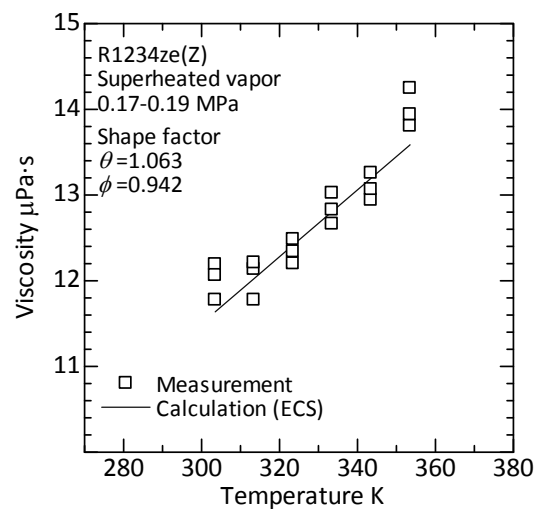


Fig. 10.3.11 Measurement and calculation results (superheated vapor)

$$f = \frac{T_C}{T_{C,0}} \theta, \quad h = \frac{\rho_{C,0}}{\rho_C} \varphi \quad (10.3.18 \text{ a, b})$$

Functions θ and φ in Eq. (10.3.18) are known as shape factors, and these are linked to the relationship between the residual contribution of the interest fluid, $\Delta\eta$, and the reference fluid, $\Delta\eta_0$.

Function $F_\eta(T, \rho)$ in Eq. (10.3.15) is expressed using function f and h in Eq. (10.3.19), as below:

$$F_\eta = f^{1/2} h^{-2/3} \left(\frac{M}{M_0} \right)^{1/2} \quad (10.3.19)$$

In the case of R1234ze(Z), the parameters can be regarded as constant values, which resulted in experimental data fitting and their values are obtained as Eq. (10.3.20):

$$\theta = 1.063, \quad \varphi = 0.942 \quad (10.3.20 \text{ a,b})$$

As shown in Figs 10.3.10 and 10.3.11, there is a good agreement between the measurements and the calculations. It is intended that in future studies, more data will be obtained over wider temperature and pressure ranges, in order to apply the calculation model for wider pressure and temperature ranges.

10.4 Assessment of Cycle Performance Using Low-GWP Refrigerant Mixtures

From the drop-in experiment, it was demonstrated that the heat pump cycle using HFO-1234ze(E) alone exhibits a considerably low COP (coefficient of performance) relative to the conventional refrigerant R410A. Because of the small volumetric capacity of HFO-1234ze(E), a higher volumetric refrigerant flow rate is required to maintain a certain cooling/heating capacity. Therefore, mixing HFC-32 and CO₂ in HFO-1234ze(E) was attempted, in order to increase the volumetric capacity. With HFC-32/HFO-1234ze(E) and CO₂/HFC-32/HFO-1234ze(E), the comparable (or somewhat higher) COP was obtained in comparison with using R410A. This year, refrigerant mixture of HFC-32/HFO-1234yf were assessed using the drop-in experiment, where HFO-1234yf is the isomer HFO-1234ze(E).

10.4.1 Experimental apparatus and method

Figure 10.4.1 illustrates the experimental apparatus used in this study. The refrigerant loop consists of an inverter-controlled hermetic-type rotary compressor, an oil separator, a condenser, a solenoid expansion valve, and an evaporator. Four mixing chambers were installed between the main components in the refrigerant loop, and these were used to measure the bulk-mean temperature and pressure of the refrigerant flow at a steady state. Using constant-temperature baths, a heat sink and heat source water were supplied to the condenser and the evaporator. In the water loops, mixing chambers were also installed at the inlet and outlet of the heat exchangers to measure the water bulk mean temperature. The heat exchangers were a double-tube type in a counter flow configuration, wherein the refrigerant flowed in the inner tube and the water flowed in the annulus. Table 10.4.1 specifies the dimensions of these heat exchangers.

Table 10.4.2 lists the tested refrigerants and their GWP, NBP (Normal Boiling Point), volumetric capacity, and temperature glide. The cycle performance of the refrigerant mixtures HFC-32/HFO-1234yf (42/58 mass% and 28/72

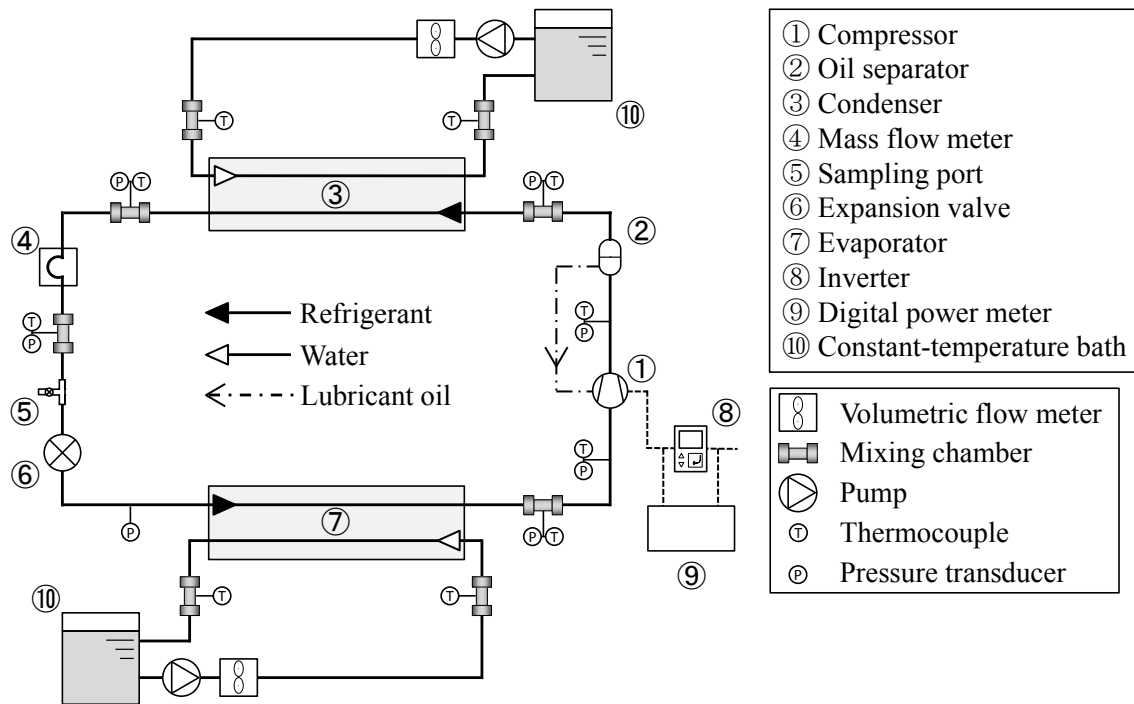


Fig. 10.4.1 Experimental apparatus

Table 10.4.1 Dimensions of heat exchangers

	Outer diameter [mm]	Inner diameter [mm]	Length [mm]	Type
Outer tube	15.88	13.88	7200	Plain
Inner tube	9.53	7.53	7200	Micro-grooved

Table 10.4.2 Test refrigerants

Refrigerant	GWP [-]	NBP [°C]	Volumetric capacity* [kJ · m ⁻³]	Temperature glide* [K]
R410A	2088	-51.4	11043	0.1
HFC-32/HFO-1234yf	42/58 mass%	285	8233	5.4
	28/72 mass%	190	7184	7.1
HFC-32/HFO-1234ze(E)	42/58 mass%	285	7040	9.6
	28/72 mass%	190	5969	11.7

*At bulk temperature 20°C

Table 10.4.3 Test conditions

	Heating mode	Cooling mode
Heat source temperature [°C]	15→9	20→10
Heat sink temperature [°C]	20→45	30→45
Superheat Δt [K]	> 3	> 3
Capacity [kW]	1.6-2.6	1.4-2.4

mass%) were compared to that of HFC-32/HFO-1234ze(E) (42/58 mass% and 28/72 mass%) and R410A. Those compositions are determined from the criteria: the GWPs are nearly equal to 200 and 300. The GWP was obtained from the GWP of the components, and was simply weighed using the mass fraction. For instance, HFC-32/HFO-1234yf (42/58 mass%) and HFC-32/HFO-1234ze(E) (42/58 mass%) exhibits a GWP of 300. At this composition, HFC-32/HFO-1234yf exhibits a 20% greater volumetric capacity, and a 4 K smaller temperature glide than HFC-32/HFO-1234ze(E).

Table 10.4.3 lists the experimental conditions for the heating and cooling modes used. Each experiment was performed based on the specified conditions of the specified heat source/sink temperatures, the degree of superheat at the evaporator, and the heating/cooling capacity.

10.4.2 Experimental results

Figs 10.4.2 and 10.4.3 show the variations in COP against the capacity for the heating and cooling modes; and Figs. 10.4.4 and 10.4.5 compare the irreversible loss breakdown for the heating and cooling modes at capacities of 2.2 kW and 2.0 kW.

As shown in Fig. 10.4.2, values of COP decrease with increasing capacity. At a heating capacity of 2.2 kW, the heating COP of (HFC-32/HFO-1234ze(E): 42/58 mass%) is the highest among the tested refrigerants. The COP in descending order is as follows: (HFC-32/HFO-1234ze(E): 42/58 mass%), (HFC-32/HFO-1234yf: 42/58 mass%), R410A, (HFC-32/HFO-1234yf: 28/72 mass%), and (HFC-32/HFO-1234ze(E): 28/72 mass%). The COPs of the refrigerant

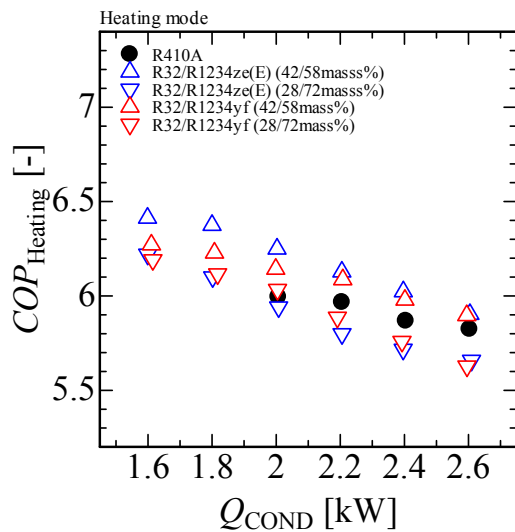


Fig. 10.4.2 COP for heating mode

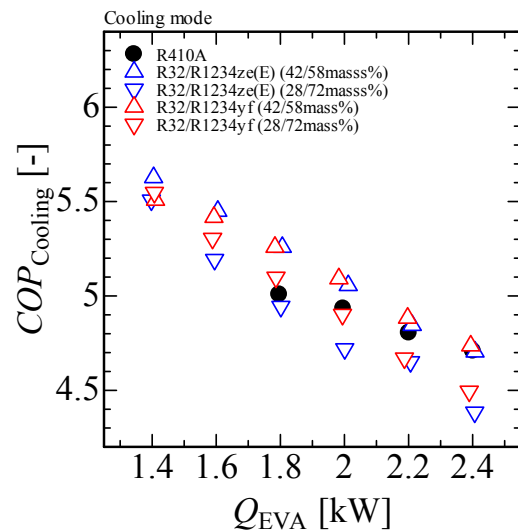


Fig. 10.4.3 COP for cooling mode

mixture with GWP 300 exceed that of R410A. Comparing the refrigerant mixtures with the same GWP 300, (HFC-32/HFO-1234yf: 42/58 mass%) exhibits a lower COP than that of (HFC-32/HFO-1234ze(E): 42/58 mass%) because of matching the temperature glide with the heat source/sink water temperature changes. Figure 10.4.6 shows the temperature distributions of refrigerants and water flows in the condenser and evaporator. In the evaporator with a water temperature change of 6 K, the average temperature difference between the refrigerant and the water decreases because of the smaller temperature glide of HFC-32/HFO-1234yf, and thus, the irreversible loss in the evaporator decreases. However, in the condenser with a water temperature change of 25 K, a large temperature difference is encountered, and thus, the irreversible loss in the condenser of HFC-32/HFO-1234yf is larger than that of HFC-32/HFO-1234ze(E). This loss cancels out the advantage gained in the evaporator. As a result, the effect of the temperature glide on the reduction of irreversible loss is more evident with HFC-32/HFO-1234ze(E) in the heating mode.

A comparison of the mixtures with GWP 200 and GWP 300 shows that the mixture with GWP 200 exhibits the larger irreversible loss in the compressor. Because the volumetric capacity of the mixture with GWP 200 is smaller than that with GWP 300, higher volumetric flow rate is required to maintain the heating capacity for the mixture with GWP 200, and therefore, the larger irreversible loss occurs in the compressor.

As shown in Figure 10.4.3, at a cooling capacity of 2.0 kW the descending order of COP is as follows: (HFC-32/HFO-1234yf: 42/58 mass%), (HFC-32/HFO-1234ze(E): 42/58 mass%), R410A, (HFC-32/HFO-1234yf: 28/72 mass%), and (HFC-32/HFO-1234ze(E): 28/72 mass%). For the cooling mode, the water temperature change in the condenser was 15 K, and thus, the effect of the temperature glide on the reduction of irreversible loss was not evident for HFC-32/HFO-1234ze(E). Consequently, the total irreversible loss in the condenser and evaporator of HFC-32/HFO-1234ze(E) was comparable to that of HFC-32/HFO-1234yf.

From the above results, it was found that the COP of HFC-32/HFO-1234ze(E) and HFC-32/HFO-1234yf were almost comparable at a composition with the same GWP. However, at a composition with a GWP of 300, the COPs of these mixtures exceeded that of R410A.

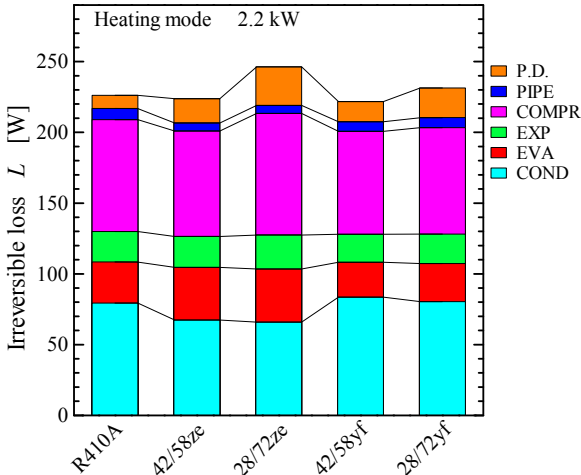


Fig. 10.4.4 Irreversible loss for heating mode

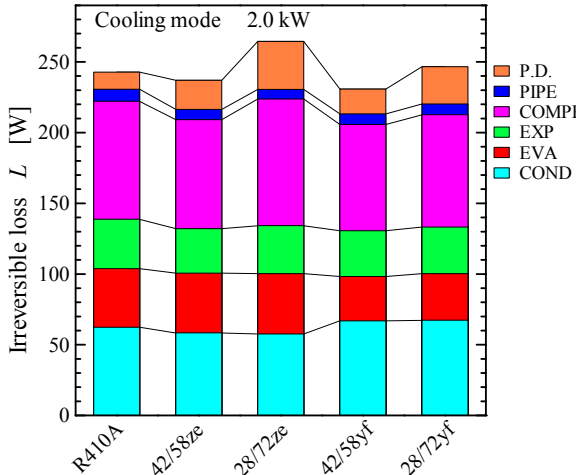


Fig. 10.4.5 Irreversible loss for cooling mode

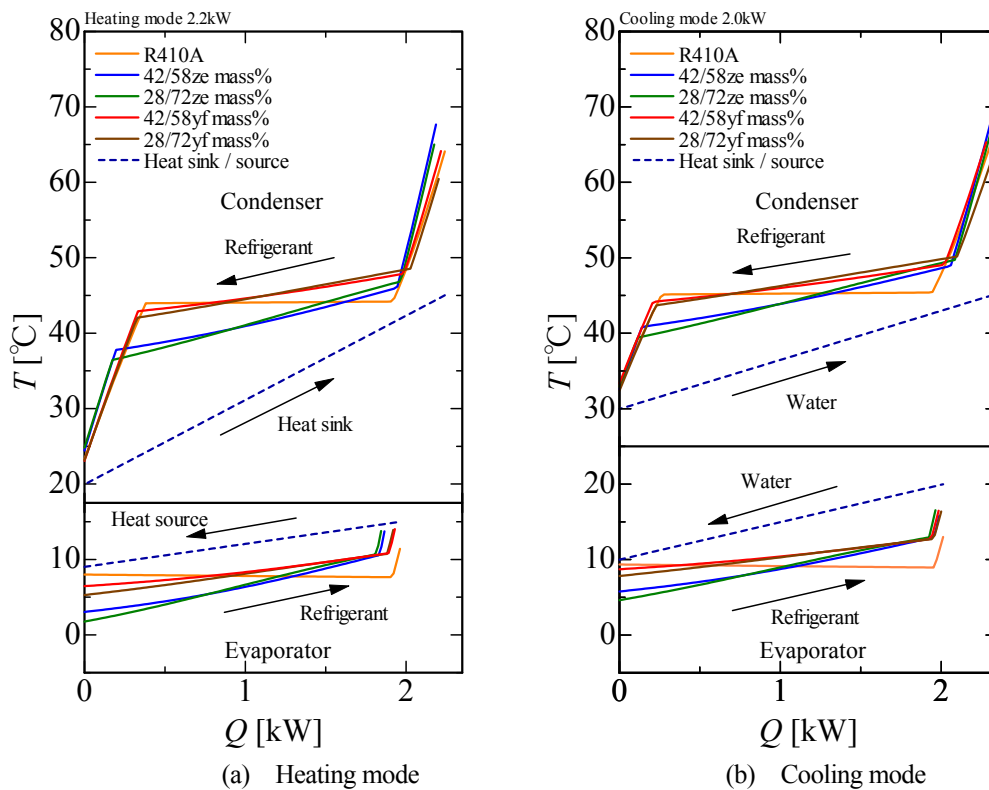


Fig. 10.4.6 Temperature distribution in heat exchanger

10.5 Conclusions

In this year, the thermodynamic properties of HFO-1243zf, the surface tension for a number of low-GWP refrigerants, and the transport properties of HFO-1234ze(Z) were measured. The equation of state for R1243zf was proposed, and the cycle performance test for a binary refrigerants mixture of HFO-32/HFO-1234yf was also carried out. The conclusions obtained are as follows:

- (1) The pressure-density-temperature ($P\rho T$) properties, vapor pressures, and saturated liquid and vapor densities for HFO-1243zf were measured with two types of isochoric methods. Then, critical temperature T_c and critical density ρ_c are determined from the present measured data. The critical pressure P_c and the saturated vapor pressure correlation are also determined for HFO-1243zf.
- (2) A fundamental equation of state explicit in the Helmholtz energy are formulated for R1243zf using the critical parameters and saturated liquid and vapor densities obtained in in the present study. It is confirmed that thermodynamic properties predicted by the formulated equation of state agree with existing experimental data. A FLD file for REFPROP based on the equation of state is also provided.
- (3) The surface tension was measured with the capillary elevation method for HFO-1243zf, HFO-1234ze(Z), and HCFO-1233zd(E). Then, the empirical correlations of the van der Waals type were proposed.
- (4) The thermal conductivity of HFO-1234ze(Z) was measured with a transient hot-wire technique using two fine wires of different length for HFO-1234ze(Z) both in saturated liquid state and superheated vapor state in the temperature range of 280 to 350 K. The extended corresponding model to predict the thermal conductivity of

HFO-1234ze(Z) is also developed based on the present study. It is confirmed that there are good agreement between the measurement and the prediction.

(5) The viscosity thermal conductivity of HFO-1234ze(Z) was measured with a tandem capillary tubes method based on the Hagen-Poiseuille theory both in subcooled liquid state and superheated vapor state. The extended corresponding model to predict the viscosity of HFO-1234ze(Z) is also developed based on the present study. The experimental data are predicted well with the extended corresponding model.

(6) In the present study, the cycle performances of several refrigerants were evaluated using a water heat source heat pump loop. In this year, binary zeotropic mixtures of HFC-32 and HFO-1234yf (42/58 mass% and 28/72 mass%) were tested. The cycle performance of the refrigerant mixtures HFC-32/HFO-1234yf (42/58 mass% and 28/72 mass%) was compared to that of HFC-32/HFO-1234ze(E) (42/58 mass% and 28/72 mass%) and R410A. Then, it was found that the COP of HFC-32/HFO-1234ze(E) and HFC-32/HFO-1234yf were almost comparable at the composition with same GWP and at the composition with GWP of 300, the COPs of these mixtures exceeded that of R410A.

Appendix 1: List of Committee Members

Chair

Eiji HIHARA, Professor

- Graduate School of Frontier Sciences, The University of Tokyo.

Associate Chair

Satoru FUJIMOTO

- The Japan Refrigeration and Air Conditioning Industry Association. (JRAIA)
(Daikin Industries, Ltd.)

Committee Members

Sigeru KOYAMA, Professor

- Interdisciplinary Graduate School of Engineering Sciences, Kyushu University.

Osami SUGAWA, Professor

Tomohiko IMAMURA, Junior Associate Professor

- Department of Mechanical Engineering, Faculty of Engineering, Tokyo University of Science, Suwa.

Chaobin DANG, Associate Professor

- Graduate School of Frontier Sciences, The University of Tokyo.

Hiroyuki SUDA, Group Leader

Kenji TAKIZAWA, Senior Researcher

- Research Institute for Innovation in Sustainable Chemistry, National Institute of Advanced Industrial Science and Technology (AIST).

Tei SABURI, Senior Researcher

Yuji WADA, Group Leader

- Research Institute of Science for Safety and Sustainability, National Institute of Advanced Industrial Science and Technology (AIST).

Kenji MATSUDA, Senior Manager of Engineering Department

Kazuhiro HASEGAWA, Section Manager of Engineering Department

- The Japan Refrigeration and Air Conditioning Industry Association. (JRAIA)

Kenji TAKAICHI, Staff Engineer

- The Japan Refrigeration and Air Conditioning Industry Association. (JRAIA)
(Appliances Company Corporation Engineering Division, Panasonic Corporation.)

Takeshi WATANABE, Staff Engineer

- The Japan Refrigeration and Air Conditioning Industry Association. (JRAIA)
(Appliances Company Corporation Engineering Division, Panasonic Corporation.)

Ryuzaburo YAJIMA

- The Japan Refrigeration and Air Conditioning Industry Association. (JRAIA)
(Daikin Industries, Ltd.)

Kenji UEDA

- The Japan Refrigeration and Air Conditioning Industry Association. (JRAIA)
(Machinery, Equipment & Infrastructure Air-Conditioning & Refrigeration Division Chiller & Heat Pump Engineering Department, Mitsubishi Heavy Industries, Ltd.)

Takeshi ICHINOSE, Group Leader

- Business Affairs Department, Japan Automobile Manufacturers Association, Inc. (JAMA)

Atsushi OOKI, Group Manager

- Japan Automobile Manufacturers Association, Inc. (JAMA)
(Toyota Motor Corporation.)

Tetsuya SUZUKI, Researcher

- Japan Automobile Manufacturers Association, Inc. (JAMA)
(Japan Automobile Research Institute.)

Jun ICHIOKA

- Safety Committee, Japan Society of Refrigeration and Air Conditioning Engineers. (JSRAE)
(Toyo Engineering Works, Ltd.)

Kenji TSUJI

- Safety Committee, Japan Society of Refrigeration and Air Conditioning Engineers. (JSRAE)
(Daikin Industries, Ltd.)

Observers

Takashi ICHIKAWA, Assistant Director

- Fluoride Gases Management Office, Chemical Management Policy Division, Ministry of Economy, Trade and Industry

Noboru KANUMA, Assistant Director

- Industrial Machinery Division, Ministry of Economy, Trade and Industry

Masamichi ABE, Director

Noboru TAKARAYAMA, Project Coordinator

Mika SUZAWA

- Environment Department, New Energy and Industrial Technology Development Organization. (NEDO)

Moriaki IINUMA, Manager

- Refrigeration Safety Division, High Pressure Gas Safety Department, The High Pressure Gas Safety Institute of Japan

Yasuhisa NAKASO, Manager (Energy Utilization Research)

- Sales Department, The Kansai Electric Power Co, Inc.

Hiroaki OKAMOTO, Project Researcher

- Graduate School of Frontier Sciences, The University of Tokyo.

Appendix 2: List of Authors

Chapter 1

Eiji HIHARA/ The University of Tokyo

Chapter 2

Kenji TAKIZAWA/ AIST

Contributor: Eiji HIHARA, Chaobin DANG, Makoto ITO/ The University of Tokyo

Chapter 3

Tomohiko IMAMURA, Osami SUGAWA/ Tokyo University of Science, Suwa

Contributor: Eiji HIHARA, Chaobin DANG, Tomohiro HIGASHI/ The University of Tokyo

Chapter 4

Tei SABURI, Yuji WADA/ AIST

Chapter 5

Kenji TAKAICHI/ Panasonic

Contributor: Ryuzaburo YAJIMA, Satoru FUJIMOTO/ Daikin Ind.; Kenji UEDA/ Mitsubishi Heavy Ind.; Takeshi WATANABE/ Panasonic

Chapter 6

Kenji TAKAICHI/ Panasonic

Shigeharu TAIRA/ Daikin Ind.

Contributor: Madoka UENO/ Sharp; Katsunori MURATA, Akio TASAKA, Satoru FUJIMOTO/ Daikin Ind.; Koichi YAMAGUCHI/ Toshiba Carrier; Ryoichi TAKAFUJI/ Hitachi Appliances; Toshiyuki FUJI/ Fujitsu General; Hiroaki MAKINO/ Mitsubishi Elec.

Chapter 7

Takeshi WATANABE/ Panasonic

Contributor: Tsuyoshi YAMADA, Ryuzaburo YAJIMA, Shigeharu TAIRA, Takashi HASEGAWA/ Daikin Ind.; Akihiro SUZUKI, Hiroichi YAMAGUCHI/ Toshiba Carrier; Kazuhiro TSUCHIHASHI, Shunji SASAKI/ Hitachi Appliances; Toshiyuki FUJI/ Fujitsu General; Kenichi MURAKAMI, Kenichi MURAKAMI, Tetsuji FUJINO/ Mitsubishi Heavy Ind.; Yasuhiro SUZUKI, Takuho HIRAHARA, Naoshi TAKIMOTO/ Mitsubishi Elec.; Kenji TAKAICHI/ Panasonic; Kazuhiro HASEGAWA/ JRAIA

Chapter 8

Ryuzaburo YAJIMA/ Daikin Ind.

Contributor: Yukio KIGUCHI, Hiroichi YAMAGUCHI/ Toshiba Carrier; Katsuyuki TSUNO, Kenji TAKAICHI/ Panasonic; Shunji SASAKI, Tetsushi KISHITANI, Eiji SATO/ Hitachi Appliances; Shuntaro ITO, Takahiro MATSUNAGA/ Fujitsu General; Koji YAMASHITA/ Mitsubishi Elec.; Tatsumi KANNON/ Mitsubishi Heavy Ind.; Shinya MATSUOKA, Masato YOSHIZAWA/ Daikin Ind.; Kazuhiro HASEGAWA/ JRAIA

Chapter 9

Kenji UEDA/ Mitsubishi Heavy Ind.

Contributor: Masayuki AIYAMA/ Hitachi Appliances; Mikio ITO/ Ebara Ref. Equip. Systems; Isao IBA, Hiroichi YAMAGUCHI/ Toshiba Carrier; Naoki KOBAYASHI, Yosuke MUKAI/ Mitsubishi Heavy Ind.; Tetsuji SAIKUSA, Yoshihiro SUMIDA, Koji YAMASHITA, Takuho HIRAHARA/ Mitsubishi Elec.; Mamoru SENDA/ Panasonic; Tomokazu TASHIMO/ Kobe Steel; Shuji FUKANO/ Maekawa Mfg.; Hiroaki OKAMOTO/ Univ. Tokyo

Chapter 10

Shigeru KOYAMA, Chieko KONDO/ Kyushu Univ.

Yukihiro HIGASHI/ Iwaki Meisei Univ.

Ryo AKASAKA/ Kyushu Sangyo Univ.

Akio MIYARA, Keishi KARIYA/ Saga Univ.